AER/AGS Open File Report 2019-06

Alberta Energy Regulator

A Risk-Based Methodology for Commingled Well Abandonment – Southeastern Alberta Gas Field Case Study

AGS
ALBERTA GEOLOGICAL SURVEY

AER/AGS Open File Report 2019-06

A Risk-Based Methodology for Commingled Well Abandonment – Southeastern Alberta Gas Field Case Study

T.G. Lemay[1], A. Singh[1], K. Parks[2], A. Wiersma[3], D. Palombi[1], M. Babakhani[1], H. Berhane[1], B. Hathway[1], P. Vermeulen[3] and A. Marsman[3]

[1] Alberta Energy Regulator
Alberta Geological Survey
[2] Alberta Energy Regulator
[3] Deltares

August 2019

ISBN 978-1-4601-3993-6

If you use information from this publication in other publications or presentations, please acknowledge the AER/AGS. We recommend the following reference format:

Lemay, T.G., Singh, A., Parks, K., Wiersma, A., Palombi, D., Babakhani, M., Berhane, H., Hathway, B., Vermeulen, P. and Marsman, A. (2019): A risk-based methodology for commingled well abandonment – southeastern Alberta gas field case study; Alberta Energy Regulator / Alberta Geological Survey, AER/AGS Open File Report 2019-06, 76 p.

Author addresses:
K. Parks
Alberta Energy Regulator
Suite 1000, 250 – 5th Street SW
Calgary, AB T2P 0R4
Canada
403.297.8390
Email: Kevin.Parks@aer.ca

A. Wiersma, P. Vermeulen, A. Marsman
Deltares
Boussinesqweg 1
2629 HV Delft
P.O. Box 177
2600 MH Delft
Netherlands
+31 883357176
Email: ane.wiersma@deltares.nl

Published August 2019 by:
Alberta Energy Regulator
Alberta Geological Survey
4th Floor, Twin Atria Building
4999 – 98th Avenue
Edmonton, AB T6B 2X3
Canada

Tel: 780.638.4491
Fax: 780.422.1459
Email: AGS-Info@aer.ca
Website: www.ags.aer.ca

Contents

Tables

Figures

Acknowledgements

We thank the following people for their contributions to this report:

- Brian Smerdon (AGS) for his scientific advice and review as well as project leadership,
- Bas van der Grift (formerly with Deltares, now with KWR Water Cycle Research Institute) for his contributions in evaluating and constructing conceptual models of the petroleum systems as well as his leadership of the Deltares team,
- Geoff Zimmel (Deltares) for his contributions in the model conceptualization phase of the project,
- Kelsey MacCormack and Tyler Hauck (AGS) for their assistance in geological mapping and modelling of the gas-bearing and water-bearing units in the case study area,
- Nevenka Nakevska (AGS) for her contributions to the initial mapping of the water chemistry in the case study area,
- Jordan Brinsky (AGS) for contributing to an example of a hydrostratigraphic column,
- Rick Huff (AGS) and Jim Hendry (University of Saskatchewan) for their insights on groundwater modelling and methane concentrations in groundwater, respectively, and
- Mark White (Pacific Northwest National Laboratory) for his advice and support throughout the two-phase flow modelling work.

Abstract

Commingled gas production is the production of gas from more than one geologically distinct zone in an unsegregated manner within a single borehole. Tens of thousands of commingled wells are producing natural gas across Alberta, all of which will eventually require abandonment. The abandonment of wells is strictly enforced using very specific requirements. The intent of these requirements is to prevent any unwanted impacts on the environment through gas or fluid migration, and on the ability of resource production companies to produce their fair share of hydrocarbon resources. At the time of publication, the Alberta Energy Regulator (AER) is examining if it can allow variances from the abandonment requirements for commingled zones where there is demonstrated low risk. The cost savings of such variances could be substantial to Alberta's oil and gas industry, provided it can be shown that there is no intolerable increase in risk to the AER's outcomes. A risk-ranking screening tool was developed using the Alberta Table of Formations to qualitatively display the relative probability of risk from commingled well abandonments. This derivation uses knowledge of the regional geology and hydrogeology of the Alberta sedimentary basin to provide a stratigraphic zonation of groups and formations. If commingled zones or formations fall within green-coloured intervals, the risks to the AER's outcomes are relatively low. If commingled zones or formations fall within red-coloured intervals, the risks to the AER's outcomes will be relatively high. The orange-coloured intervals represent a moderate risk to the AER's outcomes. The risk rankings can guide a commingled well operator on how to apply for variances from abandonment requirements for certain geological units, and can be used by the regulator to guide the operator through the waiver request process. The different risk categories can be used to guide what is required to substantiate the application and satisfy the AER's requirements in achieving its regulatory outcomes. Although green intervals might have fewer requirements in assessing risks and red intervals will likely have more, this does not necessarily mean that commingled well abandonments in red intervals will not be allowed, but rather that additional supporting materials will have to be provided to support any applications for red-interval wells. To assess what a red interval assessment might look like, the AER decided to look at the potential for the abandonment of a large number of commingled gas wells within the Southeastern Alberta Order area (Commingling Order No. MU 7490). The AER and Alberta Geological Survey undertook a detailed geological, hydrogeological, and petrophysical mapping and modelling exercise to understand the extent and properties of the gas-bearing and water-bearing units in the Milk River Formation and the Alderson and Medicine Hat members in the southeastern Alberta gas field. The geological, petrophysical mapping, and modelling results were used for numerical modelling of single-phase groundwater flow and two-phase gas and groundwater flow modelling to understand the consequences of allowing widespread commingled well abandonments. In assessing the petroleum system and groundwater literature for the area, it was found that there are multiple plausible conceptual models of how the gas field petroleum system functions and the nature of regional groundwater flow. After compilation of the literature, five conceptual models were constructed. Each conceptual model was translated into a distinct groundwater flow model and two-phase flow model creating five equally plausible scenarios for a multimodelling exercise. In four of the five models, gas migration did not migrate into areas of potential concern during commingled well abandonment conditions, but for one of the models gas migration was observed in an area of concern. This suggests the need for further model validation achieved through additional data collection and environmental monitoring to ensure that the AER's outcomes are satisfied.

1 Commingled Wells and Pools in Alberta – A Risk-Based Path to Safe and Affordable Permanent Well Abandonment

Commingled gas production in Alberta is gas that is allowed under Alberta regulation to be produced from more than one geologically distinct zone or pool in an unsegregated manner within a single borehole. Commingled production improves the economic recovery of smaller or thinner natural gas deposits by removing the requirement for an additional dedicated energy well. As a result, fewer wells are needed, thereby reducing the surface footprint of gas production including a reduction in well pads, roads, pipelines, gathering facilities, etc. This further improves economics of marginal gas deposits while avoiding proliferation of surface works.

In 2018, the Alberta Energy Regulator (AER) estimated that there were over 18 000 distinct geological zones or pools in Alberta with commingled hydrocarbon production involving over 73 000 wells (Alberta Energy Regulator, pers. comm., 2018). Commingling practice has combined about 18 000 geological pools into about 4300 commingled entities. Administratively, commingled production is administered through one of over 600 commingling orders from the AER. The commingling orders specify zones or pools that can be commingled. Commingled production is also managed through special administrative orders wherein commingling is allowed for all zones and pools between specific geological markers rather than by specifying the actual zones and pools. This latter group of administrative constructs include the AER's Southeastern Alberta Order (Commingling Order No. MU 7490), Development Entity No. 1, and Development Entity No. 2 (Alberta Energy Regulator, 2019b).

When operators abandon commingled wells, the AER's expectation is that the commingled zones will be segregated in the borehole with a bridge plug capped with cement. The technical requirements are detailed in AER *Directive 020* (Alberta Energy Regulator, 2018). The intention of these requirements is to remove any risk to subsurface outcomes protected by the AER's defining legislation, rules, and other instruments. These outcomes include prevention of migration of H_2S from 'sour' zones into 'sweet' zones; prevention of wasting or sterilizing resources; prevention of impacts on other operators, including interfering with their rights to a fair opportunity to get their share of production; prevention of crossflow of fluids between otherwise naturally separated geological strata that would induce pressure, temperature, or chemical change; and protection of the environment from inadvertent loss of containments in the subsurface affecting groundwater quality. During production, all fluids are induced to flow into the wellbore thereby creating little to no risk of any of these impacts during the operational phase of well life. Thus it was reasoned that zonal re-segregation at abandonment of these wells is the best and least-risk approach to ensure there will be no impacts of this nature after production ceases.

At the time of publication, the AER is examining if it can allow variances from *Directive 020* requirements for zonal re-segregation of commingled zones where there is demonstrated low risk to outcomes. The cost savings of such variances could be substantial to Alberta's oil and gas industry, provided it can be shown that there is no unacceptable increase in risk to the AER's outcomes. Raucher (1983) created an economic framework to determine if money spent on groundwater protection provides real value in terms of subsurface or environmental protection, or would such money be better spent on other risks that yield more social and environmental benefits over the long term. It is this philosophy that the AER is open to, finding safe ways to allow industry to capture savings through allowing waivers to segregated abandonments that do not create equal or greater costs in terms of risk, thereby allowing industry to deploy their abandonment budgets in ways that better benefit the operators' and Alberta's outcomes in terms of cost-benefit trade-offs (e.g., https://www.aer.ca/regulating-development/project-closure/liability-management-programs-and-processes/area-based-closure).

The Alberta Geological Survey (AGS) of the AER has been asked by the AER to provide technical advice on risk assessment of commingled well abandonments based on the geology and hydrogeology of the Alberta Basin. The specifics were to:

- create a risk-based screening tool that can be used to quickly identify candidate pools or zones that would present low risk if commingled well abandonment were allowed through *Directive 020* variances;
- evaluate if the wells in the Southeastern Alberta Order area with commingled production from the Medicine Hat and Alderson members can be safely and permanently abandoned if left in a commingled state;
- based on the results from the two items above, identify and propose a risk-based approach that can be used to evaluate risks to groundwater and other shallow receptors in the event that commingled wells involve very shallow gas production.

The risk-based screening tool is described in Section 2 of this report. The assessment of commingled abandonments of Medicine Hat–Alderson gas wells in the Southeastern Alberta Order area is described in Sections 3, 4, 5, 6, and 7 of this report. Recommendations on how to implement a risk-based decision in southeastern Alberta, which can also be used in future cases, are found in Section 8.

2 A Screening Tool for Assessment of Subsurface Risk for Commingled Well and Pool Abandonments in Alberta

by D. Palombi and K. Parks

The risk-based screening tool developed for the assessment of commingled well abandonments combines Alberta's official Table of Formations from the AGS (Alberta Geological Survey, 2015) with an overlay of green, orange, and red, which are typically used on 'heat maps' in risk evaluations (Figure 1). Heat maps are a qualitative graphical device wherein relative probability of a risk event is cross-plotted against the relative scale of consequences of the event. Green indicates combinations of probability and consequence values where risk is low, orange or yellow indicates combinations of concern, and red indicates combinations where risk is high.

It is recommended that the utilization of the risk-based screening tool based on Figure 1 operates at the pool or zone rather than the well scale. A pool is defined in the AER regulation as a distinct subsurface accumulation of hydrocarbons. Pools have administrative names and their edges and thicknesses are mapped within the AER's Board Order System (Alberta Energy Regulator, 2019a). Zones are vertically distinct producing parts of pools connected to wells by perforations. For example, one commingled well producing from any two or more zones or pools means that the zones and pools are in pressure and fluid communication regardless of the state of other wells completed in the zones or pools. For this reason, working at the zone and pool level is more efficient than working at the well scale to assess commingled well abandonments. All wells connected to each zone and pool should be abandoned in the same way in order to consistently manage risks and also ensure equity between different operators.

It should be noted that this screening tool is not intended to address any wellbore-specific migration risks associated with damaged or compromised boreholes, including any damaged or compromised cement and casing.

The placement of colours on the Table of Formations in Figure 1 should be read like a heat map when assessing commingled zone or pool abandonments. If commingled zones or pools fall within green-coloured formations, the risks to outcomes are relatively low if wells, zones, and pools are left permanently unsegregated at abandonment. The risk is qualitatively and relatively ranked low because either the probability of an undesirable event is low or the consequences of the event will be low. If commingled zones or pools fall within red-coloured formations, the risks to outcomes will be relatively high either because the probability of an undesirable event is high or the consequences of the event will be high. The orange-coloured formations fall in between with respect to the probability of the event occurring as well as related consequences.

Note that risk events are cumulative as one goes through the colour ramp classification from green to red. The legend in Figure 1 provides the heat ranking and concerns for each type of interval. The risk rankings correlate to outcomes in the following way:

- single green intervals – local H_2S could migrate from sour to sweet zones; energy resources could be wasted or sterilized; there may be interference or offense to equity between nearby operators (laterally or vertically) during the expected duration of current or reasonably foreseeable energy development;
- multiple green intervals – local H_2S could migrate from sour to sweet zones; energy resources could be wasted or sterilized; there may be interference or offense to equity between nearby operators (laterally or vertically); there could be crossflow of formation fluids between hydrostratigraphic zones leading to undesirable physical, pressure, temperature, or chemical changes;
- orange intervals – local H_2S could migrate from sour to sweet zones; energy resources could be wasted or sterilized; there may be interference or offense to equity between nearby operators (laterally or vertically); there could be crossflow of formation fluids between hydrostratigraphic zones leading to undesirable physical, pressure, temperature, or chemical changes; crossflow could lead to contamination of deep industrial-quality (saline to brackish chemical composition) groundwater resources;
- red intervals – local H_2S could migrate from sour to sweet zones; energy resources could be wasted or sterilized; there may be interference or offense to equity between nearby operators (laterally or vertically); there could be crossflow of formation fluids between hydrostratigraphic zones leading to undesirable physical, pressure, temperature, or chemical changes; crossflow could lead to contamination of deep industrial-quality groundwater resources; crossflow could lead to contamination of nonsaline groundwater; natural gas could escape to surface causing public safety hazards.

In a scenario where an operator is considering the abandonment options for commingled wells, or the regulator is evaluating a request for commingled abandonment, there are many factors being considered. The following list describes some of these considerations and proposes how the screening tool could be applied in the process:

1) An operator makes a decision to apply for variances from AER *Directive 020* in the form of a waiver, such as leaving commingled wells in a commingled state at abandonment.
2) To prepare the request for a variance, the operator and regulator would refer to the commingling order and well-completion details to identify geological formations that have been produced in the well(s) without segregation in the borehole. Where odd, archaic, or unfamiliar geological names are used in the source of record, the AGS can be contacted to map these names to the modern Table of Formations.
3) The operator and regulator may use the heat map intervals to identify what elements of risk are of most concern for the operations in question. In the event that the commingled wells cross boundaries of different risk-associated colours, it is assumed the highest risk will be used for the evaluation.
4) The operator and regulator may use subsurface information and contextual information to evaluate the likelihood that any one of the identified concerns would actually be applicable to their circumstance.
5) The operator takes steps necessary to reduce the chance for undesirable risk that would occur in the event of commingled well abandonment, or reduce the degree of consequence to a level acceptable to the regulator.
6) The regulator accepts or denies the request for the *Directive 020* variance depending on the evidence as per standard AER operating procedures.

The colours and their boundaries are informed by knowledge of hydrostratigraphy, regional hydrogeology, and petroleum systems of Alberta. This is explained in more detail below including the knowledge used to define potential consequences.

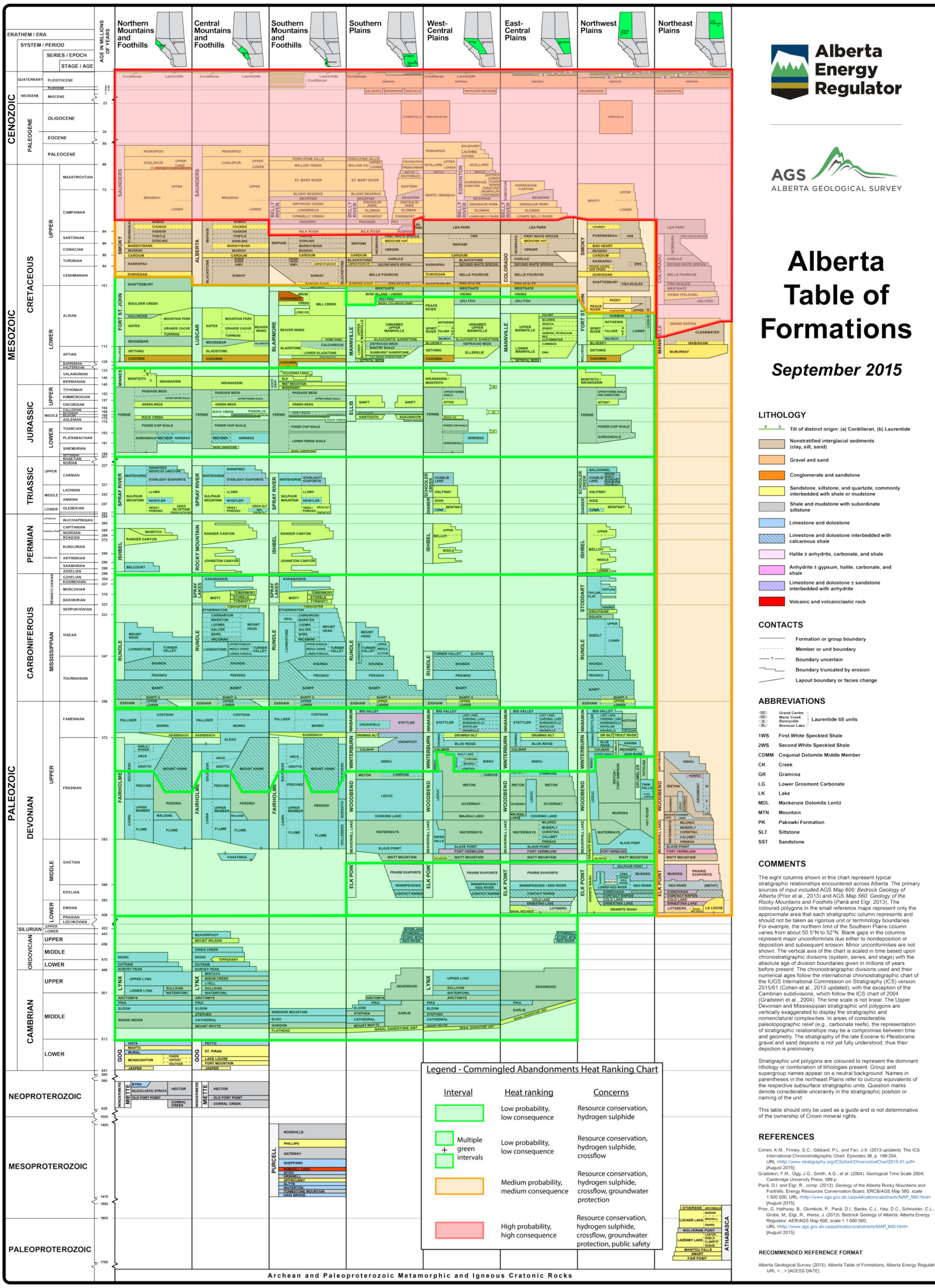

Figure 1. Alberta Table of Formations (modified from Alberta Geological Survey, 2015) denoted with heat rankings associated to possible cumulative risks with commingled well abandonments. This derivation forms the risk-based screening tool for identifying candidate pools and/or zones for low-risk commingled well abandonments.

Figure 1 is based on Alberta's Table of Formations (ToF) published by the AER in September 2015 (Alberta Geological Survey, 2015). The ToF was selected as the foundation for the screening tool because the AER's geological administrative systems use these formation names as part of well and pool identifiers, making it important to be able to cross-reference risk levels to geological formation names for the purposes of assessing risks associated with commingled well abandonments.

The ToF shows the named geological formations in Alberta arranged by age, with the oldest on the bottom and youngest at the top, with the names arranged by geographic area of use. A geological formation is a formal rock unit that is distinct and identifiable by its age, characteristics, and from what lies below and above it. The ToF presents the geological age in a nonlinear scale along the vertical axis and therefore breaks or white spaces exist that indicate geological time intervals where rocks were not deposited or are missing due to later erosion. The reason for the different names for rock formations of the same age and type in different geographic areas of Alberta is partly an artifact of history and partly a recognition of the complicated and variable nature of rock formations across a province as big as Alberta. Figure 2 shows what the ToF might look like if the time breaks were removed and the columns assigned to the appropriate geographic zones of Alberta (still with no true vertical scale).

The formations in the ToF have different rock and hydraulic properties. Alberta's ToF uses standard geological colours to represent the dominant lithology, or rock type, of each formation, e.g., sandstone is yellow, halite (i.e., salt) is pink, and so on. Formations can often be broken down into finer units of different dominant lithologies or other properties called members, and these can be separated further to the bed or lamination scale. The naming convention for formations and members that Alberta follows is the North American Stratigraphic Code (North American Commission on Stratigraphic Nomenclature, 2005). The Stratigraphic Code recognizes that properties in addition to lithology and age can be useful ways to subdivide rock units. One way to subdivide Alberta's rocks is by properties relevant to the movement of the fluids that saturate the pore and fracture spaces. Fluids like groundwater and hydrocarbons will move through rock formations over geological time. They move in response to driving forces like gravity, buoyancy, chemical gradients, and rock compression or dilation. The rate of movement is controlled by the permeability of the rock, a measure of pore or fracture interconnectedness and pore-scale resistance to flow, and by the viscosity and density of the fluid (rock and fluid properties together are referred to as the hydraulic conductivity of a unit).

If one examines the layers of rock underground, the subsurface can be divided in terms of rocks that permit groundwater motion relatively easily and those that impede the motion of groundwater. The geometrical architecture within a rock framework based on such hydraulic properties is called the hydrostratigraphy. The subdivisions between and within the green, orange, and red intervals on Figure 1 are based on the hydrostratigraphy of the Alberta Basin (e.g., Bachu, 1999).

The simplest hydrostratigraphic divisions that are used in Alberta hydrostratigraphy are the categories of aquifer, aquitard, and aquiclude. An aquifer is defined as a body or layer of rock that can transmit groundwater flow easily under natural conditions. An aquitard is a body or layer of rock that transmits groundwater flow very slowly under natural conditions. An aquiclude is a body or layer of rock that does not transmit groundwater flow at all or very minimally. Lithology, hydraulic conductivity, heterogeneity, and scale (spatial and temporal) all affect the classification of a rock unit as an aquifer, aquitard, or aquiclude. Scale is important because at a regional scale a rock body can act as an aquifer, but at a local scale parts of that rock body may act like an aquitard due to geological heterogeneity. The hydrostratigraphy of Alberta has been defined on the basis of formation lithology and then by hydraulic evidence as to its long-term behaviour with respect to flow and chemical composition of groundwater.

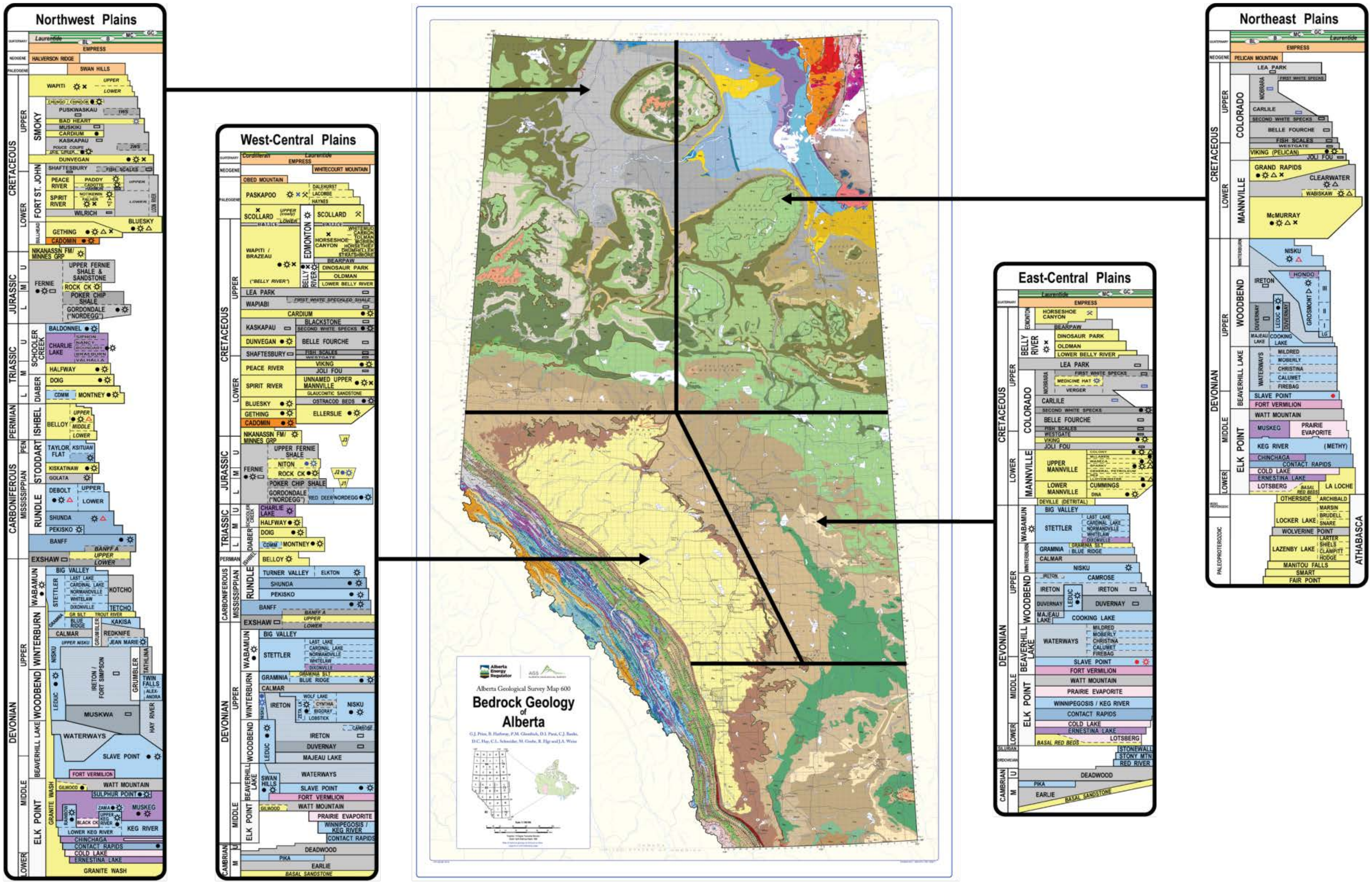

Note: There is no vertical scale on the Table of Formations columns, so the thicknesses do not reflect true vertical thickness. The Southern Plains column is not included on the figure since it will be discussed in a later section of the report.

Figure 2. A stacked representation of the Alberta Table of Formations (ToF; from Alberta Geological Survey, 2015) by geographic area of Alberta (base map from Prior et al., 2013). There is no vertical scale on the ToF columns, so the thicknesses do not reflect true vertical thicknesses.

Figure 3 provides an example of how lithology from the ToF was translated into hydrostratigraphic units. Across their depositional extent, the Bow Island, Viking, and Peace River formations can be grouped to form a mixed aquifer/aquitard system (Peace River / Viking / Bow Island hydrostratigraphic unit), which shows sufficient lateral continuity to generally be in hydraulic communication at that spatial scale. It is not always a simple correlation of lithologies, like sandstones to aquifers or shales to aquitards. For example, the sandstone of the Horseshoe Canyon Formation in central Alberta is regionally an aquifer relative to the Bearpaw Formation shale below it, but locally is often an aquitard due to plugging of sandstone pores with bentonite clay. Likewise, the Clearwater Formation in northeastern Alberta is a shale that is regionally regarded as an aquitard, but locally can be used for water supply or waste-water injection like an aquifer.

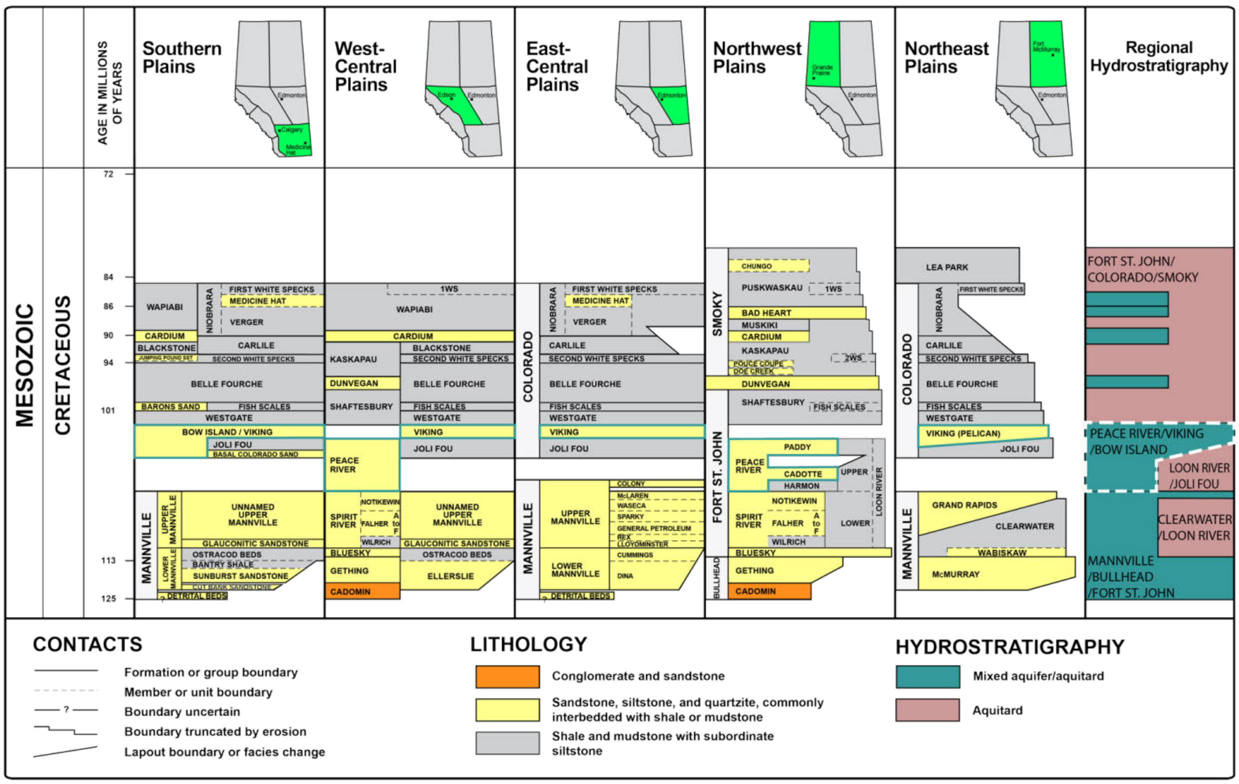

Figure 3. Example translation of the Alberta Table of Formations (Alberta Geological Survey, 2015) stratigraphic formations into hydrostratigraphic units.

The hydrostratigraphy of Alberta was used to demarcate the risk identification on Figure 1 with the following logic.

Single green intervals: These green intervals contain regional hydrostratigraphic aquifers consisting of one or more geological formations. Though the geological formations vary in lithology, age, thickness, permeability, etc., their bulk properties are dominated by aquifer-like properties and they are sufficiently well interconnected laterally and vertically that they behave like single hydraulic units over the long-term with respect to the hydrogeology of the Alberta subsurface at the regional scale. Predevelopment groundwater chemistry, hydraulic heads, and pore pressures, and even petroleum types tend to be very similar within these units.

From a risk management point of view on commingled well abandonments, there is little risk of causing significant regional hydraulic disturbance in the single green intervals because the units are hydraulically connected on the regional spatial scale over geological time. The largest risks associated with leaving unsegregated or commingled zones lie in their impact to production of residual or future adjacent hydrocarbons and other uses of rock formations or pore space. This is why a proponent of commingled well abandonments at this scale should focus on these kind of risks: H_2S migration between zones with different original H_2S content, particularly if one is naturally H_2S free or sweet whereas the other has naturally occurring H_2S and is sour; impacts that might sterilize hydrocarbon recovery now or in the future; or impacts that may interfere with another operator's opportunity to get their fair share of production from their mineral leases or freehold rights.

Multiple green intervals: The green interval on Figure 1 is divided by solid green lines. These lines correspond to regional aquitards or aquicludes that separate regional aquifers. Because the aquitards do not transmit groundwater or other fluids easily, the pressure, flow, and geochemical regimes inside the aquifers on either side may have evolved to different states over geological time. Allowing a permanent connection via commingled well abandonments across these aquifers may create a pathway that will drive fluid motion, in response to unequal forces, chemistry, pressures, etc., between aquifers naturally isolated or separated by the aquitards. The migration of fluids in the wellbores in response to these differences in the zones outside the wellbore will generate crossflow via the wellbore. The impacts of crossflow may be negligible or significant and must be assessed on a case-by-case basis at the pool scale by a hydrogeologist with knowledge of Alberta regional hydrostratigraphy, groundwater flow, and hydrogeochemistry.

Orange intervals: The orange and red intervals in Figure 1 are found in the shallower formations of the ToF and in the formations of the northeast plains. In the case of the orange-coloured formations, the additional risk comes from possible contamination of useable but still low quality groundwater from crossflow. The units in orange are shallow enough to be reached by industrial water–source wells and may have local-scale aquifers even though regionally they act as aquitards in terms of hydrostratigraphy. The northeast plains area has deeper formations in the orange interval because they occur in shallower geological settings in comparison to the rest of the province due to the structural downward dip of most formations to the south and west.

Red intervals: In the case of the red interval, there are more risks to consider because the red-coloured formations are close to or exposed at the land surface and lie above the Base of Groundwater Protection (Lemay, 2009). They contain local and regional aquifers that offer nonsaline groundwater to domestic, irrigation, industrial, and municipal users. They supply baseflow to surface waterbodies and support groundwater-dependent ecosystems. Crossflow of deep formation waters or petroleum fluids from commingled wells could compromise these aquifers. Furthermore, there are not many regional aquitards in these formations, which overlie the Cretaceous Colorado Group shale units and equivalents in Alberta, so stray or fugitive gas, oil, or formation water migrate in, alongside and away from, as well as within boreholes. Such fugitive emissions and releases could reach shallow aquifers or surface infrastructure and pose a public safety or environmental hazard if allowed to collect in a confined space.

Although the sections above present a method of evaluating potential risks associated with specific commingled units, they do not outline a methodology for evaluating the actual risks associated with allowing widespread commingled well abandonments. The following sections present an example of how the risk assessment process above can be followed by a technical assessment phase and a recommendations phase on how to proceed. The assessment phase provides the critical inputs necessary for a more detailed risk analysis for scenarios where widespread commingled well abandonments could be allowed. The recommendations phase puts together ideas on an appropriate decision on how to proceed and what decision validation processes could be implemented. The specific example will be for the commingled gas wells in the Alderson and Medicine Hat members in the southeastern Alberta gas field, the latter member of which is within a red interval using the heat map screening tool.

3 Introduction to the Case Study

In 1883, a Canadian Pacific Railway crew drilling for water in southeastern Alberta encountered natural gas near what came to be known as the town of Alderson (Alberta Culture and Tourism, 2019). Little did those drillers know that they discovered what would become one of the largest natural gas accumulations in North America, the southeastern Alberta gas field.

The area of interest for this case study extends from the Canada–United States border in the south to Township 32 in the north, and from the Alberta–Saskatchewan border in the east to the 5th Meridian in the west (Figure 4). The case study area is slightly larger than the AER's Southeastern Alberta Order area (Commingling Order No. MU 7490), which specifies well completion requirements for gas wells within its boundaries (Energy Resources Conservation Board, 2010). The southeastern Alberta gas field is found within the boundaries of the commingling order. With the exception of the cities of Calgary, Medicine Hat, and Lethbridge, the region is home to a largely rural population, many of whom depend on groundwater resources for their domestic, agricultural, and industrial needs. There are numerous previous studies of the geology of the gas field and of the primary aquifer in the region, the Milk River aquifer. The Milk River aquifer is a transboundary aquifer extending into Saskatchewan as well as into Montana in the United States. These previous studies on the geology and hydrogeology have shown that geological formations that contain gas within the gas field become water saturated farther south. These same water-saturated formations can directly overlie units of the Milk River aquifer that residents and industries of the area access for groundwater. This has raised a number of questions regarding how well connected the water-bearing and gas-bearing units are stratigraphically, lithologically, and hydraulically, and how the petroleum and groundwater systems interact.

Many hypotheses have been proposed on why and how the natural gas system developed and what its relationship is to water-bearing units to the south; however, no clear consensus exists to date.

As of December 2016, more than 40 000 wells had been drilled in the field to produce natural gas (assessment completed based on data extract from Accumap™ [IHS Markit, 2018]). Natural gas commodity prices have decreased substantially over the last decade with these low prices likely to persist into the foreseeable future. In response to economic and reservoir production trends, many of the gas wells in the field are nearing the end of their economic life. The companies operating wells in this field are preparing for, or will be faced with, the need to abandon a large numbers of gas wells.

Abandonment regulations in Alberta place environmental and societal protection at the forefront of decision-making. These decisions integrate information on the natural system to understand the current state of the environment and include assessments of the geological and hydrogeological setting of the area in question. The AER/AGS undertook a case study of the area (evaluated as potential high risk in the screening tool) to examine the potential issues that might arise as it regulates the eventual abandonment of not just a single well, but many hundreds or thousands of wells at around the same time. To accomplish this, the AER/AGS completed a geological and hydrogeological mapping, characterization, and modelling exercise. This report 1) describes the geology of the case study area; 2) discusses the properties of the geological units and results of property modelling in three dimensions (3D); 3) provides an overview of the natural gas and water resource systems; 4) summarizes natural gas and water resource development in the southeastern Alberta gas field; and 5) presents simulations of groundwater flow and discusses the mechanics of two-phase flow within gas-bearing units.

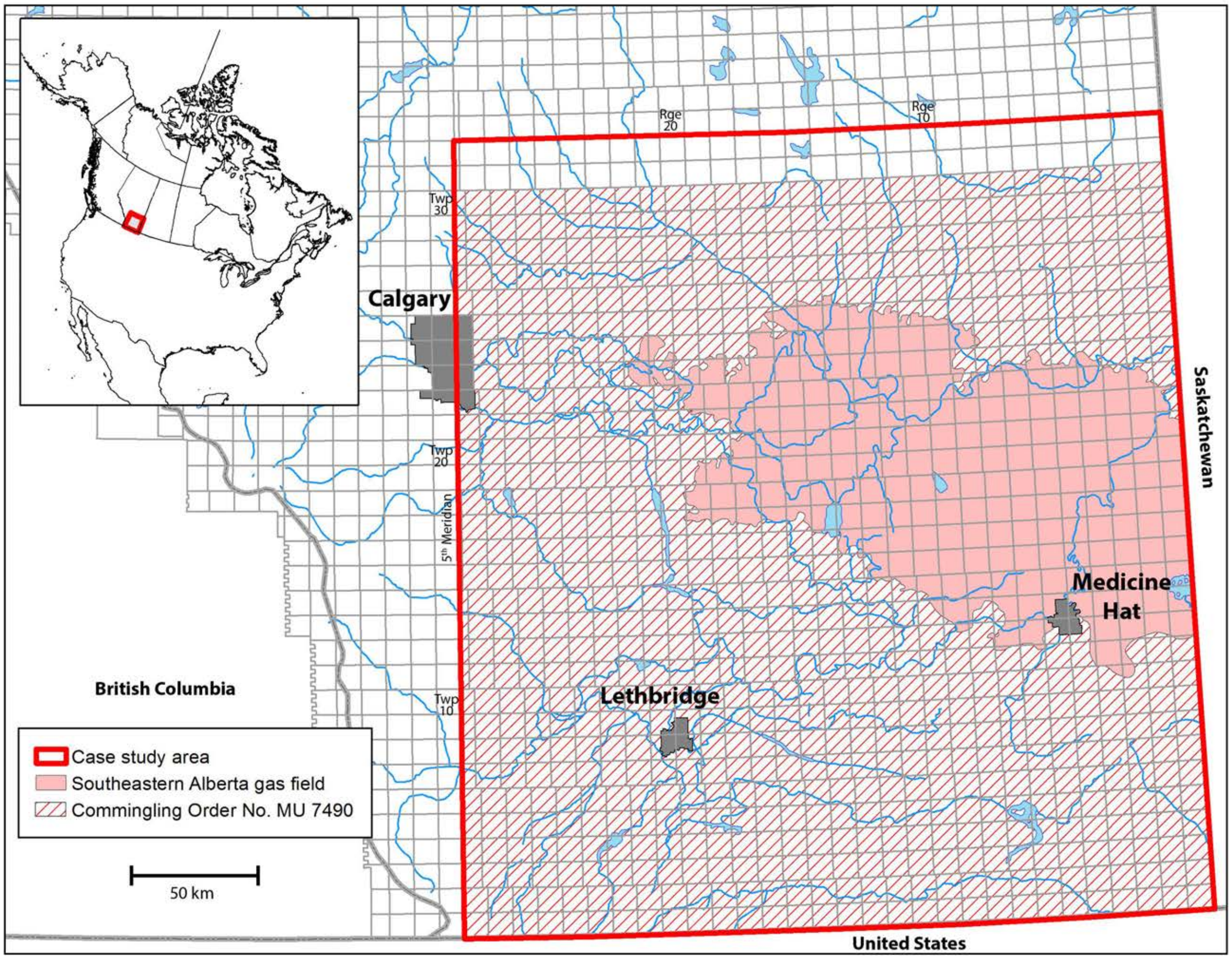

Figure 4. Map of the case study area, southeastern Alberta.

4 Geological Setting and Methodology

The geological units of interest in the case study area include all the strata in bedrock extending down from top of the bedrock surface to the base of the Cretaceous (Turonian) Niobrara Formation (Figure 5). All of the bedrock units in the case study area were deposited in a foreland basin setting, and are Cretaceous in age, with the exception of the upper part of the Willow Creek Formation and the Porcupine Hills Formation, which are Paleogene in age. A number of depositional models have been proposed to explain how the sediments in these different formations were deposited. These include eustatic sea-level changes (Williams and Stelk, 1975; Kauffman, 1977); regional tilting (Mitrovica et al., 1989); and lowstand or forced regression shoreface models (Plint et al., 1986; Plint, 1988; Walker and Plint, 1992; O'Connell, 2014).

Yang and Miall (2008) and Yang (2011) proposed that the mid-Cretaceous successions in the Cordilleran foreland basin were deposited as part of tectonically driven cycles made up of two components: proximal, continental-dominated strata captured in a foreland trough paralleling a rising mountain belt coupled with distal marine-dominated strata deposited in a relatively broad, shallow, and underfilled basin separated from the foreland trough by a basement high, termed the forebulge. Such examples of contrasting depositional styles help explain the deposition of 1) strata deposited in underfilled basins, and 2) strata deposited in overfilled basins. They explain how elements as different as widespread fine-grained clastic units, high frequency coarsening-upwards cycles, and erosive-based sandstones enclosed in mudstone could be contemporaneously deposited in sedimentary basins near rising mountain fronts. The geology of southern Alberta may ultimately be best understood in this kind of theoretical paradigm under such conditions.

The spatial relationships between the bedrock units are highlighted in Figures 6 and 7. The oldest geological unit of interest for this case study is the Niobrara Formation of the Colorado Group. Nielsen et al. (2003) described this formation as a being made up of marine shale, siltstone, and fine-grained sandstone with layers of chert pebbles. They subdivided it into three members. From oldest to youngest, they are the noncalcareous shaly Verger Member, the sand-rich Medicine Hat Member, and calcareous shaly First White Specks Member. The Medicine Hat Member consists of a series of coarsening-upwards units consisting of interbedded mudstone, siltstone, and sandstone. Abundant natural gas resources are found in the Medicine Hat Member.

Unconformably overlying the Niobrara Formation in the southern portion of the case study area is the Milk River Formation. It is described as being deposited in a transitional marine to continental environment (Meijer Dress and Mhyr, 1981; Leckie et al., 1994; O'Connell, 2003). O'Connell (2014) describes the members of the Milk River Formation as forming a succession of shallowing-upwards facies from offshore sandstones and shales to shoreface and tidally formed sandstones, as well as estuarine deposits, and heterolithic coal-bearing deposits. Tovell (1956) divided it into three members, the lowermost interbedded sandstone and shale of the Telegraph Creek Member, the middle fine- to medium-grained sandstone of the Virgelle Member, and the uppermost interbedded shale, sandstone, and coal of the Deadhorse Coulee Member.

The Alderson Member of the Lea Park Formation unconformably overlies the Niobrara Formation in the northern part of the case study area, and onlaps the Milk River Formation farther south. Descriptions of the unconformity at the base of the Alderson Member are provided by Ridgley (2000) and O'Connell et al. (1999). In the south, this regional unconformity between the Milk River Formation and Alderson Member might not be as extensive as previously thought. Recent magnetostratigraphic assessments of core from the Milk River Formation and Alderson Member (Anwar et al., 2017; Mumpy and Catuneanu, 2019) have shown that there is a time equivalence between the Deadhorse Coulee Member of the Milk River Formation and the lower part of the Alderson Member, indicating a possible genetic link between the two units. Mumpy and Catuneanu (2019) place the southern extension of the basal Alderson unconformity within the Deadhorse Coulee Member, which is supported by the recent geological mapping of this case study. In addition to the presence of a basal unconformity, Ridgley (2000) and O'Connell (2003) have mapped additional bounding surfaces within the Alderson Member. Ridgley (2000) has mapped the presence of an unconformity dividing the Alderson Member into two units. O'Connell (2003) has mapped a transgressive surface of erosion (TSE) and a sequence boundary (SB), dividing the Alderson Member into three units. Recent mapping by the AGS shows the presence of two intra-Alderson unconformities, which divide the member into the lowermost Alderson C, middle Alderson B, and uppermost Alderson A. These three units are broadly equivalent to O'Connell's (2003) lower Alderson, lower upper Alderson, and upper upper Alderson divisions. In the northern portion of the case study area, the unconformities can no longer be reliably mapped and the Alderson Member is mapped as an undifferentiated unit. The Alderson Member is described as being marine in origin and heterolithic consisting generally of very fine grained muddy sandstones, siltstones, and shales (O'Connell, 2014). Like the Medicine Hat Member, the Alderson Member is also an important gas reservoir in the case study area. Gas in the Alderson Member is found in laminated muddy, low-permeability sandstones and siltstones (O'Connell, 2014).

Overlying the Milk River Formation and Alderson Member is the Pakowki Formation. It is a marine shale that Glass (1990) describes as being composed of mudstone with some occurrences of siltstone to very fine grained sandstone.

The Pakowki Formation grades upwards into the marine to continental sandstone formations of the Belly River Group, which are from oldest to youngest the Foremost Formation, the Oldman Formation, and the Dinosaur Park Formation. In places in the northeastern part of the case study area, the Belly River Group may be capped by erosional remnants of the marine shales of the Bearpaw Formation. Towards the west and north in the case study area, younger bedrock units are encountered including the Blood Reserve, Eastend, St. Mary River, Willow Creek, and the Porcupine Hills formations.

The top of bedrock in the case study area is overlain by unconsolidated sediment. Paleogene and Neogene sediments are found on the top of the Cypress Hills, whereas successively younger sediments are found at lower elevations, reflecting processes of widespread subaerial erosion and re-deposition of sediments over the last 45 million years. There are significant channels carved in the bedrock that are preglacial, subglacial, postglacial, and modern in origin (Figure 8). The channels are often lined with preglacial sand and gravel and/or glaciofluvial and glaciolacustrine sediments at their base because they acted as loci of meltwater collection and sediment deposition during glacial retreats of the Pleistocene (Andriashek, 2003). Glacial sediments infilling the valleys are composed of coarse-grained glaciofluvial or fine-grained glacial lacustrine or heterolithic, undifferentiated till and were deposited as part of Laurentide or Cordilleran glacial events.

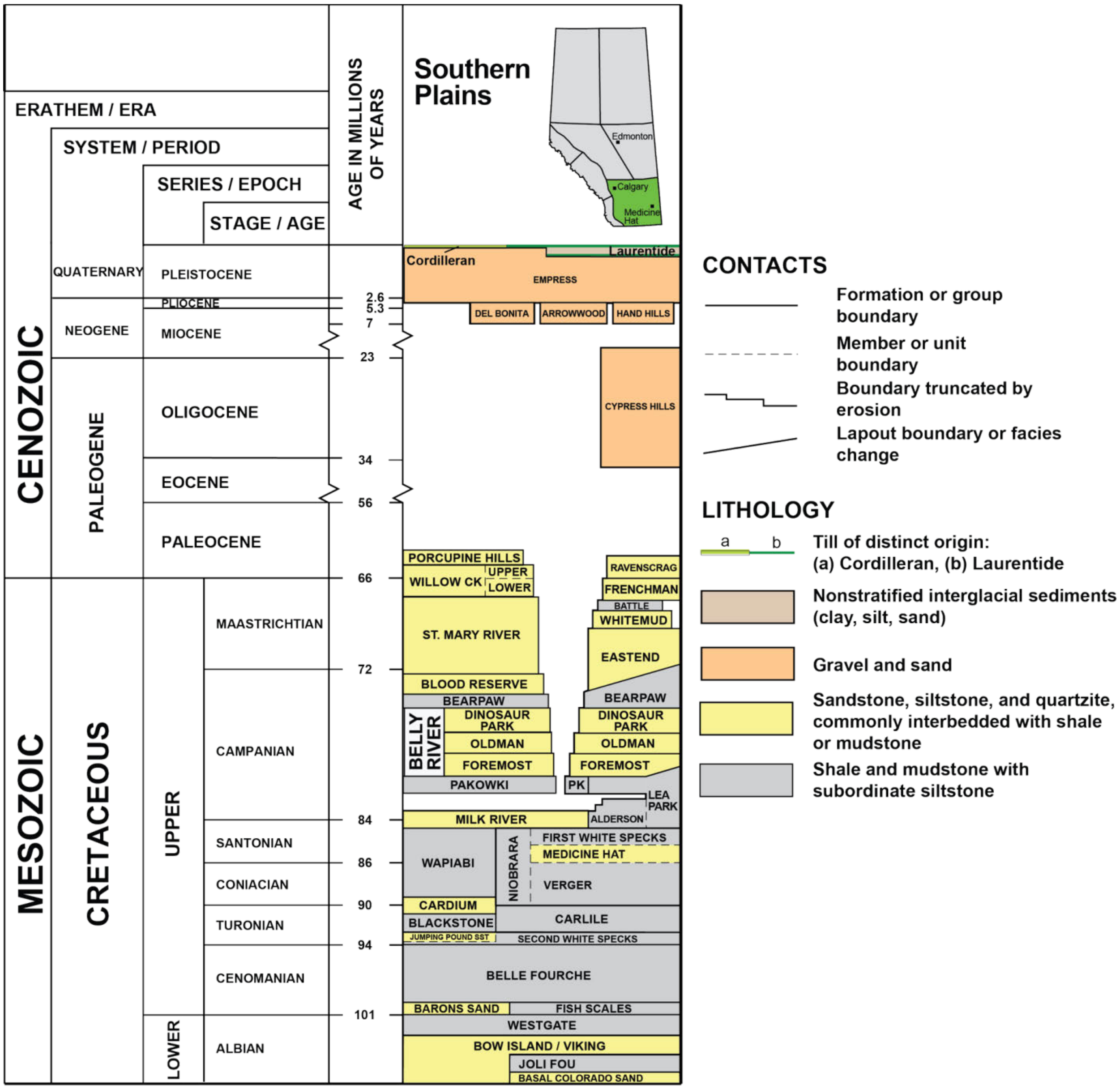

Figure 5. Stratigraphic chart for the case study area (modified after Alberta Geological Survey, 2015).

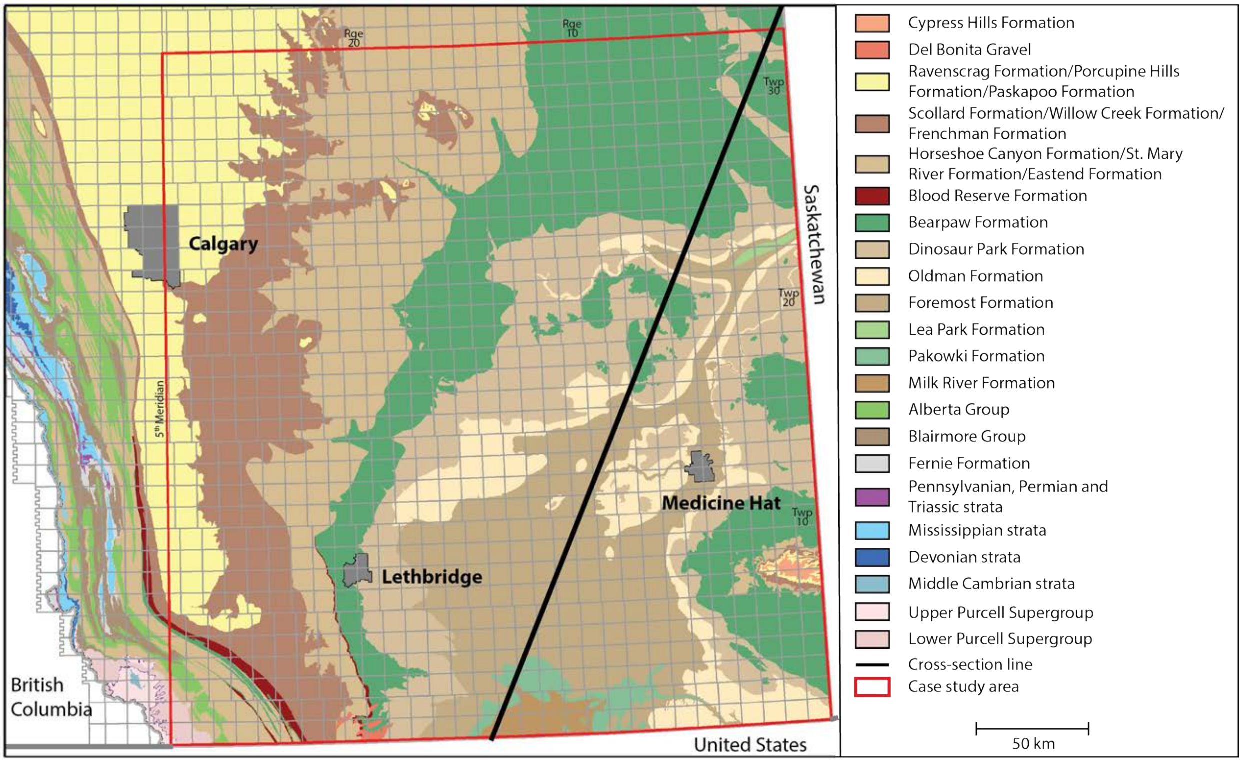

Figure 6. Bedrock geology map of case study area (modified from Prior et al., 2013).

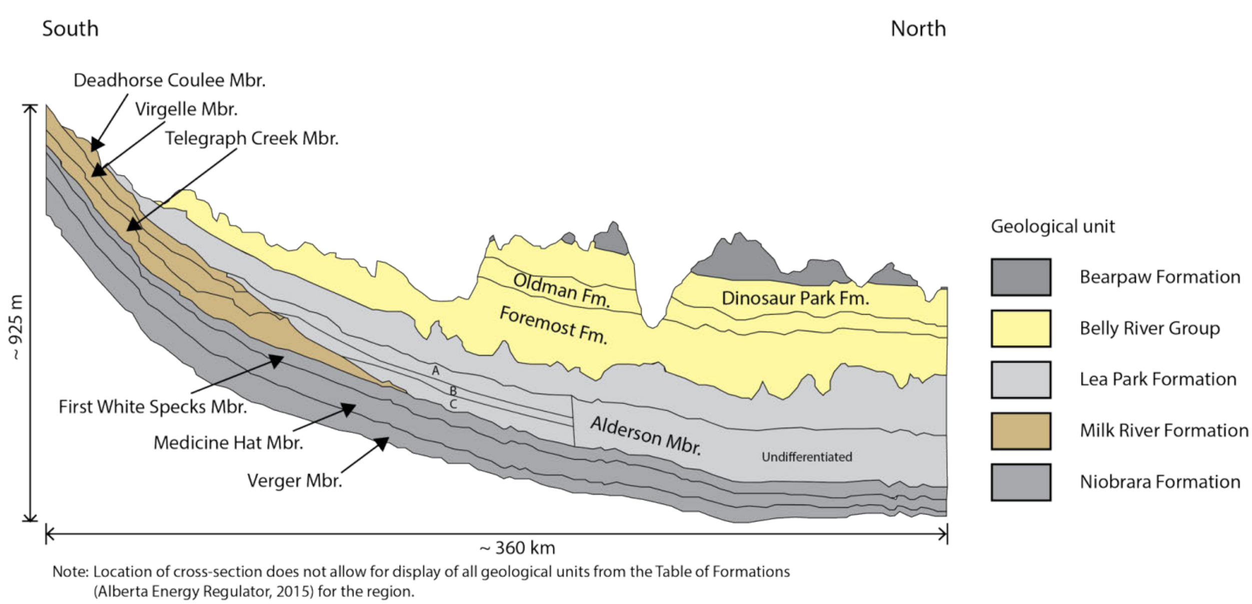

Figure 7. Bedrock cross-section (see Figure 6 for location) in case study area.

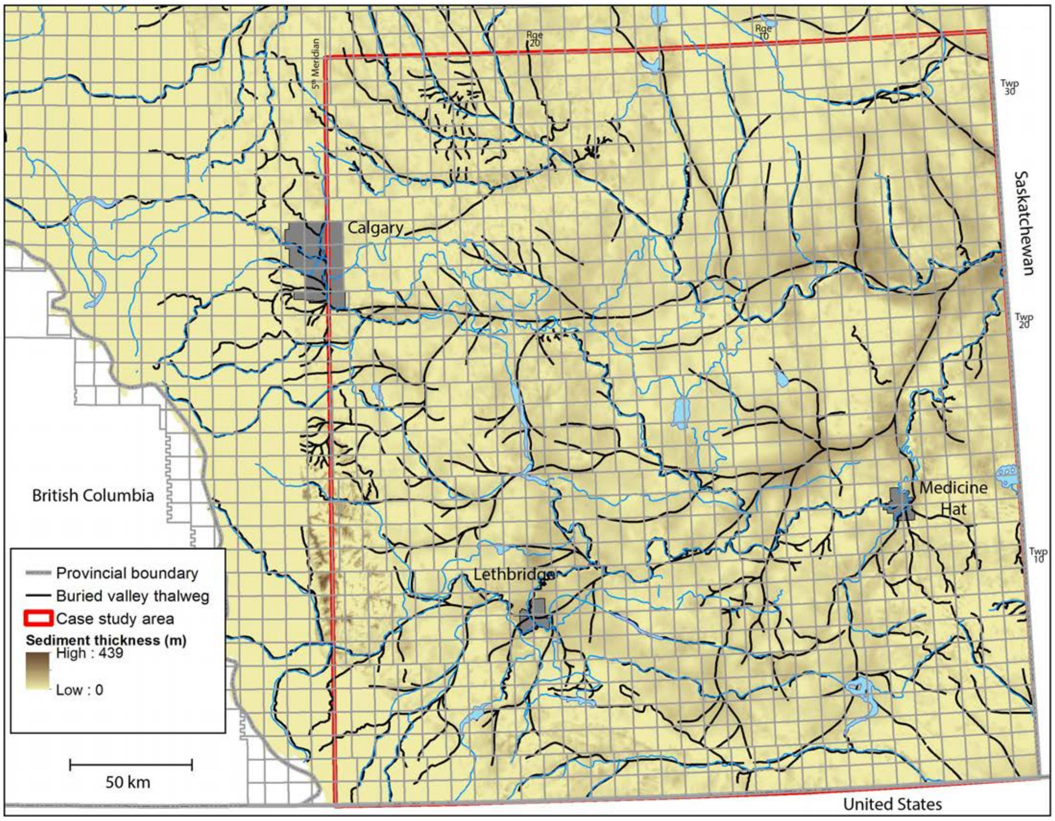

Figure 8. Sediment thickness map and location of buried bedrock valleys (modified from Atkinson and Lyster, 2012, and Andriashek, 2018).

4.1 Log Analysis

Petrophysical data analysis enabled an understanding of the rock properties (including porosity and permeability) to evaluate gas-water migration within the southeastern Alberta gas field and potentially the regional Milk River aquifer. The analysis also provided geological properties required for the groundwater modelling and analysis, including grain density, porosity, water saturation, and permeability. For the analysis, a two-step approach was implemented; firstly, data quality culling and secondly, borehole data interpretation within the respective stratigraphic formations.

From the available dataset of 19 000 wells with stratigraphic picks, 5300 wells with Milk River Formation, Alderson Member, and Lower Cretaceous picks and digital curves (two nuclear magnetic resonance [NMR] logs) were selected for the analysis. Figure 9 shows well data distribution for petrophysical analysis, which includes 5300 wells with logs, 50 wells with routine core analysis (RCA), and two wells with X-ray diffraction (XRD) analysis. The well logs were used to analyze gamma ray (GR), bulk density (RHOB), deep resistivity (RESD), neutron porosity (PHIN), sonic (DT) and when available, spectral GR and elemental curves. Prizm™ (LMKR, 2015) was used to normalize the well logs and to calibrate the results where available.

For the permeabilities of modelled units, a relationship between permeability and porosity was established using the core data. Figure 10 shows the cross-plot of core permeability with core porosity used for the porosity-permeability relation during the groundwater modelling and analysis.

To estimate uncertainty in the porosity-permeability relation, various permeability curves were generated using the different porosities for comparison and statistical analysis for groundwater modelling. Figure 11 shows one of the two available NMR logs along with different porosity and permeability estimates. These logs were used to estimate the parameter values for the multiphase (gas-water) numerical modelling.

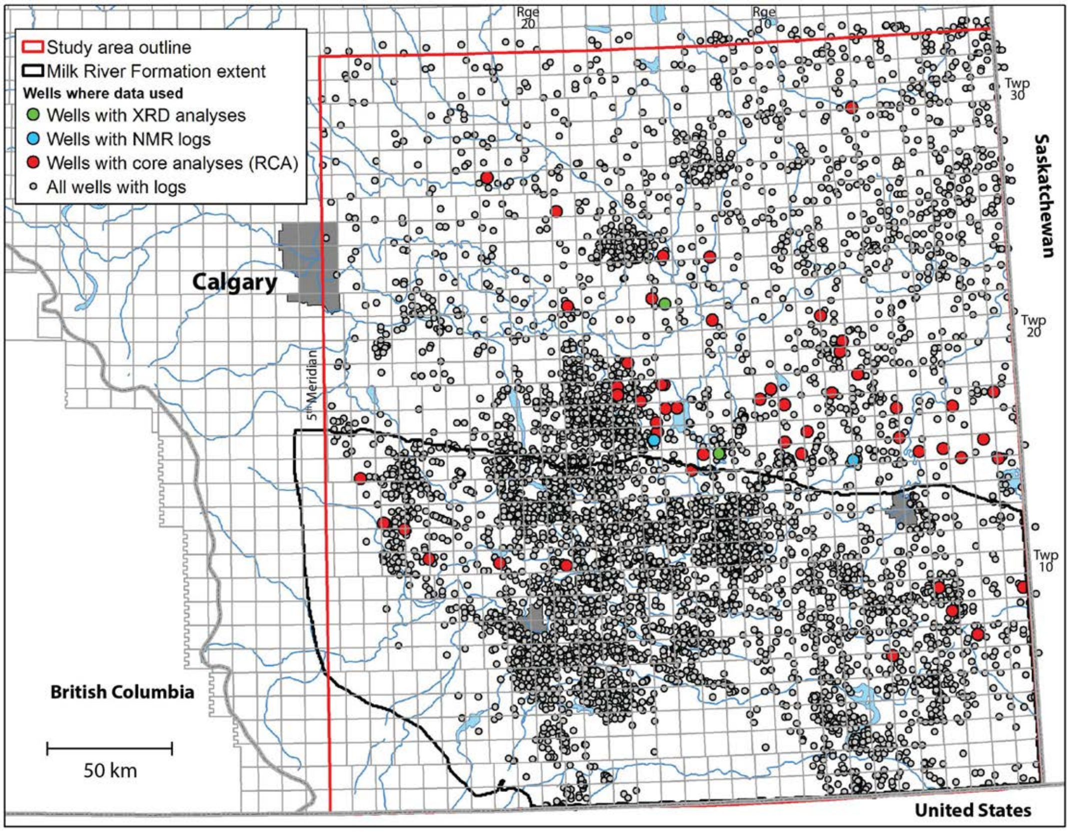

Figure 9. Map of wells used in petrophysical analysis for the case study area. Abbreviations: NMR, nuclear magnetic resonance; RCA, routine core analysis; XRD, X-ray diffraction.

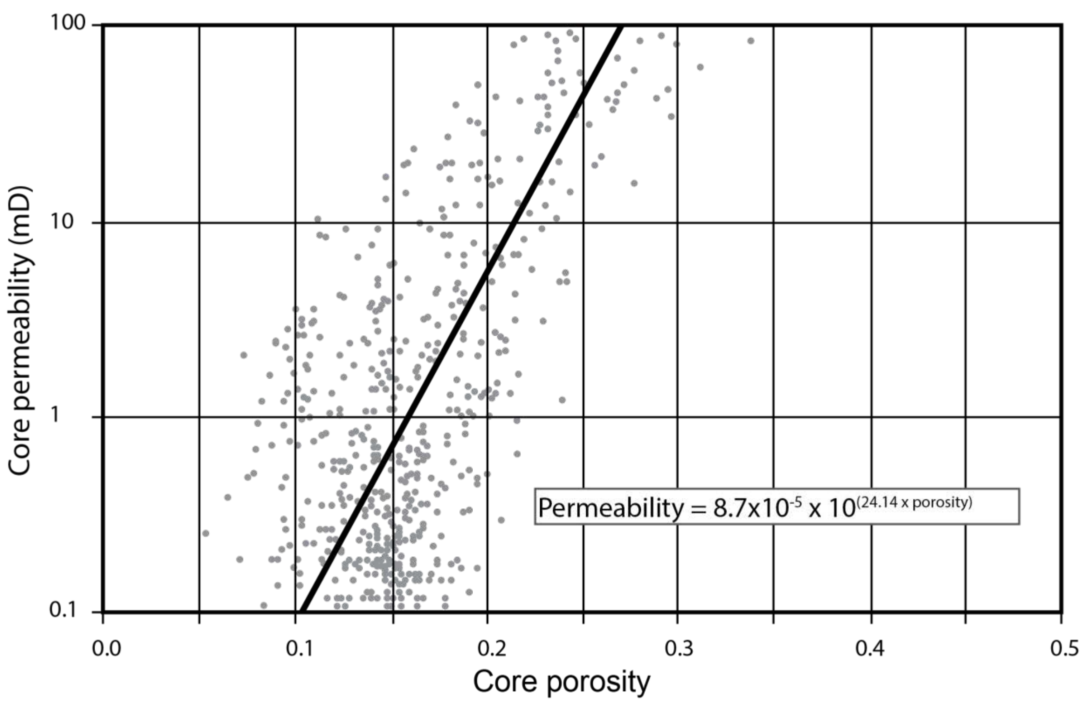

Figure 10. Cross-plot of core porosity versus core permeability used to establish a porosity-permeability relation. Abbreviation: mD, millidarcy.

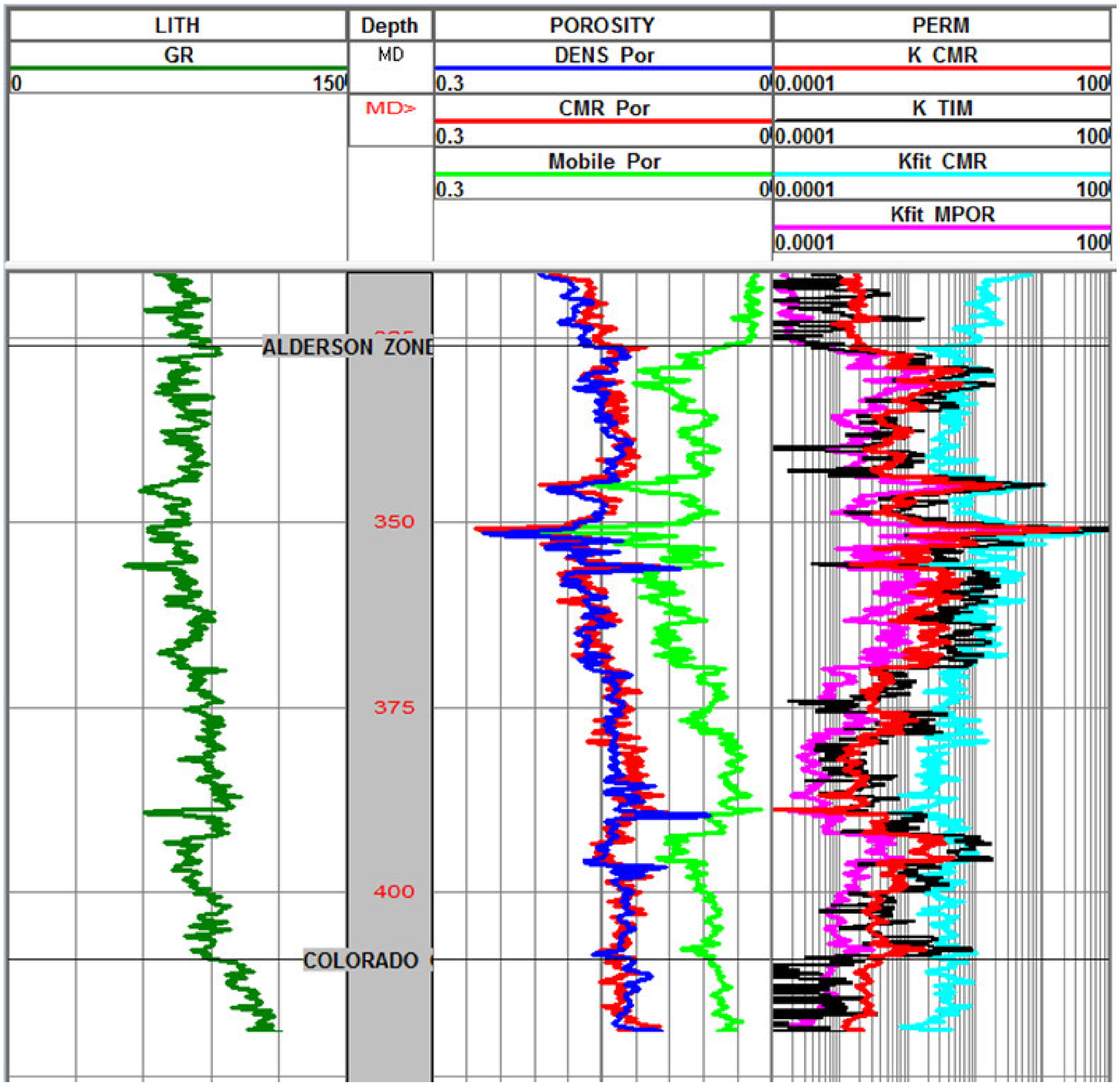

Figure 11. Example of nuclear magnetic resonance log along with various porosity and permeability estimates. Abbreviations: Colorado, top of Colorado Group; CMR, combinable magnetic resonance; DENS, density; GR, gamma ray; K, permeability; Kfit, permeability from cross-plot; LITH, lithology column; MD, measured depth in metres; MPOR, mobile porosity; PERM, permeability column; Por, porosity; TIM, Timur (1968).

4.2 Property Modelling

A 3D property model was created to reveal the internal structure of the Milk River Formation and Alderson Member including the properties within them. The property model was created using Petrel 2015 (Schlumberger Limited, 2015) software and exported to nonproprietary formats for use in numerical modelling. The modelled properties include 1) total porosity; 2) permeability; 3) water saturation; and 4) lithology (V_{sh} [volume of shale]). The geological framework for the Milk River Formation and the Alderson Member property model was mapped using 13 major stratigraphic units between the top of the Milk River 'shoulder' (a distinct geophysical log response that separates the Milk River Formation from the overlying Pakowki Formation [Glombick and Mumpy, 2014]) to the top of the Niobrara Formation (bottom of the Milk River Formation; Figure 12).

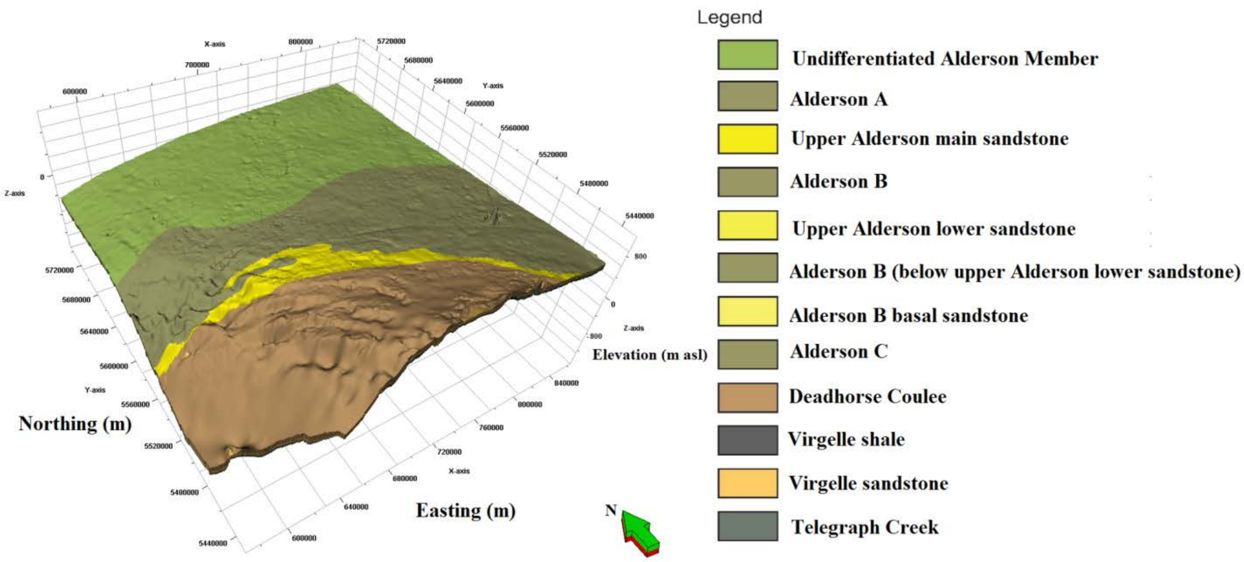

Figure 12. Geological model of the Milk River Formation and Alderson Member stratigraphic units.

The model was subdivided into 3D geocellular grids to create the property model. Each geocellular grid was then populated with four petrophysical properties (i.e., total porosity, permeability, water saturation, and lithology) using the geostatistical methods as described in Appendix 1.

Figures 13 and 14 present the averaged total porosity and water saturation properties for the Milk River Formation and Alderson Member units along with the respective property model cross-sections. The cross-sections demonstrate relatively higher porosity and water saturations near the Canada–United States border with a decreasing trend towards the north.

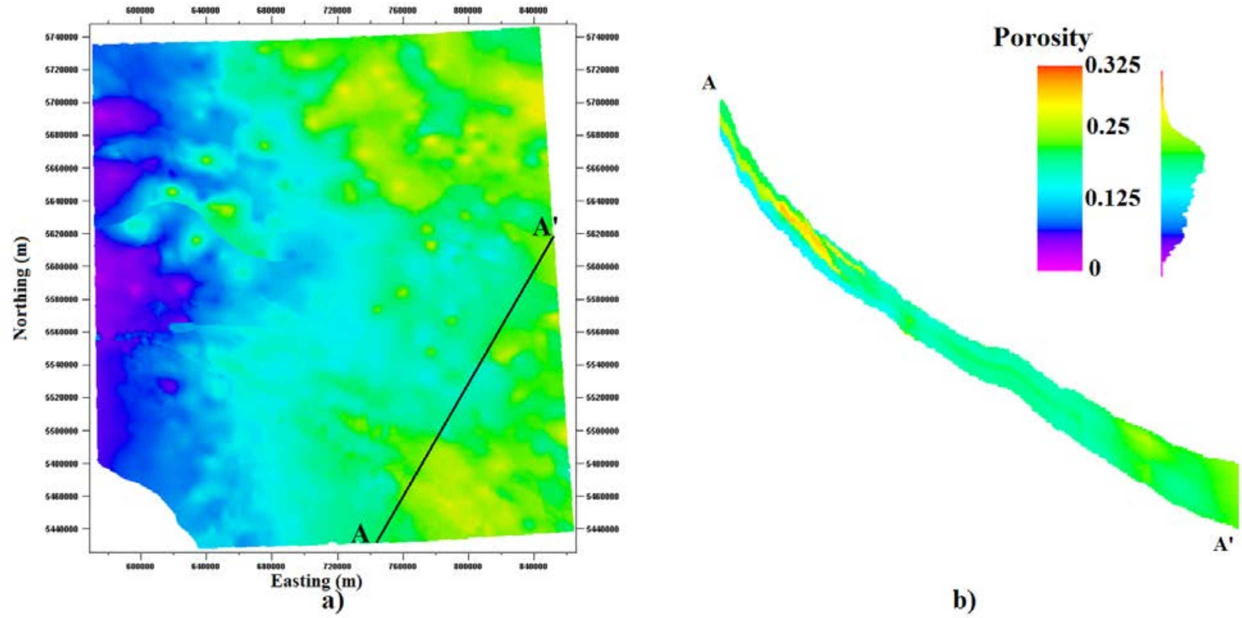

Figure 13. Porosity model for Milk River Formation and Alderson Member stratigraphic units with relatively higher porosities in the eastern part of study area: a) averaged for all subunits, and b) along the cross-section A–A′.

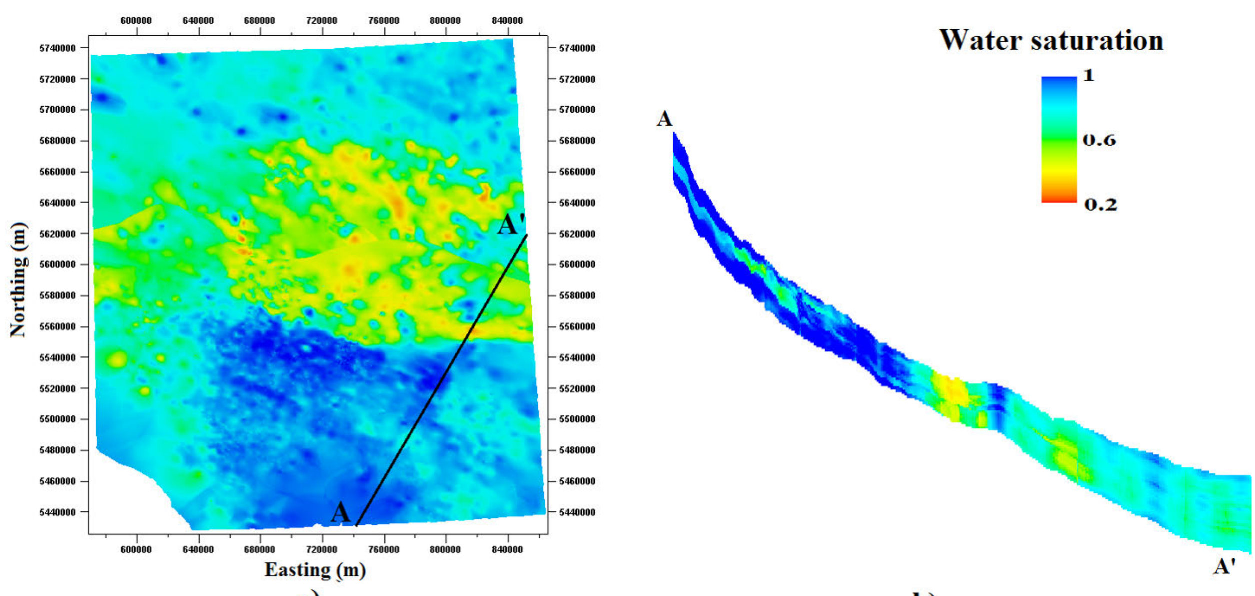

Figure 14. Water saturation model for the Milk River Formation and Alderson Member stratigraphic units with higher saturations in Milk River Formation part of study domain: a) averaged for all subunits and b) along cross-section A–A′.

5 Water Resources and Natural Gas System

5.1 Hydrogeology and Hydrostratigraphy

Meyboom (1960) indicated that recharge of the Milk River Formation occurs largely in northern Montana, where sandstones of the Milk River Formation are exposed at the surface, with groundwater flowing towards the northeast and west at a rate of 6 m/year or less. Artesian conditions were found throughout the extent of the Milk River Formation. Meyboom (1960) estimated that the total recoverable groundwater resources were approximately 263 x 10^6 m^3, cautioning that at the observed rates of withdrawal, the reserve of groundwater could last 200 years, only with careful development, justifying extensive conservation efforts. Meyboom (1960) also highlighted the presence of natural gas in the aquifer, estimating the maximum gas production rate of approximately 230 m^3/d would be possible from a well producing water at 0.03 m^3/d. Swanick (1982) noted many Milk River Formation water wells produced methane gas during pumping with gas concentrations estimated to have been only a few percent to 50 percent of the pumped volume. Hendry et al. (1991) proposed that methane concentrations in the aquifer could be the result of methane fermentation during decomposition of organic carbon. Evidence in support of the source of organic carbon is lacking, and Hendry et al. (1991) state that carbon could therefore be from within the aquifer or from the confining shales.

Schwartz et al. (1981) found that stable isotopes of oxygen and hydrogen in the Milk River Formation water were predominantly similar to those found in meteoric water, with the exception of some downdip locations where water samples resembled water from the underlying Bow Island Formation. These different compositions suggested to Schwartz et al. (1981) that a mixing process was occurring in the Milk River Formation between meteoric water recharging the formation and connate water, complicated by leakage of water through the top and bottom of the Milk River Formation.

Swanick (1982) used a groundwater flow model and ^{14}C dating to determine the age of groundwater in the Milk River Formation. The model predicted maximum ages for groundwater of approximately 500 ka near the northwestern extent of the Milk River Formation. Carbon-14 dating of samples closer to the recharge areas differed from model calculated ages for those same areas by approximately +20%.

Hitchon (1984) indicated that recharge occurs in areas where the Milk River Formation outcrops/subcrops in southern Alberta, in the Cypress Hills, in the regions between the Red Deer and South Saskatchewan rivers, and at the Hand Hills. Discharge is occurring in the major river valleys and Pakowki Lake. Flow was judged to be upwards from the Milk River Formation into the Pakowki Formation. Hitchon (1984) stated that the present hydrodynamic regime controls the location for shallow gas accumulations in the region.

Tóth and Corbet (1986) found that the potentiometric surface of the Milk River Formation closely corresponded to the bedrock surface, suggesting to them that the flow pattern within the aquifer system had adjusted to the modern land surface. Recharge was determined to occur in topographically high regions with flow paths estimated at being on the order of 50 km in length. Tóth and Corbet (1986) also highlighted the importance of buried valleys as discharge zones as well as the movement of fluids out of the Milk River Formation through overlying and underlying shale beds.

Hendry and Schwartz (1988) suggested that based on hydraulic heads, downward flow exists between the Milk River Formation and the underlying Niobrara Formation shale, and upward flow exists between the Bow Island / Viking formations and the overlying Westgate Formation shale. They developed a model to explain chemical composition of groundwater in the aquifer that accounted for advection, dispersion, and diffusion, finding that diffusion is an important factor in explaining chemical composition. They highlighted how variations in transmissivity lead to differences in transit times for groundwater, calculating groundwater residence times of between 250 and 510 ka. These values are in agreement with other estimates as presented in Schwartz and Muehlenbachs (300 ka; 1979), Swanick (500 ka; 1982), and Phillips et al. (500 ka; 1986).

Pétré et al. (2016) generated a unified conceptual model of the transboundary Milk River aquifer, reiterating the importance of features such as the outcrop and subcrop areas in Montana as well as the Cypress Hills as recharge areas. Based on groundwater flux estimates, Pétré et al. (2016) estimated recharge to be 9.6 mm/year. They highlight the importance of the Milk River in intercepting northerly flowing groundwater. Pakowki Lake, buried valleys, and vertical leakage into the Niobrara Formation are also discussed as sinks for groundwater flowing through the Milk River aquifer. Dating using $^{36}Cl/Cl$ ratios suggested that ages of groundwater in the northern portions of the Milk River aquifer are greater than 2500 ka. This estimate is greater than the estimates of between 600 and 1600 ka calculated from $^{36}Cl/Cl$ ratios in Nolte et al. (1991).

The hydrostratigraphy of the case study area is summarized in Figure 15. Units with regional aquifer characteristics include the Milk River Formation, some units within the Alderson Member, and the Medicine Hat Member. The Medicine Hat Member is gas saturated throughout much of the case study area and because of this can regionally be classified as an aquitard, although there is some evidence of groundwater flow within the Medicine Hat Member in the southern portion of the case study area (Schwartz et al., 1981). Although the Milk River Formation may be regionally considered an aquifer, its members have distinct characteristics that do not always align with that regional generalization. The Telegraph Creek Member is predominantly composed of shale and is considered an aquitard. According to Pétré et al. (2015) and Meyboom (1960), the Virgelle Member hosts the most significant regional aquifer within the Milk River Formation. O'Connell (2014) described the Virgelle Member as a composite sandstone unit consisting of multiple shoreline sandstone units that have amalgamated into a thick, continuous, regional, sandstone sheet. O'Connell (2014) also indicates that shoreface sandstone of local extent is common within this unit, and that these sandstone units can be stacked to form continuous sandstone bodies, or can be separated by shaly intervals to form distinct sandstone bodies. Figure 16 shows the results of recent isopach mapping of the Virgelle Member sandstone unit. Although the Deadhorse Coulee Member does contain fluvial sandstone units, O'Connell (2014) indicates that these sandstone units are rarely continuous and are difficult to correlate between wells and the Deadhorse Coulee Member can be considered a low-permeability barrier above the Virgelle Member, suggesting it is likely an effective aquitard.

Even though the Alderson Member is regionally considered an aquitard, there is evidence of significant accumulations of coarse-grained sediments capable of forming important local to regional aquifers. O'Connell (2014) indicates that depositional cycles during the time the Alderson Member was deposited resulted in large lobate sandstone bodies that can show coarsening-upwards trends, or can form vertical blocky sandstone bodies. Figure 17 shows the extent of these sandstone bodies from recent mapping.

Where present, the upper Alderson Member sandstone unit most frequently overlies the Deadhorse Coulee Member, but there are locations (Figure 18) where the sandstone units are stacked with the Virgelle Member introducing potential pathways for hydraulic communication between the sandstone of the Alderson Member and the sandstone of the Virgelle Member. Pétré et al. (2015) acknowledged the potential for hydraulic connections but did not include the Alderson Member as part of their defined Milk River aquifer (Figure 18). Figure 19 shows the spatial extent of the Milk River aquifer as defined by Pétré et al. (2015).

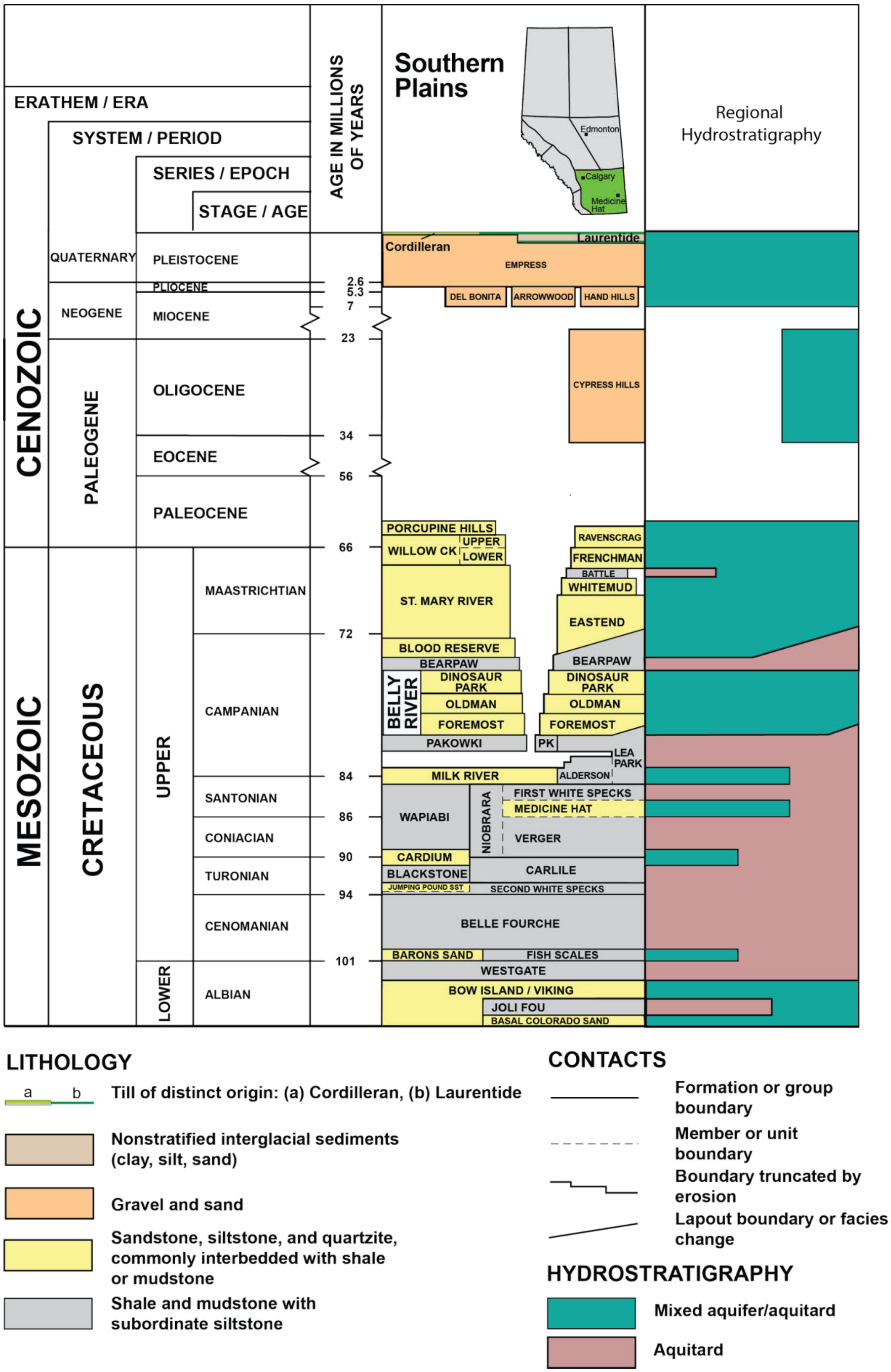

Figure 15. Hydrostratigraphy of the case study area. Table of Formations from Alberta Geological Survey (2015).

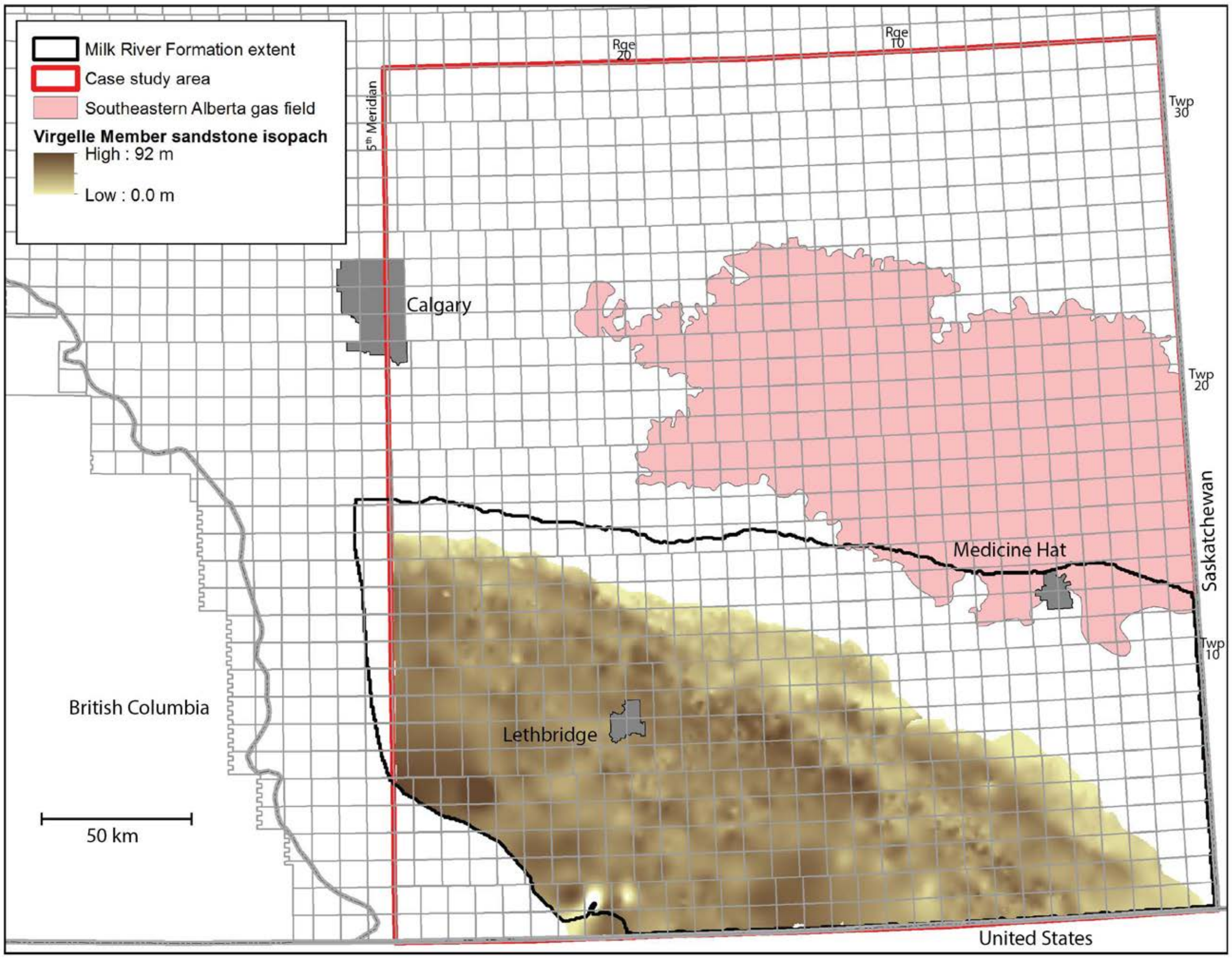

Figure 16. Isopach map of the Virgelle Member sandstone unit.

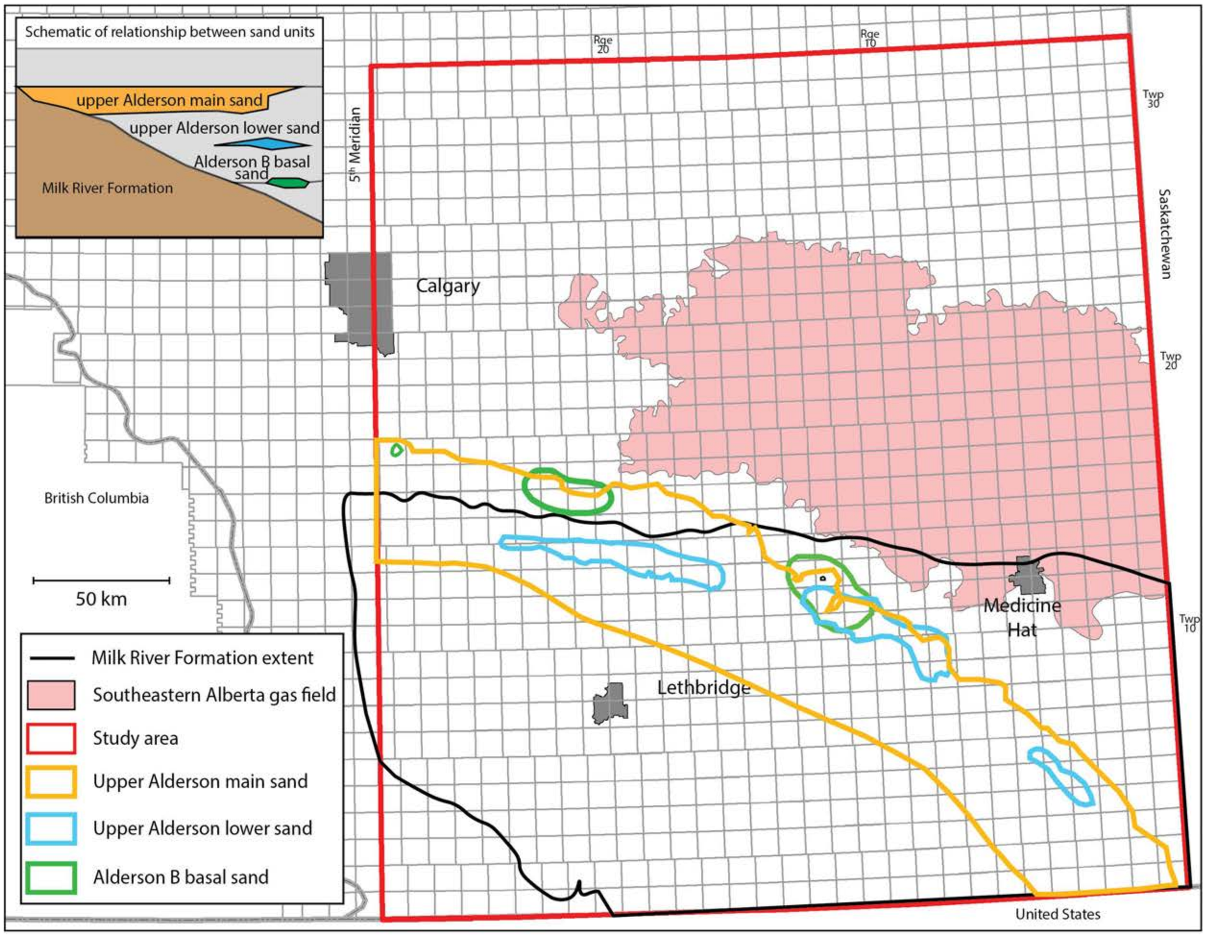

Figure 17. Alderson Member sandstone unit distribution. Abbreviation: SS, sandstone.

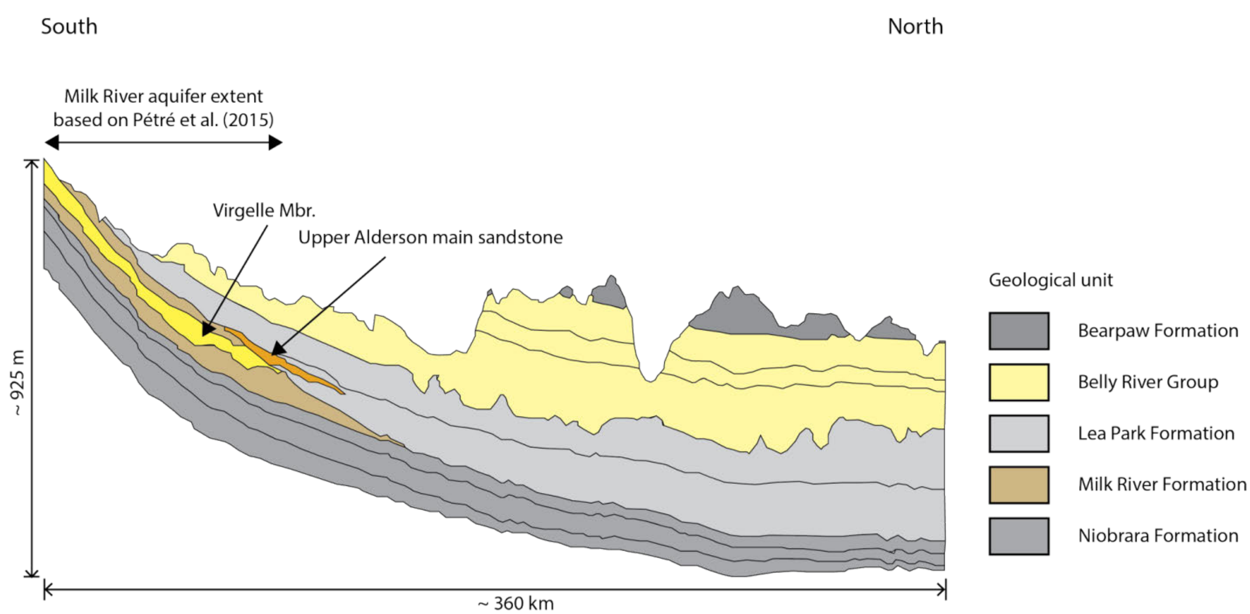

Figure 18. Occurrences of Alderson Member sandstone units directly overlying Virgelle Member sandstone units in cross-section (see Figure 6 for location).

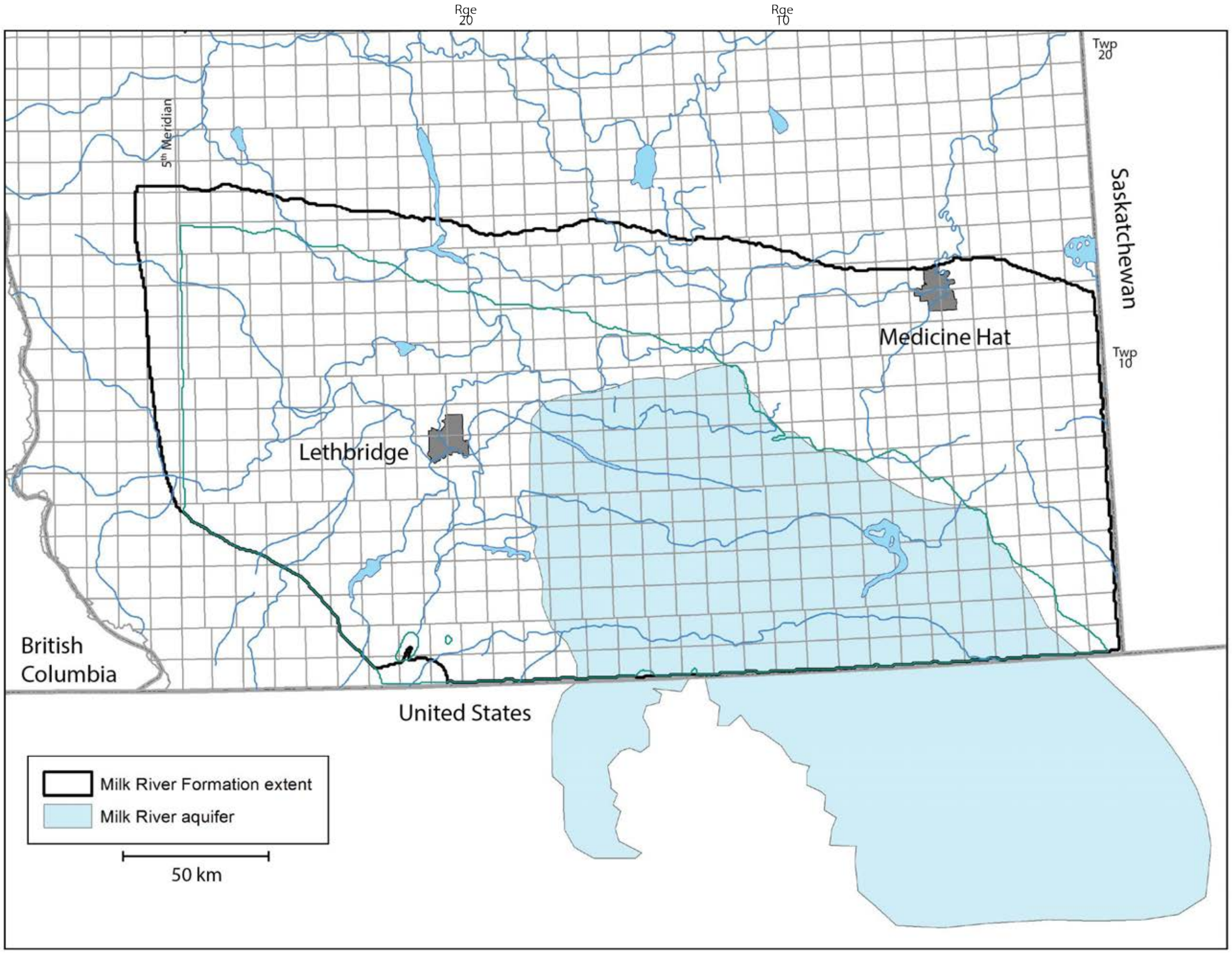

Figure 19. Extent of the Milk River aquifer (after Pétré et al., 2015).

5.2 Water Resources Development History

The earliest recorded water wells completed in the Milk River Formation were drilled in the early 1900s. Since then and up to the end of 2017, approximately 24 000 wells (source of data, Alberta Environment and Parks, 2017a) have been drilled within the geographic extent of the Milk River Formation, of which, approximately 350 water wells can be definitively assigned to the Milk River Formation based on recent mapping and available water well completion details. Another approximately 480 water wells can be assigned to the Milk River Formation based on the total depth of the wells drilled. The remaining approximately 23 000 wells were either allocated to a unit other than the Milk River Formation, or were missing well completion details necessary for allocation.

Figure 20 shows the distribution of all water wells within the extent of the Milk River Formation, and the wells identified as likely being completed in the Milk River Formation. Figure 21a shows a chart of when these water wells, which can be definitively allocated to the Milk River Formation, were drilled and the purpose of those wells. Figure 21b shows the history of groundwater licensing in the Milk River Formation (source of data, Alberta Environment and Parks, 2017b). Table 1 summarizes the number of wells drilled by decade, beginning in 1902 to 1910 and ending with the wells drilled between 2011 and 2016.

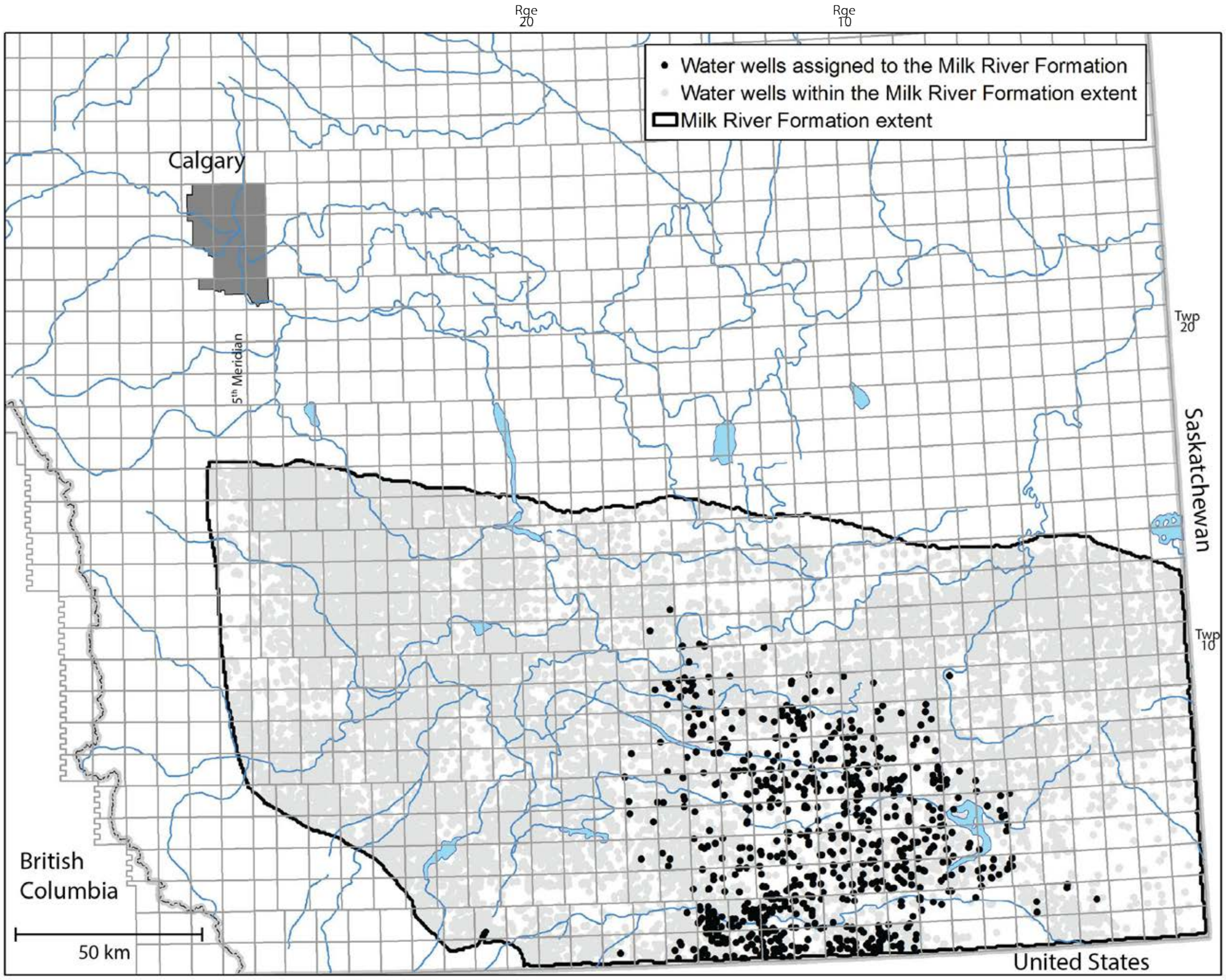

Figure 20. Water wells drilled within the Milk River Formation extent in southeastern Alberta.

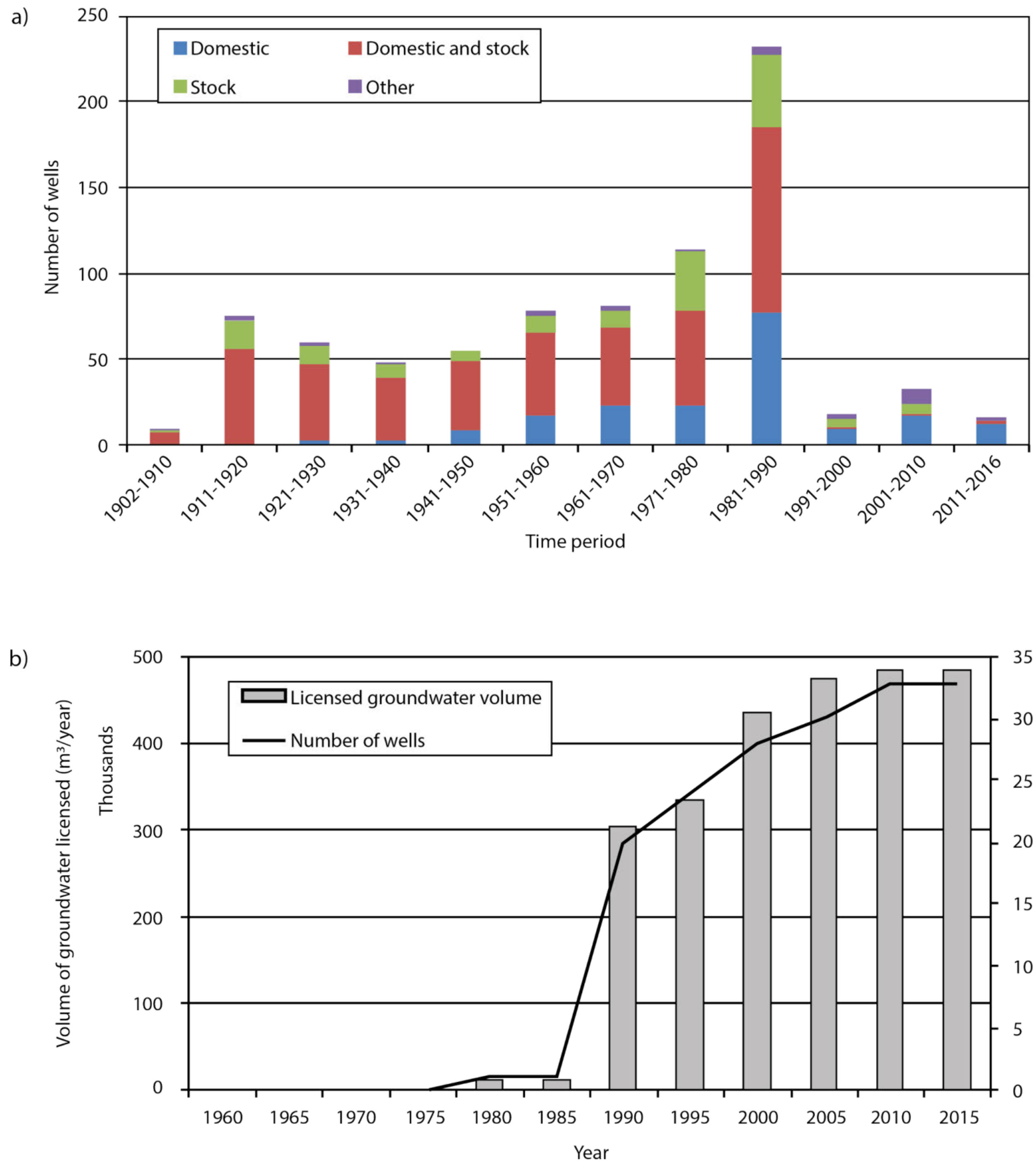

Figure 21. Water wells completed in the Milk River Formation, southeastern Alberta: a) number of wells drilled by year and type; and b) number of licensed wells by year and licensed volumes.

Table 1. Number of water wells completed in the Milk River Formation (southeastern Alberta) by time period and type of use.

Time Period	Domestic Wells	Domestic and Stock Wells	Stock Wells	Other Wells	Total Wells
1902 to 1910	0	7 (78)	1 (11)	1 (11)	9
1911 to 1920	0	56 (75)	16 (21)	3 (4)	75
1921 to 1930	2 (3)	45 (75)	11 (18)	2 (3)	60
1931 to 1940	2 (4)	37 (77)	8 (17)	1 (2)	48
1941 to 1950	8 (15)	41 (75)	6 (11)	0	55
1951 to 1960	17 (22)	48 (62)	10 (13)	3 (4)	78
1961 to 1970	23 (28)	45 (56)	10 (12)	3 (4)	81
1971 to 1980	23 (20)	55 (48)	35 (31)	1 (1)	114
1981 to 1990	77 (33)	108 (47)	42 (18)	5 (2)	232
1991 to 2000	9 (50)	1 (6)	5 (28)	3 (17)	18
2001 to 2010	17 (53)	1 (3)	6 (19)	8 (25)	32
2011 to 2016	12 (75)	2 (13)	0	2 (13)	16

Notes: Values in parentheses show the percentage of the total number of wells drilled that the particular well type represents. Because of rounding, percentage values might not add up to 100%.

Over the time series of water well drilling there seems to be two periods of greater activity. The first occurs between 1911 and 1940. The second occurs between 1941 and 1990. The total number of wells drilled after 1990 decreases substantially compared to the two previous time periods. The uses of the wells appears to shift from being primarily for a combined domestic and stock purpose in the 1900 to 1940 time period, to more diverse uses between 1941 and 1990, and then predominantly for domestic uses after 1990.

Pétré et al. (2015) summarized previous exercises in estimating the use and number of wells producing from the Milk River Formation, stating that previous authors had estimated use at between 1.2×10^6 m^3/year from approximately 400 wells in the 1960s, to 2.0×10^6 m^3/year in the early 1990s from approximately 1000 wells, and a return to water use of approximately 1.2×10^6 m^3/year in the 2000s. Pétré et al. (2015) suggested that decreasing population and reliance on regional water supply systems might be responsible for the overall decrease in groundwater use from the Milk River aquifer over time.

In order to update and further refine the time series of estimates of groundwater use from the Milk River Formation, information on the number of active water wells was gathered, as were estimates of how much water those wells could be extracting. The process for determining water use is described in the Appendix 1.

The previous work on water use estimates referenced in Pétré et al. (2016) did not map use over the entire extent of the Milk River Formation, but rather to the portion of the formation defined as the Milk River aquifer. To make the comparison of the results from this assessment of use to those of previous exercises a smaller extent than the entire extent of the Milk River Formation had to be selected. Recent preliminary mapping completed by the AGS of the total dissolved solids (TDS) concentration in the Milk River Formation defined an extent of the zone within the formation where the water is considered nonsaline (Figure 22). Using this extent, wells completed in the Milk River Formation could be selected and use volumes could be estimated. The results of the assessment are presented in Figure 23 and provide minimum and maximum annual groundwater extraction volume estimates, as well as a calculated average annual groundwater extraction volume estimates for the 1960 to 2015 period at five-year increments.

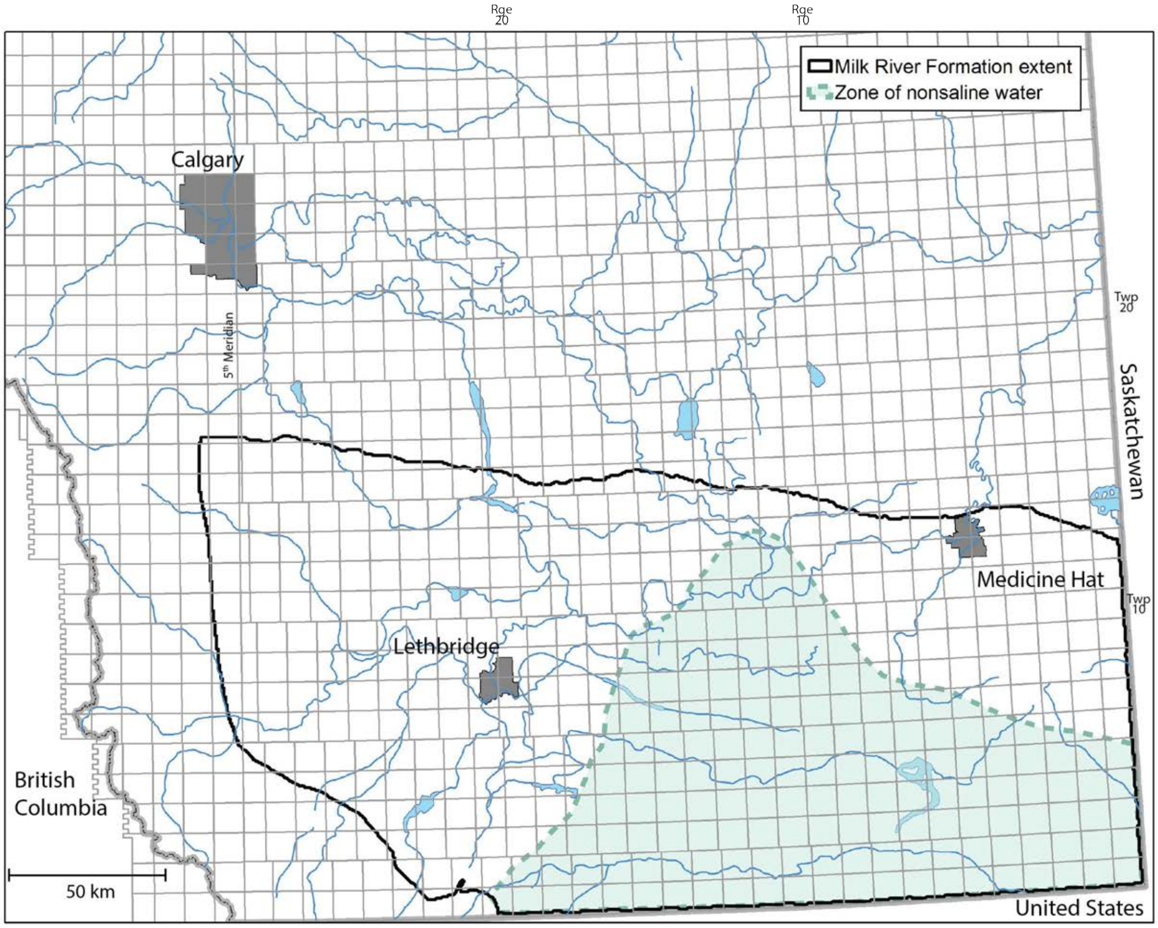

Figure 22. Approximate extent of nonsaline water within the Milk River Formation.

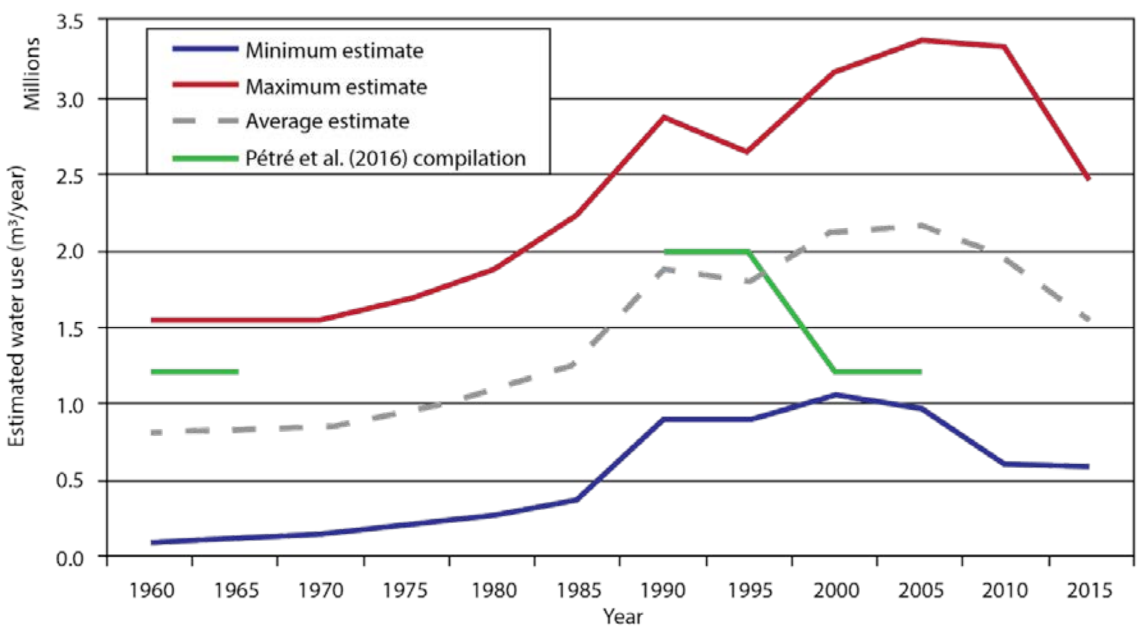

Figure 23. Estimated annual groundwater use for the area of nonsaline water within the Milk River Formation, 1960–2015.

Figure 23 shows increasing volumes of groundwater use into the year 2000 for the low use scenario and 2005 for the high use scenario. Groundwater use estimates then begin to decrease after the year 2000 for the low use scenario and 2005 for the high use scenario. These trends are consistent with the number of wells being drilled by year (Figure 21), as well as the increase in produced volumes from licensed water wells (Figure 21). The highest numbers of wells were drilled from 1971 to 1991, with high numbers of wells also being drilled from 1951 to 1970. As discussed in Appendix 1, produced volumes were calculated assuming that wells could be active for 20, 30, or 40 years after being drilled and put into service. A well drilled in 1971 that is active for 20 years would cease pumping in 1990, but if it were active for 40 years, it would stop pumping in 2010. The difference between the ages of wells used in the analyses causes the slight shift in the maximum use curve as compared to the minimum use curve.

Water wells being used for domestic and stock purposes are the dominant type of wells up to 1990, after which domestic wells become the most frequently drilled type of well completed in the Milk River Formation. Domestic and stock wells are allowed to use six times the amount of water, and stock wells are allowed to use five times the amount of water that a domestic well is before needing to be licensed (Government of Alberta, 2017). The decrease in domestic and stock, and stock wells in the mix of wells being drilled appears to have contributed to the reduction in groundwater production.

The Pétré et al. (2015) summary of groundwater use estimates falls within the range of groundwater use presented in this case study (Figure 23). The 1960s era estimates summarized in Pétré et al. (2015) plot closer to the maximum estimate from this case study. Estimates of use from the 1990s plot close to the average use estimates from this case study. Lastly, the estimates from the 2000s plot close to the low use estimates from this case study.

Although there is consistency between previous estimates and the results in Figure 23, the question remains if these results are reasonable. Recent work on estimates of groundwater storage variation from analysis of Gravity Recovery and Climate Experiment satellite data for Alberta completed by Huang et al. (2016) show that groundwater storage has increased by between 12 and 17 mm/year over much of southern Alberta during the period between April 2002 and October 2014. In nine of the thirteen years of the Huang et al. (2016) analysis, precipitation was between 80 to 200% of normal, whereas in the other four years, precipitation was between 50 to 120% of normal (based on data from Alberta Agriculture and Forestry, 2019). It seems reasonable to conclude that decreasing groundwater production in the 2000 to 2015 time period, coupled with what appears to be increased precipitation should result in increased groundwater storage.

Meyboom (1960) raised concerns about groundwater management in the Milk River aquifer and the potential for depletion of the groundwater resource. Klassen et al. (2018) assessed first order groundwater availability calculating maximum sustained yield values throughout southern Alberta. Maximum sustained yield (MSY) was defined as the volume of groundwater that can be removed where pumping is balanced by the maximum amount of capture, which includes induced recharge of streamflow and zero discharge. The Klassen et al. (2018) study was focused on the upper 150 m of sediment and bedrock and uses the total calculated recharge without assigning a recharge amount to any particular geological interval. The Milk River Formation over much of its extent is greater than 150 m below ground surface (Figure 24) and only approximately 35% of wells completed in the Milk River Formation were drilled to depths of 150 m or less. Comparing the estimates of groundwater production volumes to the maximum sustained yield estimates from the Klassen et al. (2018) assessment is therefore not directly applicable for this assessment, however, the definition of maximum sustained yield is useful in comparing availability to use.

Estimates of recharge to the Milk River Formation were calculated by Pétré et al. (2016) and by the AGS and Deltares; the values are approximately 9.6 mm/year, and 0.67 mm/year, respectively, over the area of expected nonsaline water in the Milk River Formation. These recharge values translate to an overall maximum sustained yield of between 144×10^6 m^3 and 10×10^6 m^3.

When groundwater use is compared to recharge estimates for the region where the Milk River Formation is inferred to be nonsaline, groundwater use does not appear to exceed the MSY. It could be that there are cases where exceedances occur locally however.

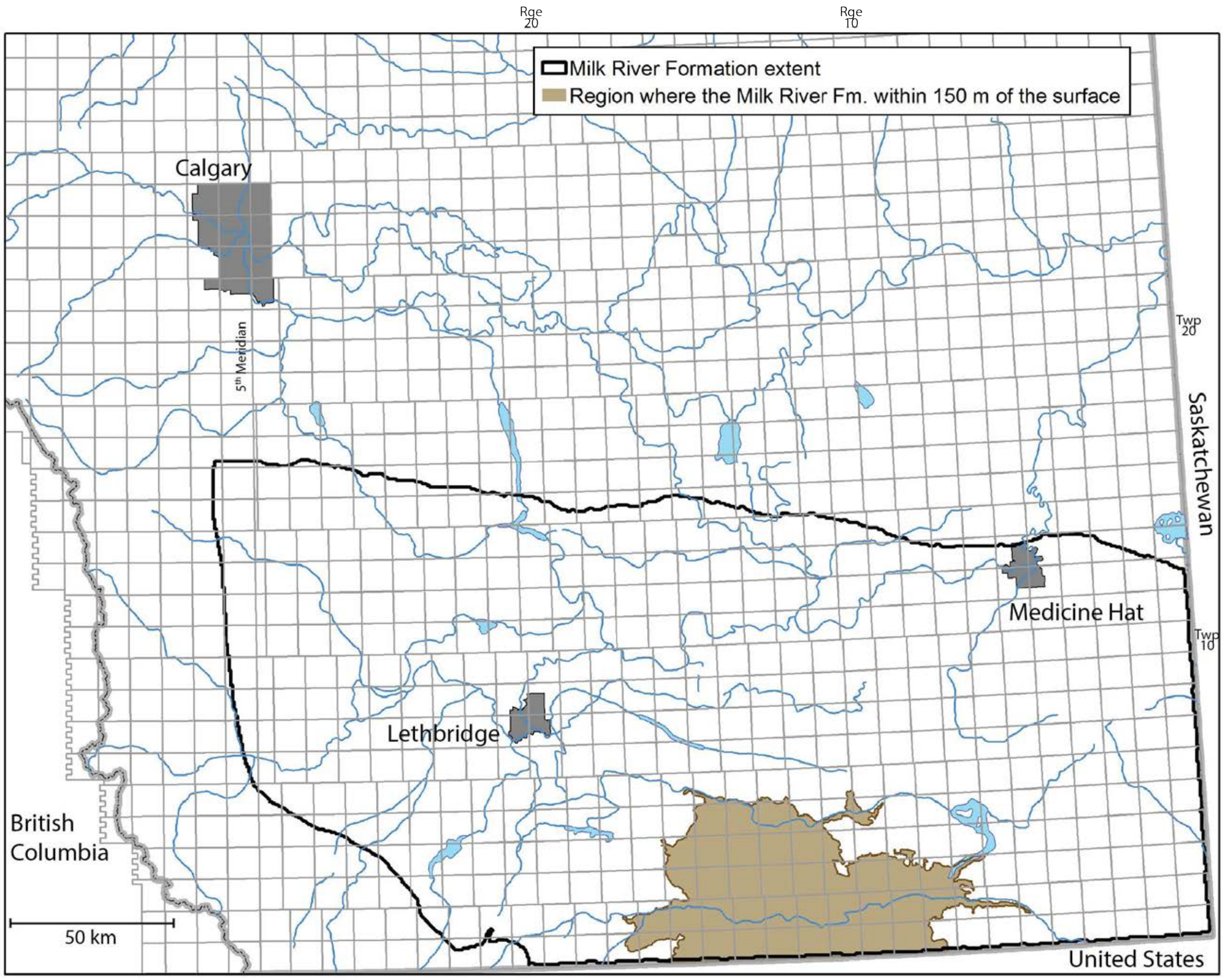

Figure 24. Extent of the Milk River Formation that is at a depth of 150 m or less from the ground surface.

5.3 Petroleum Systematics of the Medicine Hat and Alderson Members in the Southeastern Alberta Gas Field

Megill (1984), Lerche and Mackay (1999), and Rose (2001) state that the elements of petroleum systems include 1) a source of hydrocarbons; 2) a reservoir rock of sufficient quality to deliver hydrocarbons to a well at commercial rates; 3) a migration pathway between the presumed source and target reservoir rock; 4) one or more formations with the right properties to impede or halt petroleum migration at the reservoir (called the seal or cap rock); 5) a favourable three-dimensional geometry of reservoir and seal to make an enclosed volume, called the trap; 6) the right geological history or sequence to have the trap in position during hydrocarbon generation and migration; and 7) favourable conditions to preserve the hydrocarbons in the trap after it fills over geological time otherwise known as persistence.

A number of authors have discussed the origin of the natural gas and nature of the gas entrapment in the Alderson Member, including Berkenpas (1991), Ridgley (2000), Schurr and Ridgley (2002), Fishman et al. (2012), O'Connell (2014), and Chen et al. (2015). Although there was agreement between authors on some elements of the Alderson Member petroleum system, it became clear that there was no clear consensus on its overall nature. The following list discusses the similarities and differences between the interpretations of the petroleum system as presented in the cited literature.

1) Source: There is no uncertainty in the published literature about the source. The consensus view is that the gas was generated biogenically (Fuex, 1977; Rice and Claypool, 1981).
2) Reservoir: There is uncertainty in the published literature about the nature of reservoir quality as the deposit is heterogeneous and the nature of the geometry of reservoir-quality rocks that produce to gas wells is speculative. The reservoir quality is a function of porosity, permeability, volume, and interconnectedness vertically as well as horizontally.
3) Migration: There is no uncertainty about hydrocarbon migration pathways as the Alderson Member gas deposit is believed to be self-sourced. There is some uncertainty about redistribution of the gas over time.
4) Seal: There is no uncertainty about the presence of a seal of strength at least sufficient to impede any vertical or updip loss of methane for the volumes of gas in place in the Alderson Member beds at their discovery. This puts a lower bound on the strength of the seal(s) in the trap, but there is uncertainty about the maximum seal strength, given uncertainty about the internal connectivity. The scale of the seal is uncertain as well. For instance, is there a single seal or are there many internal seals?
5) Trap: There is uncertainty about the boundaries, geometry, and heterogeneity of the beds in the Milk River Formation and the Alderson Member, both reservoir/aquifer and sealing beds.
6) Timing: As the Alderson Member is both source and reservoir in the trap, there is no uncertainty about timing.
7) Persistence: As the Alderson Member trap has gone through a cycle of burial and exhumation, the persistence of the gas zone(s) must be evaluated in terms of diffusion and groundwater processes over geological time, as this will provide more certainty on the overall functioning and strength of the trap.

Elements 3, 4, and 5 from the list above hint at the potential for connection between the Alderson gas zone(s) in the northern portion of the case study area with coarser-grained units of the Milk River Formation in the south. This suggests that one additional element needs to be considered in evaluating the system. Here the key uncertainty will be the degree of hydraulic continuity between the gas-bearing and updip water-bearing units. Hydraulic continuity is defined by Tóth (1995) as the degree to which a hydraulic head change in one part of a groundwater system induces a change at another part of the system. Uncertainty in the degree of hydraulic continuity between northern and southern portions of the case study area exist, and will be a function of spatial scale, the time interval of interest, and the hydraulic diffusivity of the system.

Where uncertainties existed in the described petroleum system elements, or with the degree of hydraulic continuity, the elements can be treated as binary choices as described in Table 2. Given that these five elements of uncertainty have a binary either/or condition associated with them, there are 2^5 or 32 possible combinations, each of which could be an alternative conceptual model of the system. It can be argued that the element of trap persistence and hydraulic continuity are best assessed directly with simulation and therefore can be removed from the element set, leaving 2^3 or 8 possible conceptual models to consider for how the Alderson trap may function. Upon further review, three of the conceptual models were removed from consideration as internally inconsistent and geologically implausible, leaving five geologically plausible conceptual models to consider.

All five geologically plausible conceptual models were recognized in one or more of the papers listed earlier in this section. Some authors were very strong in their arguments for one particular model, but others left space for interpretation for there being more than one possibility to explain the functioning of the Alderson trap given the data available to them at their time of publication.

Table 2. Uncertainty statements for the Alderson Member petroleum system elements.

Element	Either	Or
Alderson reservoir rocks	Sandstones and siltstones in the Alderson gas zones are hydraulically connected (e.g., Berkenpas, 1991).	Sandstones and siltstones in the Alderson gas zones are hydraulically isolated and disconnected (e.g., O'Connell, 2014).
Alderson capillary seal(s)	Alderson shales/mudstones act as weak capillary seal(s), capable of holding gas columns of 10 m or less (e.g., Chen et al., 2015).	Alderson shales/mudstones act as strong capillary seal(s), capable of holding gas columns of 100 m or more (e.g., Fishman et al., 2012).
Alderson trap geometry	Alderson shoreface sandstones persist from the erosional edge of the Virgelle Member northward into gas zones (e.g., as suggested in Anna, 2011).	Alderson shoreface sandstones are localized along the edge of the Virgelle Member (e.g., Ridgley, 2000).
Alderson trap persistence	The Alderson trap does not lose significant gas over geological time by diffusion through sealing rocks (e.g., Berkenpas, 1991).	The Alderson trap can lose significant gas over time by diffusion through sealing rocks (to be tested).
Hydraulic continuity	Groundwater flow affects Alderson gas distribution and the system is hydraulically continuous regionally over geological or management time scales (e.g., as suggested by Hitchon, 1984).	Groundwater flow does not affect Alderson gas distribution and the system is not hydraulically continuous regionally over geological or management time scales (to be tested).

The five alternative conceptual models for the Alderson gas zone and trap at the intraformational scale are summarized and illustrated as follows:

1. Connected reservoir, strong seals, Alderson sandstone persists to the north (Figure 25)
2. Connected reservoir, strong seals, Alderson sandstone localized to the south (Figure 26)
3. Disconnected reservoir, strong seals, Alderson sandstone localized to the south (Figure 27)
4. Disconnected reservoir, strong seals, Alderson sandstone persists to the north (Figure 28)
5. Disconnected reservoir, weak seals, Alderson sandstone persists to the north (Figure 29)

The groundwater-bearing and Alderson gas regimes in the conceptual models are shown at the top of the figures in blue and red, respectively.

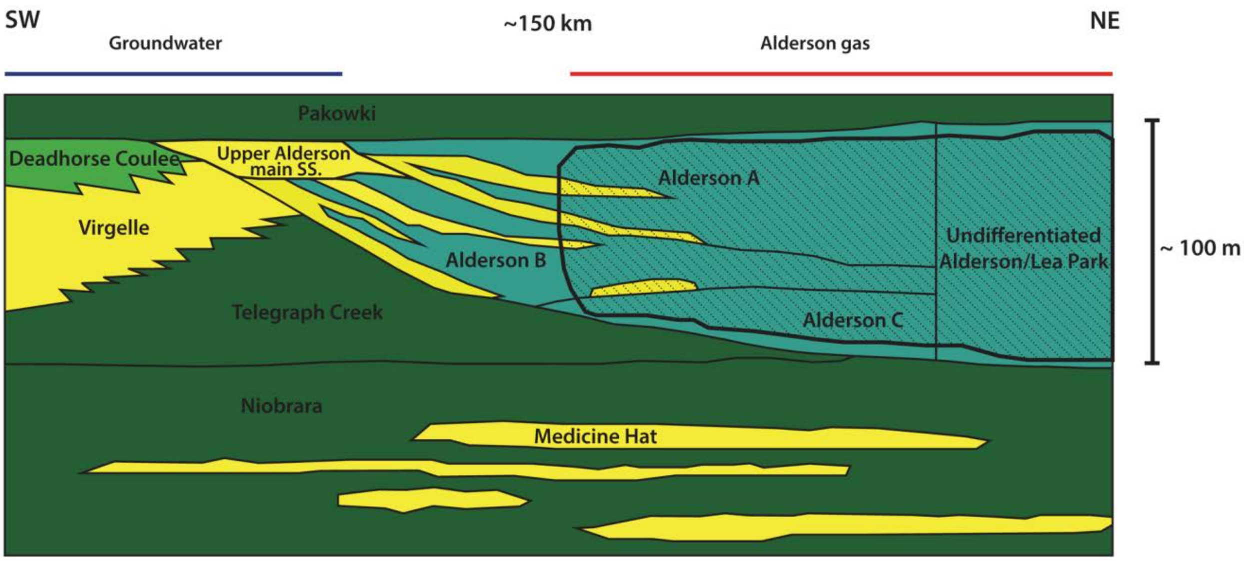

Note: Connected reservoir (cross-hatched area), strong seal (bold black line), Alderson sandstone persists to the north. Groundwater-bearing and Alderson gas regimes are shown at the top in blue and red, respectively. SS. is an abbreviation for sandstone. Modified from O'Connell (2003).

Figure 25. Conceptual model 1 for the Alderson gas zone and trap.

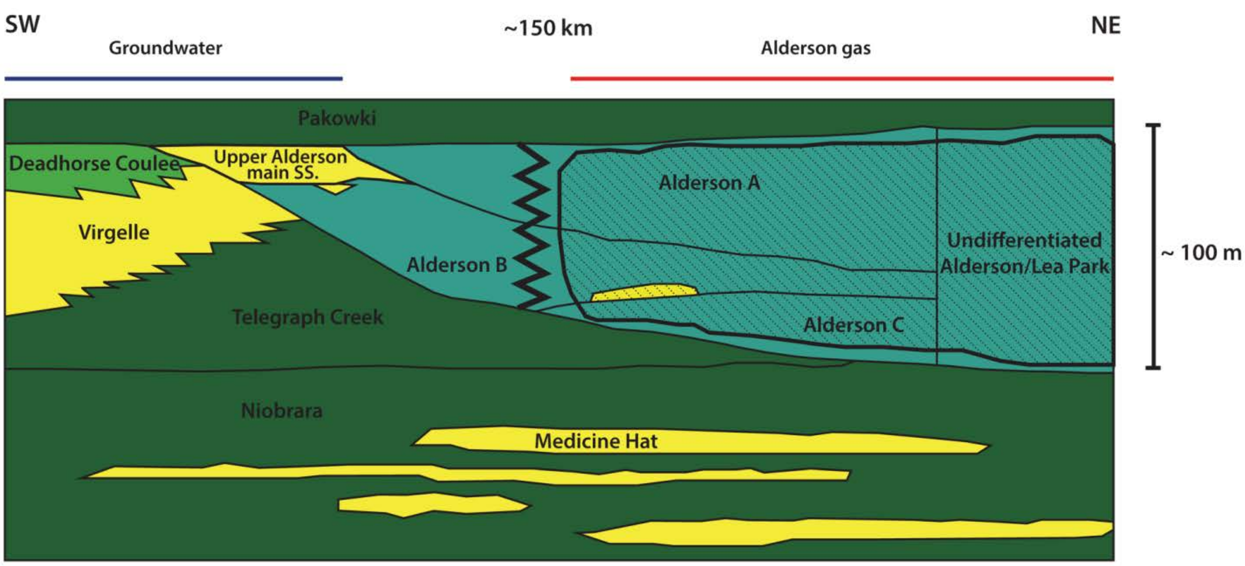

Note: Connected reservoir (cross-hatched area), strong seals (bold black lines), Alderson sandstone localized to the south. Groundwater-bearing and Alderson gas regimes are shown at the top in blue and red, respectively. SS. is an abbreviation for sandstone. Modified from O'Connell (2003).

Figure 26. Conceptual model 2 for the Alderson gas zone and trap.

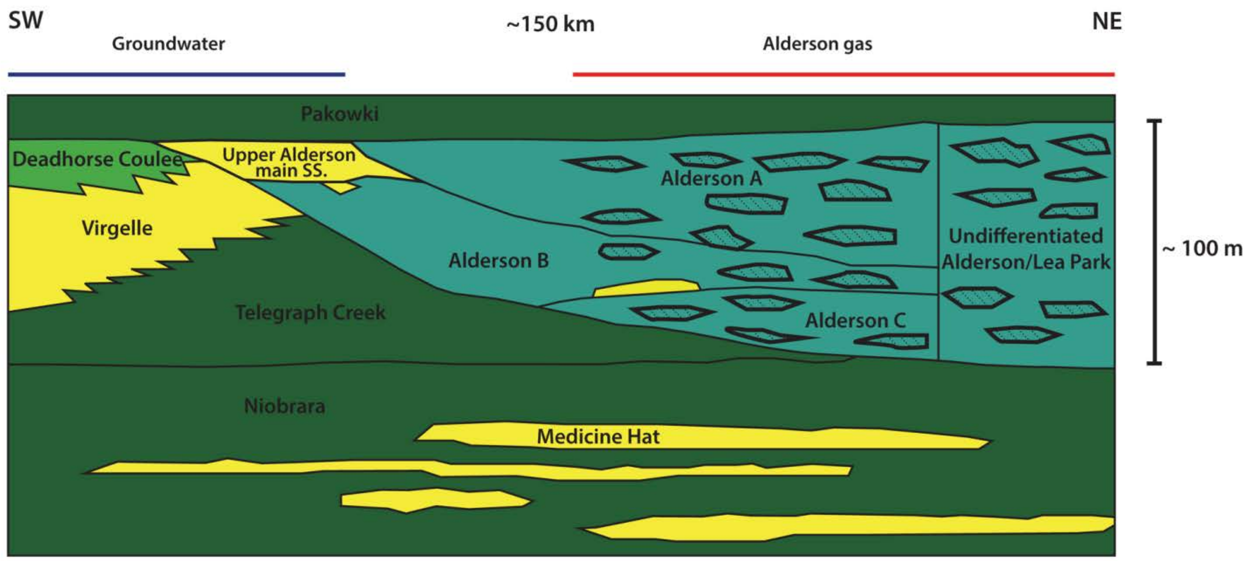

Note: Disconnected reservoirs (cross-hatched areas), strong seals (bold black lines), Alderson sandstone localized to the south. Groundwater-bearing and Alderson gas regimes are shown at the top in blue and red, respectively. SS. is an abbreviation for sandstone. Modified from O'Connell (2003).

Figure 27. Conceptual model 3 for the Alderson gas zone and trap.

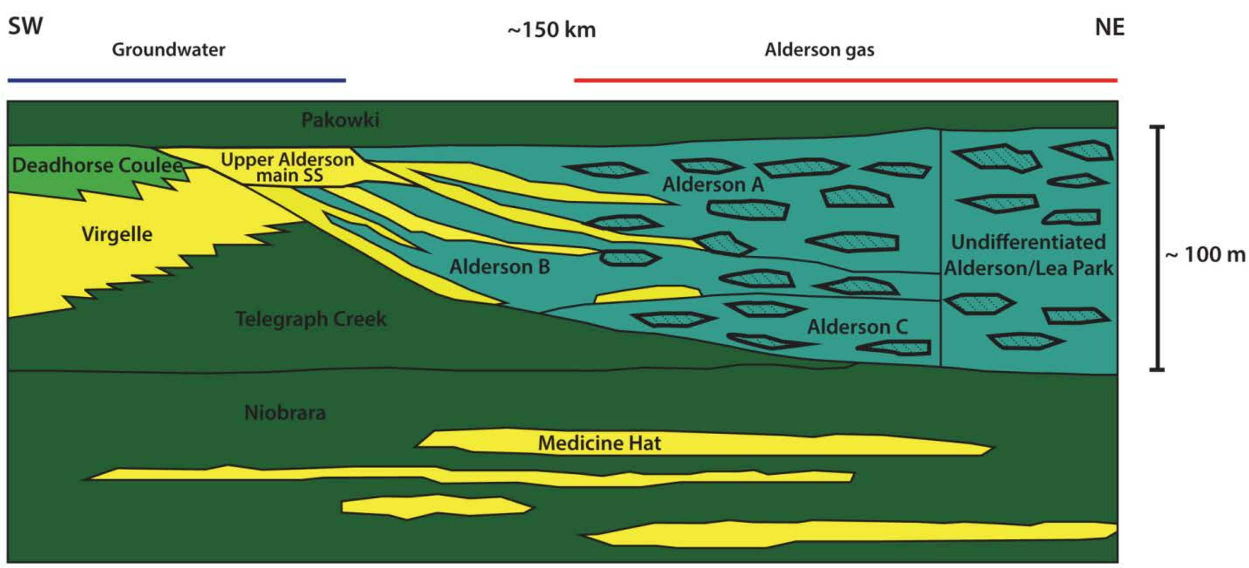

Note: Disconnected reservoirs (cross-hatched areas), strong seals (bold black lines), Alderson sandstone persists to the north. Groundwater-bearing and Alderson gas regimes are shown at the top in blue and red, respectively. SS. is an abbreviation for sandstone. Modified from O'Connell (2003).

Figure 28. Conceptual model 4 for the Alderson gas zone and trap.

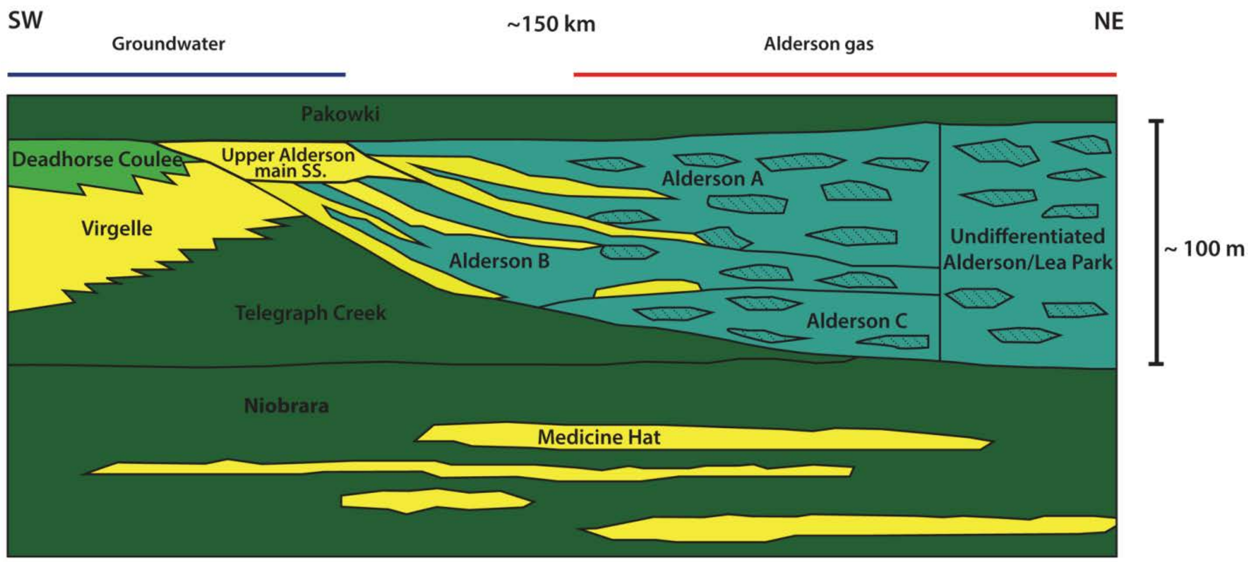

Note: Disconnected reservoirs (cross-hatched areas), weak seals (regular black lines), Alderson sandstone persists to the north. Groundwater-bearing and Alderson gas regimes are shown at the top in blue and red, respectively. SS. is an abbreviation for sandstone. Modified from O'Connell (2003).

Figure 29. Conceptual model 5 for the Alderson gas zone and trap.

5.4 Natural Gas Development History

In 1883, a crew from the Canadian Pacific Railway who were drilling near Medicine Hat, Alberta, for water discovered natural gas at a site that would eventually be known as Alderson (Alberta Culture and Tourism, 2019). In 1884, a second well close to the first well was drilled with the intent of producing gas, marking the beginning of development of the southeastern Alberta gas field. Since then, over 40 000 wells have been drilled in the area, with almost 26 000 wells targeting just the Milk River Formation, and/or the Alderson Member of the Lea Park Formation, and/or the Medicine Hat Member of the Niobrara Formation. In 2002, the AER estimated the raw gas initial volume in place in the Alderson Member–Milk River Formation–Medicine Hat Member units in southeastern Alberta to be 566 x 10^9 m^3, and the initial established reserves to be 367 x 10^9 m^3 (Alberta Energy Regulator, 2002). Based on well production data (IHS Markit, 2018), approximately 152 x 10^9 m^3 of natural gas has been produced from the area as of the end of July 2018, or approximately 41% of the initial established reserves.

Changes in gas well drilling (Figure 30) and gas well abandonment (Figure 31) are correlated with changes in commodity price. The number of wells being drilled increases as commodity prices increase with the highest levels of well drilling occurring between 1970 and 1986, and between 2000 and 2008, both periods of high inflation-adjusted commodity prices. Conversely, the number of wells being abandoned increases as inflation-adjusted commodity prices decrease. Lower commodity prices in the late 1980s to late 1990s correlate with an increase in well abandonments compared to previous years. Higher commodity prices in the 2000s correlate with low numbers of abandoned wells. More recent decreases in commodity prices also correlate with recent increases in abandonments.

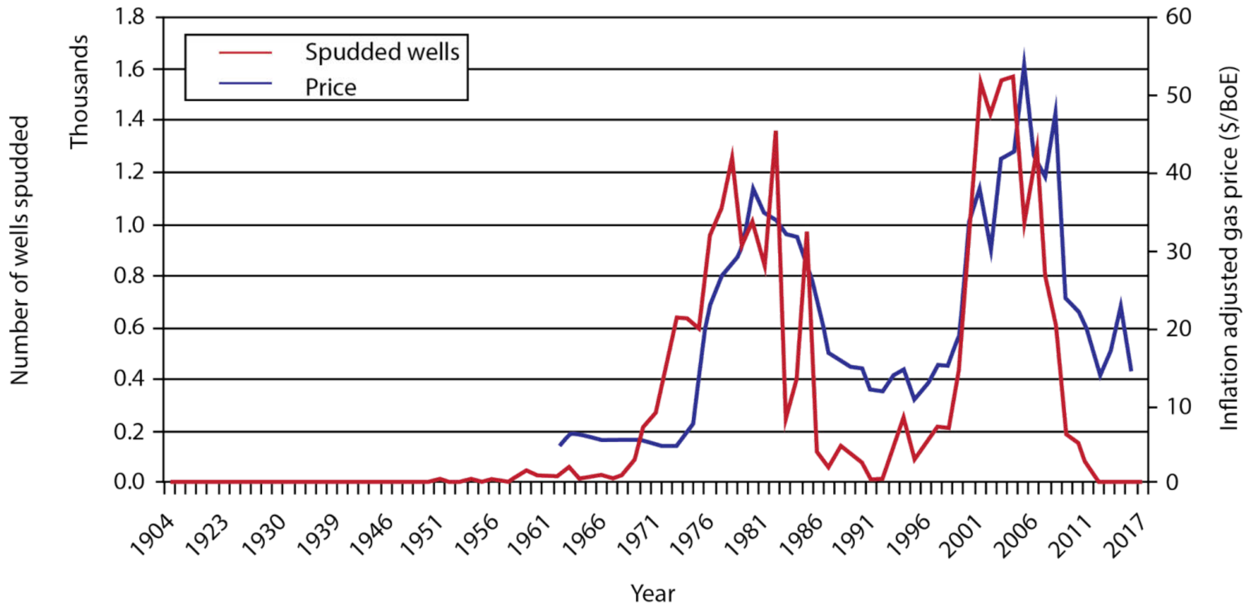

Figure 30. Inflation-adjusted gas commodity prices and the number of spudded wells in the Alderson Member and/or Medicine Hat Member per year in the southeastern Alberta gas field. Data on the number of spudded wells from IHS Markit (2018), commodity price from Alberta Energy Regulator (2016), and inflation rate from Statistics Canada (2018). Abbreviation: BoE, barrel of oil equivalent.

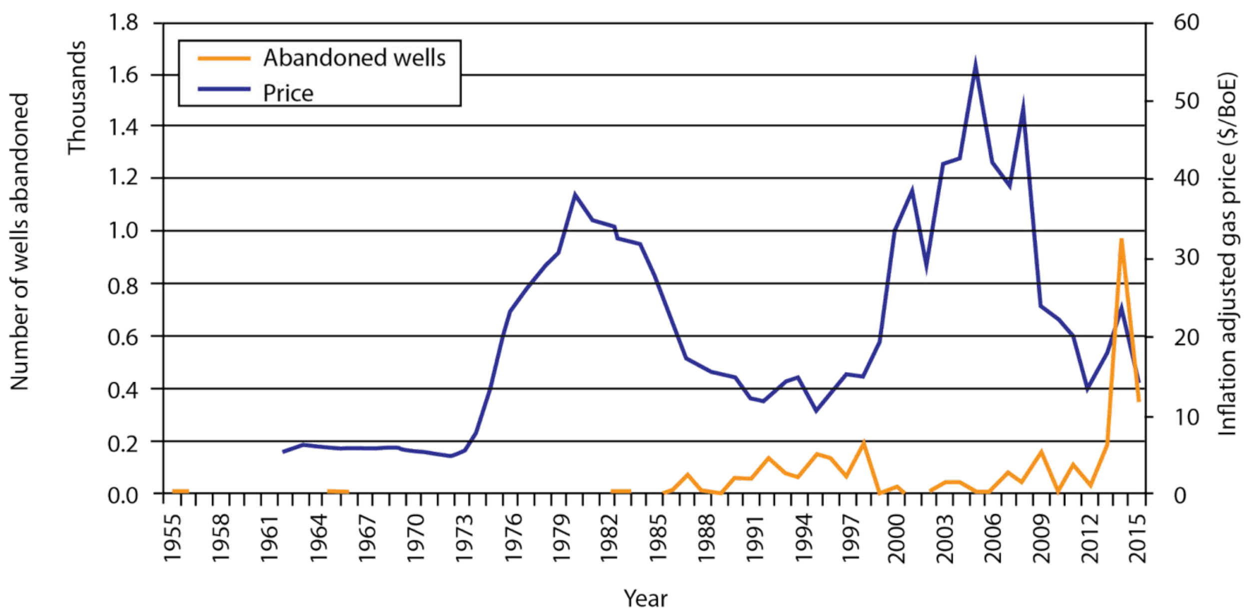

Figure 31. Inflation-adjusted gas commodity prices and the number of abandoned wells in the Alderson Member and/or Medicine Hat Member per year in the southeastern Alberta gas field. Data on the number of wells from IHS Markit (2018), commodity price from Alberta Energy Regulator (2016), and inflation rate from Statistics Canada (2018). Abbreviation: BoE, barrel of oil equivalent.

Wells in the area generally have average rates of production (source of data, IHS Markit, 2018) that differ for active production wells and for wells that have been abandoned or where production has been suspended (Figure 32). In abandoned and suspended wells, during the last three months of production for those wells, the median average rate of gas production was 3.4 mcf/d with a 99% confidence interval of 0.66 mcf/d (shaded in grey). In actively producing wells, the median of the average rate of gas production during the most recent three months of production was 5.9 mcf/d with a 99% confidence interval of 0.43 mcf/d. This suggests that the median of the average gas production rates for abandoned and suspended wells is significantly different from the median average production rate in active production wells. It also provides an indication that production rate might be a good predictor of when a well will be considered for abandonment or suspension.

Of the 17 295 wells with active production in May, June, and July of 2018, 5373 wells had an average production rate equal to or less than the median average production rate for wells that have been abandoned or suspended. An additional 1709 wells have an average production rate less than or equal to the median average production rate for producing wells, but greater than the median average production rate for abandoned or suspended wells. As production rates decline over time, these 7082 wells could be next in line for abandonment or suspension of production.

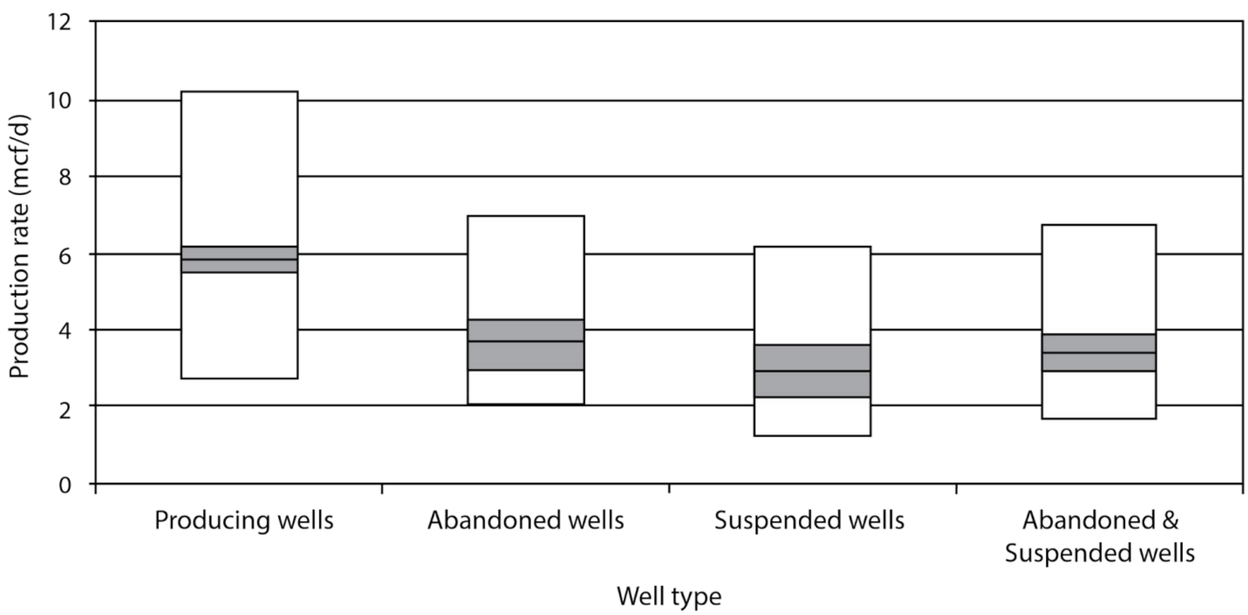

Figure 32. Box plot of daily production rates for producing, abandoned, and suspended wells in the Alderson Member and/or Medicine Hat Member in the southeastern Alberta gas field (data from IHS Markit, 2018). Confidence interval shaded in grey.

6 Groundwater Modelling

The numerical modelling to assess the risk of leakage from the Alderson gas trap under commingled well abandonment conditions with the Medicine Hat Member for this case study was done in two stages. The first stage modelled a simpler system by simulating a single phase, regional, water-dominated flow system, whereas the second stage focused on a relatively complex two-phase air-water flow system at the trap boundary itself. The objectives for the first phase were to establish initial/boundary conditions for the second stage two-phase (air and water system) scenario evaluation model. The two-phase modelling focused on evaluating all conceptual models for two scenarios, replicating and simulating the hydrogeological conditions with and without commingling. The first stage or single-phase simulation modelled the whole system from ground surface to the Medicine Hat Member whereas the second stage focused only on the Alderson Member, specifically the transition area between gas-bearing and water-bearing portions of the member, testing the potential for gas migration under commingled well abandonment conditions.

6.1 Single-Phase Modelling

A single-phase water-saturated steady state model was developed using MODFLOW2005 (McDonald and Harbaugh, 1988; Harbaugh, 2005), a finite-difference model of 3D groundwater flow. The iMOD (Vermeulen et al., 2018) graphical user interface (GUI) is used for input and output data processing.

6.1.1 Model Details

The case study area of approximately 95 956 km^2 was modelled using a 500 m cell size. Two vertical discretizations were used with the petrophysical property model being used differently in both cases. The first was a true layer approach whereas the second used the property modelling results directly for model parameterization. Initial details of the model setups are discussed in Appendix 2.

In brief, the model was constructed using a true layer approach. In the true layer approach, the model cells are arranged in layers and assigned variable thicknesses, elevations, and properties from the geological model. The thicknesses and elevations of the cells represent the structure of the stratigraphic bounding surfaces in the geological framework and the parameters are selected to be representative of the hydraulic properties of the rock volumes at that location and over that volume of rock. For some geological layers, a single cell spans the vertical thickness of the formation, whereas in others like the Milk River Formation and Alderson Member, the vertical thickness was discretized into multiple layers to capture hydraulic properties of interest. Such a trade-off of detail is often made in modelling; in order to be able to do the computations, the model needs to be simplified and this simplification is best done in the parts of lowest interest to the case study.

As the goal of the case study was to assess the risk of leakage of natural gas from the Alderson Member into the Milk River aquifer, the five different conceptual models representing possible Alderson gas reservoir and trap configurations needed to be embedded in the models while being consistent with property-model observations. The petrophysically derived parameters described above can be used directly to assign hydraulic properties to grid cells. In the direct-assignment approach, grid cells are assigned porosity, permeability, etc. values directly by point estimates from geostatistical estimation. That is, a value derived from well logs is used without any modification if present and if not, the geostatistical best-estimate is used based on neighbouring values.

However, the direct-assignment parameterization approach does not embed any geological or hydrogeological information or conceptualization about the geometry of rock beds, stratigraphic architecture, grain size, or texture. The practice of aquifer or reservoir characterization has developed in the past several decades in hydrogeology and petroleum engineering to make better predictions of subsurface fluid behaviour by incorporating geological knowledge in parameterization. An approach based on percolation theory was used in this case to modify simple point estimates of properties from well logs to grid-cell estimates of effective hydraulic properties that better represent the geological variability represented in alternative models of reservoir and trap configurations discussed above. Percolation theory states that in a binary mixture of rocks with contrasting properties, e.g., sandstone and mudstone or shale, the mixture will behave hydraulically like a sandstone if the sandstone volume exceeds a critical threshold, otherwise it will behave hydraulically like a mudstone or shale. Geological textures like laminations and beds will alter these thresholds, as does scale or persistence of discontinuous lenses of sandstone or mudstone bodies embedded in a matrix of the other.

To create an Alderson gas reservoir that was relatively discontinuous from the point estimates, a threshold was selected from the cumulative distribution of V_{sh} that resulted in the Alderson grid cells being 20% sandstone and 80% shale by volume. Any cell with an estimated V_{sh} that was less than this threshold was deemed to act hydraulically as sandstone in the model, otherwise they behaved hydraulically as a shale. Percolation theory states that in a random 3D mixture of two materials with contrasting permeability properties, one needs more than 20% of the permeable material to get connected pathways. Thus having 20% or less sandstone in the reservoir will help enforce an internally discontinuous arrangement of sandstone grid cells.

To create an Alderson gas reservoir that was relatively continuous internally from point estimates, a threshold was selected of log-derived V_{sh} that resulted in 40% of the Alderson grid blocks being sandstone and 60% shale by volume. Any cell with an estimated V_{sh} less than this was deemed to act hydraulically as a sandstone in this model, otherwise it would act as a mudstone or shale. Percolation theory states that in a random two-dimensional (2D) mixture of two materials of contrasting permeability, that having at least 40% of the more permeable mixture almost guarantees internal connectivity. As the Alderson Member in these models is discretized in three dimensions with multiple layers, the percolation threshold for internal continuity is around 20%; thus the internal reservoir continuity is really being enforced without making the Alderson Member dominantly sandstone in the model, which would not be geologically realistic.

For the numerical modelling a true layer model was built with 43 layers representing the units between the land surface and the Bow Island Formation as shown in Figure 3. Although the groundwater model had to honour the geology of the case study area, the particular focus of the modelling work was to assess changes in the Alderson Member and the Milk River Formation. In order to model groundwater flow in the proposed conceptual models, two elements of the conceptual models had to be approximated in keeping with the purpose of the groundwater modelling, as well as the results of the geological and petrophysical modelling: 1) one continuous reservoir versus several discontinuous reservoirs; and 2) the strength of the reservoir and boundary seals. To determine the extent of reservoir and nonreservoir rocks in the Alderson Member, the modelled permeability values for the unit were used. On cumulative distribution plots of permeability, two cutoffs were chosen to create two views of the distribution of reservoir and nonreservoir rocks. For the continuous reservoir case, property model cells with permeability values in the upper 40% of the range of permeability values for the Alderson Member were assigned to the reservoir category. Cells with permeabilities in the lower 60% were assigned to the seal category. For the discontinuous reservoir, the reservoir cutoff was set at the upper 20% of permeability values. Well completion details confirmed that these cutoffs were reasonable given how the gas resources were being produced. The horizontal and vertical permeability values used in the numerical model for sandstone and mudstone grid cells in the Alderson Member and for other layers in the model were based on the median of the permeability values from the property model for the modelled units, from literature values, or from earlier AGS work. For the units identified as aquifers in Figure 12, Alderson Member reservoirs and all other aquifer units were assigned an initial value of 4.32×10^{-2} m/d. Strong seals were assigned a value of 7.2×10^{-4} m/d; and weak seals were assigned a value of 2.9×10^{-3} m/d. Model fine tuning modified area-specific permeability values to achieve model stability and to give realistic results.

In the second direct-assignment modelling parameterization approach, the detailed property model was used to assign permeability values directly to the Milk River Formation and to the Alderson and Medicine Hat members from geostatistical point measurements derived from well logs. Permeability values for other layers were based on literature values or previous AGS work as described above.

A no-flow boundary condition was implemented in both model setups for all units along all edges, except for the Milk River Formation and Belly River Group along the Canada–United States border. A generalized head boundary along the border was applied based on mapped head data in the respective units. No-flow boundary conditions for other units can be justified based on thickening of low-permeability units along the case study area boundaries. A uniform net recharge (precipitation−evapotranspiration−runoff) was used for the simulations. The primary stress implemented in the numerical model was pumping from the shallower formations including the Milk River Formation (Figure 20).

6.1.2 Results

Figure 33 shows the cross plot of simulated versus observed hydraulic heads for the Milk River Formation wells in the case study area. Figure 34 shows the hydraulic head in the top layer (water table) and the hydraulic heads in three model layers (Belly River Group, Medicine Hat Member, and Bow Island / Viking formations). Results show that a topography-driven gravity flow system dominates in all the hydrostratigraphic units. The regional trend reflects the topography in general with higher heads in the foothills of the Rocky Mountains and topographically high regions discharging toward the northeast and to rivers. These patterns of flow are consistent with what is described in Section 5.1. Using the net recharge methodology the rivers are the only sink units in the model. Given the objective of the project and the first stage of numerical modelling, a detailed model calibration was not performed.

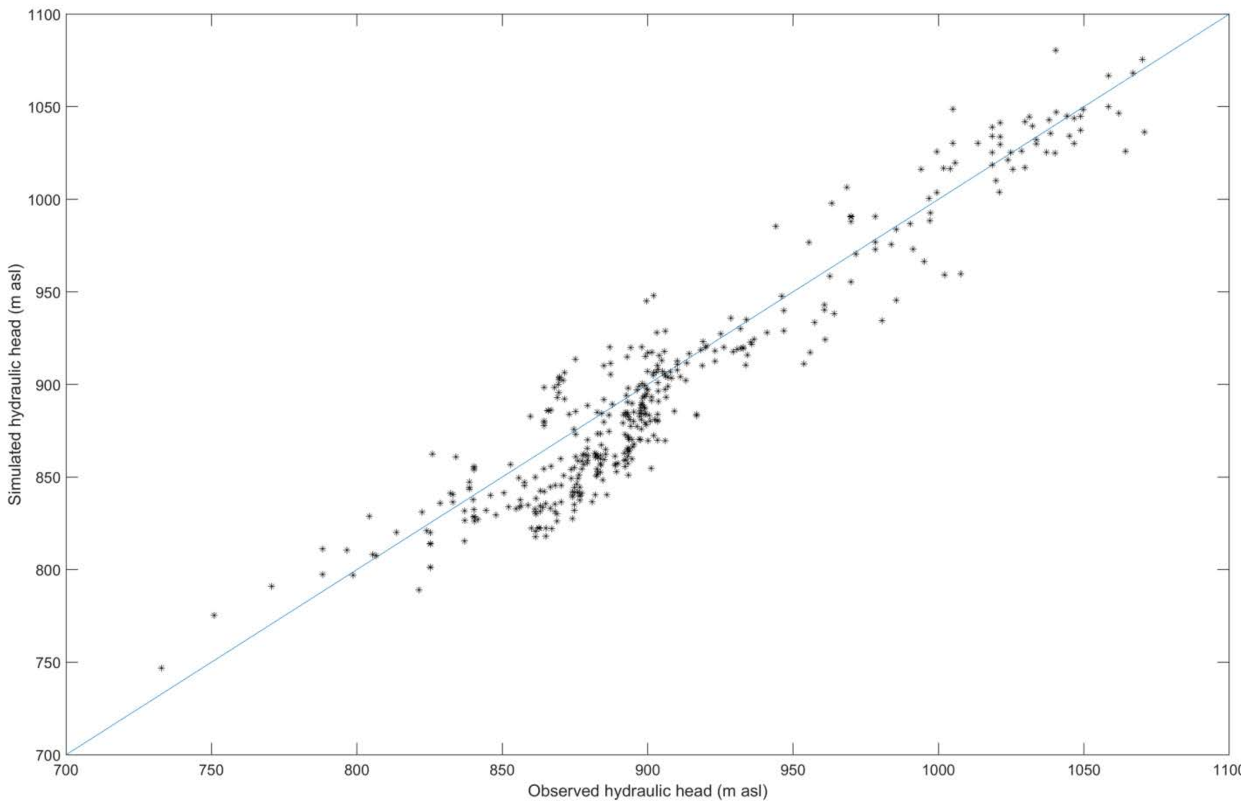

Figure 33. Cross-validation plots between the steady-state simulated hydraulic heads and the observed hydraulic heads for Milk River Formation wells, southeastern Alberta.

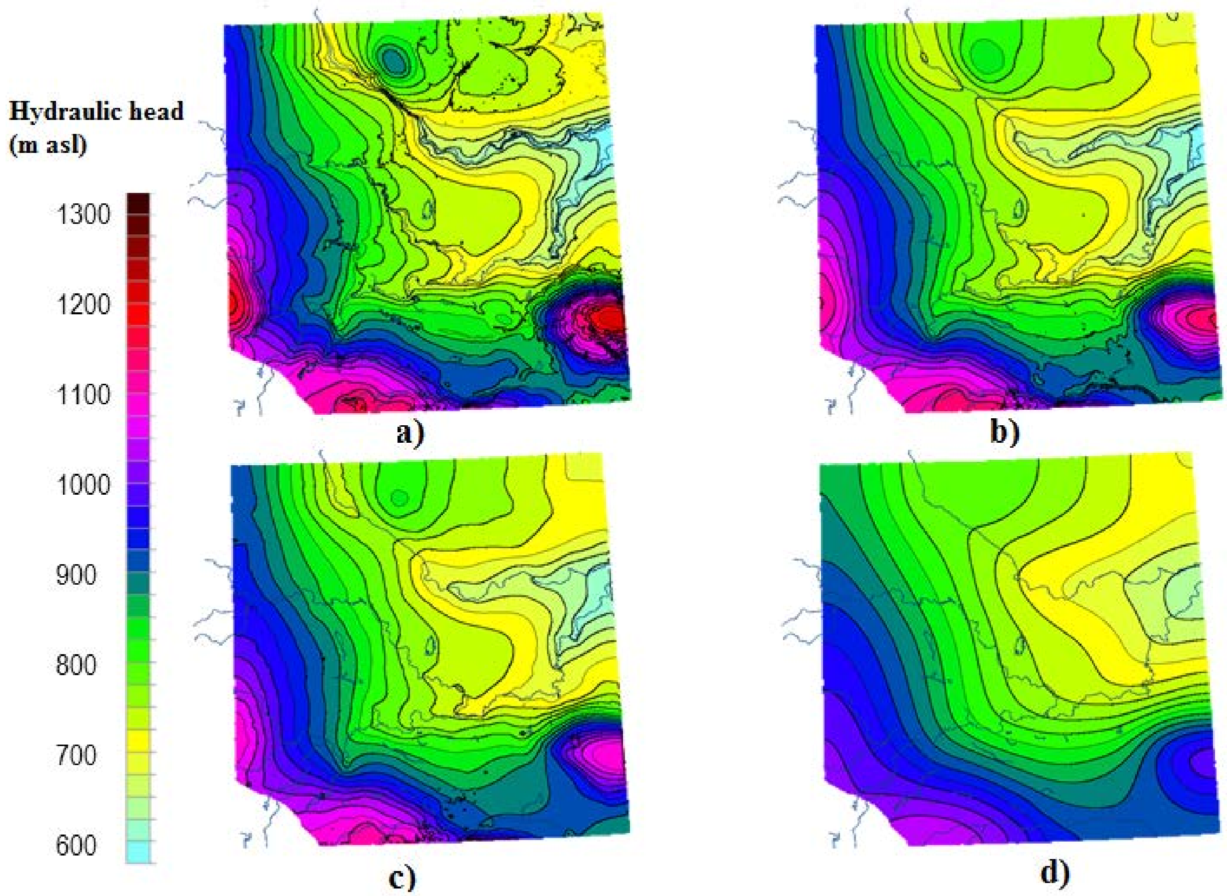

Figure 34. Hydraulic head in a) top layer (water table), b) Belly River Group, c) Medicine Hat Member, and d) Bow Island / Viking formations.

6.2 Multiphase Modelling

Two-phase air-water transport was simulated using the Subsurface Transport Over Multiple Phases (STOMP; White and Oostrom, 2006; White et al., 2015) modelling package released by Pacific Northwest National Laboratory. STOMP is a sequential numerical simulator for modelling multifluid and multiphase flow and transport through geological media. STOMP is an integrated-volume finite-difference model based on the Richards equation (Bear, 1972) and the relations developed by Lenhard and Parker (1987) and Kaluarachchi and Parker (1990). The capillary pressure-saturation relationships can be chosen from different empirical relationships. This case study uses the van Genuchten (1980) capillary pressure saturation relationship.

6.2.1 Multiphase Modelling Setup

Multiphase flow simulations for this case study were run to simulate potential multiphase flow 500 to 5000 years into the future once gas production has ceased in the gas field. The high computational expense of a fully three-dimensional (3D) multiphase simulation led to the decision to focus the modelling on a 2D cross-section in the study area. Figure 35 shows the location of the cross-section chosen for this case study. The area of pink represents the southeastern Alberta gas field and the black outline represents the extent of the Milk River Formation. Given the purpose of the modelling, the modelled section also focused exclusively on the Alderson Member. The discretization implemented for the model was 500 m (horizontal) to 5 m (vertical). The starting pressure conditions for the conceptual models were imported from the 3D single-phase model.

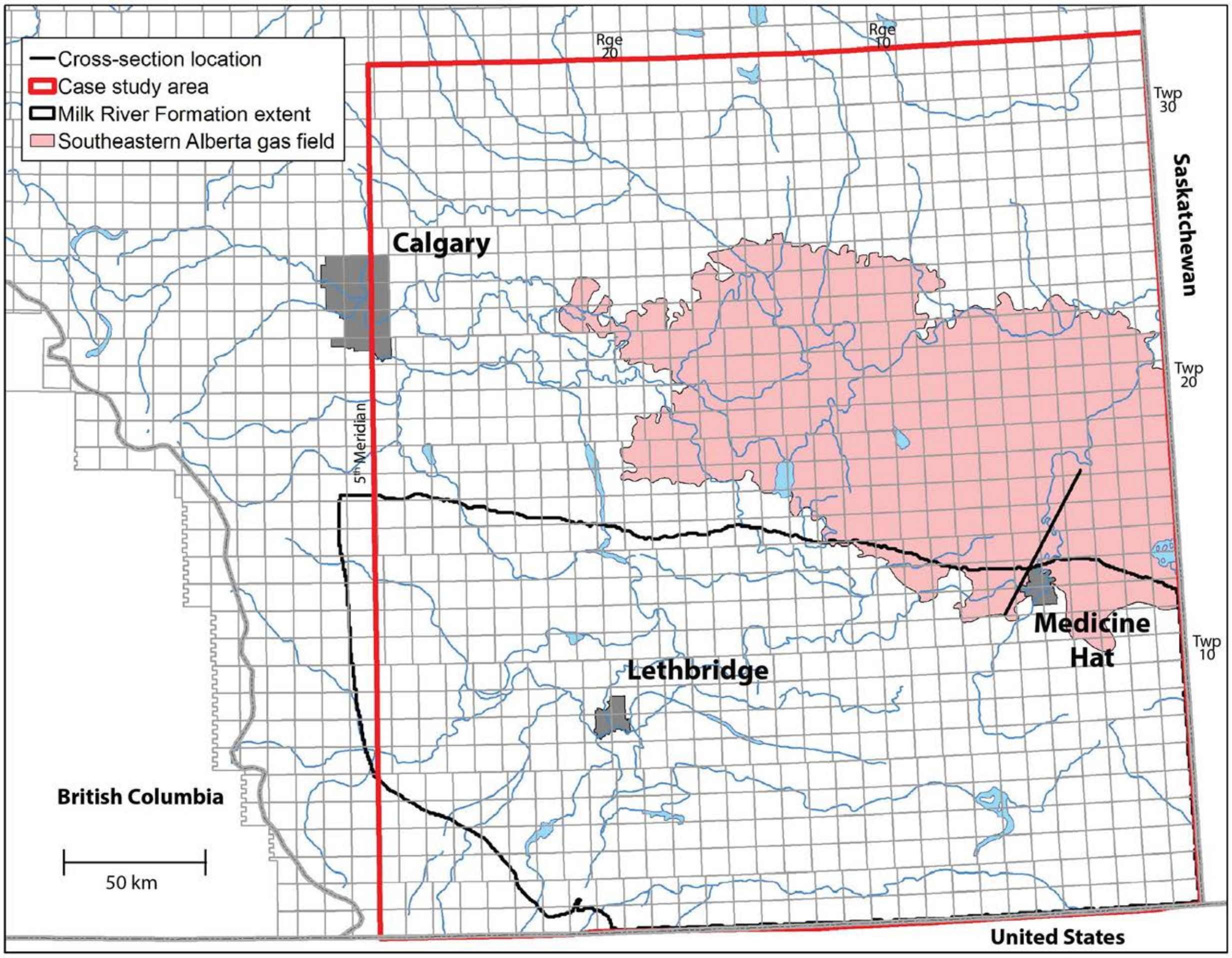

Figure 35. Location of the two-dimensional cross-section chosen for the two-phase air-water simulation.

6.2.2 Conceptual Models to Numerical Models

For any simulation model, groundwater or otherwise, the conceptualized system being simulated needs to be expressed in a grid-based discretized form. This section explains how the property model and hydrocarbon production history for the case study area were used to discretize the conceptual models. The property model was used to define uniform property zones. Overlaying gas well completion information helped define two potential reservoir conceptual models, the single and multiple reservoir models. The properties of these zones were parameterized based on literature (van Genuchten, 1980; Carsel and Parrish, 1988) and the petrophysical analysis with subsequent 3D modelling.

Table 2 highlights the major differences among the alternative conceptual models. The two different reservoir concepts were discretized differently. These discretizations were parameterized to simulate all alternative conceptual models.

Figure 36 shows the implemented discretization schema for the two different reservoir systems. Figure 36a shows the porosity cross-section along the chosen section overlaid by the perforations within 30 m of the section. Figure 36b shows the schema for the connected reservoir system used for simulating conceptual models 1 and 2. Figure 36c shows the schema for the disconnected reservoir system used for simulating conceptual models 3, 4, and 5. For the parameters or the rock properties at the intraformational or smaller scale, the lithology-associated property was estimated from petrophysical modelling and literature. Table 3 lists these parameters for simulating the conceptual models.

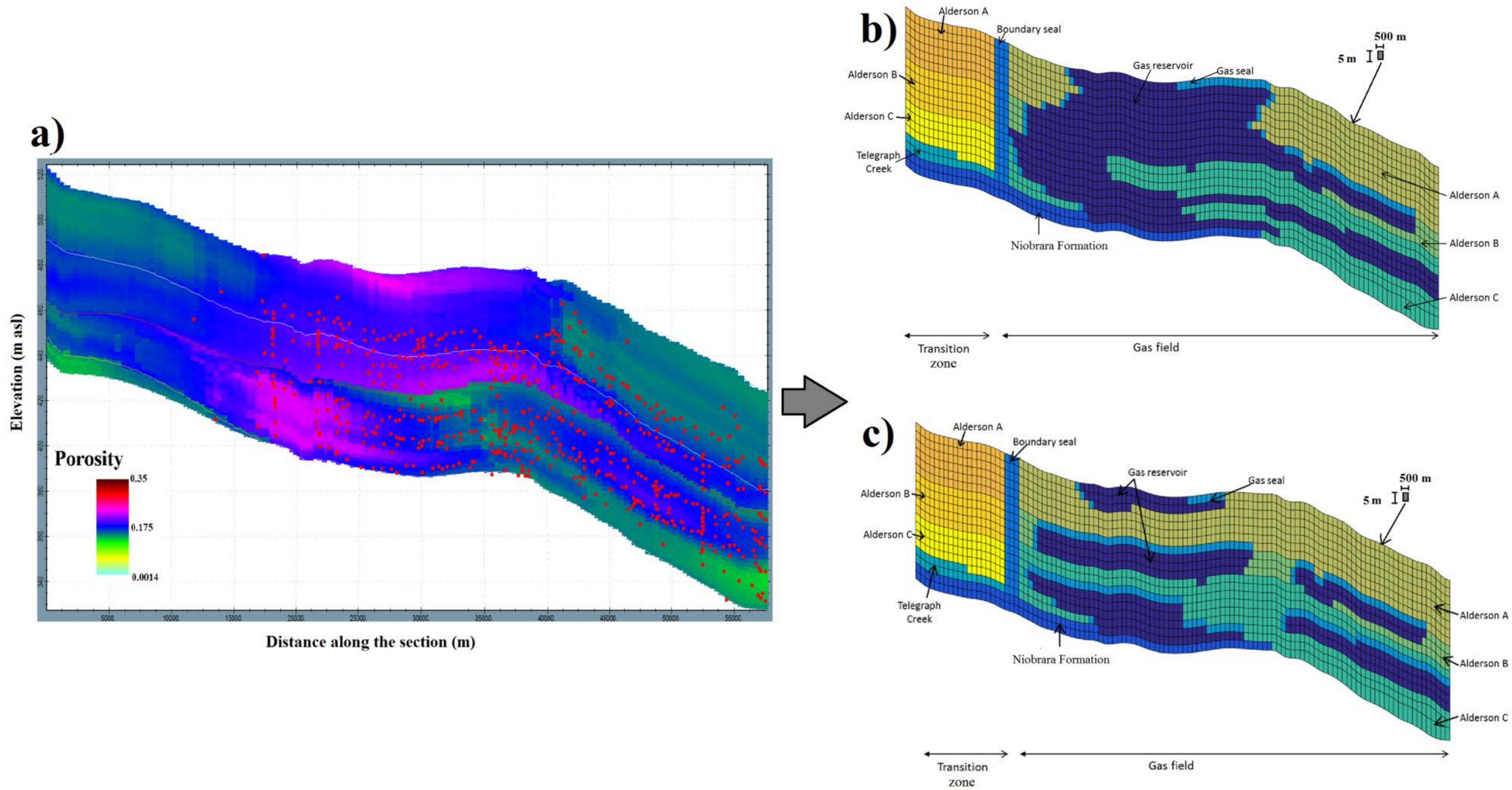

Figure 36. Model discretization: a) porosity cross-section with perforations within 30 m of the section; b) connected reservoir system for conceptual models 1 and 2; c) disconnected reservoir system for conceptual models 3, 4, and 5. Line of cross-section is shown in Figure 35.

Table 3. Porosity and permeability parameterization for alternative conceptual model simulation highlighted for strong and weak seals. Abbreviation: mD, millidarcy.

	Model 1		Model 2		Model 3		Model 4		Model 5	
	Connected reservoir, strong seals, Alderson sandstone persists to the north		Connected reservoir, strong seals, Alderson sandstone localized to the south		Disconnected reservoir, strong seals, Alderson sandstone localized to the south		Disconnected reservoir, strong seals, Alderson sandstone persists to the north		Disconnected reservoir, weak seals, Alderson sandstone persists to the north	
	Porosity	**Permeability(mD)**	**Porosity**	**Permeability(mD)**	**Porosity**	**Permeability(mD)**	**Porosity**	**Permeability(mD)**	**Porosity**	**Permeability(mD)**
Reservoir	0.2	5.87	0.2	5.87	0.2	5.87	0.2	5.87	0.2	5.87
Reservoir seal	0.12	6.80E-02	0.03	4.60E-04	0.03	4.60E-04	0.03	4.60E-04	0.12	6.80E-02
Boundary seal	0.03	4.60E-04	0.03	4.60E-04	0.03	4.60E-04	0.03	4.60E-04	0.12	6.80E-02
Alderson A[1]	0.1	2.30E-02	0.1	2.30E-02	0.1	2.30E-02	0.1	2.30E-02	0.1	2.30E-02
Alderson B[1]	0.1	2.30E-02	0.1	2.30E-02	0.1	2.30E-02	0.1	2.30E-02	0.1	2.30E-02
Alderson C[1]	0.1	2.30E-02	0.1	2.30E-02	0.1	2.30E-02	0.1	2.30E-02	0.1	2.30E-02
Colorado Group shale	0.03	4.60E-04	0.03	4.60E-04	0.03	4.60E-04	0.03	4.60E-04	0.03	4.60E-04
Transition zone	0.15	0.36					0.15	0.36	0.15	0.36

[1] see Figures 25, 26, 27, 28, and 29

6.2.3 Model Scenarios: Predevelopment and Commingled Conditions

Hydrogeological modelling for this case study focused on evaluating the risk of migration of natural gas through the Alderson Member to the geologically adjacent Milk River Formation if commingled abandonment of wells in the southeastern Alberta gas field is widely allowed. Since the Milk River Formation is a primary source of groundwater in southern Alberta, if gas were to migrate into the Milk River Formation the groundwater supply in the region could be degraded. The assessment used a numerical model to evaluate two scenarios that tested system behaviour under predevelopment (discovery) conditions and then under commingled conditions. The first scenario simulated the system behaviour prior to any gas development. In this scenario, the water pressure profile was imported from the single-phase model and used parameterization such that it could hold gas in place (within reservoir) with very short columns. A pressure elevation (PE or PZ) analysis was used to approximate the gas column heights. Typically, the gas column height represents the elevation difference between the gas-pressure recorder and the intersection of a gas density gradient projected down to the local waterline, which was calculated from pressure and elevation data for the geological units in that region. Local pressure conditions can mean that this line might not fall on a typical hydrostatic gradient. This case study used the top of a member to calculate the gas column height instead of the recorder elevation as recorders can be located throughout the drill-string (sometimes above and or below the testing interval). Figure 37 shows the gas gradient values used in the gas column height calculation for the Alderson Member, the drillstem test (DST) locations along with the respective pressure-elevation plot. Similarly, Figure 38 shows the gas gradient lines used in the analysis for the Medicine Hat Member. Table 4 summarizes the calculated gas column heights for the Alderson and Medicine Hat members. The red values in Table 4 highlight the regions where the entire member is gas saturated. The table also shows that the minimum gas column height for the Alderson Member is approximately 12.4 m whereas the maximum combined gas column height for the Alderson and Medicine Hat members is estimated to be approximately 170 m (extreme scenario of gas column, which is the sum of red values within gas saturated members).

Under discovery conditions, the 10 m high gas column as discussed in Chen et al. (2015) was implemented for the model, as it is a part of the model ensembles and is approximately the same as the value calculated above (12.4 m). Under the commingled well abandonment scenario, the water pressure profile was again imported from the single-phase model but a 230 m high gas column pressure buildup was implemented for the gas pressure profile instead of the calculated 117.3 m gas column height from the pressure elevation analysis. The 230 m gas column height reflects the worst case estimate of gas buildup, which coincides with the maximum elevation difference between the Medicine Hat Member and the Alderson Member. The commingled scenario assumes a sudden 230 m gas column buildup, which is extremely unlikely given the long production history in the gas field and the resulting decrease in pressure in the commingled reservoirs. Figure 39 shows the starting pressure profiles along the cross-section under the discovery conditions with gas column height (relative pressure jump in Figure 39b as compared to Figure 39a being the only difference between the predevelopment and commingled conditions). Groundwater pumping from the Milk River Formation was incorporated by applying a 100 m drawdown boundary condition on the southern end of the section. The assessment of groundwater production through time suggests that a 100 m drawdown very much represents a worst condition drawdown scenario.

Table 4. Calculated gas column heights (in m) for the Alderson and Medicine Hat members. Locations shown on Figure 37.

Location	Alderson	Medicine Hat
1	20.1	15
2	41.2	51
3	12.4	28
4	117.3	

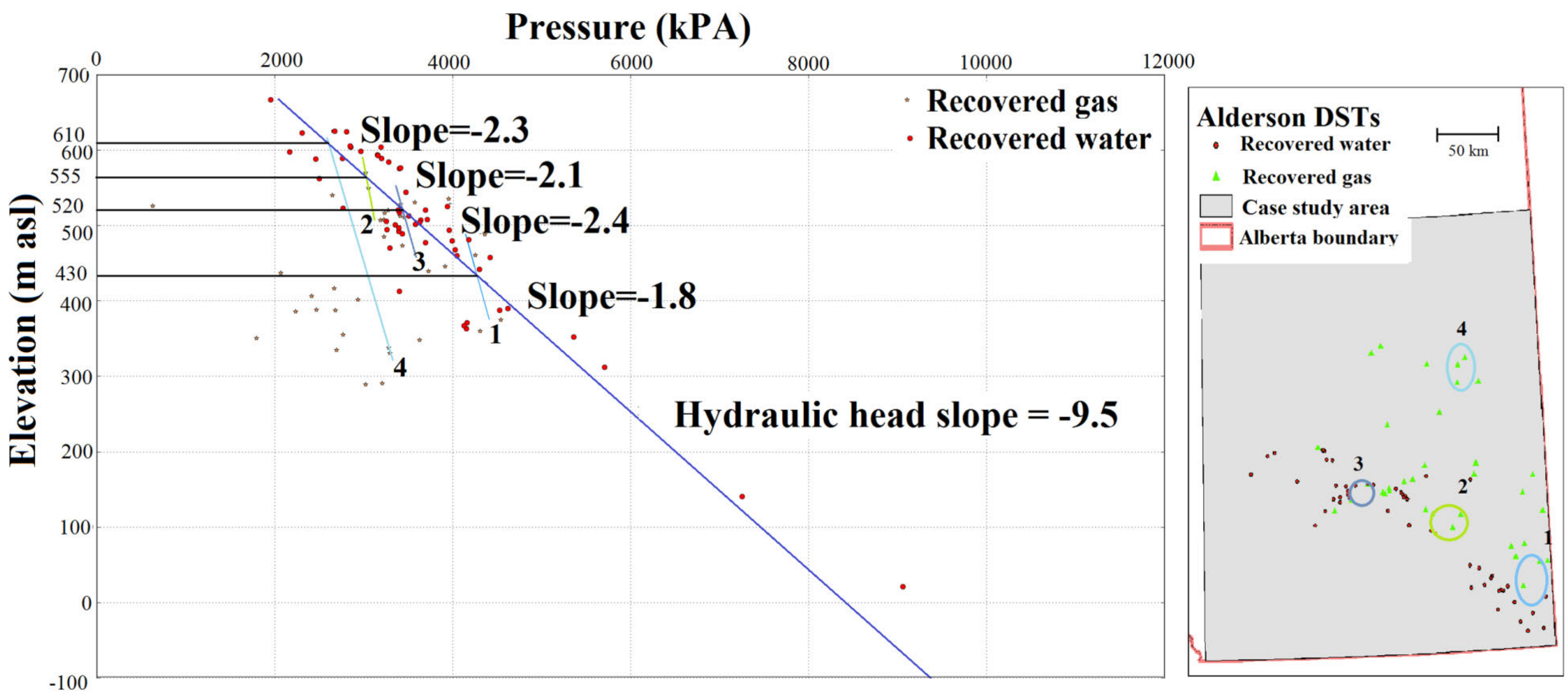

Figure 37. Pressure-elevation analysis for the drillstem tests (DSTs) in the Alderson Member. Numbered locations on the chart correspond to the numbered locations on the map and were used in gas column height calculations.

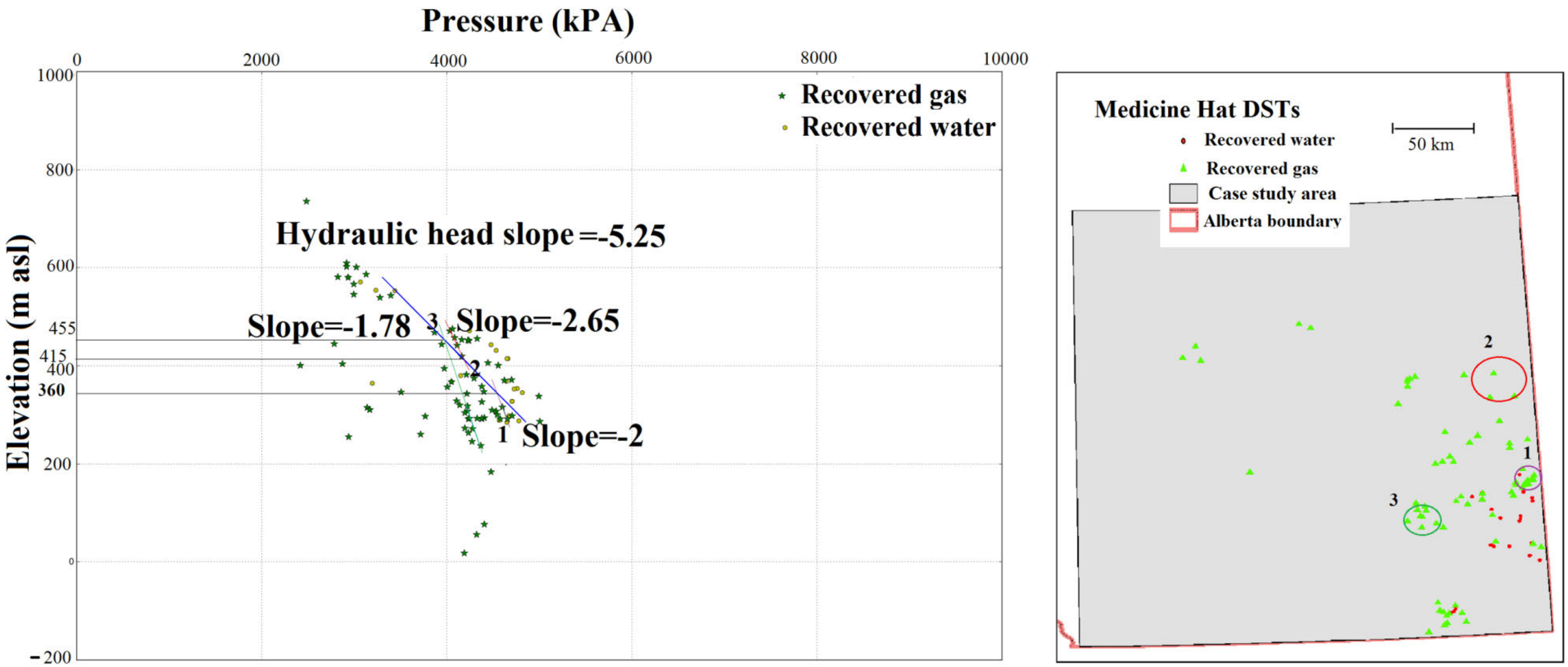

Figure 38. Pressure-elevation analysis for the drillstem tests (DSTs) in the Medicine Hat Member. Numbered locations on the chart correspond to the numbered locations on the map and were used in gas column height calculations.

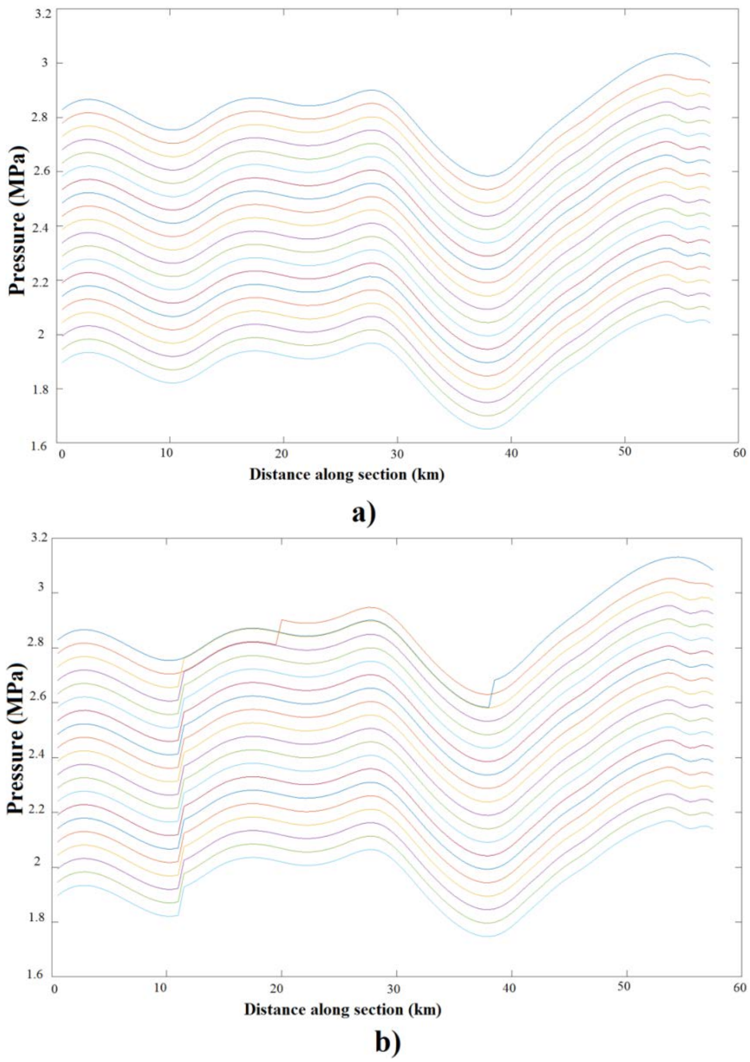

Figure 39. Initial pressure conditions along cross-section (see Figure 35 for location): a) water pressure conditions, and b) gas pressure conditions displaying 10 m gas column height.

6.2.4 Results

The results of the two-phase STOMP model were evaluated using air concentration/saturation profiles along the cross-section and breakthrough curves at specific locations along the cross-section. Both the models were run under discovery and commingled scenarios for 5000 years following abandonment with a constant groundwater-pumping effect (100 m hydraulic head drop at the southern end [left side] of the section). Figures 40 and 41 show gas migration for the conceptual models of a connected reservoir under discovery conditions and Figures 42, 43, and 44 show gas migration for the conceptual models of a disconnected reservoir under discovery conditions. Figures 45 and 46 show gas migration for the conceptual models of a connected reservoir under commingled conditions and Figures 47, 48, and 49 show gas migration for the conceptual models of a disconnected reservoir under commingled conditions. Results show that commingling creates a slight increase in gas saturation near the southern edge over the simulated 5000 years. Model 5 displays higher saturations than the other four models with no effects felt at 6 km south of the reservoir in 5000 years. The results show that the shaly nature of the Alderson Member lessens the effects of even an exaggerated groundwater pumping boundary condition suggesting that the Alderson Member behaves as an effective seal and aquitard.

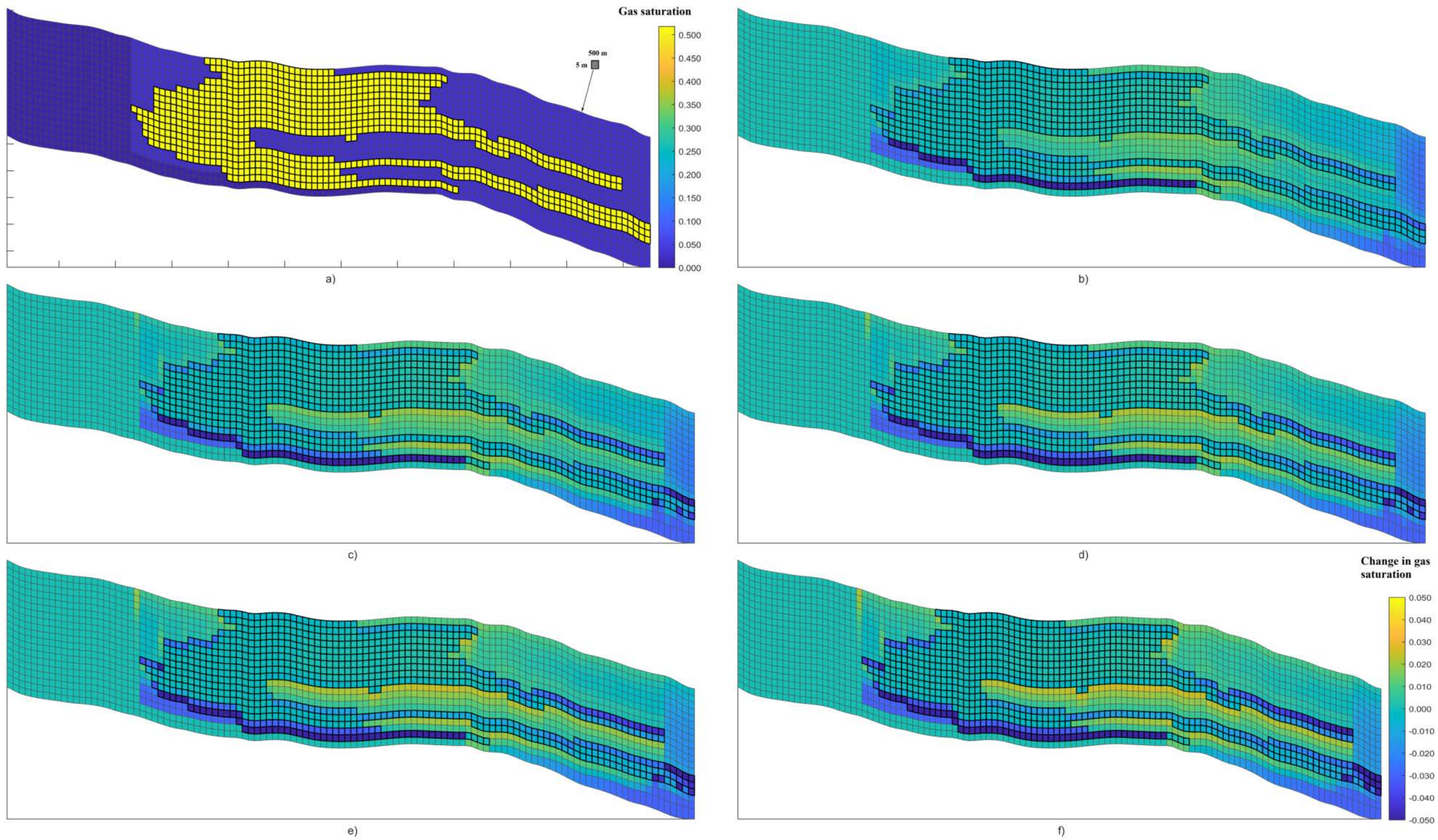

Figure 40. Gas migration for model 1 (connected reservoir, strong seals, Alderson sandstone persists to the north) under discovery conditions: a) initial gas saturation profile, b) gas saturation change in 1000 years, c) gas saturation change in 2000 years, d) gas saturation change in 3000 years, e) gas saturation change in 4000 years, f) gas saturation change in 5000 years. Gas saturation changes in b) to f) are plotted with same colour scale; see legend in f). Line of cross-section shown in Figure 35.

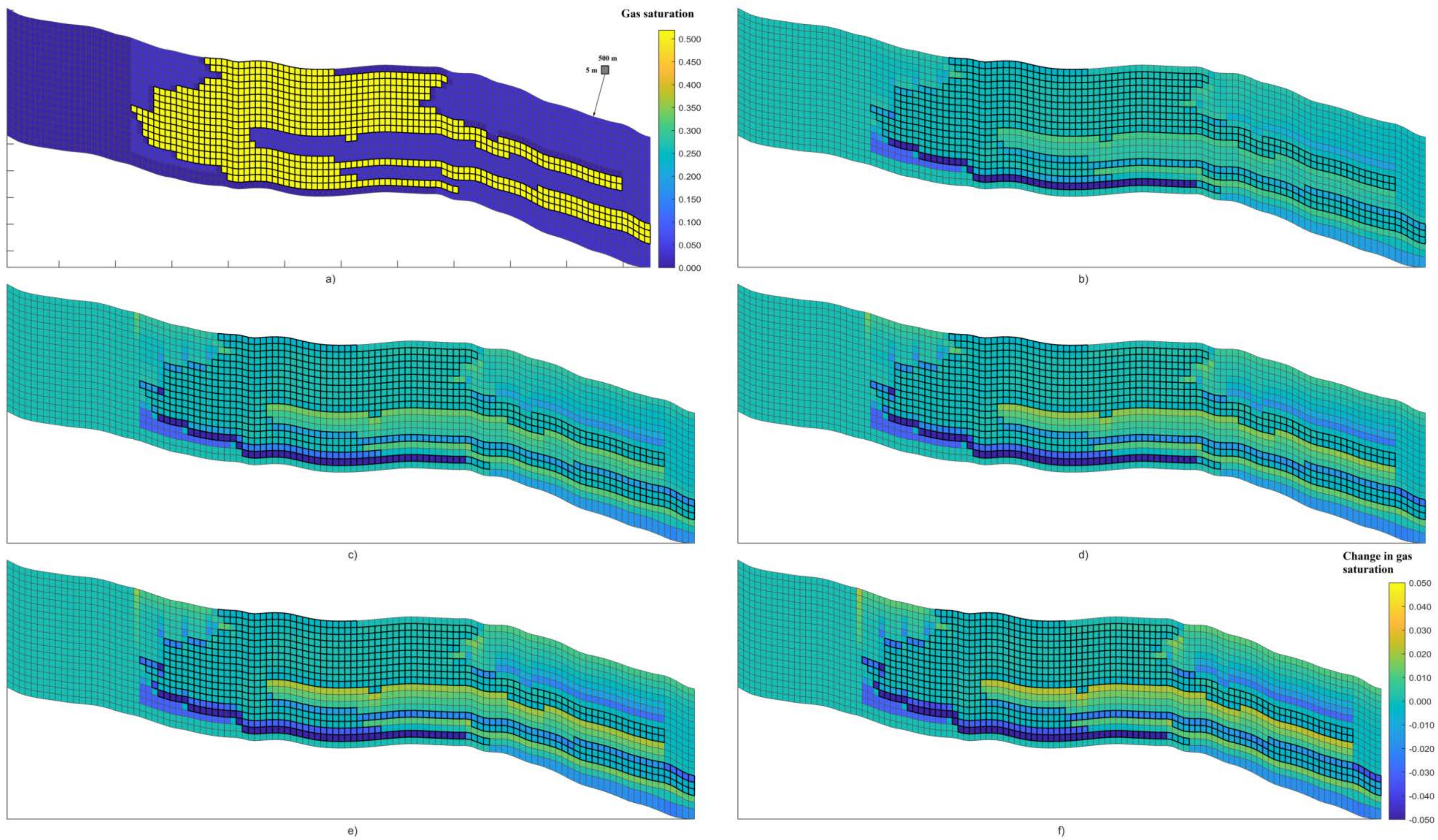

Figure 41. Gas migration for model 2 (connected reservoir, strong seals, Alderson sandstone localized to the south) under discovery conditions: a) initial gas saturation profile, b) gas saturation change in 1000 years, c) gas saturation change in 2000 years, d) gas saturation change in 3000 years, e) gas saturation change in 4000 years, f) gas saturation change in 5000 years. Gas saturation changes in b) to f) are plotted with same colour scale; see legend in f). Line of cross-section shown in Figure 35.

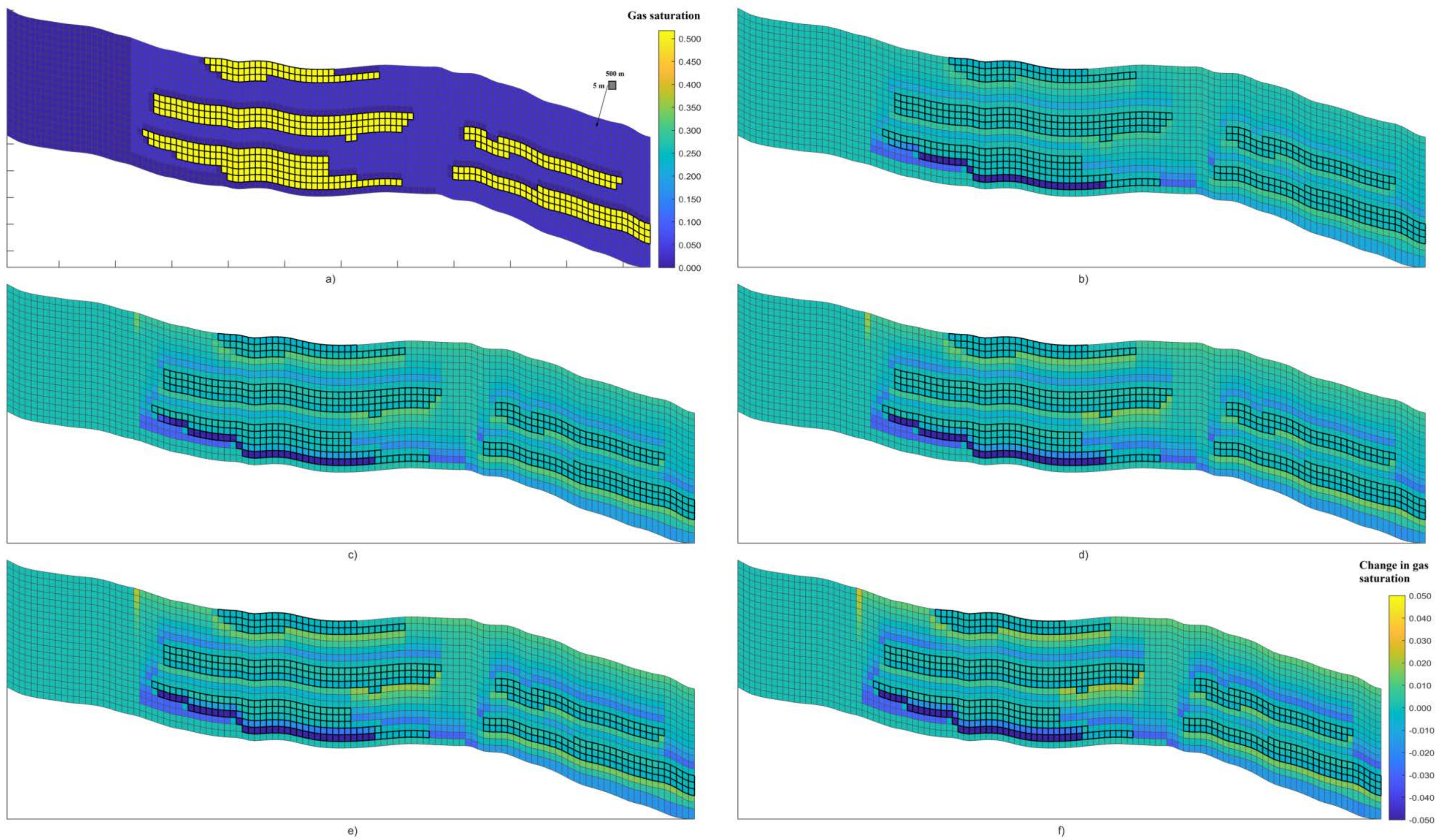

Figure 42. Gas migration for model 3 (disconnected reservoir, strong seals, Alderson sandstone localized to the south) under discovery conditions: a) initial gas saturation profile, b) gas saturation change in 1000 years, c) gas saturation change in 2000 years, d) gas saturation change in 3000 years, e) gas saturation change in 4000 years, f) gas saturation change in 5000 years. Gas saturation changes in b) to f) are plotted with same colour scale; see legend in f). Line of cross-section shown in Figure 35.

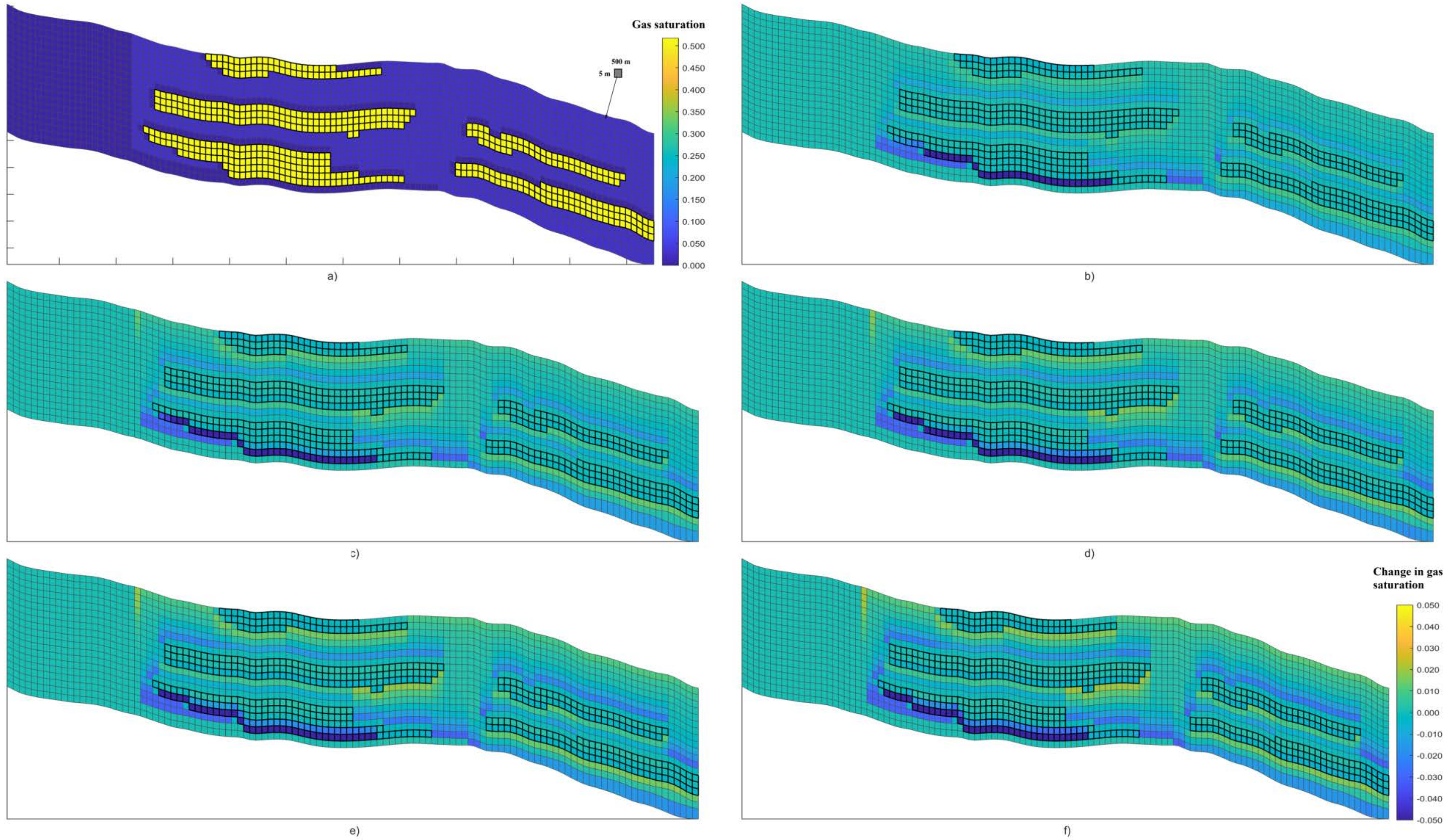

Figure 43. Gas migration for model 4 (disconnected reservoir, strong seals, Alderson sandstone persists to the north) under discovery conditions: a) initial gas saturation profile, b) gas saturation change in 1000 years, c) gas saturation change in 2000 years, d) gas saturation change in 3000 years, e) gas saturation change in 4000 years, f) gas saturation change in 5000 years. Gas saturation changes in b) to f) are plotted with same colour scale; see legend in f). Line of cross-section shown in Figure 35.

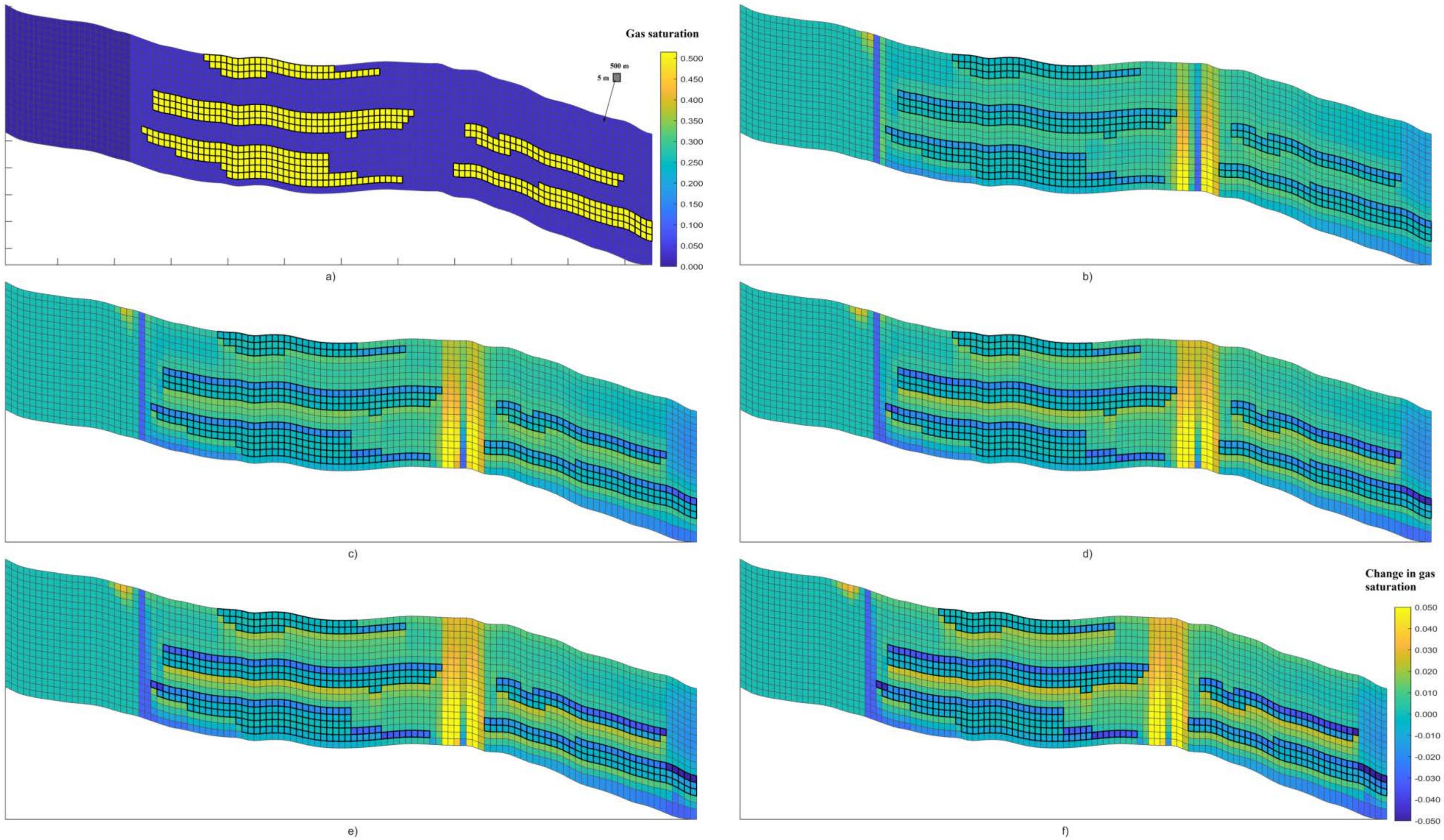

Figure 44. Gas migration for model 5 (disconnected reservoir, weak seals, Alderson sandstone persists to the north) under discovery conditions: a) initial gas saturation profile, b) gas saturation change in 1000 years, c) gas saturation change in 2000 years, d) gas saturation change in 3000 years, e) gas saturation change in 4000 years, f) gas saturation change in 5000 years. Gas saturation changes in b) to f) are plotted with same colour scale; see legend in f). Line of cross-section shown in Figure 35.

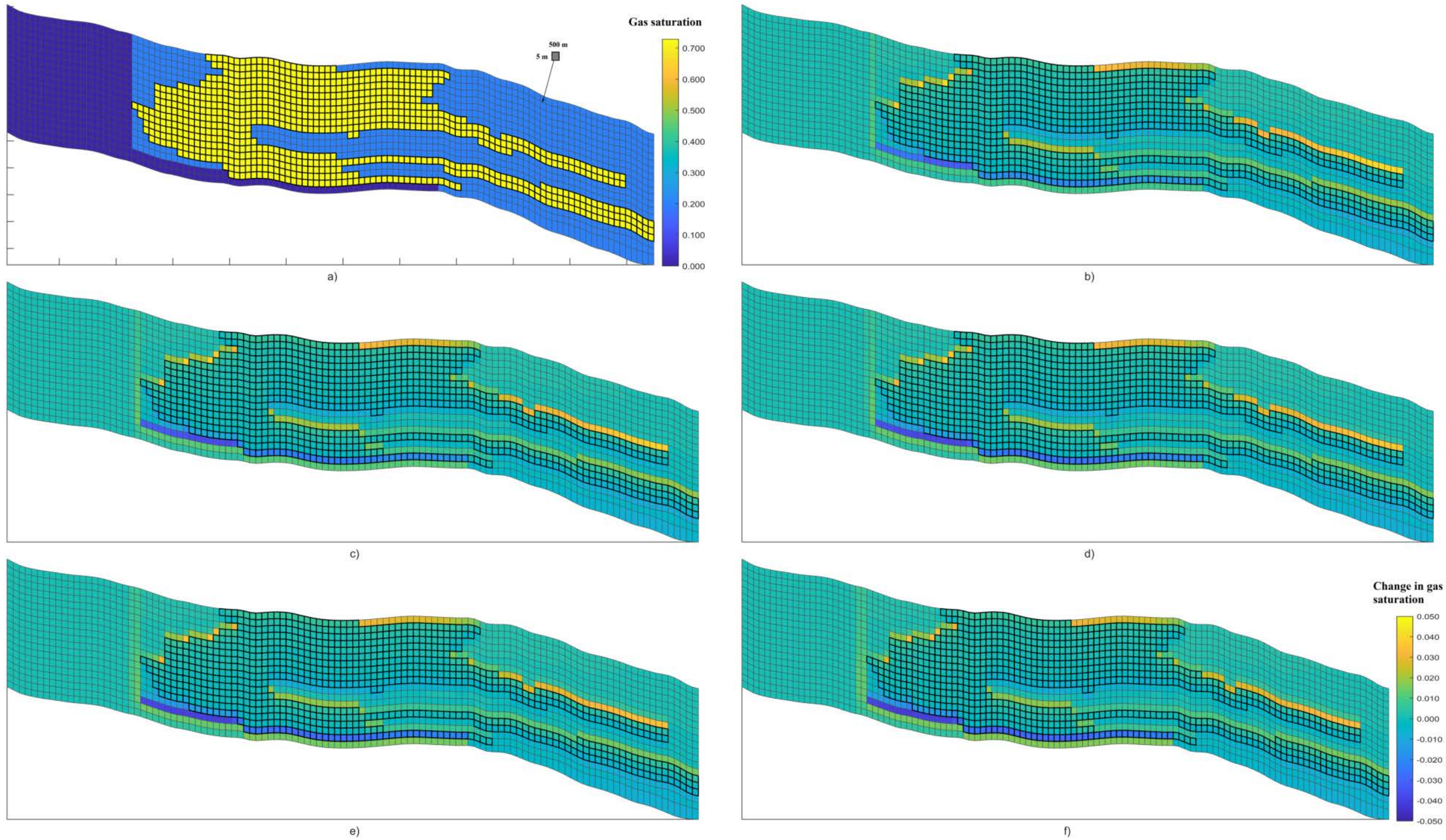

Figure 45. Gas migration for model 1 (connected reservoir, strong seals, Alderson sandstone persists to the north) under commingled conditions: a) initial gas saturation profile, b) gas saturation change in 1000 years, c) gas saturation change in 2000 years, d) gas saturation change in 3000 years, e) gas saturation change in 4000 years, f) gas saturation change in 5000 years. Gas saturation changes in b) to f) are plotted with same colour scale; see legend in f). Line of cross-section shown in Figure 35.

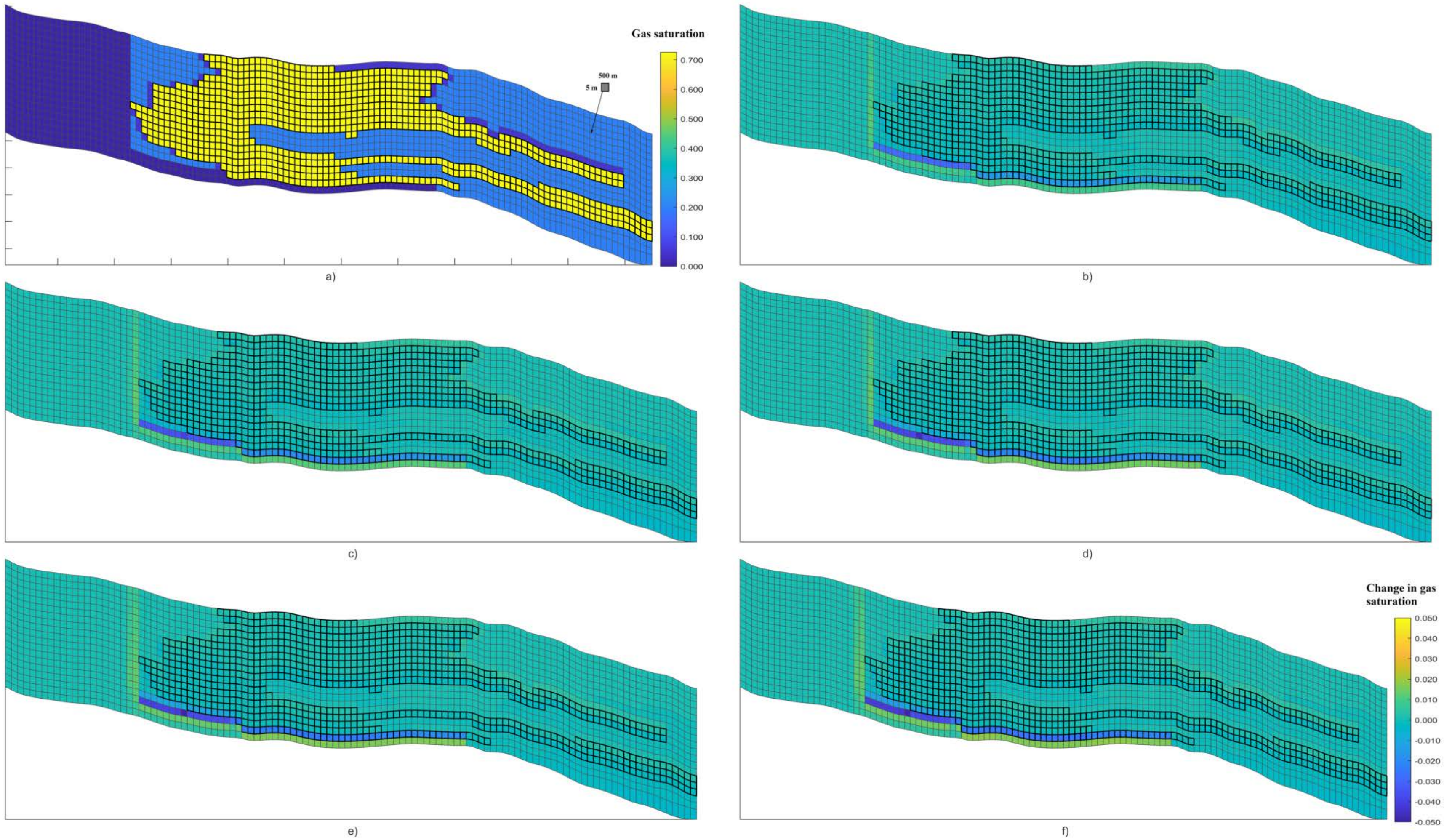

Figure 46. Gas migration for model 2 (connected reservoir, strong seals, Alderson sandstone localized to the south) under commingled conditions: a) initial gas saturation profile, b) gas saturation change in 1000 years, c) gas saturation change in 2000 years, d) gas saturation change in 3000 years, e) gas saturation change in 4000 years, f) gas saturation change in 5000 years. Gas saturation changes in b) to f) are plotted with same colour scale; see legend in f). Line of cross-section shown in Figure 35.

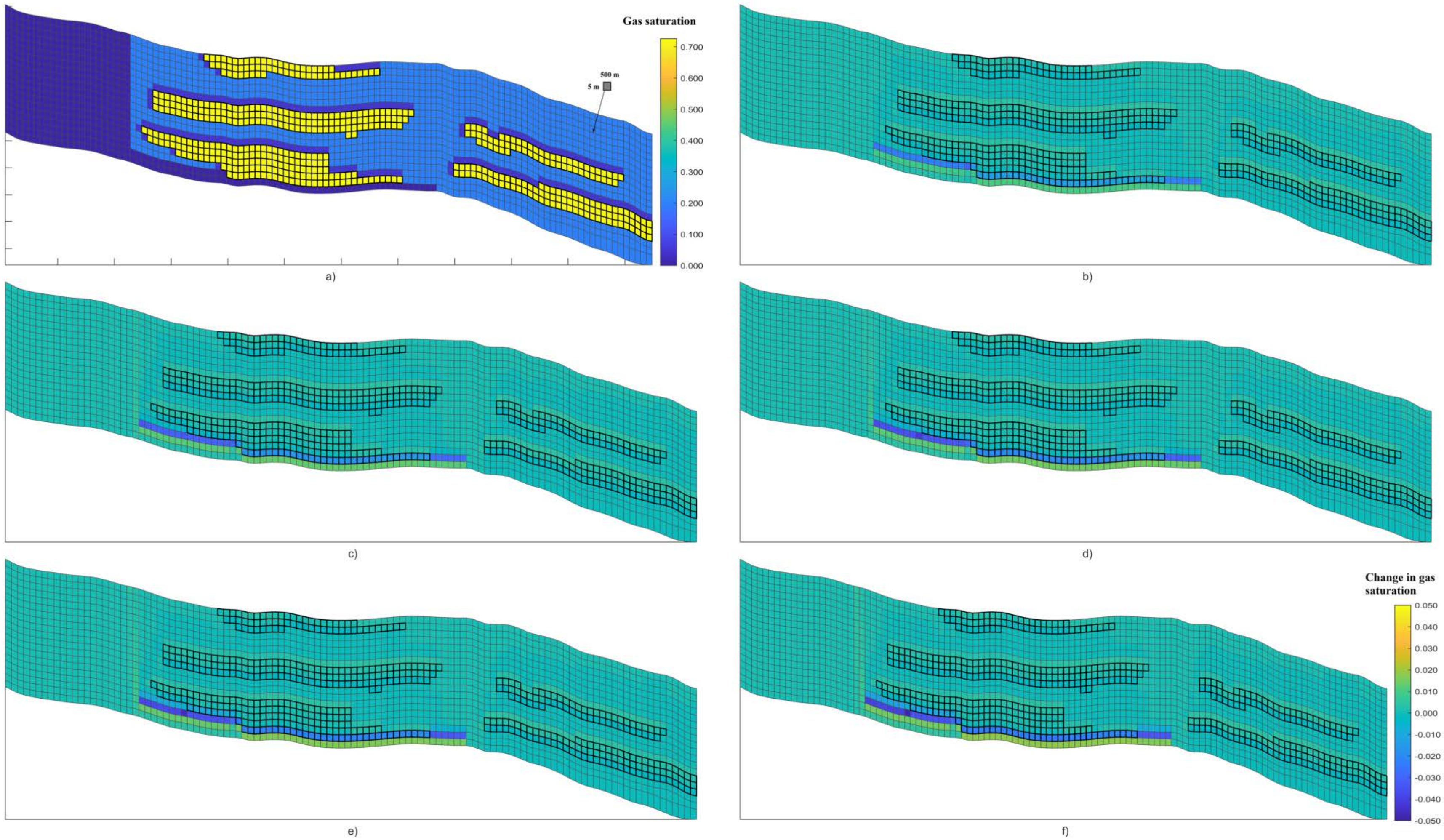

Figure 47. Gas migration for model 3 (disconnected reservoir, strong seals, Alderson sandstone localized to the south) under commingled conditions: a) initial gas saturation profile, b) gas saturation change in 1000 years, c) gas saturation change in 2000 years, d) gas saturation change in 3000 years, e) gas saturation change in 4000 years, f) gas saturation change in 5000 years. Gas saturation changes in b) to f) are plotted with same colour scale; see legend in f). Line of cross-section shown in Figure 35.

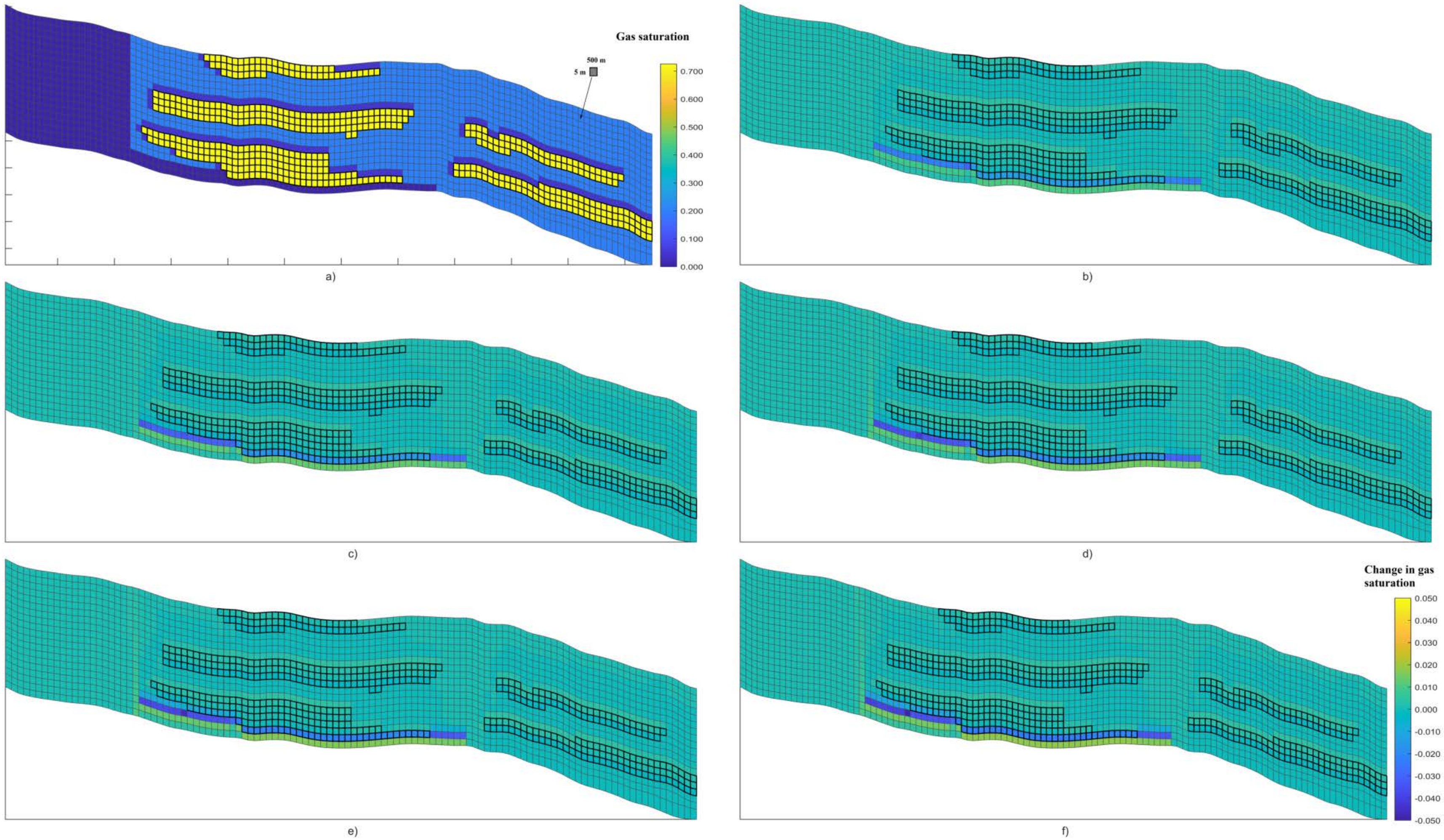

Figure 48. Gas migration for model 4 (disconnected reservoir, strong seals, Alderson sandstone persists to the north) under commingled conditions: a) initial gas saturation profile, b) gas saturation change in 1000 years, c) gas saturation change in 2000 years, d) gas saturation change in 3000 years, e) gas saturation change in 4000 years, f) gas saturation change in 5000 years. Gas saturation changes in b) to f) are plotted with same colour scale; see legend in f). Line of cross-section shown in Figure 35.

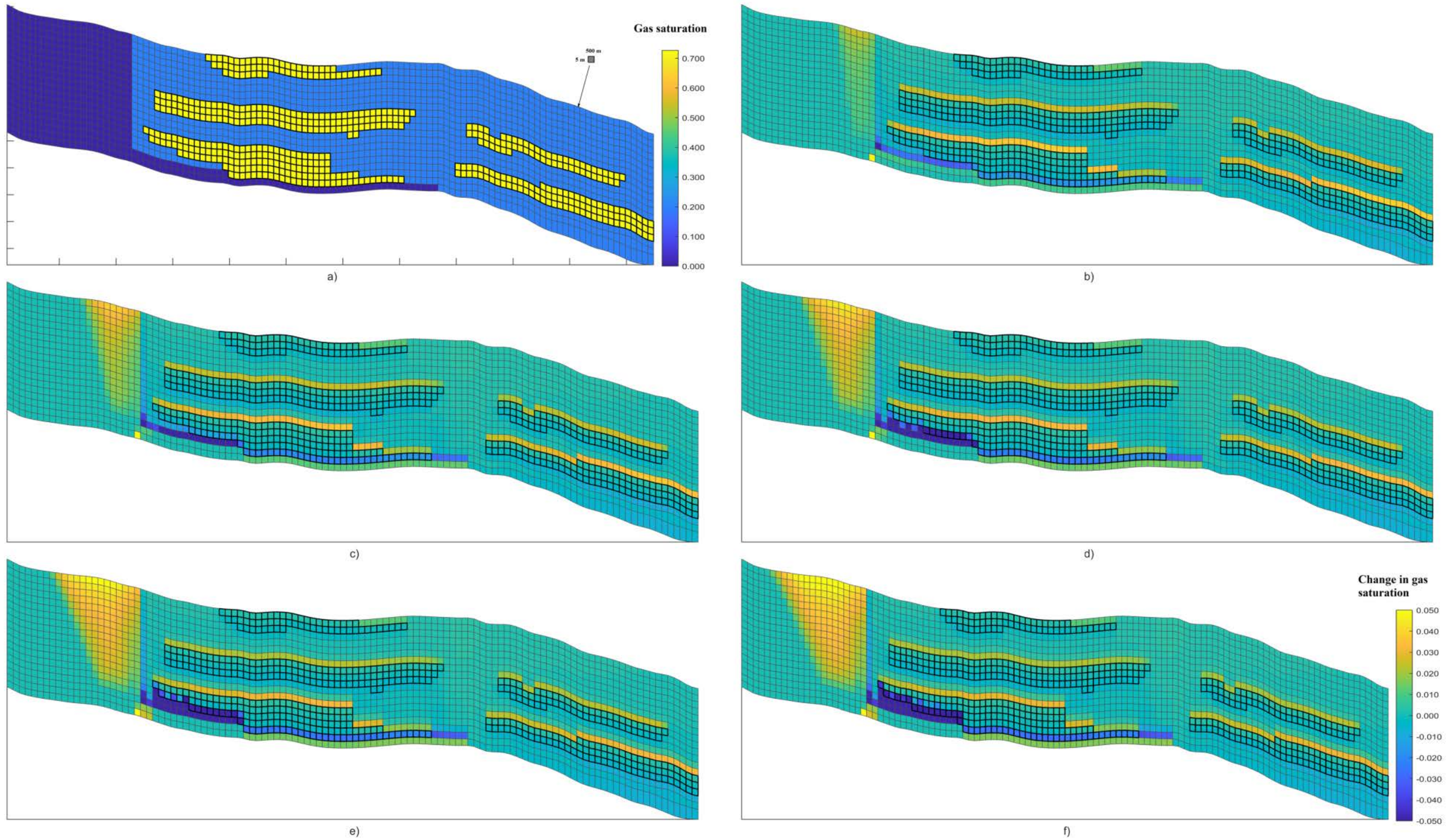

Figure 49. Gas migration for model 5 (disconnected reservoir, weak seals, Alderson sandstone persists to the north) under commingled conditions: a) initial gas saturation profile, b) gas saturation change in 1000 years, c) gas saturation change in 2000 years, d) gas saturation change in 3000 years, e) gas saturation change in 4000 years, f) gas saturation change in 5000 years. Gas saturation changes in b) to f) are plotted with same colour scale; see legend in f). Line of cross-section shown in Figure 35.

The simulation results were also analyzed in terms of breakthrough curves. The purpose of the curves was to represent the change in concentrations at three depths at one location. The curves show these changes in concentration over the simulated time period for each of the five conceptual models under both the discovery and commingled abandonment scenarios. The three vertical observation points chosen for describing the change in concentration for the curves are approximately 50 km from the Milk River Formation boundary (Figure 50). The observation points were chosen within the boundary seal so that potential gas migration out of the petroleum system can be observed. The plots (Figures 51, 52, 53, 54, and 55) show the concentration profiles at the three observation points (Figure 50 shows the location of points) at the chosen location. The results show that for models 1, 2, 3, and 4, the gas behaviour is almost static with a slight increase in concentrations at 1 km south of the gas reservoir after approximately 2000 to 3000 years. For model 5 under commingled conditions, the effects 1 km south of the gas reservoir are felt after 1000 years.

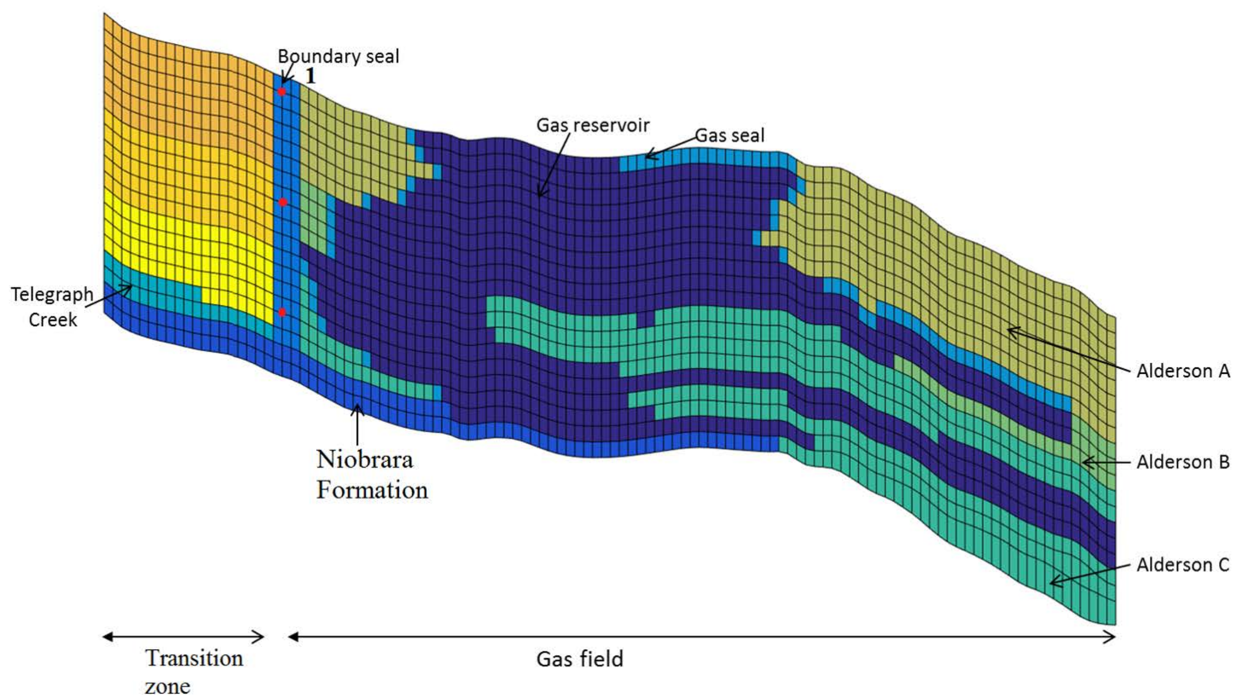

Figure 50. Breakthrough curve points (red) at section 50 km from the Milk River Formation boundary (three vertical observation points). The 1 indicates the point location for the breakthrough curves (Figures 51, 52, 53, 54, and 55).

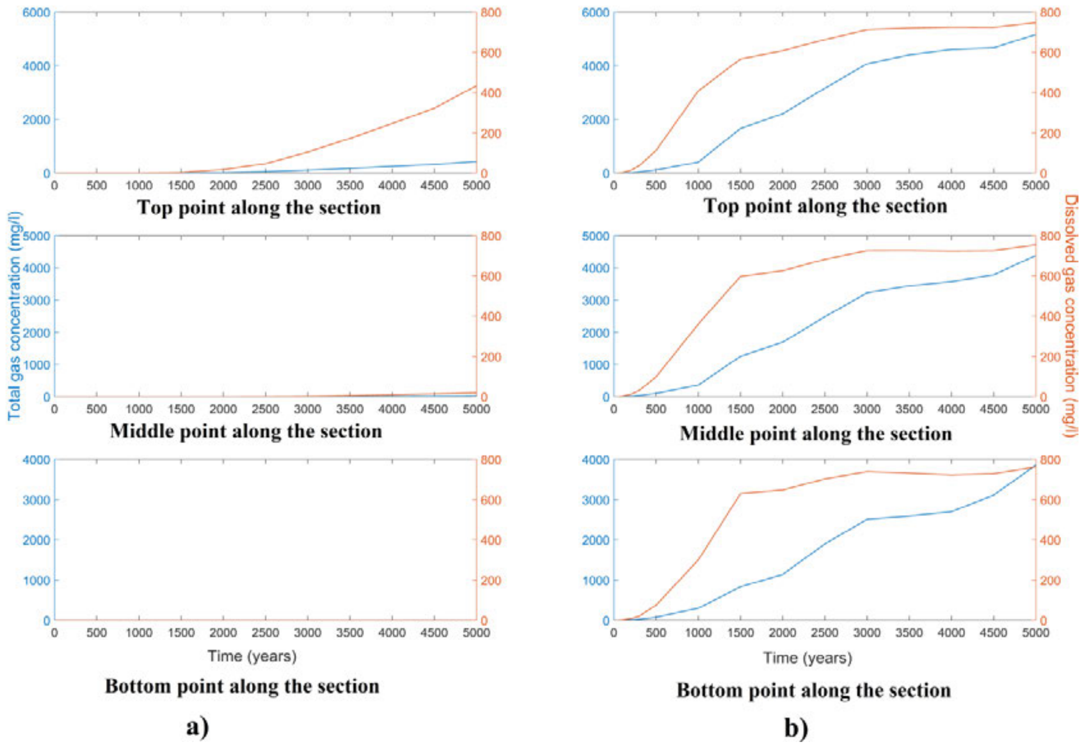

Figure 51. Breakthrough curves comparison for model 1 for three vertical observation points (see Figure 50) at 50 km from the Milk River Formation boundary: a) discovery conditions, b) commingled conditions.

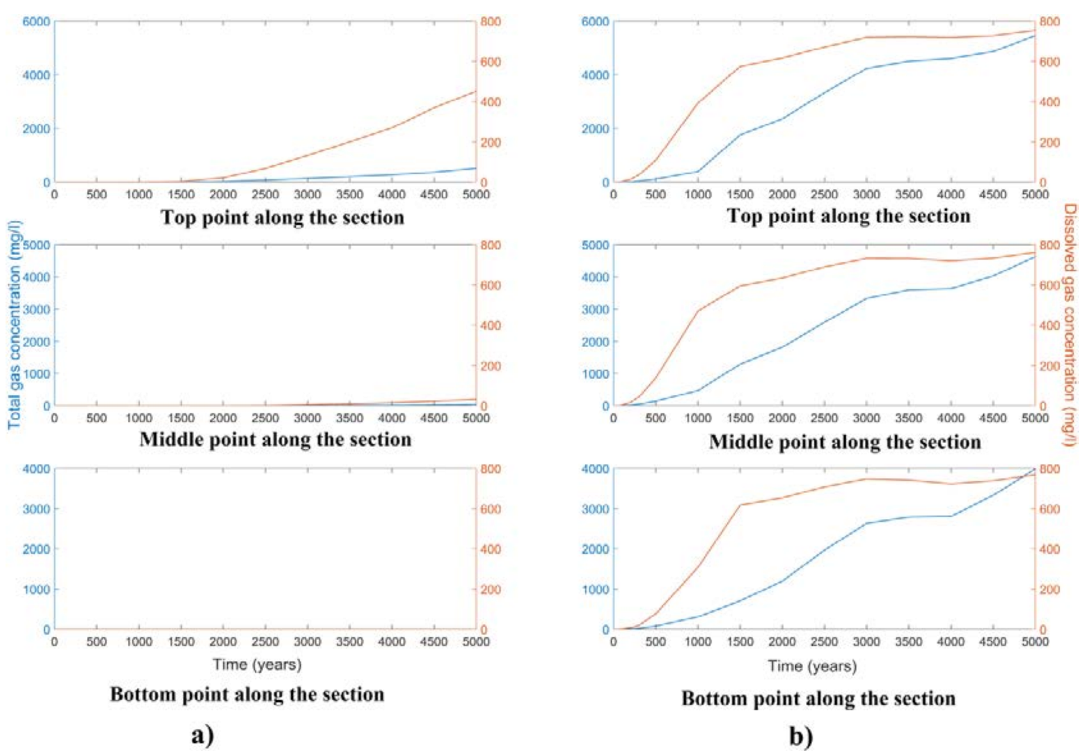

Figure 52. Breakthrough curves comparison for model 2 for three vertical observation points (see Figure 50) at 50 km from the Milk River Formation boundary: a) discovery conditions, b) commingled conditions.

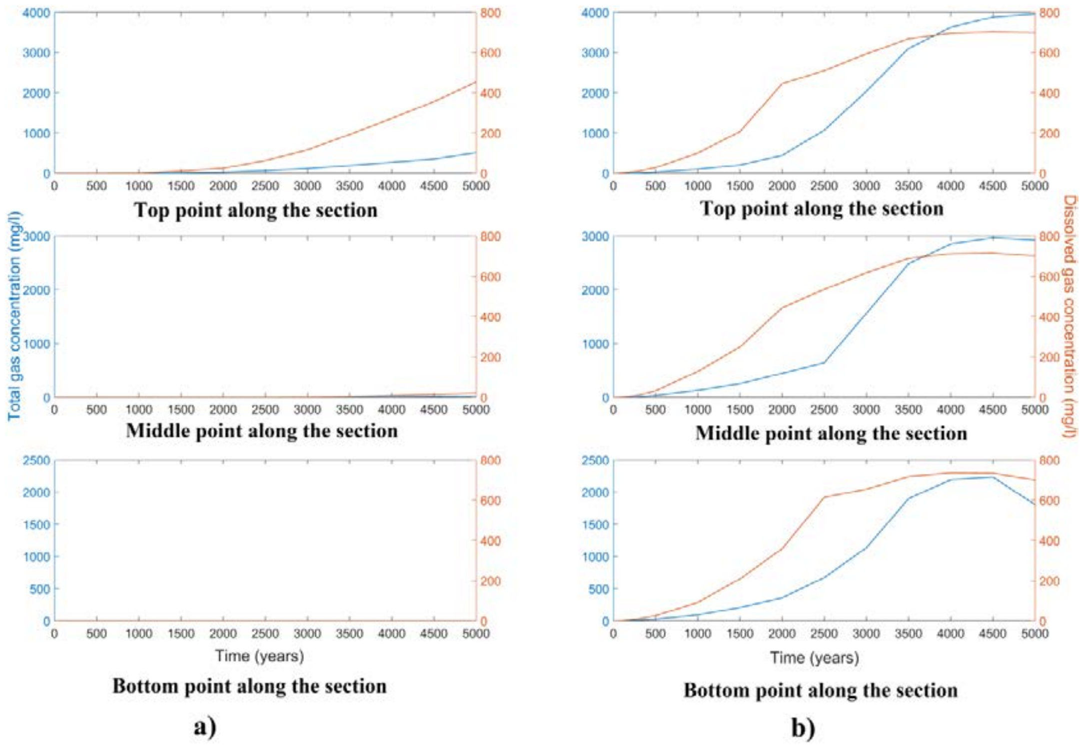

Figure 53. Breakthrough curves comparison for model 3 for three vertical observation points (see Figure 50) at 50 km from the Milk River Formation boundary: a) discovery conditions, b) commingled conditions.

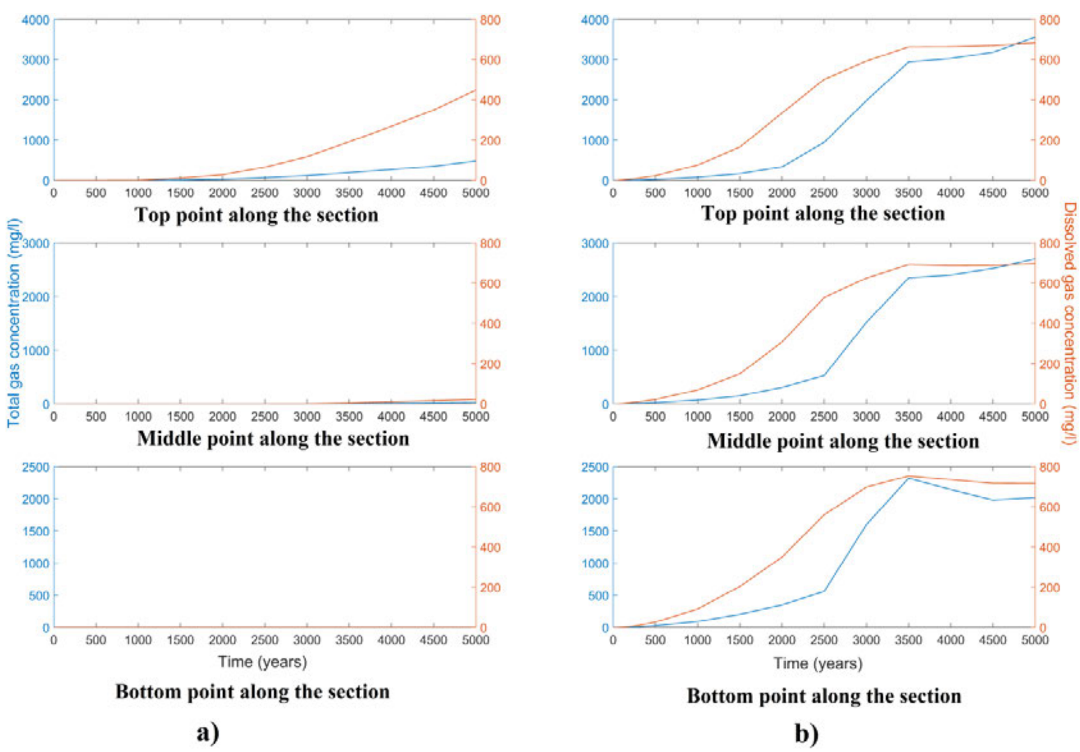

Figure 54. Breakthrough curves comparison for model 4 for three vertical observation points (see Figure 50) at 50 km from the Milk River Formation boundary: a) discovery conditions, b) commingled conditions.

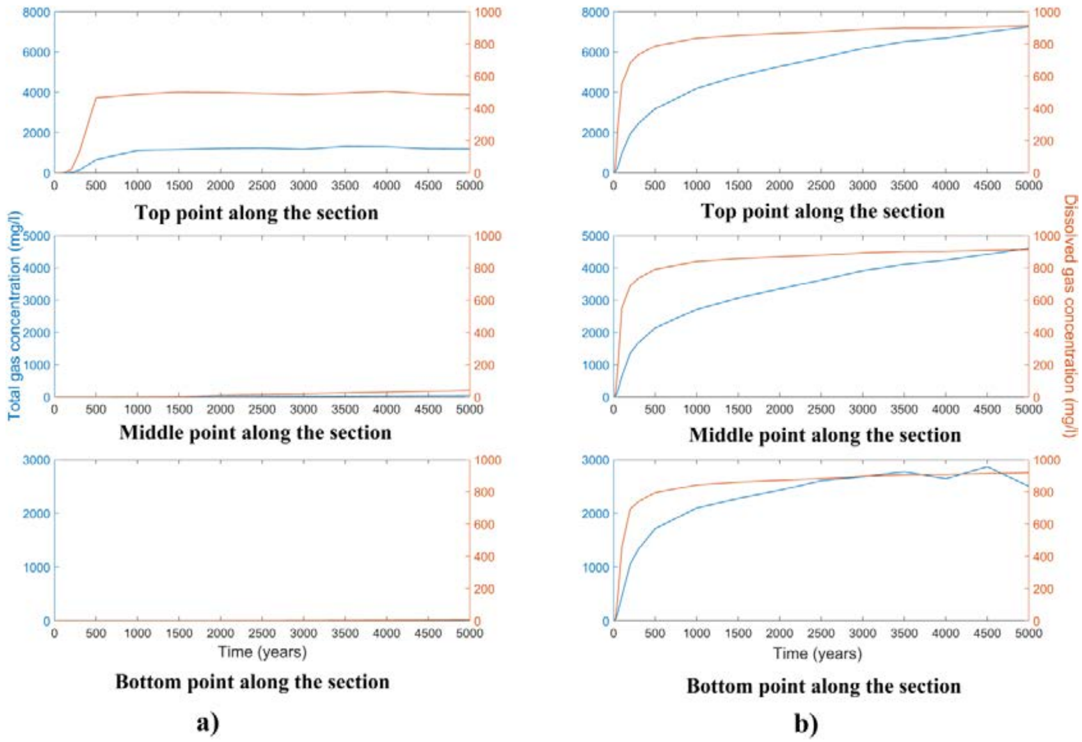

Figure 55. Breakthrough curves comparison for model 5 for three vertical observation points (see Figure 50) at 50 km from the Milk River Formation boundary: a) discovery conditions, b) commingled conditions.

6.2.5 Sensitivity Analysis

The sensitivity of the numerical model was evaluated for all input parameters. The objective of this analysis was to evaluate how each numerical model parameter affected the two-phase flow model results and through this understand the uncertainty in the numerical models. The input parameters for specific zones were individually varied over an order of magnitude whereas all other input parameters for all other zones were kept constant as detailed in Table 3. The sensitivity of the models was evaluated in comparison to the base case scenario (Table 3) for the total air mass at the locations where breakthrough-curve concentrations were measured. This was done to assess the sensitivity of the model results at the same point regardless of scenario or conceptual model being tested. For all discovery and commingled well abandonment simulations of models 1, 2, 3, and 4, the gas never breached the boundary seal whereas for model 5, gas migration through the boundary seal occurred in two simulations. Tables 5, 6, 7, 8, and 9 present the sensitivity results, showing percentage change in total air mass for systematic changes to porosity, permeability, and the van Genuchten parameters. Pumping drawdown at the southern end of the two-phase flow numerical model section was also varied to assess its impact on model results. It was found that the numerical models were not sensitive to changes in drawdown due to pumping, so these results are not included in the tables. The results show that boundary seal zone porosity and permeability affect the air mass the most, indicating that these models are most sensitive to these parameters.

Table 5. Sensitivity analysis table for model 1 with percentage change in total air mass at location 1 (see Figure 50). Negative values (bolded) indicate a decrease and positive values (unbolded) indicate an increase.

	Porosity		Permeability		Alpha (van Genuchten parameter)		n (van Genuchten parameter)	
(Multiplier)	0.75	1.25	0.1	10	0.25	4	0.9	1.1
Gas zone	10.8	5.4	**19.8**	17.4	2.4	1.3	3.7	0.5
Boundary seal	19.8	9.3	**98.5**	82	**3.2**	36.8	14.6	**26**
Gas seal	2.8	**4.3**	**2.5**	4.3	4.2	2.5	11	19.2
Alderson Member	0.6	**2.1**	0.6	**1.2**	3.8	20.3	2.2	20

Table 6. Sensitivity analysis table for model 2 with percentage change in total air mass at location 1 (see Figure 50). Negative values (bolded) indicate a decrease and positive values (unbolded) indicate an increase.

	Porosity		Permeability		Alpha (van Genuchten parameter)		n (van Genuchten parameter)	
(Multiplier)	0.75	1.25	0.1	10	0.25	4	0.9	1.1
Gas zone	5.6	6.8	**11**	3.8	1.3	7.5	0.8	1.8
Boundary seal	2.5	6.6	**97.9**	73.3	3.6	30.1	2.3	**30.1**
Gas seal	6.8	**7.6**	**1.2**	0.8	**0.8**	3.2	3.2	**10.1**
Alderson Member	**3.2**	**3.1**	10.3	**0.1**	1.2	8.9	**8.9**	2.4

Table 7. Sensitivity analysis table for model 3 with percentage change in total air mass at location 1 (see Figure 50). Negative values (bolded) indicate a decrease and positive values (unbolded) indicate an increase.

	Porosity		Permeability		Alpha (van Genuchten parameter)		n (van Genuchten parameter)	
(Multiplier)	0.75	1.25	0.1	10	0.25	4	0.9	1.1
Gas zone	**18.6**	5.7	**70.1**	3.2	**6.8**	**5.7**	**1.9**	**6.1**
Boundary seal	**8.7**	11.9	**96.8**	83.2	**1.31**	3.5	**1.9**	**27.1**
Gas seal	**17.1**	37.2	10.1	2.34	15.3	2.3	2.8	10.1
Alderson Member	0.04	**3.7**	**69.1**	**26.2**	16.1	**1.4**	0.1	11.1

Table 8. Sensitivity analysis table for model 4 with percentage change in total air mass at location 1 (see Figure 50). Negative values (bolded) indicate a decrease and positive values (unbolded) indicate an increase.

	Porosity		Permeability		Alpha (van Genuchten parameter)		n (van Genuchten parameter)	
(Multiplier)	0.75	1.25	0.1	10	0.25	4	0.9	1.1
Gas zone	**22.3**	0.8	**51.5**	10.9	**6.9**	1.3	14.2	7.1
Boundary seal	1.2	6.2	**96.8**	121.6	**8.1**	14.2	12.1	**11.2**
Gas seal	**4.6**	48.5	23.8	15.2	20.2	13.0	13.0	23.7
Alderson Member	12.7	17.2	**57.1**	**34.3**	23.4	11.2	24.9	12.4

Table 9. Sensitivity analysis table for model 5 with percentage change in total air mass at location 1 (see Figure 50). Negative values (bolded) indicate a decrease and positive values (unbolded) indicate an increase.

	Porosity		Permeability		Alpha (van Genuchten parameter)		n (van Genuchten parameter)	
(Multiplier)	0.75	1.25	0.1	10	0.25	4	0.9	1.1
Gas zone	**2.1**	**3.2**	**10.3**	24.9	2.14	**0.4**	85.1	0.9
Boundary seal	**8.2**	**6.3**	**17.5**	47.4	**13.6**	11.4	**14.6**	29.4
Gas seal	**2.6**	**2.5**	13.3	10.3	**1.7**	7.2	**11**	9.2
Alderson Member	**14.1**	3.34	**3.8**	4.17	**0.6**	**4.9**	**6.5**	1.29

7 Southeastern Alberta Gas Field Case Study Summary

The southeastern Alberta gas field has been in operation for many decades, most often producing gas from wells completed in one or more of the Milk River Formation, the Alderson Member, the Medicine Hat Member, and sometimes units deeper than the Niobrara Formation as permitted in the Southeastern Alberta Order (Commingling Order No. MU 7490). Due to the age of the gas field, many wells are nearing the end of their commercial life. As part of the AGS's ongoing Provincial Groundwater Inventory Program and its role of supporting the AER in its regulation of the oil and gas sector, a geological and hydrogeological case study of the Milk River Formation and the Alderson Member was undertaken in the vicinity of the southeastern Alberta gas field.

In order to better understand the geological and hydrogeological factors at play in the region and provide information on the area to colleagues within the AER, the case study involved detailed geological mapping of the various members of the Milk River Formation, and of the various units of the Alderson Member. The mapping clarified the relationships between the Milk River Formation in the southern extent of the case study area and the onlapping Alderson Member to the north, as well as the overlying Pakowki Formation, and underlying Niobrara Formation. In particular, the mapping provides resolution of the overlapping coarse-grained sandstone in the Virgelle Member of the Milk River Formation, and overlying coarse-grained sandstone in the Alderson Member. It also raised some questions about the depositional history and setting of the Alderson Member that will require additional study to fully unravel.

Following geological mapping, 3D property modelling of the rock units was completed. Properties modelled included porosity, the volume of shale (V_{sh}), and water saturation. Based on core measured porosity and permeability relationships, permeability values were calculated and subsequently modelled. Using the outputs from the porosity modelling, the V_{sh} values were determined and modelled. Lastly, based on the V_{sh} and characteristics of the fluids found in the area, water saturation was determined. Porosity and permeability modelling enhanced the interpretation of the points of direct contact between overlying sandstone units by confirming or disproving that both units were permeable. The overlapping permeable and porous zones within the model show where fluids and gases are more likely to migrate towards as they move through the subsurface. Like the geological mapping and modelling, the results of the property modelling also raised questions regarding the depositional setting and history of the area, and specifically the nature of interconnections between the Alderson Member gas deposits and the Milk River Formation through pathways with potentially just enough permeability to allow gas to move should pressure conditions be sufficient to allow migration to occur. Water saturation modelling was very effective in showing the extent of the water-bearing and gas-saturated portions of the Milk River Formation and Alderson Member. It also pointed out some other zones of potential gas accumulation.

A 3D multiphase flow model was developed to further understand the gas migration risks that could develop under commingling well abandonment conditions. The numerical modelling results for all the alternative models show that the gas seal along with the transition zone acts as an effective trap for the gas. Of all the runs including the sensitivity analysis runs, there were only a few extreme case scenarios where the gas seal was breached but the transition zone was never breached during the 5000 year modelling runs. Under commingled well abandonment conditions for the weakest alternative model with extreme pumping implemented, the effects at 1 km are felt after 1000 years, and thus under realistic conditions the time for effects to reach the Milk Formation edge (>50 km) would be significantly more.

The Milk River Formation is an important reservoir of groundwater in southern Alberta and northern Montana. It contains both nonsaline and saline groundwater with its water use history dating back to the early 1900s and possibly further back in time. Groundwater use from the nonsaline portion of the aquifer is difficult to determine requiring a number of assumptions. To account for uncertainties in use estimates, a high use case and a low use case were calculated using different estimates of use rates and the lifespan of a water well. Groundwater use volumes were highest around the year 2000, and decreased substantially after. The increase appears related to increased numbers of wells drilled over time, the types of uses for the water wells, and the increase in groundwater licensing that increased substantially in the 1990s. After the 2000s, the purpose for wells had shifted to types of uses that typically use lower volumes of water, such as domestic use. Other demographic or policy reasons for changes were not examined, although they likely play an important part in the changes.

These trends in decreasing water use after 2000 are consistent with recent estimates of increases in groundwater storage in the region and what looks like increases in precipitation over the same period. In comparing groundwater use to groundwater availability, it appears that groundwater use is less than the annual amount of recharge the Milk River Formation receives within the portion of the formation that contains nonsaline groundwater. Although this suggests that taken as a whole, groundwater is not being overexploited, this does not indicate that there is no effect from groundwater withdrawals, nor does it indicate that at a more local scale there aren't more pronounced effects on groundwater levels caused by pumping.

Like groundwater production, natural gas production in the southeastern Alberta gas field has also occurred since the late 19th century. Since then more than 40 000 wells have been drilled in the gas field, of which approximately 26 000 wells are producing from one or more of the Milk River Formation, Alderson Member, and Medicine Hat Member. Median production rates for active wells versus production rates for wells that have recently been abandoned or where production has been suspended are statistically different. The number of active wells where production rates are approaching rates where historically other wells have been abandoned or suspended is growing. This highlights the gas field as being a mature field, as well as the large-scale abandonment efforts that will be required to close the field.

A review of the literature found that there are diverging opinions on the elements that control gas accumulations in the Alderson Member, specifically the type and size of the gas reservoir(s), the nature of the seals holding the gas within the reservoirs, and the nature of the seal that marks the southern edge of the gas field. There is substantial disagreement between authors, resulting in no clear consensus on a conceptual model for the gas accumulation(s). Instead of evaluating the competing conceptual petroleum system models and selecting one, the AGS chose to evaluate the entire set of conceptual models, arriving at five plausible conceptual models for the petroleum system. Four of the models (scenarios 1 to 4) showed very little potential for gas migration under a commingled well abandonment scenario with one (scenario 5) showing the potential for some gas migration given the right geological and pressure conditions.

8 Recommended Next Steps Towards Safe and Affordable Permanent Abandonment of Commingled Medicine Hat and Alderson Gas Wells in the Southeastern Alberta Gas Field

by K. Parks and D. Palombi

The hydrogeological studies in this report show that out of five reasonably possible hydrogeological models of the Alderson Member gas trap, four show the natural system would probably trap the gas remaining in a commingled Medicine Hat–Alderson geobody, preventing it from migrating updip and southwards into the Milk River aquifer after production ceases. However, one model shows that a commingled Medicine Hat–Alderson geobody might not trap gas after production ceases.

Each of these geological and hydrogeological models has been presented in peer-reviewed scientific literature and each can be reasonably argued to be consistent with the available data. The state of affairs where observations are consistent with more than one explanation is called the non-uniqueness problem. Non-uniqueness is commonly encountered in hydrogeological investigations. Non-uniqueness is problematic when important hydrogeological decisions need to be made on the basis of predictions of future behaviour of a system, but where the competing models offer different outcomes. If stakeholders have different values in the predictions, then hydrogeological decision-making can devolve into an argument about the strengths of competing models. Such an argument will almost always be unresolved because of the inherent non-uniqueness problem in hydrogeological models.

In this case study, the hydrogeological decision is whether to permit gas wells to remain permanently commingled with respect to completions in the Medicine Hat and Alderson members in the southeastern Alberta gas field in view of the possibility of leakage of residual natural gas updip and to the south into the Milk River aquifer. Four of five hydrogeological models of the system suggest it would be safe to do so, but one remaining hydrogeological model suggests it may not be. Model sensitivity analysis indicates that uncertainty within each of the five models is not sufficient to change this situation. Rather the uncertainty in predicted outcomes is dominated by the difference between the five models rather than parameter uncertainty within them. This situation is shown diagrammatically in Figure 56.

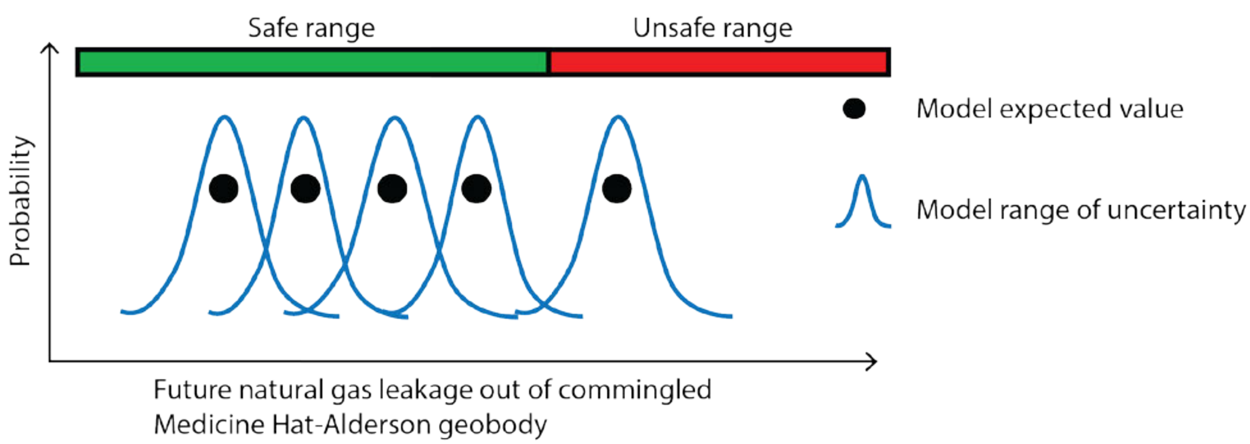

Figure 56. Diagram showing five models predicting future natural gas leakage from the commingled Medicine Hat–Alderson geobody.

The black dot in the figure above indicates the expected gas concentration value and the blue distributions indicate the range of uncertainty around that expected value due to model parameter uncertainty (the range of input values consistent with the conceptual model and existing data). In this diagram, four of the five models have an expected value in the ‘safe range’ and their range of uncertainty is not great enough to fall outside the safe range. The fifth model has its expected value outside the safe range and its range of uncertainty is not great enough to have a significant chance it is actually in the safe range.

Ferré (2017) offers a path forward for decision makers and stakeholders faced with non-uniqueness in hydrogeological models who must make an informed decision about a hydrogeological issue that will impact the future. The recommendation is to keep all the competing models in an ensemble termed the ‘multimodel’ and look for ways to first eliminate models before addressing the consequences of those that remain.

The multimodel ensemble should contain all of the plausible models consistent with the observations and geological theory relevant to the decision at hand and not shy away from the non-uniqueness problem. The multimodel ensemble can also contain ‘advocacy models’, which are models that are hydrogeologically possible yet not well-supported by the data and observations. Advocacy models are important because they may lead to predictions that will cause harm or offense to the environment, property, or social values of particular stakeholders in the decision-making process. The multimodel methodology supports their inclusion because, as Ferré (2017) states, “rather than providing single-model predictions with quantitative uncertainties, we should develop teams of rival models that inform decision makers about what is known, what is possible, and what is unknown.” By including advocacy models in the multimodel ensemble, all stakeholders can have a degree of assurance that their concerns will be fairly considered in the decision-making process.

The multimodel methodology has two main steps after the multimodel ensemble is assembled. The first step is to examine predicted outcomes associated with each model in the multimodel ensemble with respect to stakeholder values, fears, or regulatory limits. If there are no consequential impacts with respect to stakeholder values or fears, or to regulatory limits in any model, there will be no value in determining which member of the multimodel ensemble is the best. All possible futures are acceptable so there is no utility in doing further work to resolve the non-uniqueness.

If instead one or more members of the multimodel ensemble, including advocacy members, predict outcomes that are negative or harmful in some way to stakeholders or violate regulations, then there is value in doing additional work.

The additional value-added work also comes in two steps. The first step is to design a new data collection program that would scientifically test the members of the multimodel ensemble that cause concern. This program will not seek to prove or support a favoured or feared member. Rather, the new data will be selected to try and disprove or ‘falsify’ them and thus remove them, and their predictions, from the multimodel ensemble. Additional value is not achieved from trying to ‘prove’ a more favourable member of the multimodel ensemble is better because inherent non-uniqueness will likely still keep the unfavourable member in the ensemble, and no progress is made towards an acceptable decision that is satisfying to all stakeholders.

It also may be that the cost of falsifying the unfavourable member with new data will be higher than the economic cost of mitigating or accepting possible negative consequences. In this case, the decision maker can decide not to support data collection and just do the mitigation. This decision can be made ahead of time before the data are collected, ensuring the best use of scarce resources.

There is also the possibility that no new data can be collected that will uniquely falsify a member of concern such that it can be eliminated from the multimodel ensemble. In this case, numerical techniques can be deployed that measure the relative geostatistical goodness of fit of all existing observations to predictions from each multimodel member. In this process, the best overall fit of model predictions to available observations is used as a proxy measure of likelihood of a model being true in relation to the others. Such goodness-of-fit measurements can be converted into likelihood-weighted probabilities of outcome, so likelihood-weighted costs can be used to make decisions based on quantitative risk. These are complex calculations and may actually cost more to execute than mitigating or accepting the consequences of unfavourable models in the first place.

Figure 57 shows diagrammatically what the process of falsifying a member would look like. In this diagram, one member of the five-member multimodel ensemble has been disproven or falsified by new field observations (shown as light grey model expected value symbol). As such, it is no longer in the multimodel ensemble. The other members remain in the multimodel ensemble and since all predict future outcomes in the safe range, there is no value or utility in the decision maker examining them further.

Figure 58 shows an illustrative example how geostatistical goodness-of-fit calculations might work to rescale the multimodel ensemble members to an aggregated quantitative risk profile. In this schematic diagram, different members of the multimodel ensemble have been falsified or disproven by further observations but they are in the safe range of outcomes. The remaining members still represent both safe and unsafe outcomes. A geostatistical goodness-of-fit computational exercise could be conducted to determine multimodel member likelihoods and incorporate these likelihoods into the overall quantitative risk profile of future system behaviour. The decision maker can make a quantitative risk-informed decision at this point or start an additional cycle of field observations and data gathering to reduce uncertainty.

The recommended path forward on whether to permit commingled energy boreholes to remain in that state between the Medicine Hat and Alderson members after production ceases in the future is to attempt to falsify model 5, the model showing leakage into the updip boundary seal, with further field data and monitoring observations. The collection of these data will take several years and present additional costs, but these costs should be orders of magnitude less than the cost of re-segregating all of the commingled wells to avoid the leakage associated with model 5, which may ultimately be found to be false. Moreover, the cost of new observations would be orders of magnitude less than the costs associated with damaging the Milk River aquifer with long-term subsurface migration of residual natural gas from the zones if left permanently commingled should model 5 be ultimately found true. By this logic, if new, carefully chosen data can falsify and therefore eliminate model 5 from the multimodel ensemble of this report, all stakeholders can be satisfied that commingled abandonment of the gas wells producing from the Medicine Hat and Alderson members of the southeastern Alberta gas field will be a safe and affordable strategy because all of the remaining models in the multimodel ensemble predict no future leakage.

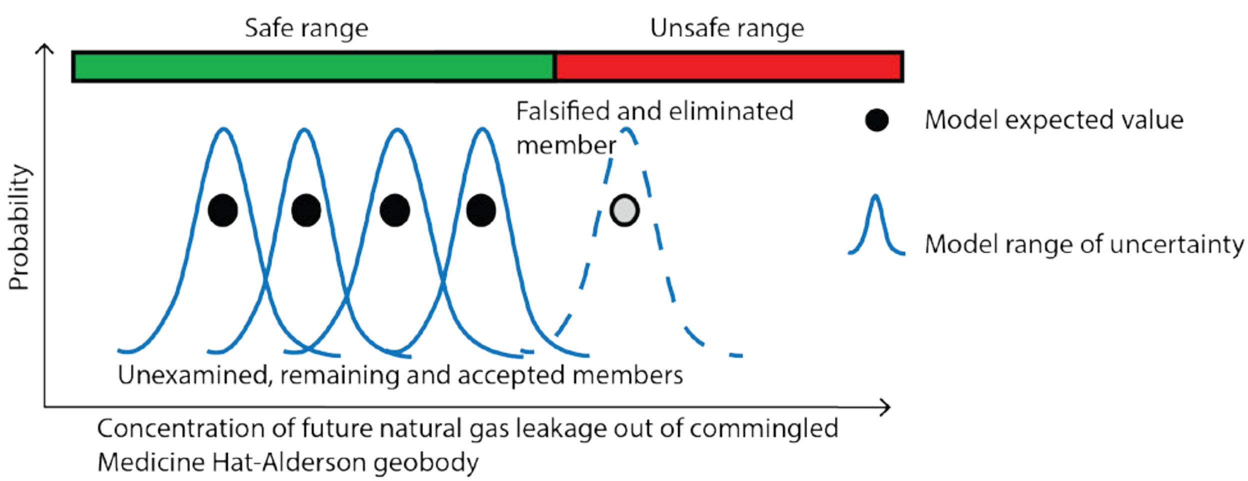

Figure 57. Falsification of one member of a multimodel ensemble through collection of new field observations. The five models predict future natural gas leakage from the commingled Medicine Hat–Alderson geobody.

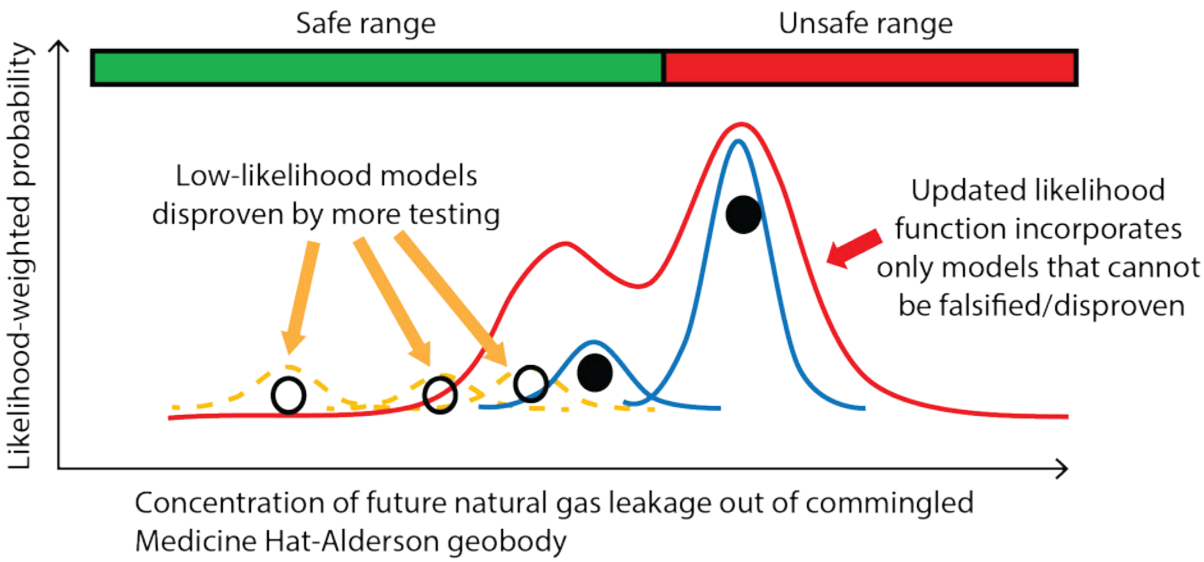

Figure 58. Illustrative example of a geostatistical goodness-of-fit exercise. The five models shown are schematic representations of future natural gas leakage from the commingled Medicine Hat–Alderson geobody. Dots show model expected value and lines show model range of uncertainty.

8.1 Recommended Data Collection Program to Address Modelling Uncertainties

For natural gas to leak from a permanently commingled Medicine Hat–Alderson geobody into the adjacent Milk River aquifer in the future under the conditions of model 5, some or all of the following factors need to be true:

- The rock beds in the boundary seal (as shown in Figure 36) need to be low permeability shale intermixed with beds of sandstone and siltstone. Any interbeds of sandstone or siltstone need to be hydraulically connected to each other and regionally continuous and persistent from the Virgelle Member and Alderson B sandstone beds to the Alderson gas zone.
- The low-permeability shale itself needs to have hydraulic properties that will allow the entry into and diffusion of gas across its extent from the southern limit of the Alderson natural gas zone.
- The gas pressure in the Medicine Hat Member and the Alderson Member will rebound to original pressures either from postproduction gas redistribution or groundwater recharge into reservoir rock.
- After postproduction redistribution of remnant gas in the Medicine Hat and Alderson members, a continuous buoyant column of gas will form within and across the Medicine Hat and Alderson natural gas zones with sufficient vertical height to exceed capillary pressure of the boundary seal acting to trap Alderson gas in its predevelopment state.

The following field-based observations are suggested as ways to falsify these statements. If possible, all of these observations should be made in order to eliminate, at least to the greatest extent practicable, all lower order parametric uncertainty and non-uniqueness problems:

- Core the vertical thickness of the Alderson Member at a location between the northern beds of the Virgelle Member and the southern limit of the Alderson gas zone, in the boundary seal. Analyze the core in detail for its stratigraphic, sedimentological, mineralogical, hydraulic, and age-related properties (e.g., magnetic age, paleontology) to address uncertainties in the stratigraphic affinities of these rocks. This information will be extremely useful in determining what formation these beds actually belong to, and from this what internal geology they may possess across their vertical and horizontal extent. The borehole will need to be logged with downhole petrophysical tools in order to correlate results to other logged but not cored boreholes in the trap area, and update the regional stratigraphic knowledge. Model 5 will be falsified if the beds of the boundary seal zone are younger than any of the members of the Milk River Formation. It will be strongly falsified if the beds of the boundary seal belong to the Pakowki Formation, a marine shale unit that overlies both of the Milk River Formation and the Alderson Member and which is a strong regional hydrogeological aquitard.

- Conduct specialized hydraulic tests on the core and in the borehole to determine the properties of rock in the boundary seal relative to both groundwater and natural gas movement and storage, including the parameters estimated for modelling under all five models of the multimodel ensemble. Model 5 will be partly falsified if the measured parameters are orders of magnitude less permeable than the parameters assumed in this case study.
- Measure groundwater and natural gas compositions and concentrations in one or more specialized monitoring wells at the location of the core (these may or may not be constructed in the same borehole). Detailed geochemical analysis can confirm if the rock is already transmitting natural gas from the Alderson gas zone as well as provide a baseline for future tests of natural gas migration after commingled production ceases under whatever abandonment conditions exist at that time. Bacteriological analyses should be conducted, as bacteria could be important controls on future gas migration south of the Alderson gas zone.
- Measure groundwater and natural gas compositions and concentrations from gas wells in the southern part of the Alderson gas zone and the underlying Medicine Hat Member. This will assist interpretation of the results of groundwater and gas sampling inside the trap zone. Dating and isotopic analysis of fluids with modern methods can illuminate some of the uncertainties that exist on the degree of natural interchange between the natural gas and groundwater system inside the Alderson gas deposit and the regional groundwater flow system of southern Alberta that sustains the Milk River aquifer. Bacteriological analyses should be conducted, as bacteria could be important controls on future gas generation in the abandoned reservoirs themselves after abandonment. Model 5 will be partly falsified if the groundwater, gas, and bacterial signatures in the boundary seal are distinctly different than that of the Alderson Member, indicating that no continuous column of natural gas had sufficient buoyancy pressure at its top to enter into the boundary seal in recent geological time.
- Measure noble gas compositions and concentrations in Alderson and Medicine Hat natural gas samples, especially helium. Noble gases are mobile and nonreactive natural tracers of crustal fluid and gas movement in rock. The presence of significant helium in the Alderson Member is already known in some parts of the deposit in Saskatchewan. If helium is found in significant quantities in the Alderson gas zone but not in the boundary seal rocks, it will be evidence that the shale in the boundary seal used in model 5 has orders of magnitude less permeability than presumed for the calculations in this case study.
- Measure and monitor gas pressure in Alderson and Medicine Hat gas zones in dedicated, noncommingled wells after local production ceases. Pressure buildup over time in these zones will help determine the rate and degree to which gas redistribution after production ceases will create a new gas column. If pressures in the Medicine Hat and Alderson gas zones do not build up sufficiently fast after production ceases, say within 10 years, a future vertically continuous column of buoyant natural gas is unlikely to form, falsifying another part of model 5.

A detailed data collection program plan giving specific technical recommendations on these steps towards falsification of model 5 from the multimodel ensemble will need to follow. The recommended practice of Ferré (2017) and other workers in this field is to involve all stakeholders and decision makers in the structure of the program before design and execution. This involvement helps ensure that all stakeholders and decision makers inform and accept the results of the falsification exercise. This is especially important when advocacy models that have high importance or utility become falsified and removed from the ensemble before final decisions are made.

9 References

Alberta Agriculture and Forestry (2019): Alberta climate and atlas maps; URL <https://agriculture.alberta.ca/acis/climate-maps.jsp> [January 2019].

Alberta Culture and Tourism (2019): Accidental industry; URL <http://www.history.alberta.ca/energyheritage/gas/creation-of-an-industry/accidental-industry/default.aspx#page-1> [April 2019].

Alberta Energy Regulator (2002): Alberta's reserves 2001 and supply/demand outlook 2002–2011; Statistical Series 2002-98, 130 p.

Alberta Energy Regulator (2016): Alberta's energy reserves 2015 and supply/demand outlook 2016–2025; Statistical Series 98-2016.

Alberta Energy Regulator (2018): Well abandonment; Directive 020, 59 p.

Alberta Energy Regulator (2019a): AER Order System; URL <https://aer.ca/regulating-development/compliance/orders/aer-order-system> [May 2019].

Alberta Energy Regulator (2019b): Commingling orders; URL <https://www.aer.ca/regulating-development/compliance/orders/commingling-orders> [May 2019].

Alberta Environment and Parks (2017a): Alberta Water Well Information Database; URL <https://www.alberta.ca/alberta-water-well-information-database-overview.aspx> [October 2017].

Alberta Environment and Parks (2017b): Water use reporting system; URL <https://www.alberta.ca/water-use-reporting-system.aspx> [October 2017].

Alberta Geological Survey (2015): Alberta Table of Formations; Alberta Energy Regulator, URL <https://ags.aer.ca/activities/table-of-formation.htm> [March 2019].

Andriashek, L.D. (2003): Quaternary geological setting of the Athabasca Oil Sands (in situ) area, northeast Alberta; Alberta Energy and Utilities Board, EUB/AGS Earth Sciences Report 2002-03, 295 p.

Andriashek, L. comp. (2018): Thalwegs of bedrock valleys, Alberta (GIS data, line features); Alberta Energy Regulator, AER/AGS Digital Data 2018-0001.

Anna, L.O. (2011): Effects of groundwater flow on the distribution of biogenic gas in parts of the Northern Great Plains of Canada and United States; United States Geological Survey, Scientific Investigations Report 2010-5251, 31 p.

Anwar, T., Mumpy, A., Blanco, D., Kravchinsky, V.A. and Catuneanu, O. (2017): Core magnetostratigraphy: chron 33r in the southern Alberta Plains; Bulletin of Canadian Petroleum Geology, v. 65, no. 4, p. 425–435.

Atkinson, N. and Lyster, S. (2012): Thickness and distribution of Quaternary and Neogene sediment in Alberta; Energy Resources Conservation Board, ERCB/AGS Map 551.

Bachu, S. (1999): Flow systems in the Alberta Basin: patterns, types and driving mechanisms; Bulletin of Canadian Petroleum Geology, v. 47, no. 4, p. 455–474.

Bear, J. (1972): Dynamics of fluids in porous media; American Elsevier, New York, New York.

Berkenpas, P.G. (1991): The Milk River shallow gas pool: role of the updip water trap and connate water in gas production from the pool; *in* Proceedings of the 1991 Society of Petroleum Engineers Annual Technical Conference and Exhibition, v. 66, p. 371–380.

Carsel, R.F. and Parrish, R.S. (1988): Developing joint probability distributions of soil water retention characteristics; Water Resources Research, v. 24, issue 5, p. 755–769, doi:10.1029/WR024i005p00755.

Chen, Z., Shuai, Y., Osadetz, K., Hamblin, T. and Grasby, S. (2015): Comparison of biogenic gas fields in the Western Canada Sedimentary Basin and Qaidam Basin: implications for essential geological controls on large microbial gas accumulations**;** Bulletin of Canadian Petroleum Geology, v. 63, no. 1, p. 33–52.

Energy Resources Conservation Board (2010): Province-wide framework for commingling of gas from coals and shales with other gas; Energy Resources Conservation Board, Bulletin 2010-25, 3 p.

Ferré, T.P.A. (2017): Revisiting the relationship between data, models and decision making; Groundwater, v. 55, no. 5, p. 604–614.

Fishman, N.S., Ridgley, J.L., Hall, D.L., Higley, D.K. and Tuttle, M.L.W. (2012): Ancient microbial gas in the Upper Cretaceous Milk River Formation, Alberta and Saskatchewan: a large continuous accumulation in fine-grained rocks; *in* Shale reservoirs—giant resources for the 21st century, J.A. Breyer (ed.), American Association of Petroleum Geologists, Memoir 97, p. 258–289.

Fuex, A.N. (1977): The use of stable carbon isotopes in hydrocarbon explorations; Journal of Geochemical Exploration, v. 7, no. 2, p. 155–158.

Glass, D.J., editor (1990): Lexicon of Canadian stratigraphy, v. 4; Canadian Society of Petroleum Geologists, Calgary, Alberta, 1423 p.

Glombick, P. and Mumpy, A.J. (2014): Subsurface stratigraphic picks for the Milk River 'shoulder', Alberta plains: including tops for the Milk River Formation and Alderson Member of the Lea Park Formation; Alberta Energy Regulator, AER/AGS Open File Report 2013-17, 29 p.

Government of Alberta (2017): Water Act; Revised Statutes of Alberta 2000, Chapter W-3, Section 19, 140 p.

Harbaugh, A.W. (2005): MODFLOW-2005, the U.S. Geological Survey modular ground-water model - the ground-water flow process; United States Geological Survey, Techniques and Methods 6-A16, 2005.

Hendry, M.J. and Schwartz, F.W. (1988): An alternate view on the origin of chemical and isotopic patterns in groundwater for the Milk River aquifer, Canada; Water Resources Research, v. 24, no. 10, p. 1747–1763.

Hendry, M.J., Schwartz, F.W. and Robertson, C. (1991): Hydrogeology and hydrochemistry of the Milk River aquifer system, Alberta, Canada: a review; Applied Geochemistry, v. 6, p. 369–380.

Hitchon, B. (1984): Geothermal gradients, hydrodynamics, and hydrocarbon occurrences, Alberta, Canada; American Association of Petroleum Geologists, Bulletin, v. 68, no. 6, p. 713–743.

Huang, J., Pavlic, G., Rivera, A., Palombi, D. and Smerdon, B. (2016): Mapping groundwater storage variations with GRACE: a case study in Alberta, Canada; Hydrogeology Journal, v. 24, issue 7, p. 1663–1680.

IHS Markit (2018): AccuMap™; IHS Markit, URL <https://ihsmarkit.com/products/oil-gas-tools-accumap.html> [September 2018].

Kaluarachchi, J.J. and Parker, J.C. (1990): Multiphase flow with a simplified model for oil entrapment; Transport in Porous Media, v. 7(1), p. 1–14.

Kauffmann, E.G. (1977): Geological and biological overview: Western Interior Cretaceous basin; Mountain Geologist, v. 14, p. 75–99.

Klassen, J., Liggett, J.E., Pavlovskii, I. and Abdrakhimova, P. (2018): First-order groundwater availability assessment for southern Alberta; Alberta Energy Regulator / Alberta Geological Survey, AER/AGS Open File Report 2018-09, 37 p.

Leckie, D.A., Bhattacharyan, J.P., Bloch, J., Gilboy, C.F. and Norris, B. (1994): Cretaceous Colorado/Alberta Group of the Western Canada Sedimentary Basin; Chapter 20 *in* Geological atlas of the Western Canada Sedimentary Basin, G.D. Mossop and I. Shetsen (comp.), URL <https://ags.aer.ca/document/Atlas/chapter_20.pdf> [January 2019].

Lemay, T.G. (2009): Description of the process for defining the base of groundwater protection; Energy Resources Conservation Board, ERCB/AGS Open File Report 2009-04, 27 p.

Lenhard, R.J. and Parker, J.C. (1987): A model for hysteretic constitutive relations governing multiphase flow; 2, Permeability-saturation relations; Water Resources Research, v. 23, no. 12, p. 2197–2206.

Lerche, I. and MacKay, J.A. (1999): Economic risk in hydrocarbon exploration; Academic Press, New York, New York, 488 p.

LMKR (2015): GeoGraphix® Prizm™; LMKR, URL <https://www.lmkr.com/geographix/by-solution/geographix-suite/prizm%E2%84%A2/> [December 2018].

McDonald, M.G. and Harbaugh, A.W. (1988): A modular three-dimensional finite-difference ground-water flow model; United States Geological Survey, Techniques of Water-Resources Investigations, Book 6, Chapter A1, 586 p.

Megill, R. (1984): An introduction to risk analysis, 2nd edition; Penwell Books, Tulsa, Oklahoma, 288 p.

Meijer Drees, N.C. and Mhyr, D.W. (1981): The Upper Cretaceous Milk River and Lea Park formations in southeastern Alberta; Bulletin of Canadian Petroleum Geology, v. 29, no. 1, p. 42–74.

Meyboom, P. (1960): Geology and groundwater resources of the Milk River sandstone in southern Alberta; Alberta Energy Regulator, Memoir 2, 103 p.

Mitrovica, J.X., Beaumont, C. and Jarvis, G.T. (1989): Tilting of continental interiors by the dynamical effects of subduction; Tectonics, v. 8, no. 5, p. 1079–1094.

Mumpy, A.J. and Catuneanu, O. (2019): Controls on accommodation during the early-middle Campanian in southern Alberta, western Canada foreland system; Journal of Geodynamics, in press, corrected proof, available online January 4, 2018.

Nielsen, K.S., Schroder-Adams, C.J. and Leckie, D.A. (2003): A new stratigraphic framework for the Upper Colorado Group (Cretaceous) in southern Alberta and southwestern Saskatchewan, Canada; Bulletin of Canadian Petroleum Geology, v. 51, no. 3, p. 304–346.

Nolte, E., Krauthan, P., Korschinek, G., Maloszewski, P., Fritz, P. and Wolf, M. (1991): Measurements and interpretations of ^{36}Cl in groundwater, Milk River Aquifer, Alberta, Canada; Applied Geochemistry, v. 6, no. 4, p. 435–445.

North American Commission on Stratigraphic Nomenclature (2005): North American stratigraphic code; American Association of Petroleum Geologists, Bulletin, v. 89, no. 11, p. 1547–1591.

O’Connell, S. (2003): The unknown giants – low permeability shallow gas reservoirs of southern Alberta and Saskatchewan, Canada; Canadian Society of Exploration Geophysicists, URL <https://cseg.ca/resources.2003-conference-abstract-n-to-z> [April 2019].

O’Connell, S. (2014): The Milk River transboundary aquifer in southern Alberta; Geological Survey of Canada, Open File Report 7751, 42 p.

O’Connell, S., Campbell, R. and Bhattacharya, J. (1999): The stratigraphy, sedimentology, and reservoir geology of the giant Milk River gas field in southeastern Alberta and Saskatchewan; *in* Proceedings, CSPG and Petroleum Society Joint Convention, June 14–18, 1999, v. 1, abstract 99-83-O, 3 p.

Pétré, M-A., Rivera, A. and Lefebvre, R. (2015): Three-dimensional unified geological model of the Milk River transboundary aquifer (Alberta, Canada – Montana, USA); Canadian Journal of Earth Science, v. 52, p. 96–111.

Pétré, M-A., Rivera, A., Lefebvre, R., Hendry, M.J. and Folnagy, A.J.B. (2016): A unified hydrogeological conceptual model of the Milk River transboundary aquifer, traversing Alberta (Canada) and Montana (USA); Hydrogeology Journal, v. 24, p. 1847–1871.

Phillips, F.M., Bentley, H.W., Davis, S.N., Elmore, D. and Swanick, G. (1986): Chlorine-36 dating of very old groundwater, 2, Milk River aquifer, Alberta, Canada; Water Resources Research, v. 22, no. 13, p. 2003–2016.

Plint, A.G. (1988): Sharp-based shoreface sequences and “offshore bars” in the Cardium Formation of Alberta: their relationship to relative changes in sea level; *in* Sea-level changes: an integrated approach, C.K. Wilgus, B.S. Hastings, C.G.St.C. Kendall, H.W. Posamentier, C.A. Ross and J.C. Van Wagoner (ed.), SEPM Society of Sedimentary Geology, Special Publication No. 42, p. 357–370.

Plint, A.G., Walker, R.G. and Bergman, K.M. (1986): Cardium Formation 6: stratigraphic framework of the Cardium in subsurface; Bulletin of Canadian Petroleum Geology, v. 34, no. 2, p. 213–225.

Prior, G.J., Hathway, B., Glombick, P.M., Pana, D.I., Banks, C.J., Hay, D.C., Schneider, C.L., Grobe, M., Elgr, R. and Weiss, J.A. (2013): Bedrock geology of Alberta; Alberta Energy Regulator, AER/AGS Map 600.

Raucher, R.L. (1983): A conceptual framework for measuring the benefits of groundwater protection; Water Resources Research, v. 19, no. 2, p. 320–326.

Rice, D.D. and Claypool, G.E. (1981): Generation, accumulation and resource potential of biogenic gas; American Association of Petroleum Geologists Bulletin, v. 65, no. 1, p. 5–25.

Ridgley, J.L. (2000): Lithofacies architecture of the Milk River Formation (Alderson Member of the Lea Park Formation) southwestern Saskatchewan and southeastern Alberta – its relation to gas accumulation; *in* Summary of Investigations 2000, Volume 1, Saskatchewan Geological Survey, Saskatchewan Energy and Mines, Misc. Rep. 2000-4.1.

Rose, P.R. (2001): Risk analysis and management of petroleum exploration ventures; American Association Petroleum Geologists, Methods in Exploration, no. 12, 123 p.

Schlumberger Limited (2015): Petrel 2015; Schlumberger Limited, URL <https://www.software.slb.com/products/petrel/petrel-2015> [December 2018].

Schurr, G.W. and Ridgely, J.L. (2002): Unconventional shallow biogenic gas systems; Bulletin of the American Association of Petroleum Geologists, v. 86, no. 11, p. 1939–1969.

Schwartz, F.W. and Muehlenbachs, K. (1979): Isotope and ion geochemistry of groundwaters in the Milk River aquifer, Alberta; Water Resources Research, v. 15, no. 2, p. 259–268.

Schwartz, F.W., Muehlenbachs, K. and Chorley, D.W. (1981): Flow-system controls of the chemical evolution of groundwater; Journal of Hydrology, v. 54, no. 1–3, p. 225–243.

Statistics Canada (2018): Consumer price index, annual average, not seasonally adjusted; Government of Canada, Table 18-10-0005-01, URL <https://www150.statcan.gc.ca/t1/tbl1/en/tv.action?pid=1810000501> [October 2018].

Swanick, G.B. (1982): The hydrochemistry and age of the water in the Milk River aquifer, Alberta, Canada; M.Sc. thesis, University of Arizona, 112 p.

Timur, A. (1968): An investigation of permeability, porosity, & residual water saturation relationships for sandstone reservoirs; The Log Analyst, v. 9, n. 4, p. 8–17.

Tóth, J. (1995): Hydraulic continuity in large sedimentary basins; Hydrogeology Journal, v. 3, no. 4, p. 4–16.

Tóth, J. and Corbet, T. (1986): Post-Paleocene evolution of regional groundwater flow-systems and their relation to petroleum accumulations, Taber area, southern Alberta, Canada; Bulletin of Canadian Petroleum Geology, v. 34, no. 3, p. 339–363.

Tovell, W.M. (1956): Some aspects of the geology of the Milk River and Pakowki formations (southern Alberta); Ph.D. thesis, University of Toronto, 118 p.

van Genuchten, M.T. (1980): A closed-form equation for predicting the hydraulic conductivity of unsaturated soils; Soil Science Society of America Journal, v. 44 (5), p. 892.

Vermeulen, P.T.M, Roelofsen, F.J., Minnema, B., Burgering, L.M.T., Verkaik, J. and Rakotonirina, A.D. (2018): iMOD user manual, version 4.3; Deltares, URL <http://oss.deltares.nl/web/iMOD> [July 2018].

Walker, R.G. and Plint, A.G. (1992): Wave- and storm-dominated shallow marine systems; *in* Facies models: responses to sea level change, R.G. Walker and N.P. James (ed.), Geological Association of Canada, p. 219–238.

White, M.D. and Oostrom, M. (2006): STOMP subsurface transport over multiple phase, version 4.0, user's guide; Pacific Northwest National Laboratory, PNNL-15782 (UC-2010), 108 p.

White, M.D., Appriou, D., Bacon, D.H., Fang, Y., Freedman, V., Rockhold, M.L. and Zhang, F. (2015): STOMP user guide; Pacific Northwest National Laboratory, URL <http://stomp.pnnl.gov/user_guide/STOMP_guide.stm> [April 2018].

Williams, G.D. and Stelk, C.R. (1975): Speculations on the Cretaceous paleogeography of North America; *in* The Cretaceous system in the western interior of North America, W.G.E. Caldwell (ed.), Geological Association of Canada, Special Paper 13, p. 1–29.

Yang, Y. (2011): Tectonically-driven underfilled-overfilled cycles, the middle Cretaceous in the northern Cordilleran foreland basin; Sedimentary Geology, v. 233, no. 1–4, p. 15–27.

Yang, Y. and Miall, A. (2008): Marine transgressions in the mid-Cretaceous of the Cordilleran foreland basin re-interpreted as orogenic unloading deposits; Bulletin of Canadian Petroleum Geology, v. 56, no. 3, p. 179–198.

Appendix 1 – Methodology

Water Use Calculation Methodology

Data sources included the Alberta Water Well Information Database (AWWID; Alberta Environment and Parks, 2017a) for unlicensed wells, and the water licenses database (Alberta Environment and Parks, (2017b). Different steps were taken in extracting relevant information from these two databases.

Data extraction from the water licenses database

1. Groundwater licenses were extracted from the database and the locations compared to the extent of the Milk River Formation. Those licenses that fell within the extent of the Milk River Formation were selected for further evaluation.
2. Using ArcGIS, the elevation values for the top and bottom of the Milk River Formation and the ground surface elevation were determined at each licensed water well location.
3. Completion depth details from the wells were converted to elevation values based on the groundwater elevation provided with the license record, or were assigned based on the ground level elevation obtained from the digital elevation model.
4. The elevations of the top and bottom of each completion interval were compared to the Milk River Formation top and bottom elevations to see which wells were completed in the Milk River Formation.
    a. If the elevation of the top of the completion interval was less than the top of the Milk River Formation and the elevation of the bottom of the completion interval was greater than the elevation of the base of the Milk River Formation, the well was assigned to the Milk River Formation.
    b. If the elevation of the top of the completion interval was greater than the elevation of the top of the Milk River Formation by 5 m or less, and the elevation of the bottom of the completion interval was greater than the elevation of the bottom of the Milk River Formation, the well was assigned to the Milk River Formation.
    c. If the elevation of the top of the completion interval was less than the elevation of the top of the Milk River Formation, and the elevation of the bottom of the completion interval was less than the elevation of the bottom of the Milk River Formation by 5 m or less, the well was assigned to the Milk River Formation.
5. The details on when the license became active and when it expires as well as the allocation volume were obtained for the wells assigned to the Milk River Formation.

Data extraction from the AWWID

1. The locations of water wells in the AWWID were compared to the extent of the Milk River Formation. Those water wells that were located within the extent of the Milk River Formation were selected for further evaluation.
2. Information on the total depth drilled, completion interval, well purpose, and well type were extracted from the database for those water wells within the extent of the Milk River Formation.
3. The elevations of the ground surface as well as the elevations of the top and bottom of the Milk River Formation were assigned to each well within the extent of the Milk River Formation.

4. Water well completion elevations were calculated by subtracting the top and bottom depths from the ground surface elevation.
5. Given the small number of wells with completion details, an effort was made to supplement the dataset with additional wells:
    a. Wells with completion details within each of the township-range-meridian combinations were identified. An average completion length as well as the standard deviation and maximum completion lengths were calculated for each township-range-meridian combination.
    b. The wells with total depths but no completion intervals were identified. A completion interval length for these wells was approximated using one of the following calculations:
        i. the average plus two times the standard deviation, but only if the average plus two standard deviations is less than the maximum completion interval length, and is less than the total depth,
        ii. the maximum length was used if the average length plus two standard deviations is greater than the maximum completion length, and the maximum length is less than the total depth,
        iii. the total depth is used if both the average completion length plus two standard deviations and the maximum completion length are greater than the total depth.
6. The actual completion interval top and bottom elevations and the approximated completion interval top and bottom elevations are compared to the top and bottom elevations of the Milk River Formation to see which water wells are completed in the Milk River Formation:
    a. If the elevation of the top of the completion interval was less than the top of the Milk River Formation and the elevation of the bottom of the completion interval was greater than the elevation of the base of the Milk River Formation, the well was assigned to the Milk River Formation.
    b. If the elevation of the top of the completion interval was greater than the elevation of the top of the Milk River Formation by 5 m or less, and the elevation of the bottom of the completion interval was greater than the elevation of the bottom of the Milk River Formation, the well was assigned to the Milk River Formation.
    c. If the elevation of the top of the completion interval was less than the elevation of the top of the Milk River Formation, and the elevation of the bottom of the completion interval was less than the elevation of the bottom of the Milk River Formation by 5 m or less, the well was assigned to the Milk River Formation.
7. The licensed wells dataset was compared to the AWWID dataset using primarily location, and completion details to remove duplicates from the AWWID dataset and generate a water well dataset without the licensed water wells.
8. Water wells were selected to find wells that were likely put into service rather than abandoned or used solely for observation or monitoring purposes.
9. Based on drilling dates or filing dates, the period of time the wells were actively producing water was determined. Three scenarios were used
    a. wells are active for 20 years after starting production,
    b. wells are active for 30 years after starting production.
    c. wells are active for 40 years after starting production.

10. Unlicensed wells are typically used for domestic, stock, or domestic and stock purposes. Estimates of production rates were determined using three scenarios for each of these types of uses:
    a. Regulatory maximum case using maximum annual volumes as described in Water Act Regulations (Government of Alberta, 2017):
        i. domestic wells maximum rate of 1250 m^3/year,
        ii. stock wells maximum rate of 6250 m^3/year,
        iii. domestic and stock maximum rate of 7500 m^3/year.
    b. Low-use census-based case where annual volumes are calculated using census of population and agriculture data to assess typical water consumption per well, assuming that each well serves one household or farm.
    c. High-use census-based case where the low use census-based volumes are multiplied by a factor to account for social and agricultural cases that might lead to increases in domestic and agricultural consumption rates
11. Statistics Canada census data from 2016, 2011, 2006, 2001, 1996, and 1991 (Statistics Canada, 2017) were used in the estimates of water usage. Data were obtained for all of Alberta as well as for the census division within the extent of the Milk River Formation:
    a. for domestic use, household size was obtained from each census;
    b. for stock use, the number of the different types of livestock along with the total number of farms for each census year were used to generate an estimate of the average livestock makeup of farms;
    c. based on farm numbers, a composite farm was generated for each census year using weightings that took into account the total number of farms and the total number of different types of livestock.
12. Population, people per households, and livestock numbers for years outside of the censuses range, or between census years, were done through extrapolation or interpolation.
13. Low use per capita water use was obtained from Environment Canada estimates of per capita residential water use (Environment Canada, 2017). Estimates of changes in per capita water use were calculated by interpolation between results, or through extrapolation to obtain estimates of water usage for earlier time periods or later time periods than data were available for. High use per capita water use was calculated by increasing per capita water use by 73% to approximate the observed behaviour noted in Environment Canada (2017) that water users who do not meter their water use tend to use higher volumes than per capita estimates.
14. Water requirements for different livestock types were obtained from Alberta Agriculture (2009).
15. Low use estimates were made by using the composite farm livestock composition based on overall Alberta farm statistics and multiplying the number of each animal by their water requirements. The higher use estimates were made by using region specific statistics for cattle populations that were higher than the Alberta average, but using the other livestock numbers as in the low use case. Summing the totals gave the overall stock use estimates.
16. Domestic and stock uses were calculated by adding the stock and domestic use volumes per well together to arrive at low and high use volumes estimates.

References

Alberta Agriculture (2009): Farm water supply requirements; URL <https://www1.agric.gov.ab.ca/$department/deptdocs.nsf/all/agdex1349/$file/716c01.pdf> [October 2017].

Alberta Environment and Parks (2017a): Alberta Water Well Information Database; URL <https://www.alberta.ca/alberta-water-well-information-database-overview.aspx> [October 2017].

Alberta Environment and Parks (2017b): Water use reporting system; URL <https://www.alberta.ca/water-use-reporting-system.aspx> [October 2017].

Environment Canada (2017): Residential water use; Government of Canada, URL <https://www.canada.ca/en/environment-climate-change/services/environmental-indicators/residential-water-use.html> [May 2019].

Government of Alberta (2017): Water Act; Revised Statutes of Alberta 2000, Chapter W-3, Section 19, 140 p.

Statistics Canada (2017): Census Program; Government of Canada, URL <https://www12.statcan.gc.ca/census-recensement/index-eng.cfm> [October 2017].

Property Modelling Methodology

1. Well log upscaling and data transformation: The well log data are recorded at an interval of 15.2 cm (6 in.), as compared to the desired modelled cell size of 500 by 500 m with 1 and 2 m layering. The petrophysical properties from the logs were upscaled to the geocellular model to be used in the property modelling. The upscaled log data is then transformed to a normal distribution for variogram development and kriging estimation.
2. Variography: The variogram model specifies the spatial variability of the regionalized variable. Almost all variables in every stationarity subset that will be used in modelling require a variogram. The variogram is also used to determine the effect of change of support in volume variance relations (Babakhani, 2014). The normal score ensures the sill of 1.0 for each variogram model. Spherical is the type of structure that was used to model the variogram in this case study. The three directions have different nugget effects and ranges.
3. Kriging estimation: Property modelling needs an estimation or simulation method to populate the data into the 3D grid cells. A kriging algorithm is used as the estimation algorithm to model the 3D property model.
4. 3D geocellular gridding: The kriging method in Petrel 2015 (Schlumberger, 2015) was used to populate the property values in a 3D geocellular grid with all active cells in the 3D grid assigned a value. The property model is populated using simple kriging for the four properties in the Milk River Formation–Alderson Member unit.

References

Babakhani, M. (2014): Geostatistical modeling in presence of extreme values; M.Sc. thesis, University of Alberta, 99 p.

Schlumberger Limited (2015): Petrel 2015; Schlumberger Limited, URL <https://www.software.slb.com/products/petrel/petrel-2015> [December 2018].

Appendix 2 – Simulation Plan

This simulation plan describes the work plan used for completing the numerical simulations of groundwater and two-phase flow for the southeastern Alberta gas field case study. The resultant report provides valuable background information on the conceptual models used to develop the groundwater and two-phase flow models, and sets out modelling approaches to assess the potential for gas migration under discovery and commingled abandonment conditions. The initial results presented in the report validate preliminary assumptions on the conceptual groundwater flow model, and discuss initial considerations on how best to complete the two-phase flow modelling. The results presented in the report represent the final formal contributions to this project from the Deltares team. The AGS team took on the tasks of completing the two-phase flow modelling incorporating the lessons learned through this initial phase of the work.

Deltares

Enabling Delta Life

Numerical modelling of groundwater flow and gas migration in the Milk River Aquifer and Alderson Member

Numerical modelling of groundwater flow and gas migration in the Milk River Aquifer and Alderson Member gas zone

Ane Wiersma
Annemieke Marsman
Peter Vermeulen

1230761-000

Contents

1 Introduction

This report summarizes the approach and steps that have been taken to deliver a series of computer simulations examining risk to groundwater in the Milk River Aquifer from the Alderson Member and Medicine Hat Member gas zones in AER's Southeast Alberta Management Unit. This report is part ot the 'Safe closure of the Medicine Hat and Alderson gas fields' project and more specific work package 4 'Risk quantification'. Not all steps have been finished and therefore this document is an interim report providing the results and discussion of the model simulations performed so far.

The purpose of the simulation is to support the process of risk assessment as defined by the ISO 31000 standard (International Standards Organization, 2009) by delivery of the first step in risk assessment, which is risk identification. Risk identification is defined in ISO 31000 as including identifying the "sources of risk, areas of impact, and events and their causes and their potential consequences." This should result in a list of risks based on events that might impact achievement of objectives.

The objective of AER in this case is to protect the environment from the impacts of oil and gas development in Alberta. The risk is that groundwater in the Milk River Aquifer (Virgelle Member) could be affected if commingled wells presently open to the gas-bearing zones in the Alderson Member and Medicine Hat Member are allowed to remain open after those wells are otherwise closed and abandoned at surface.

As discussed in the companion report on the conceptual model (AER-AGS & Deltares, 2017), there remains significant uncertainty as to whether this risk exists and if so, what are the potential consequences. The purpose of this simulation work-package is to generate a more comprehensive list of what subsurface events or circumstances could lead to the unwanted impact. This can only be done by conducting numerical experiments with computer simulations of this geosystem, especially since we have several alternative conceptual models for how the geosystem functions today. Also, there is no way other than simulation to examine how the geosystem will behave under different future management scenarios.

In this part of the project, the simulations are set up to deliver a set of results to answer a series of specific questions. This will be done for each conceptual model using a single representative realization. These results will generate a list of conditions where risk could occur per ISO 31000. At this point the level of risk will not yet be quantified, ranked, or otherwise assessed. The specific questions are:

1. Can a regional gravity-driven groundwater flow system as conceptualized be generated in the model domain, given our hydrostratigraphy and choices of boundaries when no natural gas deposits are included in the system? What is the effect of groundwater pumping?
2. If the Alderson Member gas-zone is replaced by a simple aquiclude in 1, does the gravity-flow system match observed patterns of regional gravity-driven groundwater flow in southern Alberta as conceptualized in the companion report?

3 If the Alderson Member is parameterized as conceptualized under each alternative model described in the companion report, can it trap natural gas under pre-development conditions?
4 If the Alderson Member is parameterized as conceptualized under each alternative model, can it still trap natural gas under conditions where the underlying Medicine Hat Member gas zone is left permanently commingled with the Alderson Member after the two gas zones are commercially exhausted?
5 If 4 is true, will gas leak out of the Alderson Member by diffusion?
6 Will groundwater pumping in the Milk River Aquifer (Virgelle Member) cause natural gas to pass through capillary seals that could otherwise trap natural gas under 4?
7 Will groundwater pumping in the Milk River Aquifer (Virgelle Member) affect trap leakage by diffusion?
8 If natural gas leaked out through seals in a separate phase due to buoyant forces or pumping-related reduction in capillary forces, would it go into the Milk River Aquifer (Virgelle Member) or elsewhere? Does groundwater pumping affect this?
9 If natural gas leaked through seals by diffusion instead would it go into the Milk River Aquifer (Virgelle Member) or elsewhere? Does groundwater pumping affect this?

To answer these questions, a workflow is set up which is discussed in Chapter 2. This workflow is based on the conceptual model report (AER-AGS/Deltares, 2017) with minor modifications to the sequence of simulations that consist of numerical groundwater flow and two phase flow models. In total, 8 Phases and 45 simulations are scheduled. This document reports about Phase 1, 2 and 4. In the simulations, conceptual model scenarios are tested.
Note that in this plan, the models will not be calibrated at first to replicate field data at specific conditions by optimizing the “parameters” of each model to deliver “best” predictions along with estimates of uncertainty.

Once these simulations are run, it may occur that the chosen instance of one of the conceptual models cannot replicate observed conditions, like replicating observed groundwater flow or trapping natural gas in the Alderson Member at predevelopment conditions. If this occurs, the instance may be reparameterized to make it work, even if improbable but possible parameter combinations are needed. The models will still be kept in the ensemble, but the likelihood of that model being a representation of the real system will go to zero. The model will be kept in the ensemble as it may reflect a stakeholder’s concerns even if improbable, and should be kept for the risk assessment stage to follow.

The results will be used in stakeholder conversations to discuss risk and learn what concerns all stakeholders will have. The stakeholder engagement plan is being developed and will be documented in a companion report. After contact with decision-makers and stakeholders, further simulations may be needed to test other conceptual models, assimilate other observations, or have decision makers validate that certain models can be eliminated from the ensemble based on simulation results. The simulation runs have been designed to minimize the cost needed to revisit any model or add another conceptualization of the system important to a decision-maker or stakeholder.

2 Simulation plan

2.1 Modelling workflow phases

The simulations consist of eight phases indicated in Figure 2.1. Each phase consists of a number of simulations. Every phase goes one step further compared to the previous phase, and ultimately the simulations allow us to give an assessment which members of the multimodel ensemble can leak gas into the Milk River Aquifer when the gas wells are decommissioned with commingled abandonments. The first three phases involve the hydrogeological model to investigate the hydrogeology of the area and acquire boundary conditions for the next phases. The subsequent five phases involve the two-phase flow model to investigate gas migration.

This report only discusses Phase 1, 2 and 4. The other phases will be carried out and reported in a later stage.

The objective of Phase 1 is to get insight in the hydrogeological system and get a feeling for the sensitivity of the model for parameters such as recharge and permeability values. In this phase, different boundary conditions of the hydrogeological model are tested and the effect of an impermeable gas reservoir on the groundwater flow. In the first simulation, the 44 layer model provided by AGS is tested with single value permeabilities per layer. In Simulation 2, the Milk River / Alderson model layers and Medicine Hat Sandstone model layers are replaced by voxels with the same dimensions and resolution as the property model provided by the AGS that is used in a later stage. All voxels within one hydrogeological unit have the same permeability values. This simulation aims to show the effect of increasing the resolution of the model and working with a large number of model layers. Simulation 3 is identical to simulation 1, except for the fact that the Alderson gas reservoir is mode impermeable. This allows the investigation of the effects of a reservoir with high gas saturation on the groundwater flow patterns.

In Phase 2 different scenarios are introduced to simulate the natural hydrogeological conditions prior to pumping in the Milk River aquifer and prior to gas extraction. These scenarios simulate the configuration of the gas reservoir and the connection to the Milk River aquifer. Five scenarios have been identified which are in agreement with literature, each consisting of a number of building blocks (e.g. A1, B2, C1 and D2) have been identified. These Building blocks have been described in detail in section 2.3. In addition to these five scenarios, a sixth scenario consists of the configuration of the reservoir according to the well log based property model provided by the AGS.

Phase 3 is identical to Phase 2, except for the fact that this phase includes the effect of pumping of the Milk River aquifer. The hydrogeological conditions obtained from this phase are used as input for subsequent phases 6 and 8 to simulate the effect of groundwater extraction on gas migration.

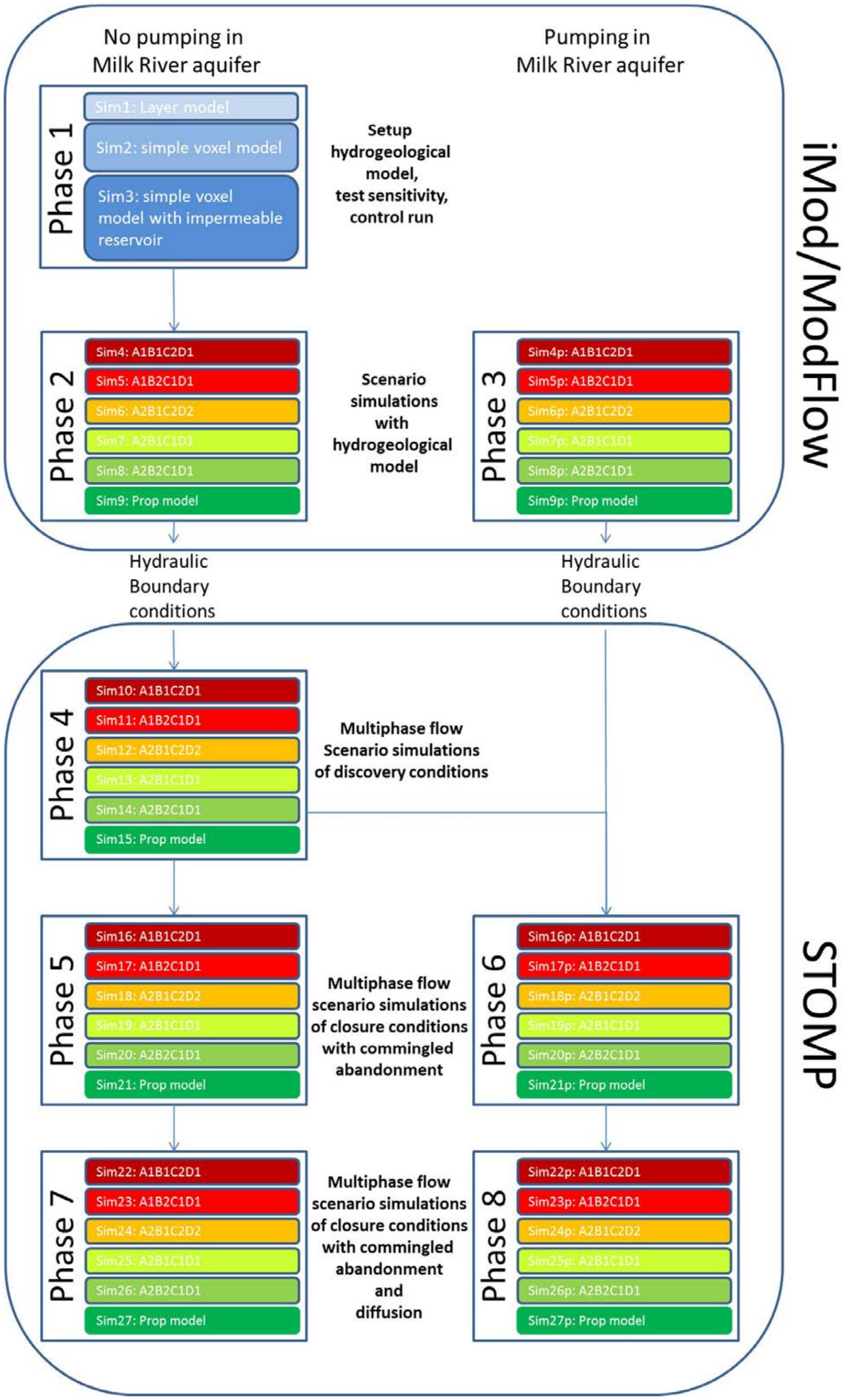

Figure 2.1 Flowchart of simulations to be performed. The codes (e.g. A1B1C2D) of the scenario simulations correspond to the building blocks used for the construction of the scenarios.

In Phase 4, two-phase flow is introduced using STOMP. In this phase, for each of the scenarios and the property model, the conditions of the gas reservoir prior to discovery are simulated. For this purpose, a representative cross section is drawn across the scenario simulations of the hydrogeological model and the hydraulic heads and pressures are used as input in STOMP. In the scenarios, the permeability values and Van Genuchten parameters are adapted to represent weak cq strong seal strengths. The weak seals are able to hold gas columns of ca. 10m, the strong seals are able to hold gas columns of 230m.

In Phase 5, the two-phase flow STOMP scenarios are taken one step further and the effect of connecting the Alderson reservoir and the Medicine Hat reservoir through commingled closed wells is simulated. The results from Phase 4 are used as input for this Phase 5. To simulate the commingled conditions, the gas pressures in the Alderson reservoir are increased, and the effect on gas migration is investigated.

Phase 6 is identical to Phase 5, but includes the effect of groundwater abstraction from the Milk River aquifer on the gas migration. This pumping could result in higher buoyancy pressures in the Alderson Formation due to the lowering of hydraulic heads, thereby potentially leading to the failure of the seals holding the gas. For this purpose, the hydraulic heads from Phase 3 are used in this phase.

Phase 7 is identical to Phase 5, except for the fact that diffusion of methane is taken into account. Similarly, Phase 8 is identical to Phase 6, but also includes diffusion of methane with groundwater.

2.2 Conceptual model simulations

Phase 2 – 8 consist of six simulations each testing a specific conceptual model. These six simulations consist of 5 conceptual model scenario simulations, and one property model simulation. This property voxel model is constructed for the Milk River – Alderson Formation and the Medicine Hat Formation and is provided by the AGS. Using log analyses, details on the lithology of the units, as well as on porosity, water saturation and permeability were provided. This property model also forms the basis for the schematisation of the conceptual model scenarios.

The conceptual models that were tested are:
The five alternative conceptual models for the hydrostratigraphy of the Alderson gas zone and trap at the intraformational scale are summarized and illustrated as follows.

1. Connected reservoir, strong seals, Alderson sandstone persists to north (Figure 2.2).
2. Connected reservoir, strong seals, Alderson sandstone localized to south (Figure 2.3).
3. Disconnected reservoir, weak seals, Alderson sandstone persists north (Figure 2.4).
4. Disconnected reservoir, strong seals, Alderson sandstone persists north (Figure 2.5).
5. Disconnected reservoir, strong seals, Alderson sandstone restricted to south (Figure 2.6).

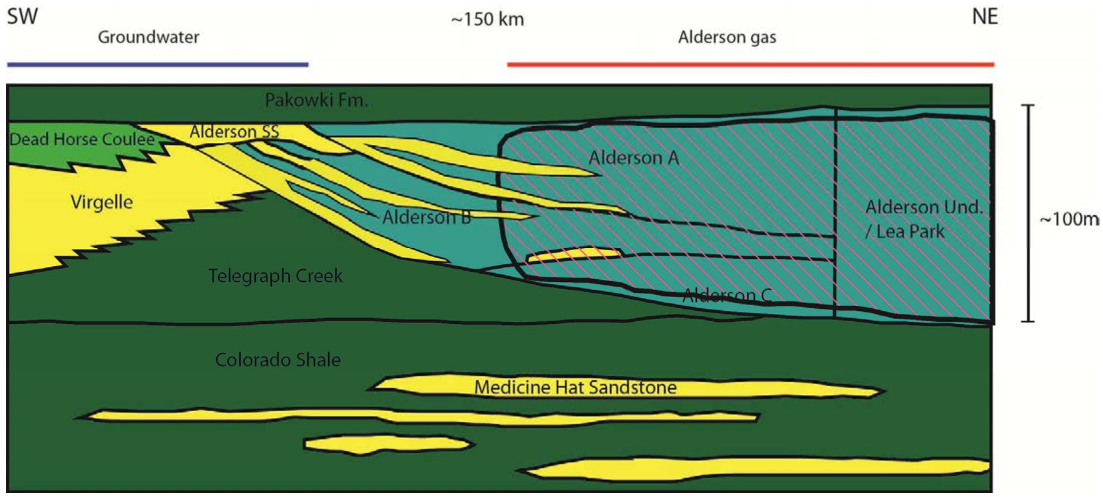

Figure 2.2 Conceptual model 1: Connected reservoir, strong seals, Alderson sandstone persists to north

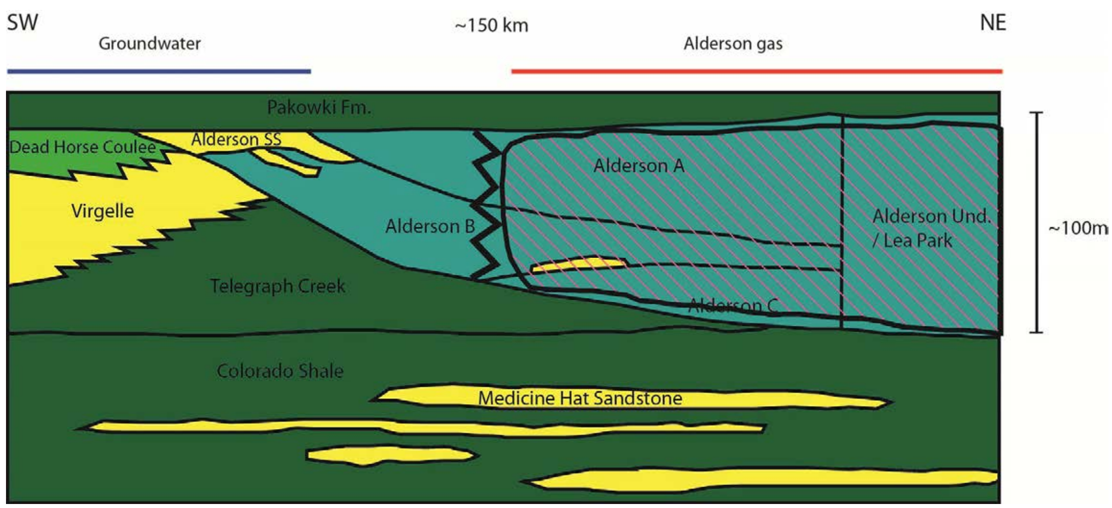

Figure 2.3 Conceptual model 2: Connected reservoir, strong seals, Alderson sandstone localized to south

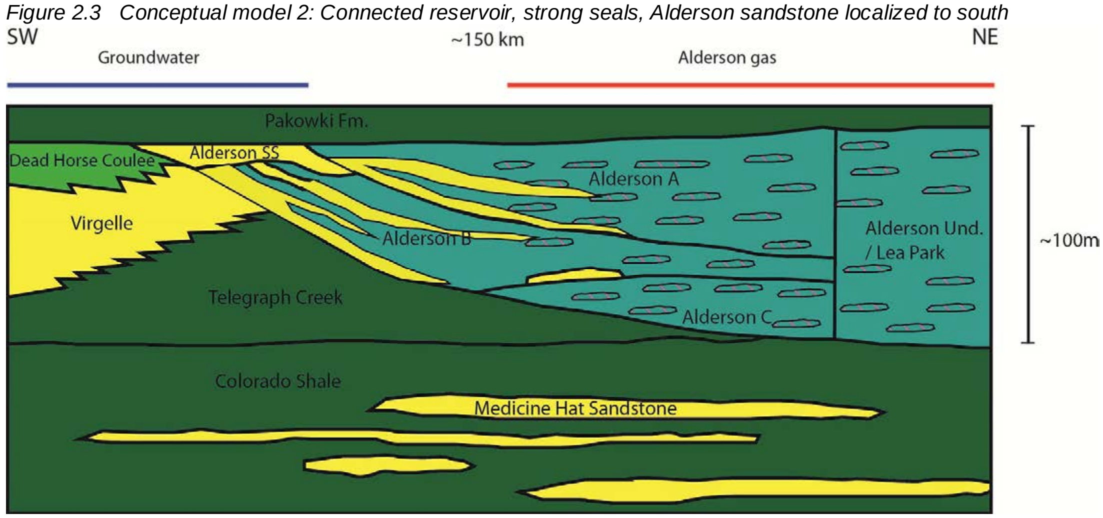

Figure 2.4 Conceptual model 3: Disconnected reservoir, weak seals, Alderson sandstone persists north

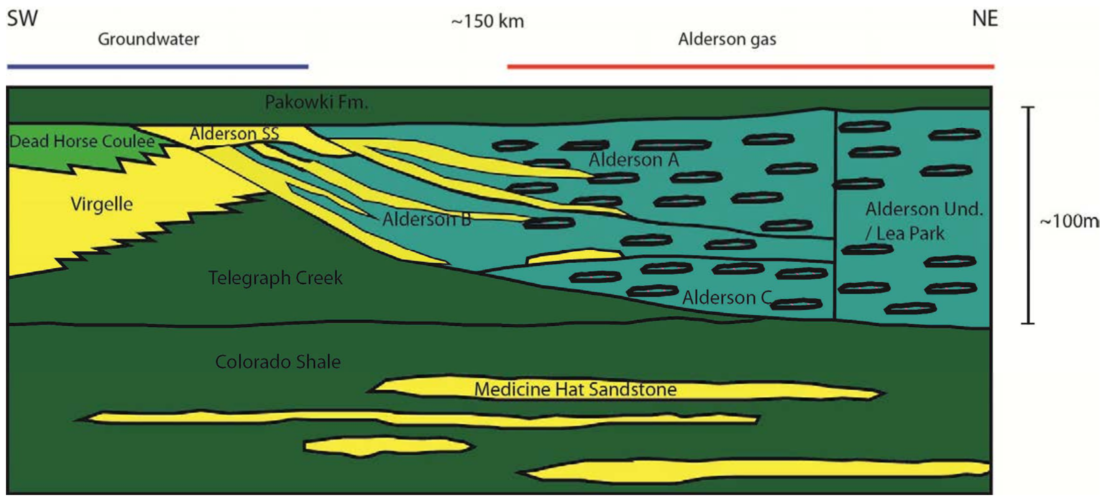

Figure 2.5 Conceptual model 4: Disconnected reservoir, strong seals, Alderson sandstone persists north

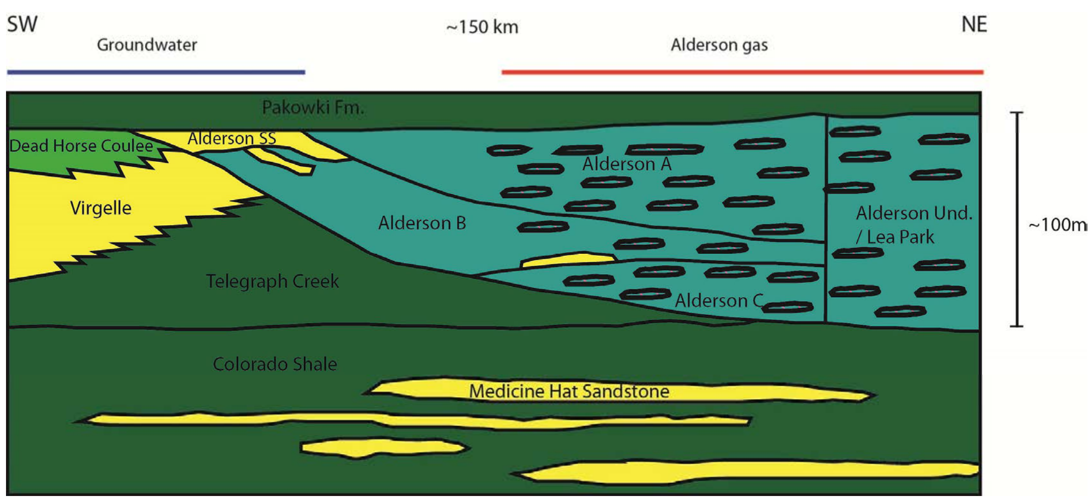

Figure 2.6 Conceptual model 5: Disconnected reservoir, strong seals, Alderson sandstone restricted to south

2.3 Schematisation of conceptual models

To schematise the conceptual models, several modifications to the property voxel model have to be made. The modifications take place in the Alderson gas reservoir and in the boundary zone between the Milk River Aquifer and the commingled Alderson gas reservoir (Figure 2.7), and consist of changing the configuration of the permeability values of voxels in the Alderson A, B and C formations in these zones. The purpose of these modifications is to simulate several possible discovery conditions of the Alderson gas reservoir. These conditions are later submitted to possible perturbations, such as pumping and commingling, to test their effect on methane migration.

The modifications are here described in four sets of two building blocks each:
A1: Connected reservoir
A2: Disconnected reservoir
B1: Alderson Sandstone persists to the north

B2: Alderson sandstone confined to the south
C1: Strong seals in reservoir
C2: Weak seals in reservoir
D1: Strong seals in Boundary zone
D2: Weak seals in boundary zone

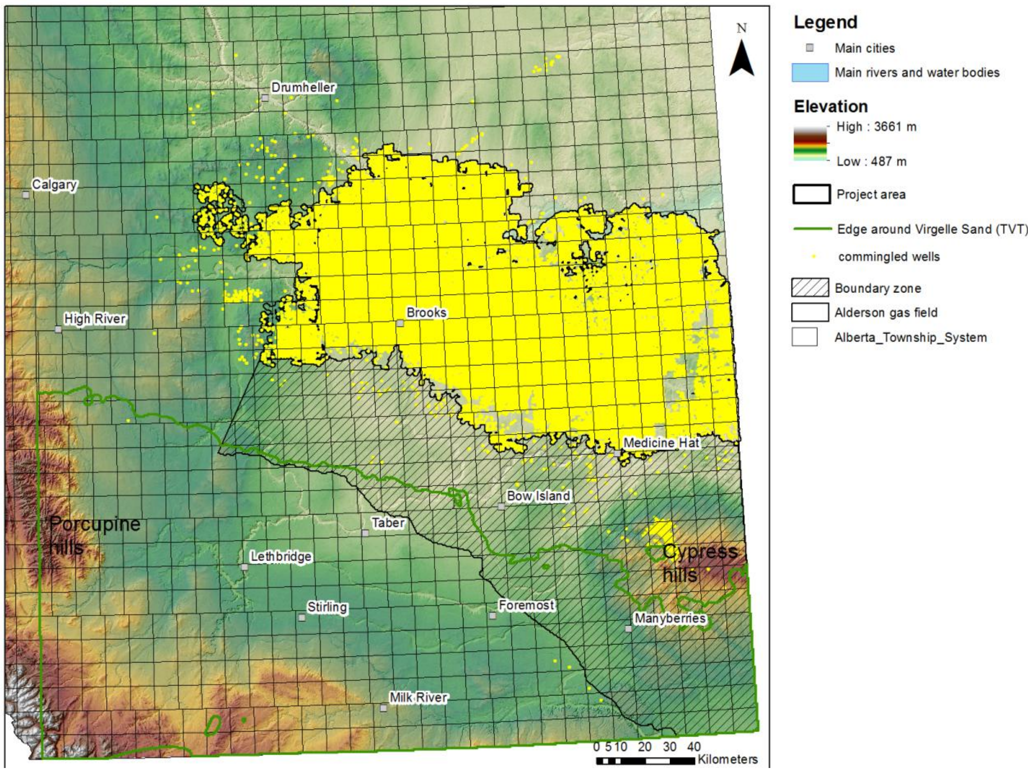

Figure 2.7 Commingled Alderson gas reservoir and boundary zone which ranges from the edge of the reservoir to the southernmost Alderson A, B and C extent.

2.3.1 A1: Connected reservoir

This building block is constructed to test the effect of large gas columns trapped in the Alderson Reservoir. For this purpose, the voxels from the property model are set to either sand or shale. To create the space for large gas columns, 40% of the voxels in the gas reservoir is set to sand, the remaining 60% is set to shale. The sand has a permeability of 4.32E-2 m/day, which is the value generally used for sandy layers in the layer model. This value agrees with a 96th percentile of permeability values in the reservoir. The permeability of the shale depends on the strength assigned to the seal.

2.3.2 A2: Disconnected reservoir

This building block is constructed to test the effect of shorter and disconnected columns of gas in the Alderson Formation. For this purpose, the voxels from the property model are set to either sand or shale. To create the space for short gas columns, 20% of the voxels in the gas reservoir is set to sand, the remaining 80% is set to shale. The sand has a permeability of 4.32E-2 m/day, which is the value generally used for sandy layers in the layer model. This value agrees with a 96th percentile of permeability values in the reservoir. The permeability of the shale depends on the strength assigned to the seal.

2.3.3 B1: Alderson sandstone persists to the north

This building block allows for the simulation of the effect of gravity driven groundwater flow downstream towards the reservoir, and its effect on gas distribution. For this purpose, in the boundary zone, the voxels of the property model are reassigned values for permeability ranging from sand in the south (near the Milk River Aquifer) gradually (log-normally) transforming into shale along the reservoir edge. The sand voxels in the south have a permeability of 4.32E-2 m/day, which is the value generally used for sandy layers in the layer model. The permeability of the shale at the northern edge of the boundary zone depends on the strength assigned to the seal.

2.3.4 B2: Alderson sandstone confined to the south

This building block allows for the simulation of minimal groundwater exchange between aquifer and reservoir. For this purpose, all voxels of the property model in the Alderson A, B or C Formations are set to shale. The permeability of the shale depends on the strength assigned to the seal.

2.3.5 Seal strength

The seal strength in the reservoir is dependent on the Van Genuchten parameters assigned to the voxels. These parameters are also related to the permeability of the rocks. The relation between the permeability and Van Genuchten parameters was established using a relation found in literature (Dobson and Houseworth, 2014). For the simulations, two seal strengths are considered: one that can hold only short columns of gas, i.e. less than 10m, and one that can hold tall columns of 230m of gas. The short columns of gas correspond to the image of authors describing the reservoir as an unconventional reservoir with small unconnected gas bodies. The tall columns correspond to the idea of authors referring to the reservoir as one connected gas column, from bottom to top. The largest distance between the deepest bottom of the Alderson to the highest top is 500m. This value was not used however, as tuning the permeabilities and Van Genuchten parameters to such a tall gas column arrived at unrealistic permeabilities for the shales in this setting. Therefore a gas column of 230m was used to tune the seals.

The permeability corresponding to a seal holding a gas column of 10m was 3.41E-08 m/day. A seal able to hold a gas column of 230m corresponds to a permeability of 8.31E-10 m/day.

2.3.6 C1: Strong seals in reservoir

All the shale voxels belonging to the Alderson A, B and C Formations in the reservoir get a permeability value of 8.31E-10 m/day. Therefore, the seal can hold a buoyancy pressure belonging to a gas column of 230m tall.

2.3.7 C2: Weak seal in reservoir

All the shale voxels belonging to the Alderson A, B and C Formations in the reservoir get a permeability value of 3.41E-08 m/day. Therefore, the seal can hold a buoyancy pressure belonging to a gas column of 10m tall.

2.3.8 D1: Strong seals in boundary zone

All the shale voxels belonging to the Alderson A, B and C Formations in the boundary zone get a permeability value of 8.31E-10 m/day. Therefore, the seal can hold a buoyancy pressure belonging to a gas column of 230m tall.

2.3.9 D2: Weak seals in boundary zone

All the shale voxels belonging to the Alderson A, B and C Formations in the boundary zone get a permeability value of 3.41E-08 m/day. Therefore, the seal can hold a buoyancy pressure belonging to a gas column of 10m tall.

2.3.10 Final schematisations

The five conceptual models are composed of the following building blocks:

1. Connected reservoir, strong seals, Alderson sandstone persists to north:A1B1C2D1 (e.g. Simulation 4)
2. Connected reservoir, strong seals, Alderson sandstone localized to south: A1B2C1D1 (e.g. Simulation 5)
3. Disconnected reservoir, weak seals, Alderson sandstone persists north: A2B1C2D2 (e.g. Simulation 6)
4. Disconnected reservoir, strong seals, Alderson sandstone persists north: A2B1C1D1 (e.g. Simulation 7)
5. Disconnected reservoir, strong seals, Alderson sandstone restricted to south A2B2C1D1 (e.g. Simulation 8)

In addition, the property model without modifications is tested (e.g. Simulation 9).

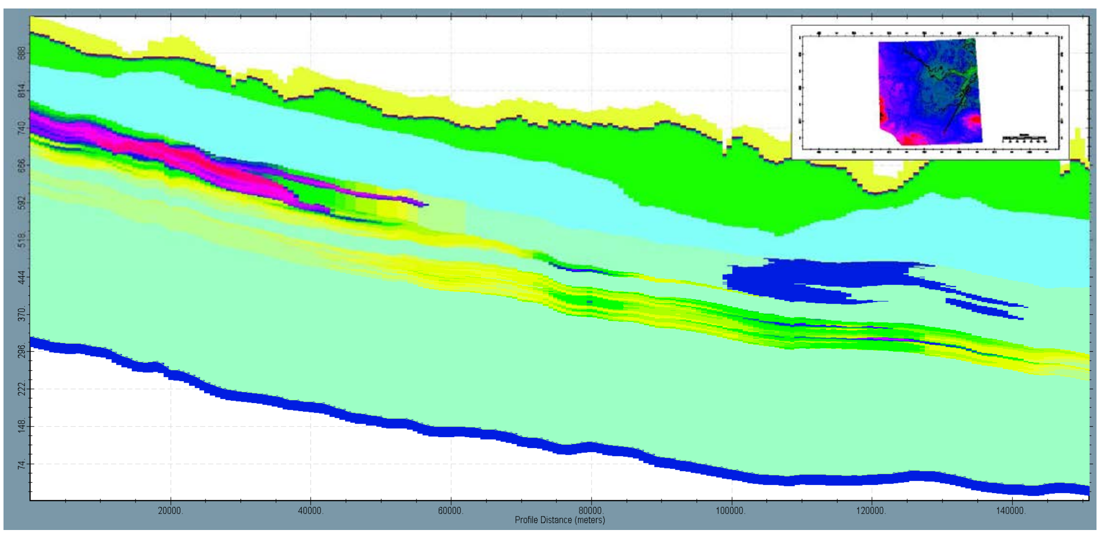

Figure 2.8 SSW – NNE cross section showing the schematisation of conceptual model 1 (e.g. Simulation 4) in permeability values. Note the gradual decrease in permeability values towards the north in the boundary zone and the connected reservoir (blue colours in the reservoir).

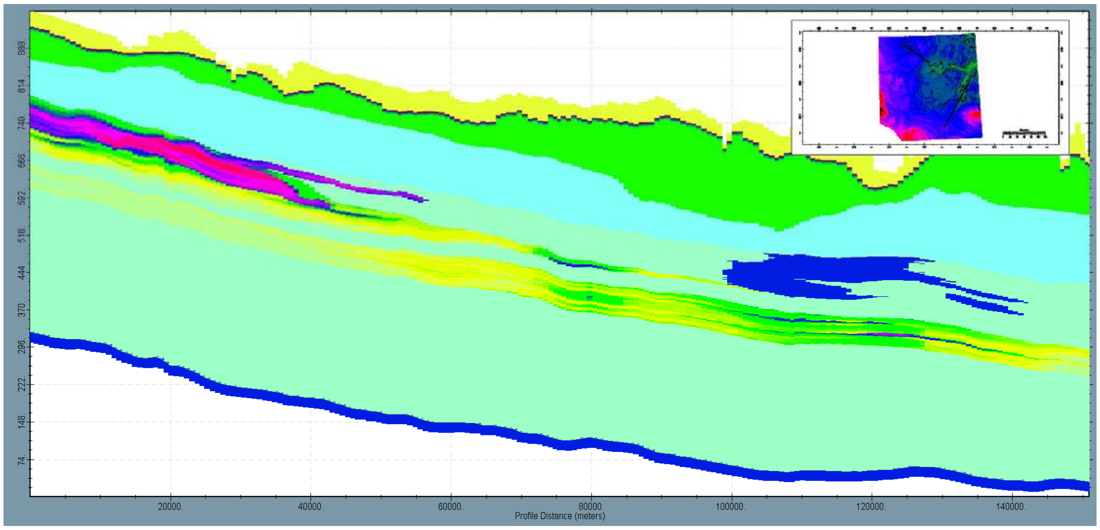

Figure 2.9 SSW – NNE cross section showing the schematisation of conceptual model 2 (e.g. Simulation 5) in permeability values. Note the low permeability values in the boundary zone and the connected reservoir (blue colours in the reservoir).

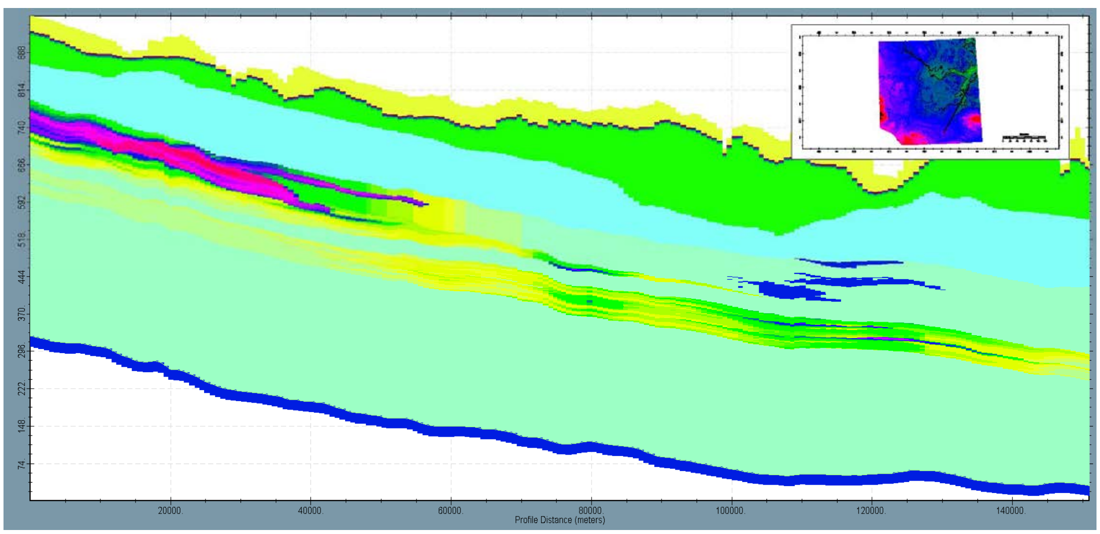

Figure 2.10 SSW – NNE cross section showing the schematisation of conceptual model 3 (e.g. Simulation 6) in permeability values. Note the gradual decrease in permeability values towards the north in the boundary zone and the disconnected reservoir (blue colours in the reservoir).

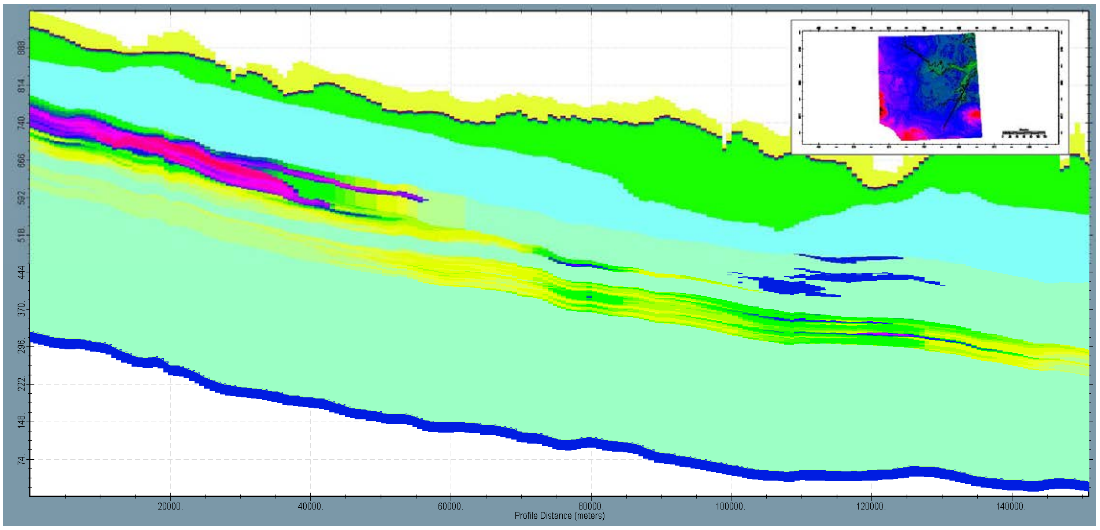

Figure 2.11 SSW – NNE cross section showing the schematisation of conceptual model 4 (e.g. Simulation 7) in permeability values. Note the gradual decrease in permeability values towards the north (but steeper than conceptual model 3) in the boundary zone and the disconnected reservoir (blue colours in the reservoir).

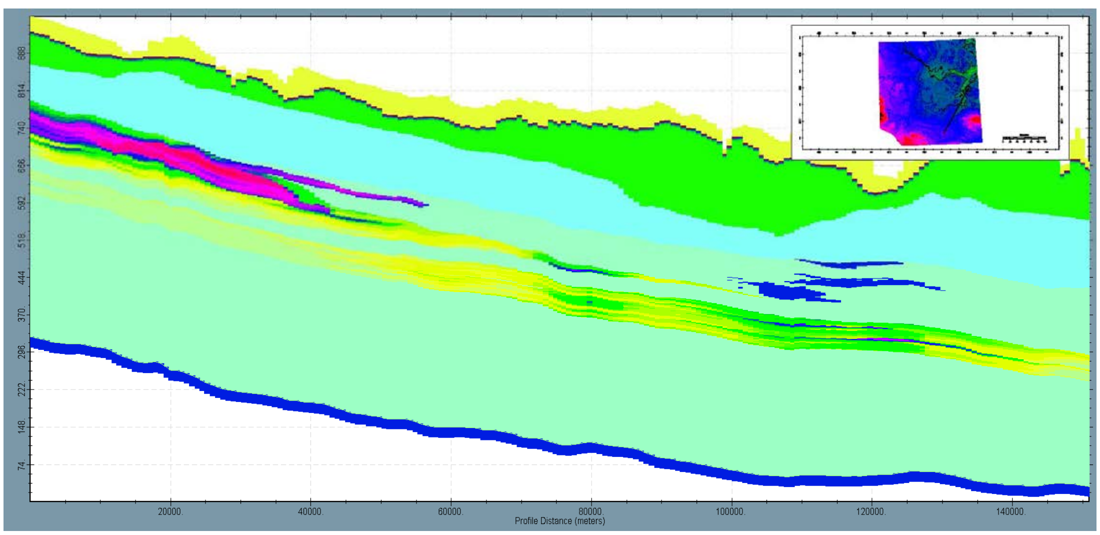

Figure 2.12 SSW – NNE cross section showing the schematisation of conceptual model 5 (e.g. Simulation 8) in permeability values. Note the low permeability values in the boundary zone and the disconnected reservoir (blue colours in the reservoir).

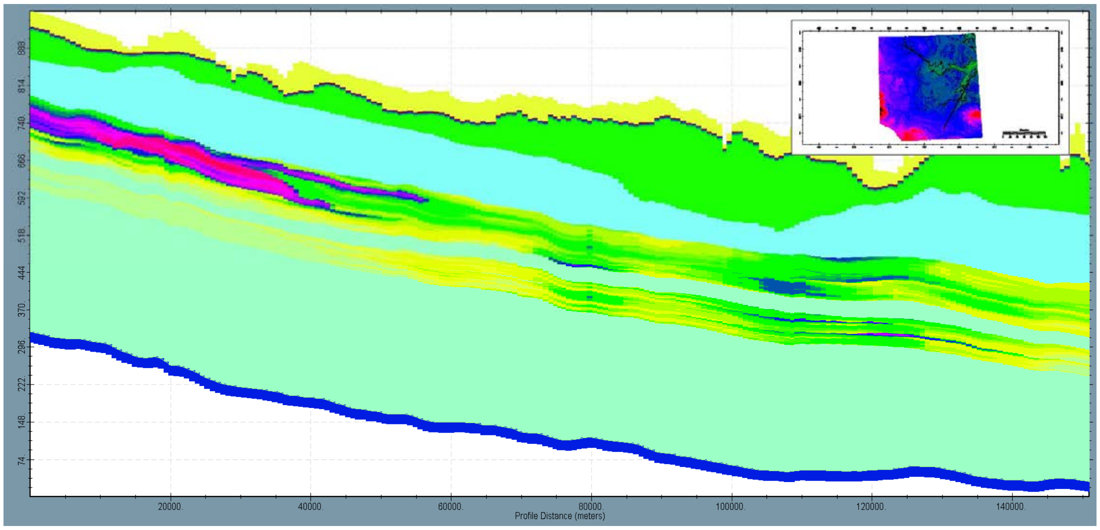

Figure 2.13 SSW – NNE cross section showing the permeability values of the property model provided by AGS (e.g. Simulation 9). Note the generally higher permeability values compared to the previous conceptual models in the boundary zone and the gas zone.

3 Theoretical Background

3.1 Groundwater

3.1.1 Numerical Concepts

To describe groundwater flow in three dimensions we use the partial differential equation based upon Darcy's law and the equation of continuity (McDonald and Harbaugh, 1988):

$$\frac{\partial}{\partial x}\left(T_x\frac{\partial h}{\partial x}\right)+\frac{\partial}{\partial y}\left(T_y\frac{\partial h}{\partial y}\right)+\frac{\partial}{\partial z}\left(T_z\frac{\partial h}{\partial z}\right)-q=S\frac{\partial h}{\partial t}$$

where h [L] is the piezometric head, x, y and z [L] are Cartesian coordinates, t [T] is the time, $T_{x/y/z}$ [LT^{-1}] are the conductivities in x, y and z directions, S [L^{-1}] is the storage coefficient and q [T^{-1}] is the discharge or recharge term.

In the Netherlands, the software package iMOD (Interactive MODeling) was developed, to support the usage and creation of high resolution, national groundwater flow models (Vermeulen, et al., 2017). The concept of iMOD minimizes the undesired high costs of repeatedly developing individual - partly overlapping - models, and to facilitate engagement of the stakeholders in the model building process. To make this happen iMOD provides the necessary functionalities to manage very large groundwater flow models, including interactive generation of sub-models with a user-defined (higher or lower) resolution embedded in- and consistent with the underlying set of model data. This feature is especially essential in the current modeling study.

3.2 Multi-Phase Flow

3.2.1 Multiphase flow: theoretical background

Gas is only slightly miscible with water. It can form a serious threat to e.g. drinking water and ecology. Due to the lower specific density of gas compared to (salt) water (1000 to 1025 kg/m^3), gas tends to "float" on groundwater. When gas leaks, it migrates upward towards the surface; a process referred to as multiphase flow through a porous medium (Marsman, 2002).

Problems involving pure phase gas are more complex than gas dissolved in plumes. A few basic concepts must be reviewed here to put the factors that control the occurrence and flow of gas into context. *Saturation* is defined as the relative abundance of a fluid or gas in a porous medium as a volume of one of the fluid or gas species present in the pores per unit void volume. The sum of saturations of the fluid or gas species is equal to one. *Capillarity* is a force that results from a combination of interfacial tension and the ability of certain liquids or gases to wet the surfaces with which they come into contact. Interfacial tension is defined as the work required to separate a unit area of one substance from another and is expressed as a force per unit length. *Wettability* is the tendency for one fluid or gas to be attracted to a surface in preference of another fluid. Water is always the wetting fluid in porous rock when co-occurring with oil or gas.

The pressure discontinuity across any curved interface separating two immiscible fluids or gases is referred to as the *capillary pressure*. Thus, the capillary pressure is directly proportional to the surface tension and inversely proportional to the radius of the curvature. Capillary pressure is a measure of the tendency of a porous medium to imbibe (or absorb) the wetting phase or to repel the nonwetting phase. As it is difficult to push a nonwetting fluid into a pore with wetting fluid or gas, capillary pressure can also be thought of as the pressure required to move a particle of nonwetting fluid or gas into a pore with a wetting fluid. Because small pores provide resistance to entry due to capillarity, nonwetting gas will tend to move through the coarser, more permeable zones of a heterogeneous medium. This behavior traps globules of water. In the unsaturated zone, capillary pressure (expressed as a negative pressure head) is referred to as suction (Domenico and Schwartz, 1998).

An important concept in multiphase flow is that of *relative permeability*. It accounts for the tendency of fluids or gases to interfere with one another as they flow through a porous medium, and can be described using Darcy's law written in terms of pressure gradients. In multi-fluid systems the relative permeability of a fluid or gas ranges between zero and one. Exactly how the relative permeability varies between zero and one when more than one fluid or gas is present is a complex function of the relative saturation, the wettability and of whether the fluid or gas is undergoing imbibition (absorbed) or drainage (repelled) (Domenico and Schwartz, 1998).

When fluid or gas enters a porous medium, the interfacial tension determines which pores and which part of these pores will be entered by the fluid or gas. Different behavior can be distinguished for different rock/soil types and fluid/gas types. Such behavior is classified by the relative permeability of the phases (gas, oil, water, air) in a certain medium. Because of the assumption that gas is the nonwetting phase compared to (salt) water, gas will enter the largest pores and water will coat the surface of the grains. In porous media with a high permeability, the gas will flow upward due to buoyancy forces, caused by the density difference between gas and water. When the gas encounters a zone of low permeability, the gas is for the largest part trapped below this layer. Spreading of the gas will be enhanced in areas with preferential groundwater flow or when the low permeable zone is tilted. In summary, where permeable porous media allow gas to flow towards the surface at high flow rates, porous media with a low permeability cause the gas to spread out over a larger area (Marsman, 2002).

3.2.2 General equations of multiphase flow

A two-dimensional isotropic and homogeneous vertical cross-section of the subsurface is considered to explain the general equations of multiphase flow (Marsman, 2002). General equations of a two-phase model (water and gas) are the mass balance equations, Darcy's law and the constitutive equations.

$$\phi \frac{\partial S_i}{\partial T} + \frac{\partial U_i}{\partial X} + \frac{\partial V_i}{\partial Z} = 0, i = w,g \tag{1}$$

where the subscript i denotes either the water (w) or the gas (g) phase. S_i is the effective phase saturation, U_i and V_i are respectively the horizontal and vertical phase velocities. T is time and X and Z are respectively the horizontal and vertical coordinates, and ϕ is the porosity. The velocities follow from Darcy's law, which is given by:

$$U_i = -\frac{Kk_{ri}}{\mu_i}\frac{\partial P_i}{\partial X} \tag{2}$$

$$V_i = -\frac{Kk_{ri}}{\mu_i}\left(\frac{\partial P_i}{\partial Z} + \rho_i g\right) \qquad i = w,g \tag{3}$$

where K is the absolute permeability, kri is the relative phase permeability, and μ_i is the phase viscosity. P is the phase pressure, ρ_i is the phase density, and g is the gravity acceleration. Combination of equations 1, 2, and 3 yields the Richards equation:

$$\phi\frac{\partial S_i}{\partial T} - \frac{\partial}{\partial X}\left(\frac{Kk_{ri}}{\mu_i}\frac{\partial P_i}{\partial X}\right) - \frac{\partial}{\partial Z}\left(\frac{Kk_{ri}}{\mu_i}\frac{\partial P_i}{\partial Z}\right) - \rho_i g\frac{\partial}{\partial Z}\left(\frac{Kk_{ri}}{\mu_i}\right) = 0 \qquad i = w,g \tag{4}$$

The constitutive relations are defined by Parker and Lenhard (1987):

$$S_w + S_g = S_t$$
$$S_w + S_{gt} = S_{wa}$$
$$S_{gf} + S_{gt} = S_g$$
$$P_{gw} = P_g - P_w$$

where S_t is the total liquid saturation. S_{wa} is the apparent water saturation, S_{gt} is the trapped gas saturation and S_{gf} is the free gas saturation, S_{gt} is the free gas saturation. P_{gw} is the gas-water capillary pressure.

To describe the entrapment of gas, a linearized equation is used according to Kaluarachchi and Parker (1992) that can be easily implemented in model codes:

$$S_{gt} = \min\left[\left(\frac{1-S_w^{\min}}{1+F_L\left(1-S_w^{\min}\right)} - \frac{1-S_{wa}}{1+F_L(1-S_{wa})}\right), S_g\right] \tag{5}$$

$$F_L = \frac{1}{S_{or}^{\max}} - 1 \tag{6}$$

where S_{gt} is the trapped gas saturation and $S_w^{\min}$ is the maximum water saturation. F_L is Land's factor, where $S_{gr}^{\max}$ is the maximum residual oil saturation. Equation (5) prevents that the trapped oil saturation becomes larger than the oil saturation Marsman (2002).

In our study, we assume there is no gas entrapment: to get insight in the strength of the seals it is worst case approach to assume that all gas is mobile and can cause a capillary pressure that can exceed the entry pressure of a seal.

3.2.3 Numerical modeling of multiphase flow

Flow models for simulating the flow of water, oil and gas through a porous medium have been in use since the 1970s, primarily in the oil and gas industry. Because the underlying principles are generic, such models can be used for environmental problems as well. Multiphase flow models for gas reservoirs, where water and gas flow simultaneously, have been used intensively, hence they can be considered thoroughly tested.

White et al. (1995) and Lenhard et al. (1995) developed a computer model called STOMP (Subsurface Transport Over Multiple Phases) to predict environmental restoration studies involving multiphase flow problems. It is a three-dimensional, three-phase, compositional engineering simulator for modeling contaminant migration and remediation technologies for the cleanup of subsurface sites contaminated with organic compounds. The STOMP model code is based on the Richards equation (see section 3.2.1) and on the constitutive relations developed by Lenhard and Parker (1987) and Kaluarachchi and Parker (1992). Flow and transport are solved numerically using an integrated-volume finite-difference scheme to discretize the governing equations. The capillary pressure-saturation relationships can be chosen from different empirical relations. In this study, the Van Genuchten capillary pressure-saturation relationship (Van Genuchten, 1980) is used (Marsman, 2002).

4 Modelling Groundwater

4.1 Model Boundaries

4.1.1 Introduction

The boundary of the model is given by the provincial border with Saskatchewan in the East, the USA-border in the South, the approximate location of the deformed belt in the West and the approximate northern-most boundary of the Alderson gas field (Figure 4.1). The width of the modelling area is 298 kilometers; the height is 322 kilometers, the total area 95,956 km^2.

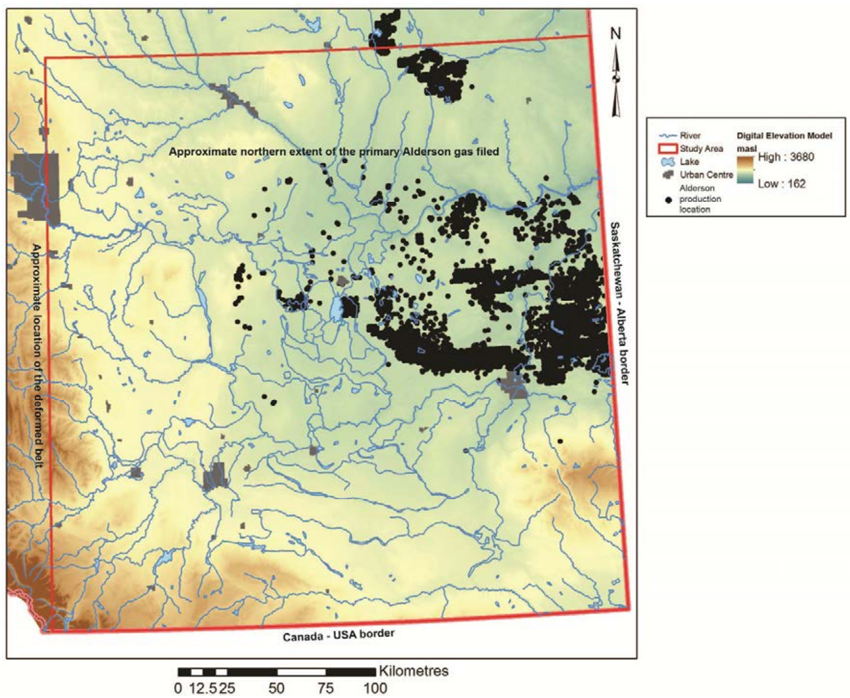

Figure 4.1 Location of the model domain.

4.1.2 Boundary Conditions

Two types of boundary conditions are used in the current model: a <u>closed boundary condition</u> which is defined as a modeling boundary over which no groundwater flow is passing, and an <u>open boundary condition</u> (Dirichlet Boundary) which is defined as a boundary over which groundwater flow is passing.

Closed Boundary Conditions

Along almost all sides of the modeling domain, throughout the base, this type of closed model boundary condition is valid. This is an assumption which is conservative in the sense that all groundwater in the model, need to origin from recharge in the model domain. There is a possibility that groundwater enters the model from the west, but since the west side is relatively far from the area of interest in the east (the gas-fields), the effect of ignoring any inflow might be neglectable.

Open Boundary Conditions
An inflow that might have an effect in the gas field is the inflow from the Sweet Grass Hills area in Montana (USA). As the more permeable formation outcrop in this area, this is seen as an important source of groundwater for the Milk River aquifer that intersects with the Alderson further north. This inflow quantity is estimated at 9 million m^3/year (Pétré et al., 2015). From experimental simulations with our model, it was impossible to inject this amount of groundwater without introducing large areas of inundation. Pétré stated: "*The total flux is probably overestimated because high transmissivity values in northern Montana corresponds to the most productive areas characterized by faults and fractures*". The current geological model in this study has a different transmissivity distribution which seems to be significant less than the one use by Pétré, therefore a Dirichlet boundary condition was chosen – also called a *constant-head boundary* – to simulate the inflow quantity from the Sweet Grass Hills in Montana and compare it with the quantity found by Pétré. From head data in the Milk River Aquifer, the isohypses of the pressure heads are estimated and interpolated using Kriging, see Figure 4.2.

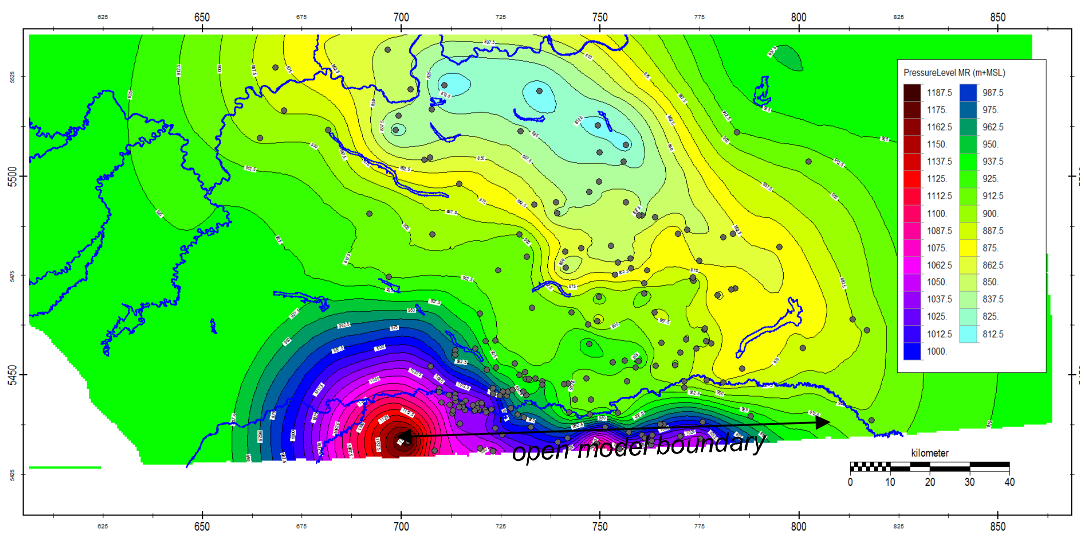

Figure 4.2 Interpolated isohypses of the pressure heads in the Milk River aquifer from head data (source: AGS, 2018)

The pressure head along the boundary are selected from the interpolated pressure head and set for the entire Milk River aquifer, from unit 14) the **Alderson Undefined** (NE) and **Dead Horse Coulee** (SW) up to unit 25) the top of the **Colorado**, see section 4.2.

4.1.3 Sub Modelling

The modelling resolution varies from 2,000 meters up to a minimal resolution of 500 meter. The first modeling resolution is used to obtain a solution of the groundwater levels for the entire region. The model consists out of 201 model layers (see section 2.3) therefore this type of model consumes 2 Gb of RAM as it contains 146 * 161 * 201 = 4.7 million nodes. The second modeling resolution is used to construct groundwater levels at the resolution of the geological maps, i.e. 500 meter. A model like this consumes 75 million nodes which is impossible to simulate on a regular computer infrastructure. To overcome this problem, a method of sub modelling is applied. From the results of the coarser model (2,000 meter resolution), Dirichlet boundary conditions are formulated for a smaller and finer modelling network at a resolution of 500 meter, each of this sub model has an overlapping boundary of

5 kilometer to avoid inaccuracies due to the open model boundary. This is illustrated on Figure 4.3. Each sub model consumed 7 Gb of RAM and contained 20.5 million nodes.

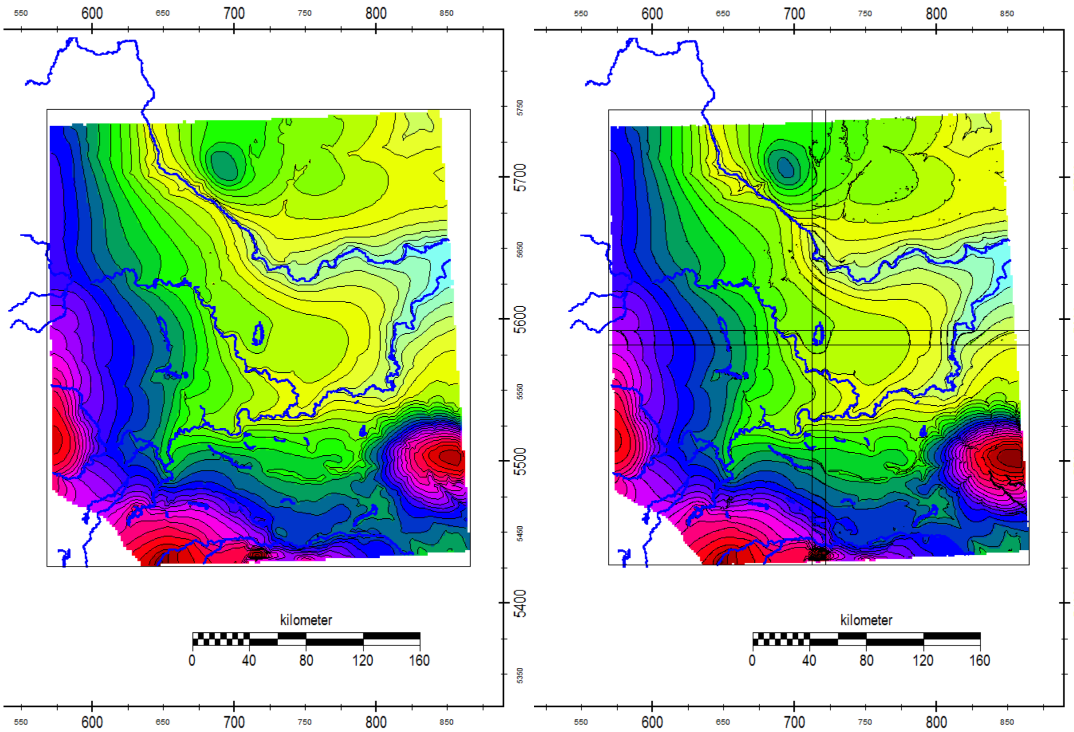

Figure 4.3 Illustration of the sub modelling concept; (left) a result on a resolution of 2,000 m for the entire modeling domain; (right) the results of 4 sub models on a resolution of 500 meter with an overlap of 5,000 meter.

4.2 Subsurface Geology

4.2.1 Introduction

The groundwater flow model is based on the detailed geological model of the study area which includes 43 different geological layers from the land surface to the Bow Island/Viking Formation. Figure 4.4 shows the hydrostratigraphic chart of the study area. As the focus of the modeling work is on the Milk River Formation, the Alderson Member of the Lea Park Formation and the Medicine Hat Member of the Niobrara Formation, additional mapping work was completed on these units. The Milk River Formation was subdivided into from oldest to youngest, the Telegraph Creek, Virgelle and Deadhorse Coulee members. The Alderson Member of the Lea Park Formation was subdivided into the Alderson A, B and C, as well as several sand units. The Medicine Hat Member of the Niobrara Formation was subdivided into several sand units as well as intervening silty/shaley intervals. All these layers were mapped at a resolution of 500 x 500 meters.

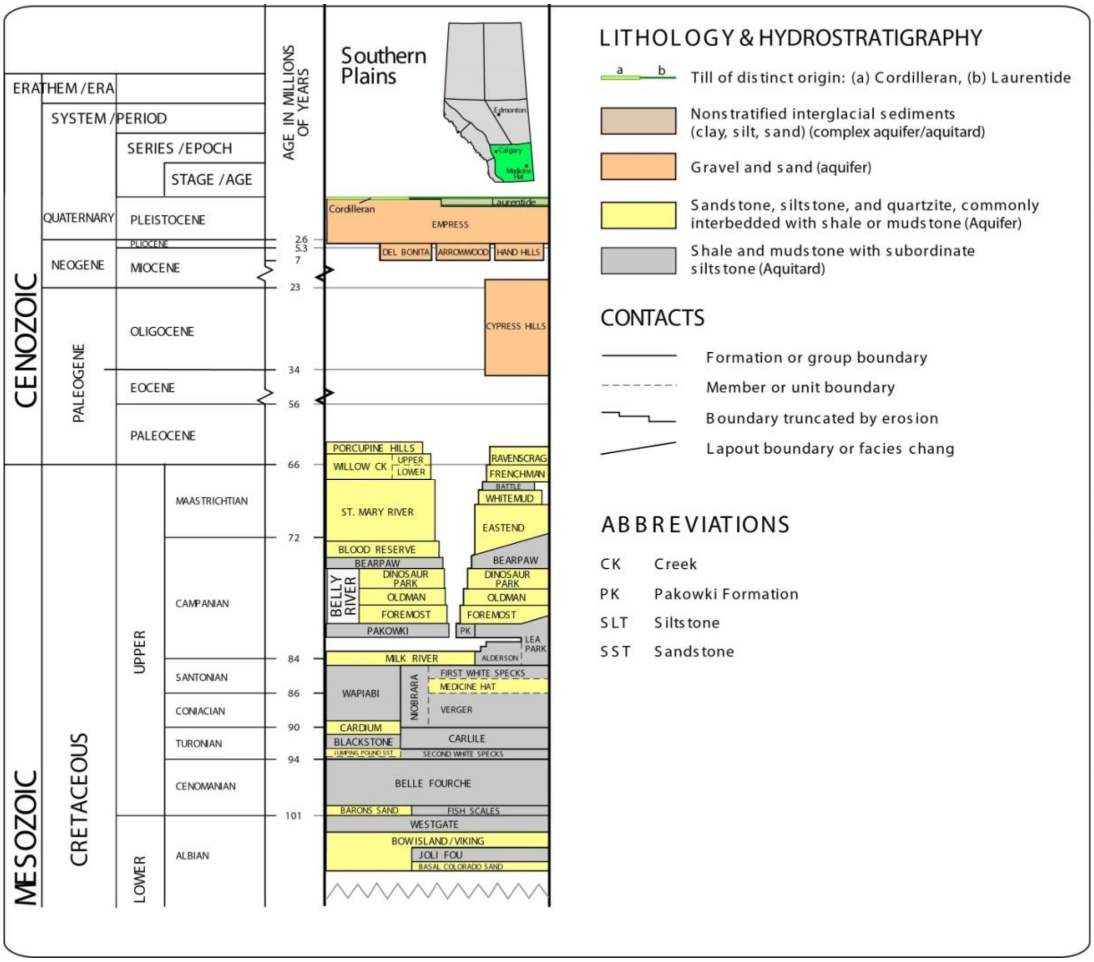

Figure 4.4 Hydrostratigraphy according to the Alberta table of Formations (left; Alberta Geological Survey, 2015, hydrostratigraphy after Pétré et al. 2015, 2016 with modifications) including dominant lithology.

Using petrophysical log analysis of approximately 6,600 geophysical well logs, and 3D geostatistical modeling, the AGS created a 3D voxel model of the distribution of permeability, porosity, gas-water saturation and shale-sand percentage for the Milk River Formation, and Alderson and Medicine Hat members. The resolution of the geostatistical model of the Milk River Formation and Alderson Member was 500 m by 500 m by 2 m. The resolution of the geostatistical model of the Medicine Hat Member was 500 m by 500 m by 1 m.

4.2.2 Model Layering

A fully 3D groundwater flow model consists of model layers that represent low- or high permeable material; aquitards and aquifers are both simulated by model layers. A strategy to reduce the number of model layers is to discretize aquitards as confining beds within a model layer. However, several units contain low- and high permeable material and therefore a clear distinction in interbeds is difficult. A minor drawback of the chosen modeling software (see section 3.1) is the enforced restriction that model layers cannot be thin out to a thickness of zero. Via a tailor-made conversion procedure, the 43 geological layers were combined with the detailed information from the geostatistical model from Petrel for the Milk River Formation and Alderson (88 layers) and Medicine Hat Members (96 layers). At the same time, model layers that tend to thin out to a zero thickness were set to a minimal thickness of 1.0 meter.

For these model layers, the permeability was set to the value of the “underlying” formation. The result of this is a 201 layered model with units that have a single permeability value (see section 4.2) and those within the 3D geostatistical modeling domain which have a high detailed variation in permeability, see Figure 4.5.

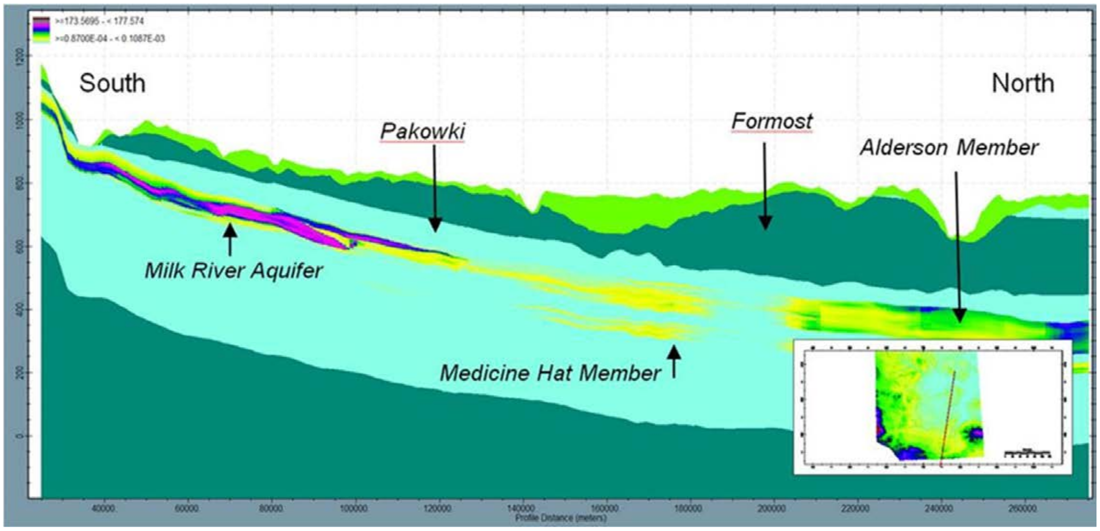

Figure 4.5 Detailed cross-section from south to north showing the incorporation of the highly detailed geostatistical model of the Milk River Formation members, Alderson Member and Medicine Hat Member, combined with the geological model. The colour shows the prior estimated permeability values.

4.2.3 Values for Permeability and Vertical Anisotropy

For the 43 units that are distinguished in the geological model, a bandwidth of permeability values is estimated if known. The current model is populated by the mid-values for each parameter. For those model layers that are populated by the geostatistical 3D voxel model has a variable permeability, though the vertical anisotropy is constant for that particular model layer.

Table 4.1 Overview of the distribution of geological units for the different model layers, the applied values for permeability and vertical anisotropy per model layer.

	Model			Permeability				Vertical	
Unit	Layer	Formation	Voxel	mid.	mid.	min.	max.	Anisotropy	Source
				m/s	m/d	m/s	m/s	[-]	
1	1	Empress		7.00E-08	6.05E-03			1.0	Robertson (1988); Hendry and Buckland (1990)
2	2	Porcupine hills		5.00E-07	4.32E-02			1.0	
3	3	Scollard		5.00E-07	4.32E-02			1.0	
4	4	Battle		1.00E-09	8.64E-05			1.0	
5	5	Horseshoe Canyon		5.00E-07	4.32E-02			1.0	
6	6	Upper Bearpaw		1.00E-09	8.64E-05			1.0	
7	7	Strathmore		5.00E-07	4.32E-02			1.0	
8	8	Lower Bearpaw		1.00E-09	8.64E-05			1.0	
9	9	Dinosaur park		5.00E-07	4.32E-02	9.00E-08	8.80E-07	1000.0	Hendry and Buckland (1990); Anna (2011)
10	10	Oldman		5.00E-07	4.32E-02	9.00E-08	8.80E-07	1000.0	Hendry and Buckland (1990); Anna (2011)
11	11	Foremost		5.00E-07	4.32E-02	9.00E-08	8.80E-07	1000.0	Hendry and Buckland (1990); Anna (2011)
12	12	Lea Park/Pakowki		1.00E-10	8.64E-06	1.00E-11	1.00E-09	5.0	Swanick (1982); Hendry and Schwartz (1988); Toth and Corbet, 1986)
13	13	Alderson Undefined (NE) and Dead Horse Coulee (SW)	x	1.00E-09	8.64E-05			1.0	
14	|	Dead Horse Coulee	x	1.00E-09	8.64E-05			1.0	
15	|	Alderson A	x	1.00E-09	8.64E-05			1.0	
16	|	Upper Alderson main sand	x	5.00E-07	4.32E-02			1.0	
17	|	Alderson B 1	x	1.00E-09	8.64E-05			1.0	
18	|	Upper Alderson lower sand	x	5.00E-07	4.32E-02			1.0	
19	|	Alderson B 2	x	1.00E-09	8.64E-05			1.0	
20	|	Alderson B basal sand	x	5.00E-07	4.32E-02			1.0	
21	|	Alderson C	x	1.00E-09	8.64E-05			1.0	
22	|	Dead Horse Coulee	x	1.00E-09	8.64E-05			1.0	
23	|	Virgelle Shale	x	1.00E-09	8.64E-05			1.0	
24	|	Virgelle Sand	x	5.00E-07	4.32E-02			10.0	Petré et al. (2016)
25	107	Telegraph creek	x	1.00E-09	8.64E-05			1.0	
26	108	Colorado		1.00E-11	8.64E-07	1.00E-12	1.00E-09	10.0	Toth and Corbet (1986); Robertson (1988); Hendry and Buckland (1990)
27	109	Medicine hat	x	1.00E-09	8.64E-05			1.0	
28	|	Medicine hat sand A	x	5.00E-07	4.32E-02			1.0	
29	|	Medicine hat	x	1.00E-09	8.64E-05			1.0	
30	|	Medicine hat Sand C	x	5.00E-07	4.32E-02			1.0	
31	|	Medicine hat	x	1.00E-09	8.64E-05			1.0	
32	|	Medicine hat sand C2	x	5.00E-07	4.32E-02			1.0	
33	|	Medicine hat	x	1.00E-09	8.64E-05			1.0	
34	|	Medicine hat sand D	x	5.00E-07	4.32E-02			1.0	
35	|	Medicine hat	x	1.00E-09	8.64E-05			1.0	
36	|	Medicine hat sand E	x	5.00E-07	4.32E-02			1.0	
37	|	Medicine hat	x	1.00E-09	8.64E-05			1.0	
38	196	Verger		1.00E-11	8.64E-07			1.0	Toth and Corbet (1986)
39	197	Carlile		1.00E-11	8.64E-07			1.0	Toth and Corbet (1986)
40	198	Second white specks		1.00E-11	8.64E-07			1.0	Toth and Corbet (1986)
41	199	Bellefourche		1.00E-11	8.64E-07			1.0	Toth and Corbet (1986)
42	200	Fish Scales		1.00E-11	8.64E-07			1.0	Toth and Corbet (1986)
43	201	Bow Viking		5.00E-07	4.32E-02			1.0	
44		Base							

The main aquifers are highlighted in Table 4.1 in green. The **Lea Park/Pakowki** formation is a very distinctive and important aquitard. From numerical simulation is appeared that a permeability of less than 1.0E^{-10} m/s yields in unrealistic inundation around the Milk River.

The total transmissivity (m^2/d), as the product of each model layer thickness multiplied with its permeability is given in Figure 4.6. Along the border with Montana (USA) there is a strong variation in transmissivity, very low values (< 1 m^2/d) within the area north of the Sweet Grass Hills in Montana, caused by the absence of the Milk River Formation and relatively high values north-east and east of the Milk River as a result of the emerging of the high permeable Virgelle sandstone member with higher permeability values of 0.0432 m/d.

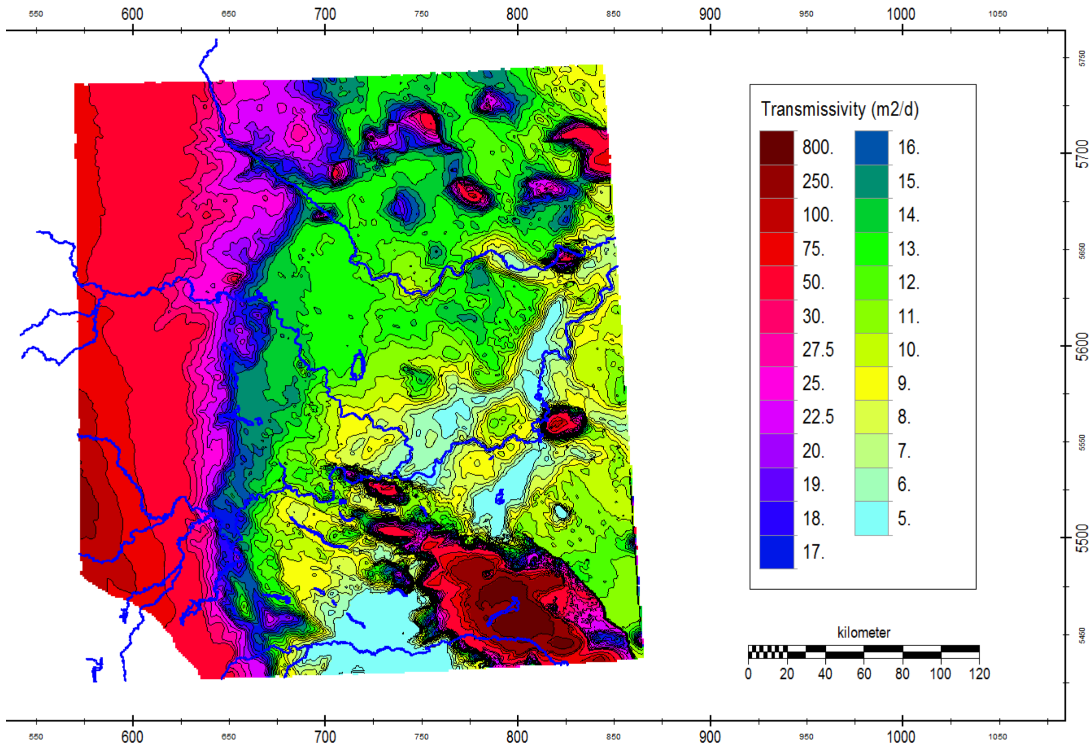

Figure 4.6 Total transmissivity (m^2/d) as a sum of all individual transmissivity value per model layer.

4.3 Surface Water Interaction – Streams and Lakes

4.3.1 Introduction

In the model domain, a few river systems are fed by surface water permanently, or most of the time. A majority of the streams are discharging water temporarily and for the underlying groundwater model – which describes a steady-state situation – irrelevant. In Figure 4.7 the location of the main rivers and lakes are depicted.

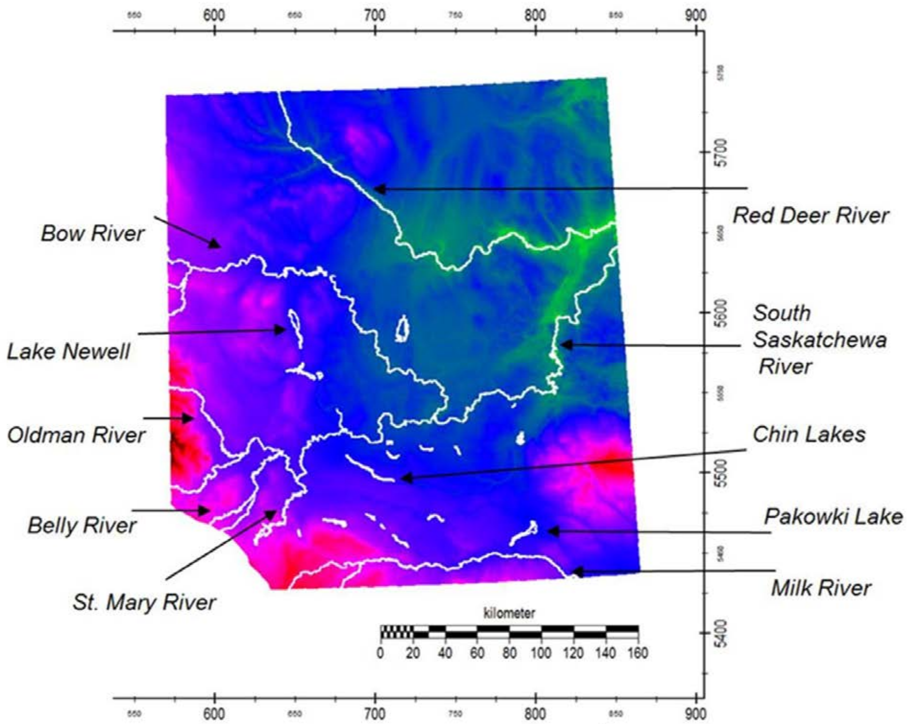

Figure 4.7 Location of the main stream in the model domain.

Based on the conceptual model, rivers are important sites of regional groundwater discharge from the Milk River Formation and Alderson Member, see Figure 4.8. The river Saskatchewan, Bow and Red Deer probably discharge groundwater underneath the Pakowki Fm. in the north and northwest of the model domain, as they are less influenced by the Milk River in the South of the model domain. As the Pakowki Fm. has an extremely high vertical resistance (> million days), the influence of the major river are still noticeable underneath the Pakowki.

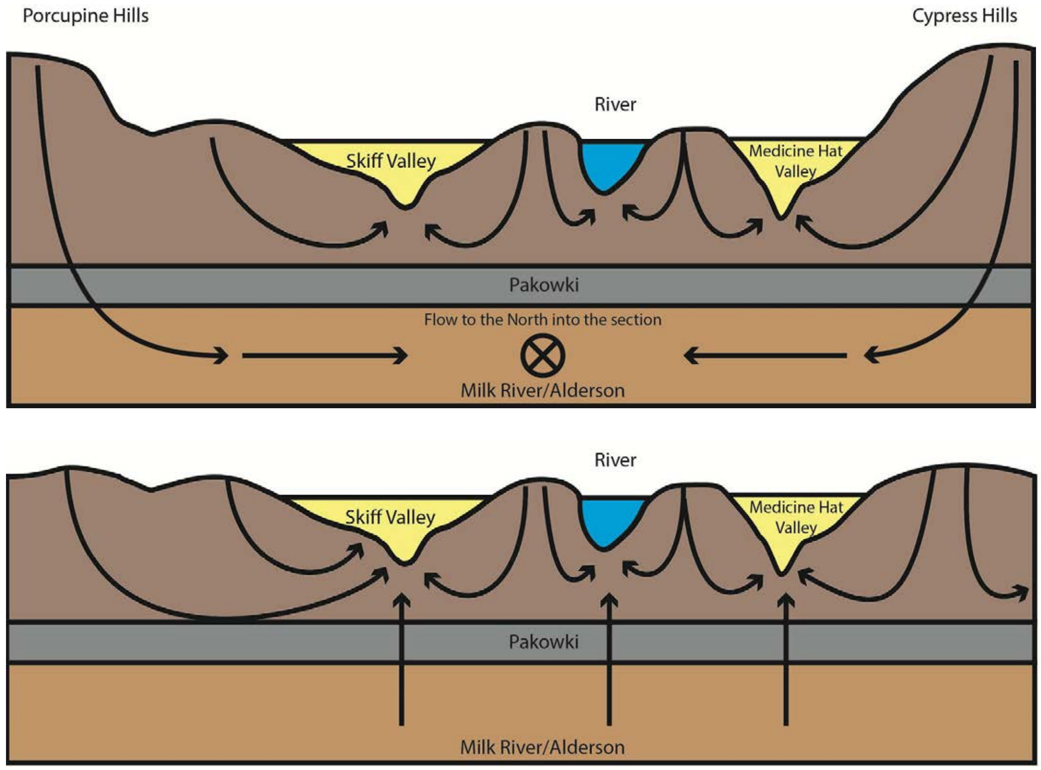

Figure 4.8 Conceptual model of the groundwater flow pattern: top) southern portion of the study area; and bottom) central portion of the study area.

4.3.2 Modelling Stream Interaction

A static surface water network overlies the groundwater flow model, and computes the flux between surface- and groundwater. It should be noted that the surface water network is not routing any surface water. Its location and stage are both derived from the provided DEM (resolution of 500 x 500 m). Therefore, an artificially drip of water is released at each location throughout the model area and following (traced) until it reaches an outlet; a) the model boundary or b) a designated outlet point within the model, such as a lake. These natural outlet points are displayed in Figure 4.7 as lakes. To estimate the stage (drainage level) of the stream, the DTM value is picked along the traced stream whereby the stage is corrected whenever a *pit cell* is concerned, see *Figure 4.9*.

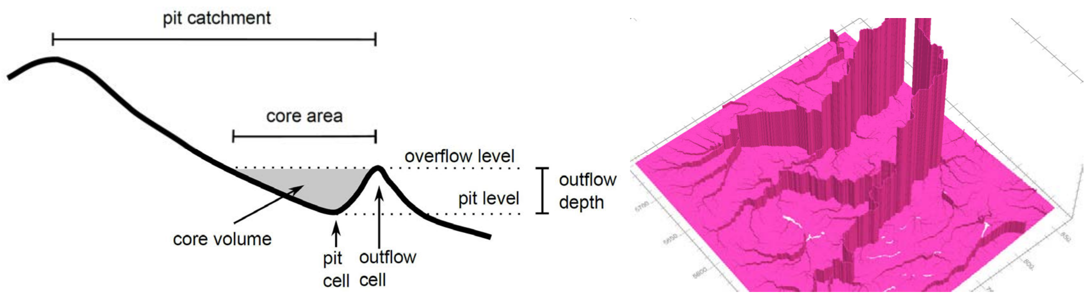

Figure 4.9 (left) Illustration of the stage correction whenever a pit is concerned; (right) the number-of-passes during a trace to delineate the surface water network, the white areas are lakes as a natural outlet for an upstream river.

In the case of a pit, the entire *core*-area receives a similar the stage which is equal the *overflow level*. The actual DTM is the minimal upscaled value for a 500 m resolution from all values inside that cell from a DTM with a resolution of 70 x 70 meter. In that manner, the DTM represents the lowest point in a valley, and therefor would be more representative for a river stage.

To estimate the conductance of a stream, the so-called *number-of-passes* is a measure for the size of the river, and therefore a measure for the conductance. Each pass is equal to 1 mm/day of precipitation. The total volume is the *number-of-passes* times the area of the cell. From there, it is assumed that 1000 m^3/d stand for a stream with a width of 50 meter and a depth of 1 meter. With this table all other streams are parameterized. As the Milk River, Oldman River, Red Deer and Belly River, all originate outside the model domain, those rivers and there downstream segments, received an additional 25,000 m^2/d as it is assumed that those rivers have a width of at least 50 meter (source: Google-Maps - *Streetview*). Stream with a conductance of <100 m^2/d were ignored, see Figure 4.10. Those small streams have drainage capabilities only, but probably are above the groundwater level and should not drain any groundwater.

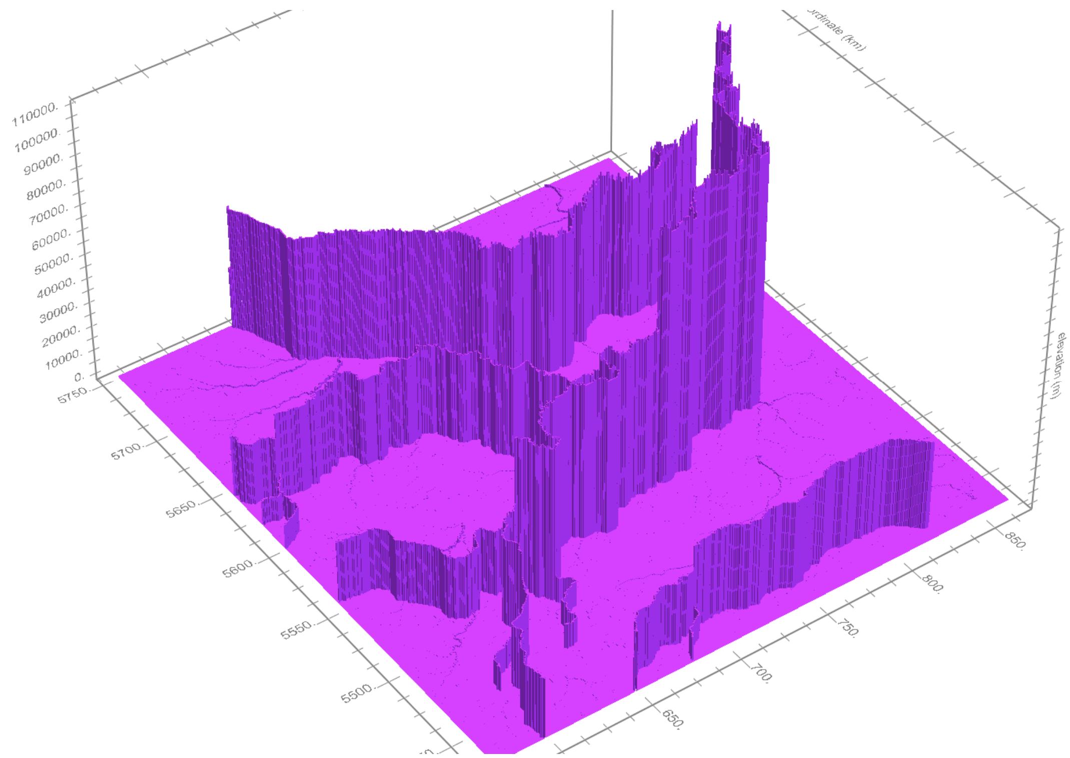

Figure 4.10 Assigned values for conductance for the major river in the study area.

The capability of infiltration is related to the conductance and for stream with a conductance more-than 1000 m^2/day (major stream in Figure 4.10) it is possible to infiltrate surface water into the groundwater as those streams may carry water year around. Those with less than 1000 m^2/d might drain groundwater and discharge it out of the system. This threshold is chosen arbitrarily, though the final distribution of water bearing and non-water bearing streams see Figure 4.11.

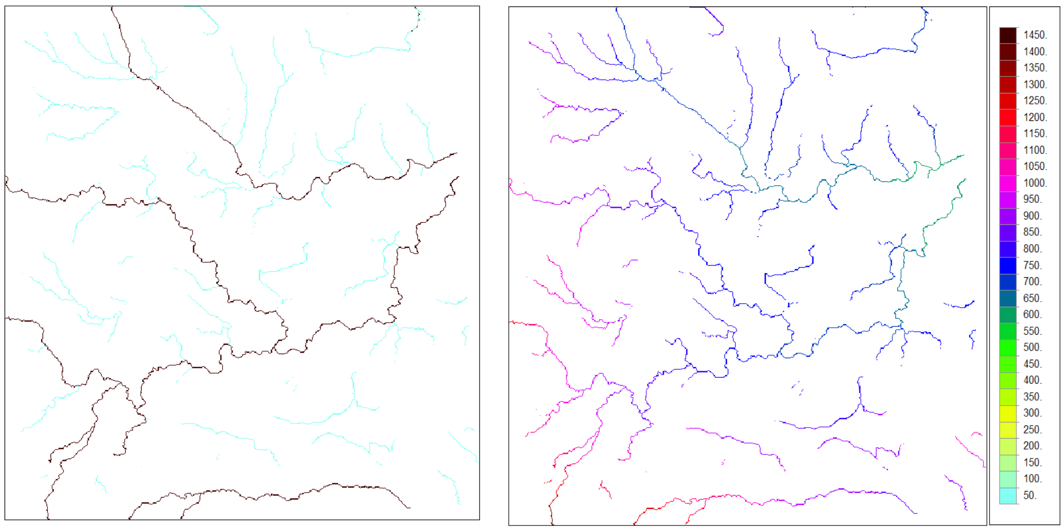

Figure 4.11 (left) Model input for the major stream that have a permanent water depth (brown) and those that probably don't (blue); (right) the estimated stage from the DTM.

4.3.3 Lakes

Several natural lakes are within the model area. Some of those lakes have a surface level that is influenced and/or steered by a weir – for most of them it is assumed that they are a) lakes that exist due to stagnant groundwater from precipitation which do not feed and/or hardly interact with groundwater; and b) lakes that are interacting with groundwater and store surface water which is drained from an upstream catchment area and might infiltrate into the subsoil. The important difference between the two is that the first does not have the ability to dis- or recharge groundwater (the surface level represents more-or-less the groundwater level and/or a perched water table), as the latter can. Due to a weir water can be maintained at a certain level to allow for drainage and/or infiltration. The first type of lake is simply ignored in the model, the second is incorporated in the model as a boundary condition with a fixed water level (from the DTM, see section 2.4.2) and a conductance of 25,000 m^2/d, which is equal to the cell size in which the lake is divided by 1 day resistance.

4.4 Recharge

The groundwater recharge is based upon the estimated quantities given by Pétré et al., 2015. The volumes are from 1.0 to 35.0 mm/year (i.e. 0.003-0.1 mm/day), see Figure 4.12. For some locations the recharge is set to 0.0 mm/year, especially along the Milk River in the southern region of the model. The reason for this is that at those locations, the Pakowki Fm. crops out, which makes it impossible to penetrate as groundwater cannot build up a pressure which is high enough to transfer water through this very low permeable formation ($k=1E^{-10}$m/s).

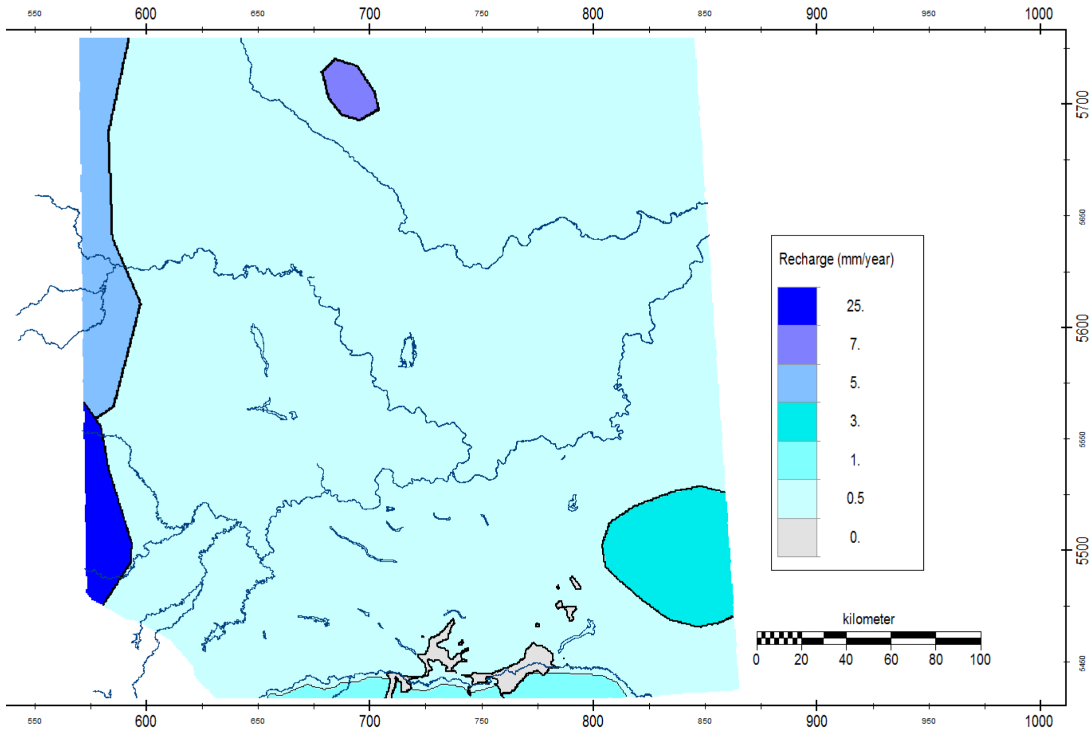

Figure 4.12 Prior-estimated recharge values in mm/year.

4.5 Extraction

4.5.1 Introduction

Within the modeling area extraction wells are drilled from the beginning of the last century up to late 2000s. The wells are drilled to the deep Milk River Formation in the south of the model (1,285 recordings) and/or into the shallower sandstone formations on top of the Pakowki (36,752 recordings), such as the Porcupine Hills, Scollard, Horseshoe Canyon, Strathmore, Dinosaur Park, Oldman and Foremost formations. All with similar permeability values as the Milk River Formation. From the records, the licensed well rate is much larger than the actual rate which is applied to extract the groundwater. Pétré found that that the consumptive use in the study area is $1.2E^6$ m^3/year (Pétré et al., 2015). From the recorded licenses the total amount of licensed rate was $23.9E^6$ m^3/year. The consumptive use is 1/20th of the total licensed rate; therefore, the model multiplies all rates with a factor 0.05 to account for a realistic extraction rate, see Table 4.2. In total, the yearly extracted amount of groundwater, in the study area is $21.4E^6$ m^3/year.

Table 4.2 Overview of the extraction rates for wells in the shallow (above the Pakowki Fm.) and deep (underneath the Pakowki Fm.) within the study area.

Formation	Max. Rate (m^3/d)	Avg. Rate (m^3/d)	St.Dev. (m^3/d)	Sum (m^3/d)	Number
Shallow	170.0	1.50	4.58	55,200.7	36,752
Deep	20.0	2.60	2.19	3,328.0	1,285
Total				58,528.7	

4.5.2 Assigning Extraction to Model Layers

Each extraction well is defined by a screen height and depth. This information is used to assign the extraction rate of the well to the appropriate model layers. Therefore, those model layers are selected that are occupied by the well screen. The actual rate that is assigned to each of those selected model layers depend on the distribution of transmissivity along those intersected model layers. Suppose a well need to be divided over 2 model layers for which one model layer has a transmissivity which is a double of the other model layer, the rate in the first model layer will be twice as high as in the second model layer. Summed up, the rates are equal to the given rate see Figure 4.13 for the locations of the shallow (above the Pakowki Fm.) and the deep well (underneath the Pakowki Fm.).

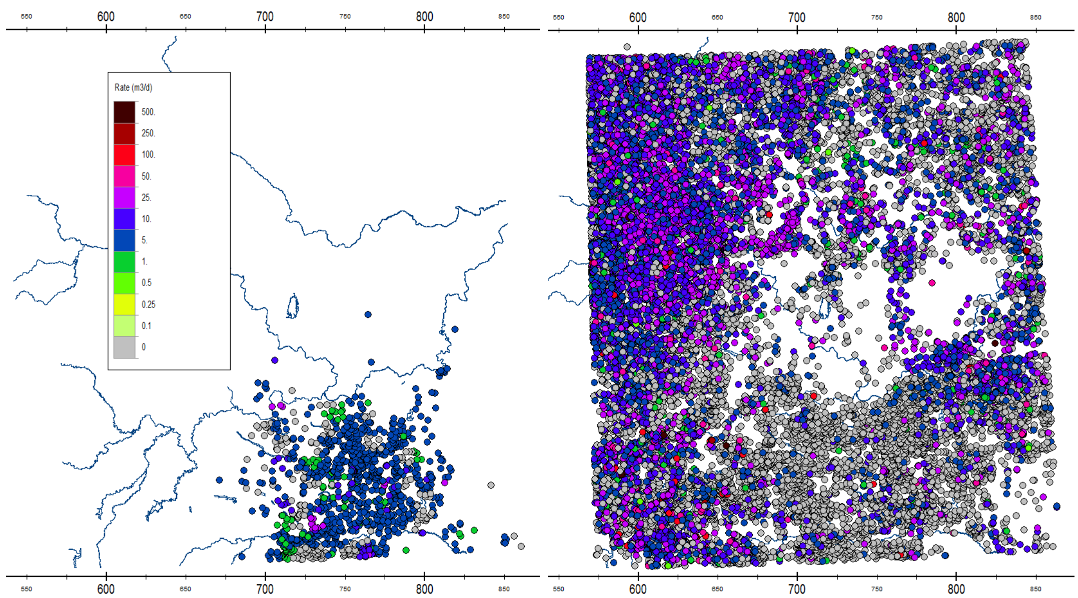

Figure 4.13 Locations of the (left) wells in the Milk River Aquifer; and (right) shallow wells above the Pakowki Formation.

4.6 Static Water Level

The static levels that are measured in the study area are not used quantify the correctness of the model. A reason for this is that a) the quality of the measurements are uncertain; a) they are measured at unknown dates; b) often only measured once; c) probably represent a local situation which is difficult to translate to the scale of the current regional model.

4.7 Confined vs Unconfined Model

The model will be simulated as a confined model in which transmissivity is not a function of saturation of corresponding model layers. This means that the used saturated transmissivity might be slightly above the transmissivity for unconfined conditions. Since, the shallow groundwater in the study area is within poor aquifers of the Empress formation (see Table 4.1), with permeability of less than $6.05E^{-3}$ m/d, there is hardly any horizontal groundwater flow. Moreover, the study aims at simulating the deeper and saturated aquifers, ignoring the unsaturated conditions in the shallow aquifers is in this perspective not relevant.

4.8 Model results

In this section the results of a 201 layer hydrogeological model are described. This model consists of the 43 layer model, but the Milk River – Alderson Formation and the Medicine Hat

Formation are replaced by the well-log derived property model provided by the AGS. This model run was used for testing the sensitivity to input parameters, and to compare the results to observations. Also Milk River aquifer groundwater extraction is included in this model.

4.8.1 Hydraulic heads

The hydraulic head of the first model layer represents the groundwater level, see Figure 4.14. The result is simulated on a 500 meter resolution; major and minor streams are clearly visible. Steep gradients are caused by sudden drops in permeability of emerging geological formations. Especially the Red Deer River and the Milk River are surrounded by very poor permeable material which implies a steep gradient. Also the discharge from the Cypress Hills is caused by the lack of permeability which causes recharge to be discharge via the natural drainage system. The effect of extraction wells are seen as well, which show a small dots. The area of influence of those wells is small due to a) the low extraction rate and b) the small values for permeability.

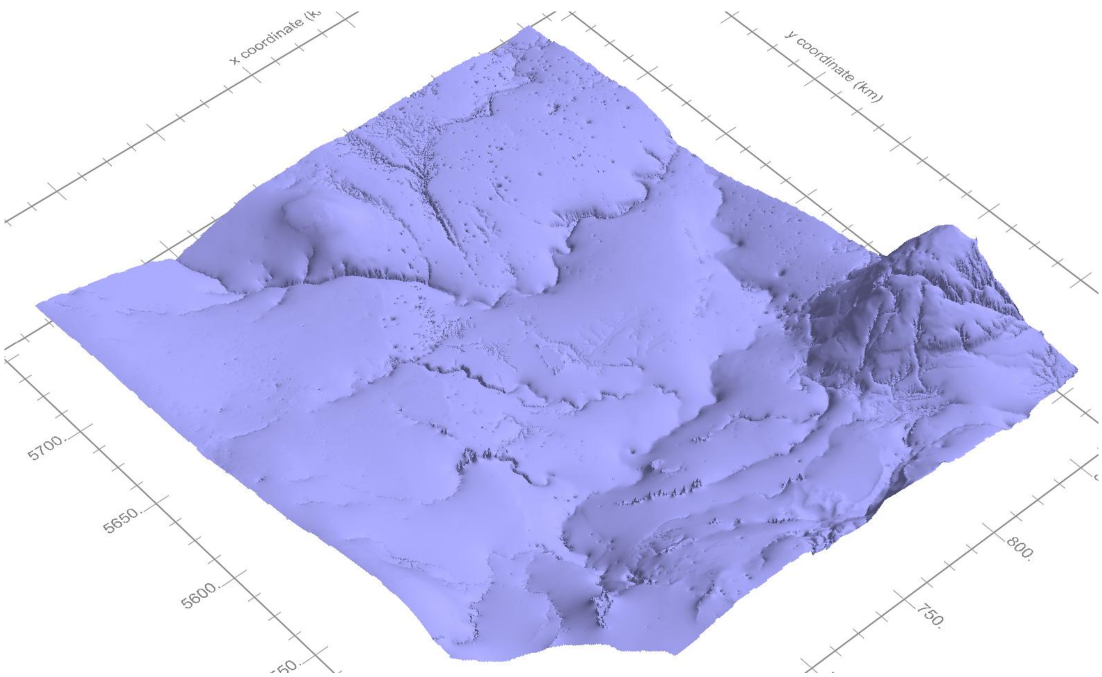

Figure 4.14 3D representation of the groundwater level.

The hydraulic heads are presented for model layer 1, 12, 108 and 201; they represent the groundwater level, the pressure head in the Pakowki Fm., Colorado Fm. and Bow Viking, respectively, see

These are all spatially distributed throughout the study area, see Figure 4.15.

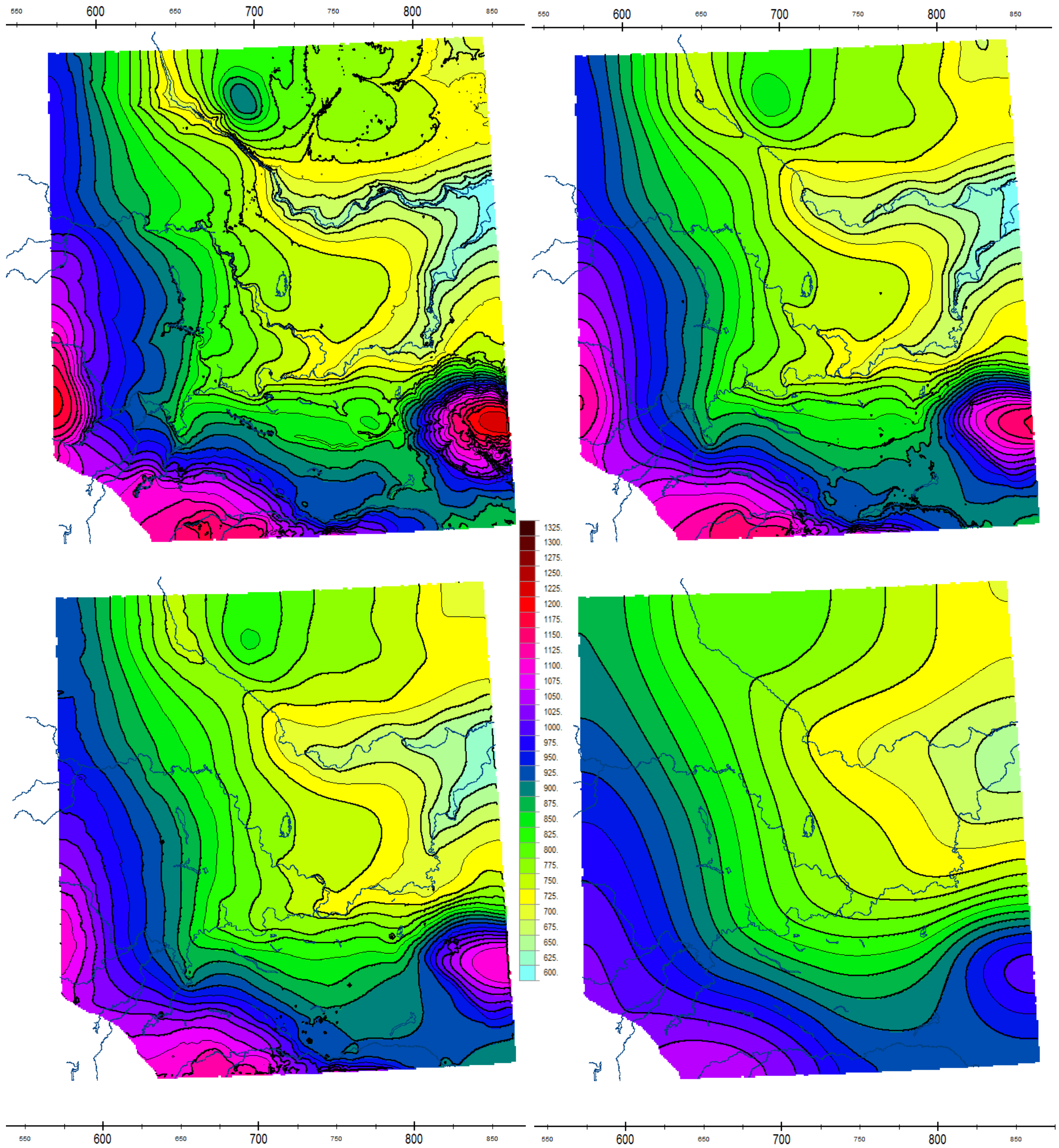

Figure 4.15 Results of the piezometric head (layer 1); the pressure head in the Pakowki Fm. (layer 12); the pressure head in the Colorado Fm. (layer 108) and the pressure head in the Bow Viking Fm. (layer 201); all head in m+MSL.

It should be noted that some of the wells are, based upon their entered screen-depths, assigned to the Colorado Fm. This yields some enormous drawdown, which are very locally due to the extreme low permeability of the Colorado Formation. For now, this unrealistic drawdown is ignored as they won't influence much of the results. In figure Figure 4.16 the computed groundwater level is presented below surface level, almost 50% of the area has groundwater levels of more than 40 meter below surface level. There are some areas present in the north, mid and south of the study area, which have higher groundwater levels of 2.5 meter below surface level, one of this area is the most eastern area of the Milk River.

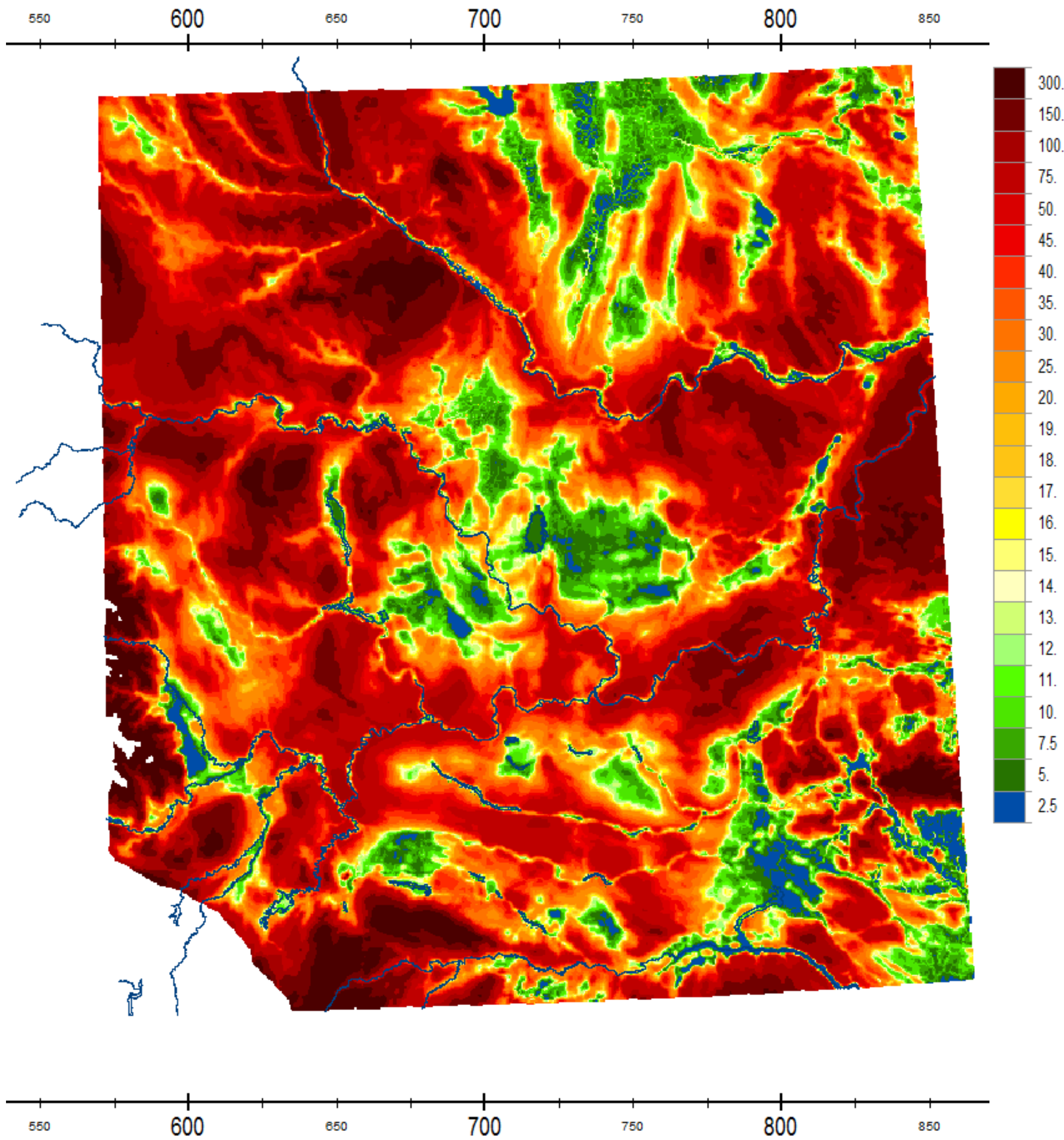

Figure 4.16 Computed groundwater levels below surface level.

4.8.2 Vertical Fluxes

It is interesting to present the spatial distribution for vertical fluxes over the Alderson/Milk River Aquifer (from model layer 12 to 13) and Medicine Hat formation (from model layer 108 and 109), see Figure 4.17. Most of the streams in the west drain most of the groundwater as Lake Pakowki in the east functions as a drainage system as well. The Saskatchewan River drains water from the shallow aquifers (above the Pakowki), as the Milk River drain water from underneath the Pakowki due to the lack of permeable aquifers on top of the Pakowki. The vertical flux over the Colorado Fm. into the Medicine Hat is very small.

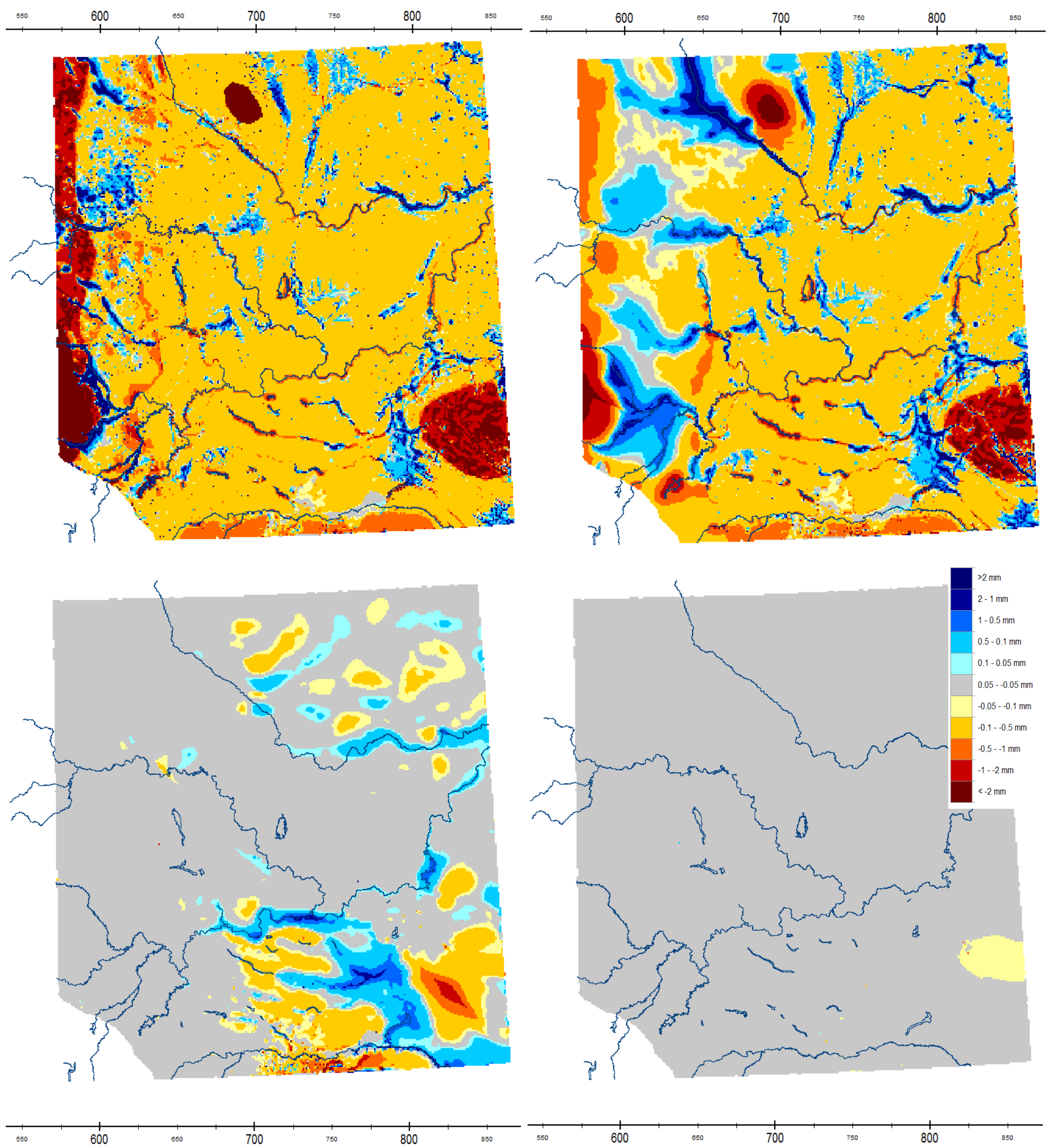

Figure 4.17 Results of the vertical flux (layer 1); the vertical flux into the Dinosaur Park Fm. (layer 8); the vertical flux into the Alderson Fm. (layer 13) and the vertical flux into the Medicine Hat Fm. (layer 108); all fluxes in mm/day.

4.8.3 Water balance

A water balance of the system presents all terms for in- and outflow, see Table 4.1. The major inflow in the current model is the net recharge: 94.3E^6 m^3/year, which is 86% of the total inflow. The rest comes from major rivers (2.8%; whereby the Belly River and the Milk River lumped infiltrate for almost 2.0% of the total river inflow); important lakes (8.7%) and inflow from Montana (1.6%). The system is drained by the major rivers for 58.3%, and 17.4% is drained by the minor drainage network. A total amount of 19.3E^6 m^3/year is extracted by wells, which is 18.3% of the total outflow.

Table 4.3 Overview of the main budget terms in the study area.

	Waterbalance						
		Inflow m3/day	Outflow m3/day	Inflow million m3/year	Outflow million m3/year	Inflow %	Outflow %
1	Inflow Montana	4712	-319	1.720	-0.116	1.59	0.11
2	River Infiltration	8363	-224430	3.052	-81.917	2.81	75.68
2a	Red Deer River	8	-45453	0.003	-16.590	0.00	15.33
2b	Bow River	1831	-11798	0.668	-4.306	0.62	3.98
2c	Belly River	3043	-7407	1.111	-2.703	1.02	2.50
2d	Old Man River	510	-69524	0.186	-25.376	0.17	23.44
2e	Saskatchewan River	486	-33208	0.177	-12.121	0.16	11.20
2f	Milk River	2479	-5445	0.905	-1.987	0.83	1.84
2g	Rest (minor streams)	5	-51595	0.002	-18.832	0.00	17.40
3	Lakes	25892	-17699	9.450	-6.460	8.71	5.97
4	Wells	0	-54112	0.000	-19.751	0.00	18.25
5	Recharge	258317	0	94.286	0.000	86.89	0.00
	Total	297283	-296559	108.508	-108.244	100.00	100.00
	Error		724		0.264		

The total sum of vertical fluxes over the Pakowki is 11,500 m^3/day (0.3358 mm/year), as the total vertical flux for the Colorado Fm. is 1,450 m^3/day (0.046 mm/year).

4.8.4 Capture Zones

Particle tracking is a methodology to trace a fictive particle through the modeling domain using the computed flow field, i.e. the velocity of flow in x-, y- and z-direction. The result of this shows an image that presents the 3D simulated path of groundwater flow. As this model is huge, with 201 model layers, a presentation of flowlines will be difficult to interpret. An efficient method is to present the maximal depth (model layer) that each particle passes through its *journey* from a starting location towards an outlet (sink). Therefore a particle has been started at the center of each model cell at the elevation of the simulated groundwater level. From there is has been traced back- (against flow direction towards its location of origin) or forward (along the flow direction towards its exit point). Both simulations yield a different map of the maximal reached layer in the model, see Figure 4.18.

On the left image of Figure 4.18, the dark red zones show the areas where groundwater infiltrates up to the mid of the Alderson/Milk River Aquifer. Only a very few locations show some infiltration up to the mid of the Medicine Hat and/or Bow Viking Fm., e.g. at the top of the Cypress Hills, from the border with Montana and on the watershed between the Red Deer River and the Saskatchewan River. The west of the study area, does not feed these deep aquifers as the infiltration does not reach formations deeper than the Foremost Fm. The right image of Figure 4.18 shows that the area north of Pakowki Lake discharges groundwater that originates from the mid Alderson/Milk River Fm. underneath the Pakowki Fm. Also the Milk River area does drain some groundwater from this deeper aquifer, mainly because of the inflow from Montana that starts at that formation.

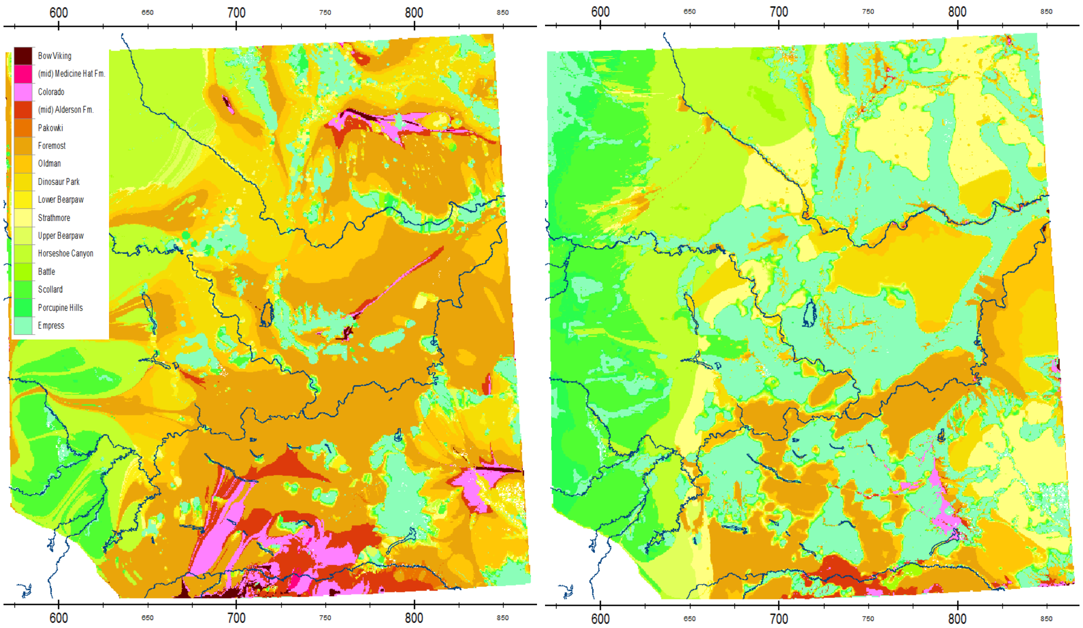

Figure 4.18 Maximal depth (expressed in Formation) for particles that (left) travel forwards to their outlet and (right) backwards to their origin.

5 Modeling Two-phase

5.1 Model schematization and input parameters

To simulate multiphase flow behavior with the STOMP model, input information is needed regarding the properties of the subsurface, and of the water and gas phases. Information required of the subsurface consists of:

- Hydraulic properties of the subsurface: porosity and intrinsic permeability of each defined rock/soil type. The values for the porosity and permeability were obtained as described in chapter 3.
- Mechanical properties of the subsurface: particle density for each defined rock/soil type. Based on these values and the values for porosity the specific storativity, compressibility, and a tortuosity function for each defined rock/soil type are calculated by the STOMP model.
- Saturation properties of the subsurface according to the saturation-capillary pressure function for each defined rock/soil type. For this function, the water retention curve by Van Genuchten is used (van Genuchten, 1980). The Van Genuchten function was chosen because it assumes that the wetting fluid drains from a porous medium whenever the capillary pressure is greater than zero. The Van Genuchten function has two parameters that are determined from data and literature:

$$S = \left(\frac{1}{1 + (\alpha h)^n}\right)^m$$

Where *S* is the saturation, *h* is the pressure head, α and *n* are the Van Genuchten parameters and $m = 1 - \frac{1}{n}$.

In the Milk River formation, mercury injections were performed for the calculation of pore size and permeability. The data includes injection pressure and saturation of the wetting phase (mercury). From these data the Van Genuchten parameters can be fitted (see Figure 5.1).

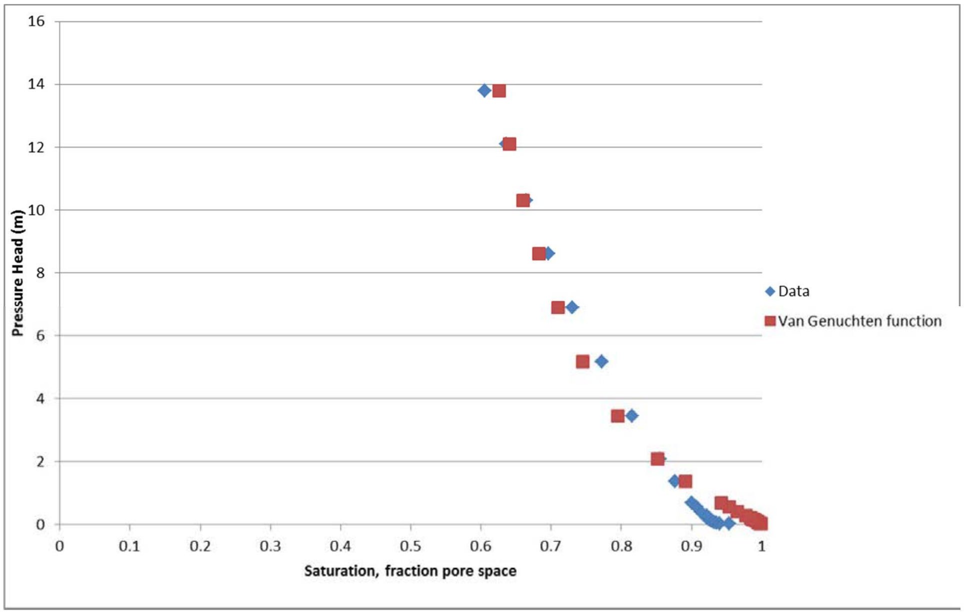

Figure 5.1 Data and fitted Van Genuchten function for mercury injection in the Milk River Formation.

The permeability of this test was 0.85 md, the porosity was 0.130. The fitted Van genuchten parameters are α is 0.1 /m and n is 1.2.

Besides the determination by data, literature was found concerning a relationship between the Van Genuchten parameters and permeability (Lawrence Berkeley National Laboratory, 2014). This type of relationship was calibrated to the few clay-shale data points available in the US. The correlation equation is,

$$\alpha = 2.01(7.37k^{-0.43})^{-1.20}$$

Where α is expressed in kPa^{-1}. In the same way, a relationship for *m(n)* was established:

$$m = 0.5 - 0.5erf\left\{\frac{\log(k) + 20.34}{3.94}\right\}$$

Since the fitted van Genuchten from the data from the Milk River Formation, fits well within these relations between permeability and the Van Genuchten relations, we have chosen to use these relations to determine these parameters for our study.

Information required of the water and gas oil phases consists of:

- The aqueous relative permeability for each defined rock/soil type; For this purpose the Mualem function is chosen since the aqueous relative permeability is dependent on the saturation function (van Genuchten) and the Mualem function is strictly applicable to the Van Genuchten function (Mualem, 1976).
- The gas relative permeability for each defined rock/soil type; for this purpose the Mualem function is used as well, because of its dependency on the Van Genuchten function.

Apart from these input parameters, the boundary and initial conditions are required as input. Application of boundary and initial conditions requires an appropriate conceptualization of the physical problem and translation of that conceptualization into boundary and initial condition form. The initial conditions are defined for time step T=0 and consist of a gas and water pressure for every gridcel of the model based on the different simulation types (see section 2.2). The boundary conditions are defined and fixed for the whole simulation period, and only at the surface (the top row of the model cells): the top surface is open for water and gas fluxes.

5.2 Column experiments for seal strength

In order to determine the strength of the weak seal and the strong seal (see 2.3.5), STOMP columns are used. For the simulations, two seal strengths are considered: one that can hold only short columns of gas, i.e. less than 10m, and one that can hold tall columns of 230m of gas. The setup was a column of 500 by 500 by 86.78 m. 500 m is the width of one cell. In the vertical direction there are 51 cells. The first 49 cells from the bottom have permeability values form the property model. The top two cells form the strong seal.

As initial condition we implemented water saturations, based on the water saturation data from the property model and adjusted them in such a way that a buoyancy pressure was established that belongs to a gas column of 230m tall. The gas pressure is 5147 kPa at the bottom with a gradient of -205 Pa per meter.

Using trial and error method the permeability and accompanying Van Genuchten parameters were changed until the seal at the top holds the gas for at least 100 years. The permeability for the strong seal is: 8.31E-10 m/day.

The same was done for a weak seal: the seal was applied at the 20th cell from the bottom: at 55.78 meter from the bottom. The applied gas pressure is now 3036 kPa with a gradient of -205 Pa per meter. The water saturation is 0.5 in the reservoir below the seal and 1.0 in the seal. Again permeability and Van Genuchten parameters are fitted so that the seal holds the gas for at least 100 years. The permeability for the weak seal is: 3.41E-08 m/day.

5.3 Cross-sections

In order to calculate the building blocks as defined in Section 2.2, for two phase flow, STOMP is used. Since STOMP has limited capabilities concerning the extend of the model and the number of cells, we have chosen to use a cross section of the 3-D groundwater model to make these calculations possible. The y-axis serves as a symmetry axis. Using this approach means that we assume there is no flow through the y-axis.

The cross section has to approach symmetry of the gas field. Furthermore we want to include the Foremost extraction and capture the areas where we see significant differences in the transmissivities between the different simulations for groundwater flow (see section 6.1). Based on these qualifications we have chosen a cross section as shown in Figure 5.2.

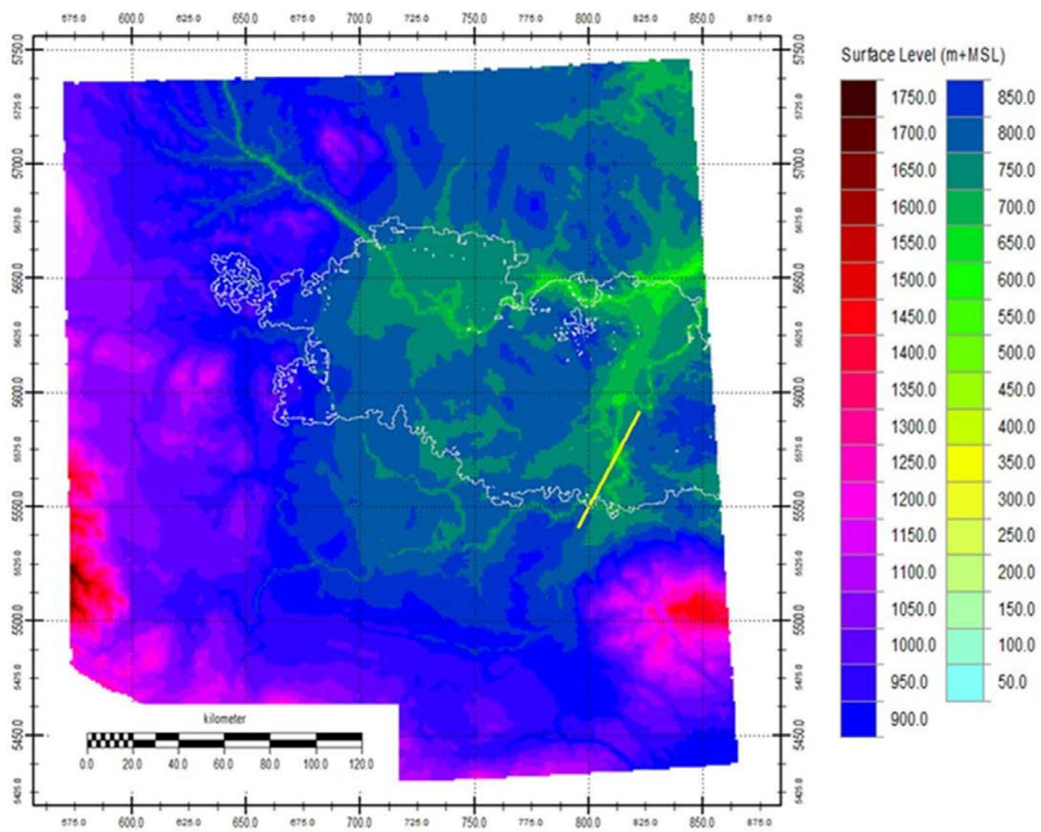

Figure 5.2 Overview of the surface level and in yellow the location of the cross section.

Figure 5.3 show the cross section in 3-D. lateral extend of the cells is 500 m in x and y direction.

With this cross section, the following simulations are calculated (see section 2.2):

10 Simulation 10: building blocks A1, C2, B1 and D1 (based on iMOD simulation 4).
11 Simulation 11: building blocks A1, C1, B2 and D1 (based on iMOD simulation 5).
12 Simulation 12: building blocks A2, C2, B1 and D2 (based on iMOD simulation 6).
13 Simulation 13: building blocks A2, C1, B1 and D1 (based on iMOD simulation 7).
14 Simulation 14: building blocks A2, C1, B2 and D1 (based on iMOD simulation 8).
15 Simulation 15: property model (based on iMOD simulation 9).

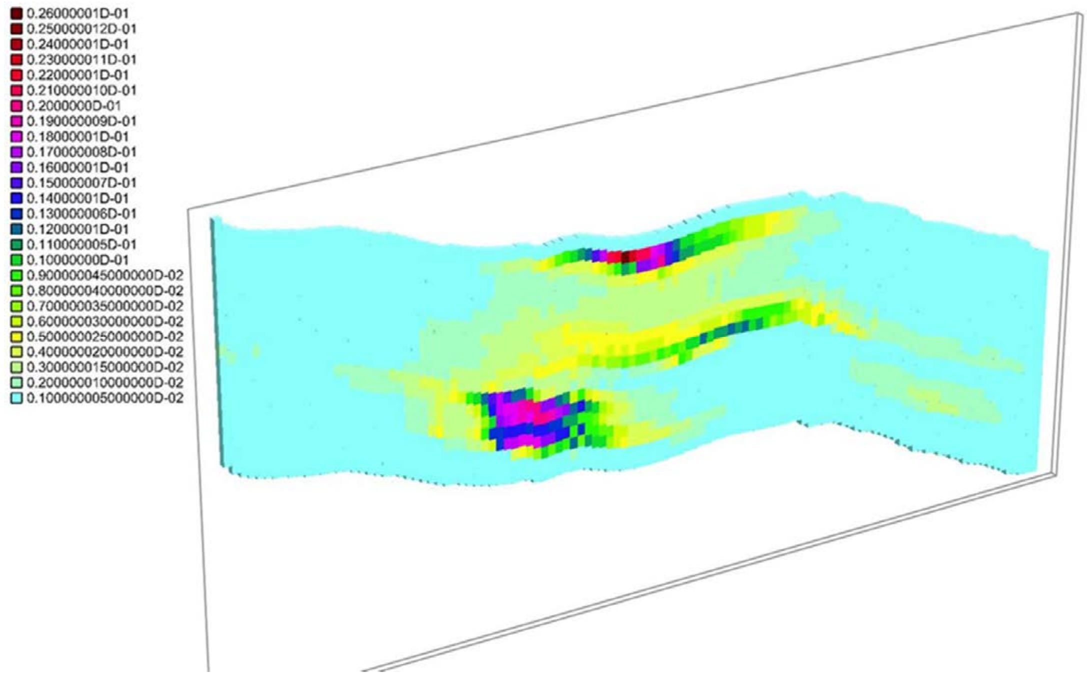

Figure 5.3 Example of the cross section in 3-D for the permeability of simulation 9. The extend of the y-axis is 500m.

5.4 Initial gas-pressure conditions

Phase 4 aims to test different conceptual scenarios to simulate the discovery conditions of the gas reservoir. For this to happen, initially two sets of models were tested. One set in which for every voxel a gas pressure was applied equal to the water pressure in that voxel (as derived from the hydrogeological simulations) plus the buoyancy pressure belonging to the previously described weak seals (96kPa). The second set was meant to represent the buoyancy pressure for the strong seals (2240kPa on top of the water pressure for each voxel). This way it was made certain that every voxel has experienced the preferred gas pressure. The reasoning was that as soon as pressures were starting to built up, it would leak away as soon as the pressures exceeded the seal strength. The remaining gas would represent the trapped gas, and hence the discovery conditions. However, it turned out that applying the additional pressure for strong seals lead to unrealistically long computing time. For this reason, in this stage only the buoyancy pressures belonging to weak seals have been applied to each voxel.

Ideally, after applying these pressures, the model should run until an equilibrium condition is reached, and no gas escapes from the top of the model anymore. However, due to time constraints and unexpectedly long simulation times, only several years up to 500 years could be competed, depending on the scenario. These results already gave a good indication of the expected response.

6 Results

In this section we show the results of the simulations described in the flowchart of Figure 2.1. First Simulation 1, 2 and 3 are described. Than Scenario 9 is described because this scenario forms the basis for Simulation 4 to 8 and is the reference simulation for these simulations that are described subsequently.

6.1 Phase 1

6.1.1 Simulation 1

6.1.1.1 Introduction and modeling adjustments

This simulation represents the geological model as a 43 layered stratigraphy of geological formations. The permeability for each geological formation is a single value and provided in Table 4.1. No groundwater pumping takes place in this model run.

6.1.1.2 Results

The water balance (Table 6.1) is reasonably in agreement with that of the simulation described in Chapter 4.8. The major inflow in the current model is the net recharge; the rest comes from rivers and lakes. The system is drained by the major rivers and the minor drainage network. No well pumping has been introduced in Simulation 1. The 43 layer model is computed without the usage of sub models as the memory consumption of the model was significantly less. The water balance is depicted in Table 6.1.

Table 6.1 Water balance for different components in Simulation 1.

	Waterbalance	Simulation 1	
		Inflow million m3/year	Outflow million m3/year
1	Flow Montana	0.492	-0.054
2	River flux	2.025	-99.130
2a	Red Deer River	0.000	-12.139
2b	Bow River	0.005	-7.152
2c	Belly River	0.967	-2.439
2d	Old Man River	0.147	-15.263
2e	Saskatchewan River	0.006	-9.723
2f	Milk River	0.900	-0.588
2g	Rest (minor streams)	0.000	-51.827
3	Lakes	9.227	-6.606
4	Wells	0.000	0.000
5	Recharge	94.297	0.000
6	Flow from Pakowki	2.320	-1.971
7	Flow from Colorado	0.762	-0.750
	Total (1+2+3+4+5)	106.042	-105.790
	Error		0.252

The water balance shows a reduced inflow from Montana which is caused by the absence of the extraction wells in the Milk River Aquifer (1.3 million m^3/year). There is more drainage to the rivers since the groundwater level will be higher compared to the model with the wells. Totally 99% is drained now to the rivers, as 81% was drained to the rivers with the extraction wells. The net inflow over the Colorado is almost zero which is correct as no other outflow is possible underneath the Colorado. Above the Colorado, there is an inflow from above over the Pakowki formation of 2.3 million m^3/year and an outflow of 1.9 million m^3/year. The difference of approximately 0.4 million m^3/year is drained by the Milk River which cuts into the members of the Alderson formation.

The main difference with the more sophisticated 201 layers model described in Chapter 4.8 is the more simplified permeability distribution over the different geological units. This leads to a significant difference in the total transmissivity (Figure 6.1). If this figure is compared with the transmissivity values of the statistical well-log derived voxel model (see Figure 4.6), the total transmissivity is significantly less in the south-east area of the study area. Differences more than 250 m^2/day are seen in the south-east area. Also, more locally, lower values for transmissivity are found in the northern regions of the study area.

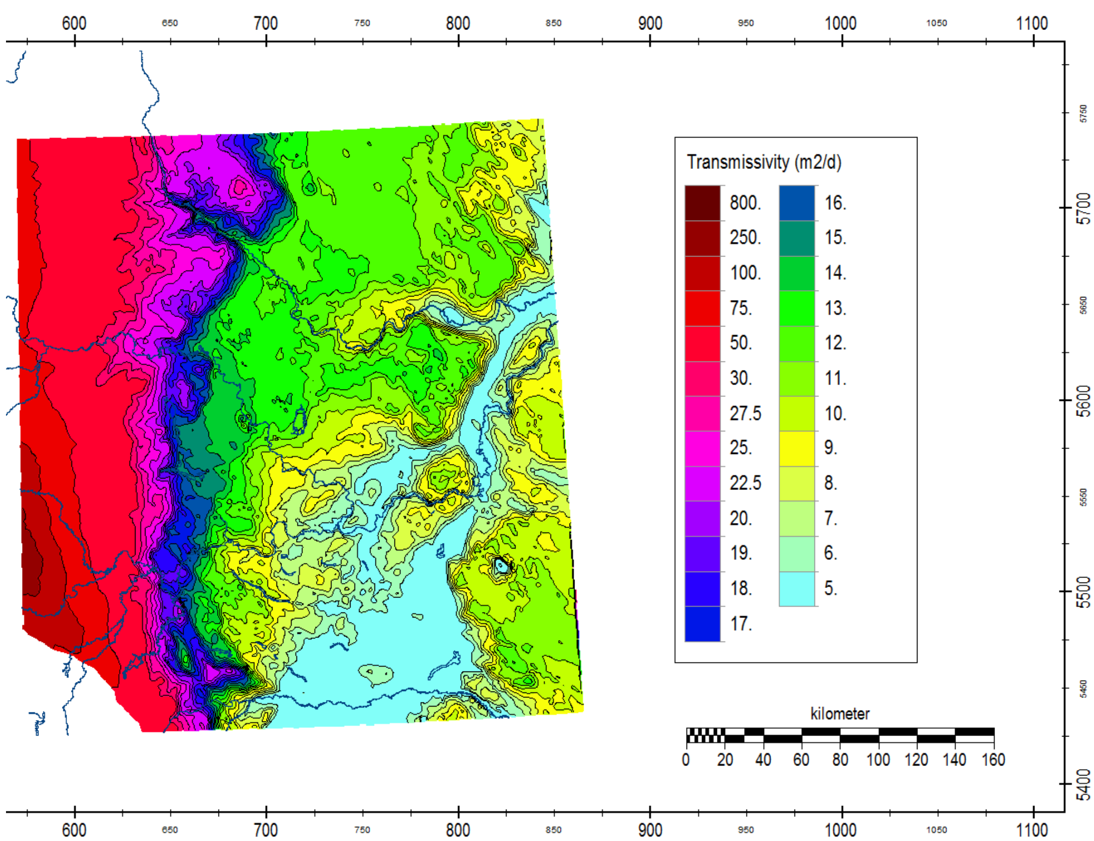

Figure 6.1 Total transmissivity (m^2/d) as a sum of all individual transmissivity values per model layer.

Figure 6.2 shows the formations reached by particles traveling to– and from locations. The dark red zones show the areas where groundwater infiltrates up to the mid of the Alderson/Milk River Aquifer. These areas are concentrated around the Milk River in the south.

Only a very few locations show some infiltration up to the mid of the Medicine Hat and/or Bow Viking Fm., e.g. at the top of the Cypress Hills, from the border with Montana and on the watershed between the Red Deer River and the Saskatchewan River. The west of the study area, does not feed these deep aquifers as the infiltration does not reach formations deeper than the Foremost Fm. The right image of Figure 6.2 shows that the area around the Milk River drains some groundwater that originates from the mid Alderson/Milk River Fm. underneath the Pakowki Fm. This is mainly inflow from Montana that is introduced in that formation, and is soon drained.

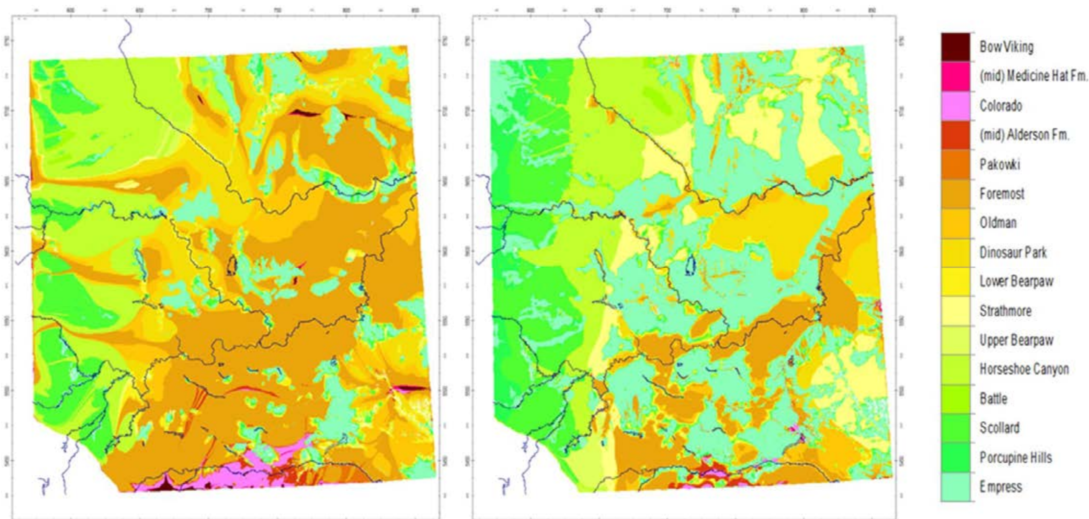

Figure 6.2 Maximal depth (expressed in Formation) for particles that (left) travel forwards to their outlet and (right) backwards to their origin for Simulation 1.

6.1.2 Simulation 2

6.1.2.1 Introduction and modeling adjustments

The second simulation is slightly more comprehensive than the 43 layer model. It uses the 201 layer model, but instead of using the conductivity values from the property model, all voxels within a formation have been assigned one conductivity value from literature. These are the same values as the values used for Simulation 1. The purpose of this simulation is to get a stable model running with the 201 layers which can act as a reference for comparison to the other simulations, together with Simulation 1.

6.1.2.2 Results

This Water balance of Simulation 2 is very similar to the water balance of the 43 layer model (Table 6.2). The most striking difference is the difference in inflow from the Pakowki Formation and from the Colorado Formation in the members of the Alderson Formation. This difference can be explained by the refinement of the layer thickness in the Alderson Formation and the Medicine Hat Formation which leads to slight changes in transmissivity. The small increase in flow entering from Montana is a result from the method used to schematize this flow which is also sensitive to changes in permeability values at the boundary.

Table 6.2 Water balances of the steady state hydrogeological model simulations 1 and 2.

	Waterbalance	Simulation 1		Simulation 2		Difference	
		Inflow million m3/year	Outflow million m3/year	Inflow million m3/year	Outflow million m3/year	Inflow million m3/year	Outflow million m3/year
1	Flow Montana	0.492	-0.054	0.541	-0.100	0.049	-0.046
2	River flux	2.025	-99.130	2.028	-99.122	0.003	0.009
2a	Red Deer River	0.000	-12.139	0.000	-12.111	0.000	0.028
2b	Bow River	0.005	-7.152	0.006	-7.124	0.000	0.028
2c	Belly River	0.967	-2.439	0.968	-2.437	0.000	0.002
2d	Old Man River	0.147	-15.263	0.147	-15.266	0.000	-0.003
2e	Saskatchewan River	0.006	-9.723	0.006	-9.790	0.000	-0.066
2f	Milk River	0.900	-0.588	0.902	-0.625	0.002	-0.037
2g	Rest (minor streams)	0.000	-51.827	0.000	-51.769	0.000	0.058
3	Lakes	9.227	-6.606	9.262	-6.620	0.034	-0.014
4	Wells	0.000	0.000	0.000	0.000	0.000	0.000
5	Recharge	94.297	0.000	94.290	0.000	-0.006	0.000
							0.000
6	Flow from Pakowki	2.320	-1.971	2.970	-2.647	0.650	-0.676
7	Flow from Colorado	0.762	-0.750	0.800	-0.795	0.038	-0.044
	Total (1+2+3+4+5)	106.042	-105.790	106.121	-105.841	0.079	-0.051
	Error		0.252		0.280		0.028

The effect of these changes on the groundwater level and hydraulic head below the Pakowki Formation is presented in Figure 6.3. The differences are compared to Simulation 1. The pattern and amplitude of the differences are strongly correlated to the differences of the model with 43 layers and constant permeability values per model layer. The cause of a slightly difference is caused by the subdividing of the Alderson and Medicine Hat members into many additional model layers. Three aspects are important:

16 As stated before, the numerical simulator which is used for the groundwater flow, does not allow model layers to thin out completely. Therefore a minimal thickness of 1 meter is applied. The parameter which is assigned to these layers is those which occupy the model layer mostly. In this way, there might be a slight difference in formation thicknesses between the 43- and 201 layer model. This yields a slightly different total transmissivity, but in the case of tiny values for permeability, as in the current study, a small difference has a huge consequence. Especially whenever the Pakowki, with permeability values of $8.64E^{-7}$ m/d is assigned slightly differently;

17 At some locations along the Milk River, the river bed cuts into the member of the Alderson Formation. Within the 43 layer model, an entire member of the Alderson is connected to the Milk River numerically as within the 201 layer model, only a few sub-layers of the same member of the Alderson Formation is connected. Numerically, the Milk River is position differently vertically between the 43- and 201 layer model;

18 The used finite-difference scheme of groundwater flow connects cells horizontally and vertically. Whenever radial flow is considered, especially near rivers, it is more accurate to simulate this with more and thin layers than with a few and more thicker layers.

The differences between the 43- and 201 layer model show a higher (numerical) resistivity, which results in higher heads at the base of the Alderson Formation in areas with a downward groundwater flow component, and lower heads in areas with an upward flow component. This is clearly visible in Figure 6.3 where the heads are lower below rivers (upward flow) and higher below recharge areas such as the Cypress Hills (downward flow). Figure 6.4 shows the difference in transmissivity between the two simulations. The fact that the changes are so small shows the sensitivity of the model to small changes in permeability and transmissivity.

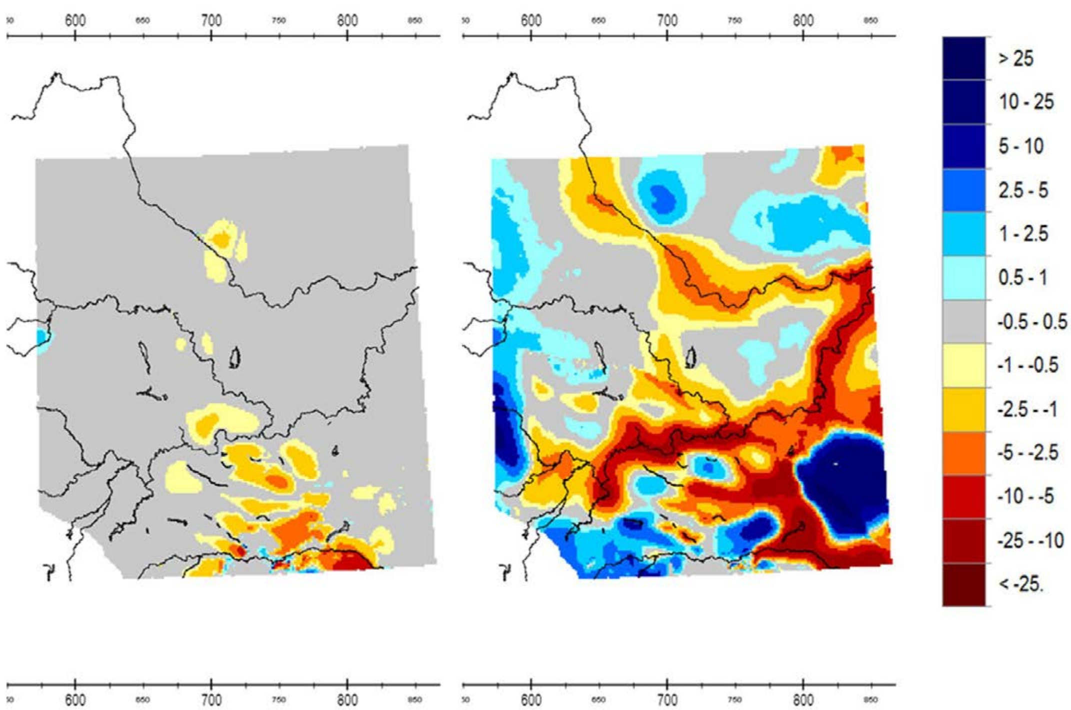

Figure 6.3 Computed difference between Simulation 2 and Simulation 1 for (left) the groundwater level and (right) the pressure head directly underneath the Pakowki Formation, all in meters of difference.

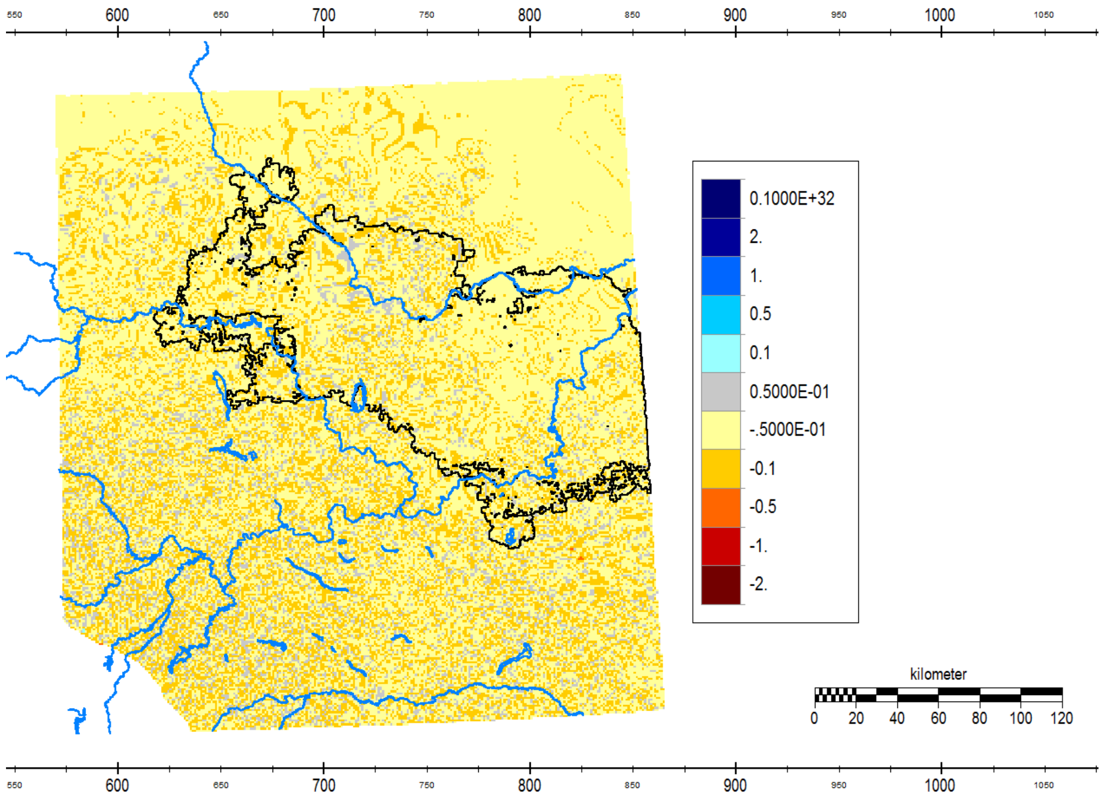

Figure 6.4 A more or less random difference in total transmissivity (m^2/day) between Simulation 1 and 2. In simulation 2 in general a small decrease occurs.

The flow patterns (Figure 6.5) of Simulation 2 are similar to Simulation 1, also the area with infiltration towards the Milk River Formation has slightly increased.

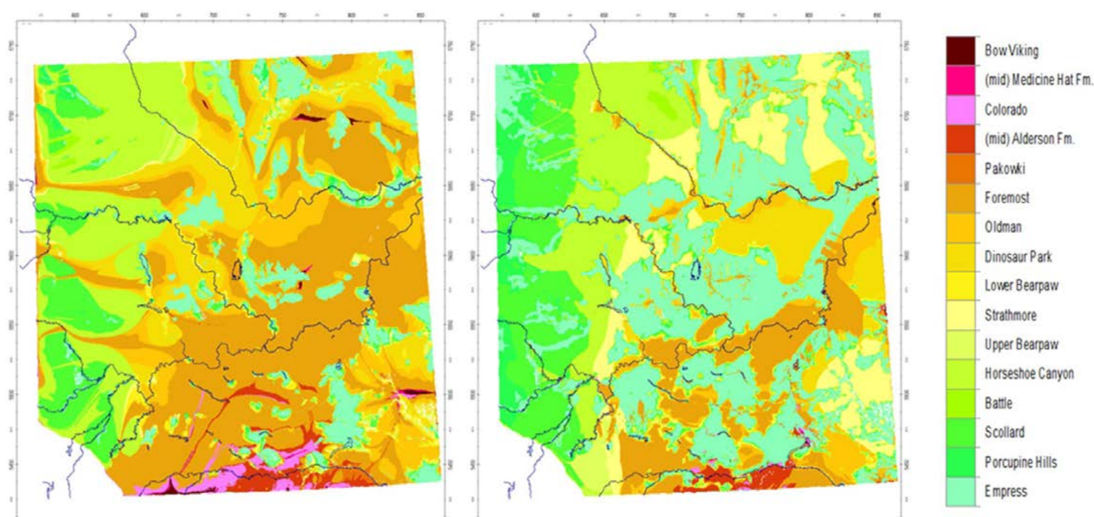

Figure 6.5 Maximal depth (expressed in Formation) for particles that travel forwards to their outlet and (right) backwards to their origin for Simulation 2.

6.1.3 Simulation 3

6.1.3.1 Introduction and modeling adjustments

The third simulation aims to simulate the effect of the gas plays with no permeability. For this purpose, the conductivity in the voxels within the zone of the gas field in the Alderson Formation (Alderson UNDF, A, B1, B2 and C) is set to zero (Figure 6.6); these are the units 13, 15, 17, 19 and 21 from Table 4.1. A comparison with Simulation 2 will show the effect of a gas field fully saturated with gas and therefore no water flux.

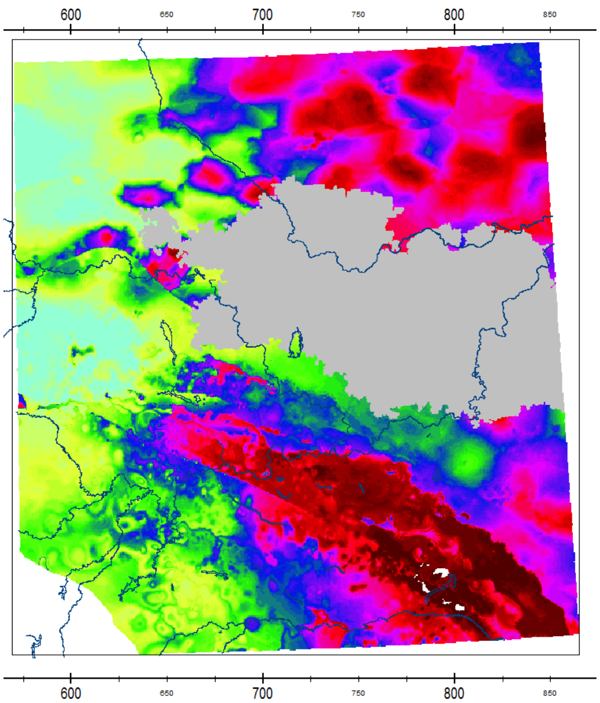

Figure 6.6 Permeability in the Milk River and Alderson Formations (red colours is high permeability, yellow is low permeability), and the conversion to a permeability of zero (grey) for one of the Alderson Members.

6.1.3.2 Results

The results of the model are presented in a water balance of the distinguished components as presented in Table 6.3 and their difference to Simulation 2. The major difference – though minor – are in the discharges of the Red Deer and Saskatchewan River. Due to the blocking of infiltrating groundwater flow through the Alderson the groundwater level rises, and therefore the modeled discharge through both mentioned rivers increases. Other, minor streams discharge less due to a drop in groundwater levels in areas with upcoming groundwater. Overall, the gas field doesn't have a significant impact on the shallow groundwater system above the Pakowki Formation (*Figure 6.7*). Moreover, the influence is limited to the hydraulic heads below the Pakowki Formation, except for a minor rise in heads around the north- and southeastern fringes of the reservoir.

A minor difference in the flow paths (Figure 6.8) occurs at the watershed between the Red Deer River and the Saskatchewan River where deep percolation up to the Bow Viking appears to be off. No changes in flow patterns occur at the southern region of the gas field.

Table 6.3 Overview of the change in water balance components between scenario 2 and 3.

	Waterbalance	Simulation 2		Simulation 3		Difference	
		Inflow million m3/year	Outflow million m3/year	Inflow million m3/year	Outflow million m3/year	Inflow million m3/year	Outflow million m3/year
1	Flow Montana	0.541	-0.100	0.541	-0.099	0.000	0.001
2	River flux	2.028	-99.122	2.028	-99.157	0.000	-0.035
2a	Red Deer River	0.000	-12.111	0.000	-12.085	0.000	0.026
2b	Bow River	0.006	-7.124	0.005	-7.140	0.000	-0.016
2c	Belly River	0.968	-2.437	0.968	-2.437	0.000	0.000
2d	Old Man River	0.147	-15.266	0.147	-15.266	0.000	-0.001
2e	Saskatchewan River	0.006	-9.790	0.006	-9.742	0.000	0.048
2f	Milk River	0.902	-0.625	0.902	-0.625	0.000	0.000
2g	Rest (minor streams)	0.000	-51.769	0.000	-51.862	0.000	-0.093
3	Lakes	9.262	-6.620	9.258	-6.623	-0.003	-0.003
4	Wells	0.000	0.000	0.000	0.000	0.000	0.000
5	Recharge	94.290	0.000	94.290	0.000	0.000	0.000
							0.000
6	Flow from Pakowki	2.970	-2.647	2.874	-2.540	-0.096	0.107
7	Flow from Colorado	0.800	-0.795	0.701	-0.707	-0.099	0.088
	Total (1+2+3+4+5)	106.121	-105.841	106.117	-105.879	-0.004	-0.038
	Error		0.280		0.238		-0.042

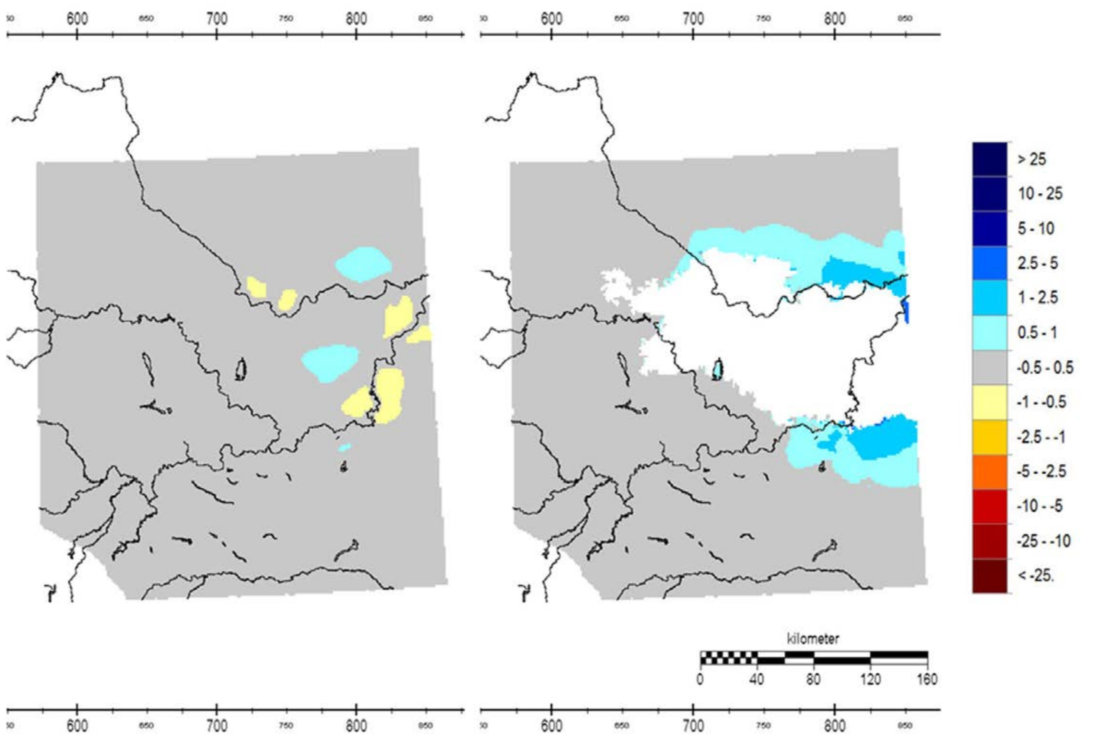

Figure 6.7 Computed difference between Simulation 3 and Simulation 2 for (left) the groundwater level and (right) the pressure head directly underneath the Pakowki Formation, all in meters of difference.

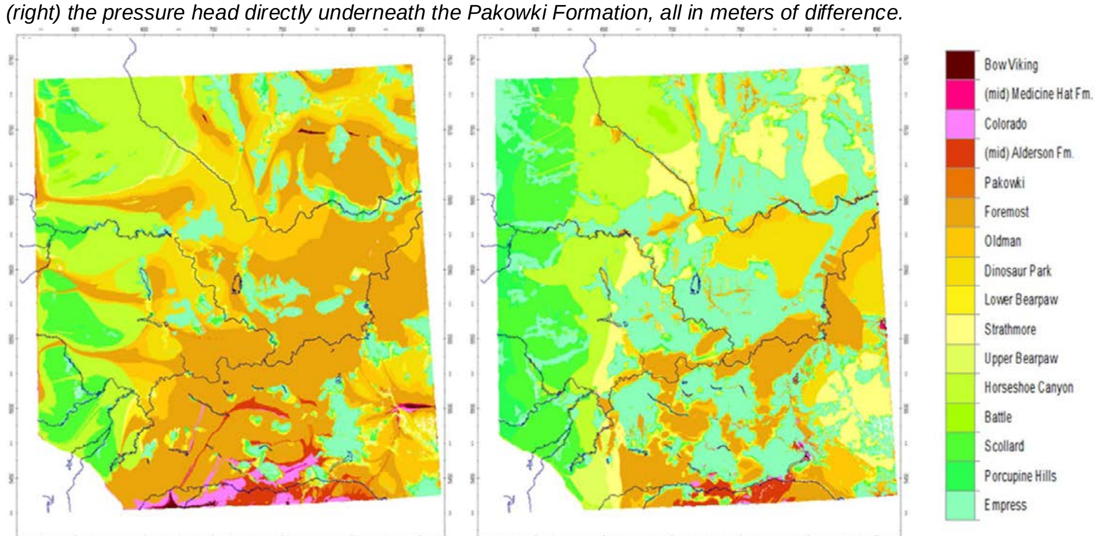

Figure 6.8 Maximal depth (expressed in Formation) for (left) particles that travel forwards to their outlet and (right) backwards to their origin for Simulation 3.

6.2 Phase 3

6.2.1 Simulation 9

6.2.1.1 Introduction

Simulation 9 represents the groundwater flow through the 201 layer model with the well-log derived permeability values for the Milk River / Alderson Formations and for the Medicine Hat Formation. Since this model forms the basis for the scenario simulations 4-8, this scenario is discussed first.

6.2.1.2 Results

The subsequent scenario simulations will be compared to the results of this model. The results of Simulation 9 will be compared to simulation 2, the 201 layer model with single permeability values per formation.

Table 6.4 Overview of the change in water balance components between scenario 2 and 9.

	Waterbalance	Simulation 2		Simulation 9		Difference	
		Inflow million m3/year	Outflow million m3/year	Inflow million m3/year	Outflow million m3/year	Inflow million m3/year	Outflow million m3/year
1	Flow Montana	0.541	-0.100	1.537	-0.080	0.996	0.020
2	River flux	2.028	-99.122	1.936	-99.943	-0.092	-0.822
2a	Red Deer River	0.000	-12.111	0.000	-12.152	0.000	-0.041
2b	Bow River	0.006	-7.124	0.006	-7.133	0.000	-0.009
2c	Belly River	0.968	-2.437	0.966	-2.423	-0.002	0.014
2d	Old Man River	0.147	-15.266	0.147	-15.313	0.000	-0.047
2e	Saskatchewan River	0.006	-9.790	0.005	-9.828	0.000	-0.039
2f	Milk River	0.902	-0.625	0.813	-0.799	-0.089	-0.175
2g	Rest (minor streams)	0.000	-51.769	0.000	-52.295	0.000	-0.526
3	Lakes	9.262	-6.620	9.215	-6.664	-0.047	-0.044
4	Wells	0.000	0.000	0.000	0.000	0.000	0.000
5	Recharge	94.290	0.000	94.290	0.000	0.000	0.000
							0.000
6	Flow from Pakowki	2.970	-2.647	4.093	-4.756	1.123	-2.109
7	Flow from Colorado	0.800	-0.795	0.533	-0.532	-0.267	0.262
	Total (1+2+3+4+5)	106.121	-105.841	106.978	-106.687	0.857	-0.846
	Error		0.280		0.291		0.012

The water balance (Table 6.4) shows a major increase in flow from Montana in Simulation 9. This is mainly caused by the increase permeability of the Virgelle Formation. The boundary condition along Montana is given by a fixed potential and by increasing permeability this yields an increased inflow as well. This flow component from Montana also introduces the increased flux over the Pakowki Formation.

The introduction of the well-log derived permeability values leads to big differences in transmissivity in the modelling area (Figure 6.9). In the northeast, the higher transmissivity values indicate a sandier part of the Alderson Formation with generally higher permeability values than the single permeability values used in Simulation 2 for the Alderson Formation. Most of the gas zone and the southern fringe of the Alderson Formation have slightly lower permeability values in the property model compared to the single value used in Simulation 2, apart from some isolated spots with higher values. In the southeast, a zone with higher transmissivity indicates the area with clean coastal sands of the Virgelle Member and the Alderson sandstones. Lastly, in the southwest, the decreased permeabilities are indicate that the Telegraph Creek, Virgelle and Dead Horse Coulee members of the Milk river formation have lower permeabilities is the property model. Hence, the property model distinguishes differences in permeability within hydrogeological units related to facies changes within the units.

The differences in transmissivity results in notable differences in groundwater level and hydraulic head below the Pakowki Formation (Figure 6.10). In areas with large differences in transmissivity result in both lowering and rising of groundwater levels. The area in the southeast with increased transmissivities generally results in higher heads and groundwater level, except for the area near the Cypress Hills where the recharge is drained easier, leading to lower groundwater tables and heads. In the northeast a similar pattern is present. Areas with downward flow show lower heads and groundwater levels, and areas with upward flow show higher heads and groundwater levels. In the area southwest with lower transmissivity the opposite is happening, with lower heads in areas with upward flow, such as rivers, and higher heads in areas with downward flow.

The flow paths (Figure 6.11) of Simulation 9 still show a similar pattern to Simulation 2. The most notable differences are streamlines reaching the Alderson and Colorado north of the gas zone and below the Cypress Hills, and slightly more percolation to these formations around the Milk River.

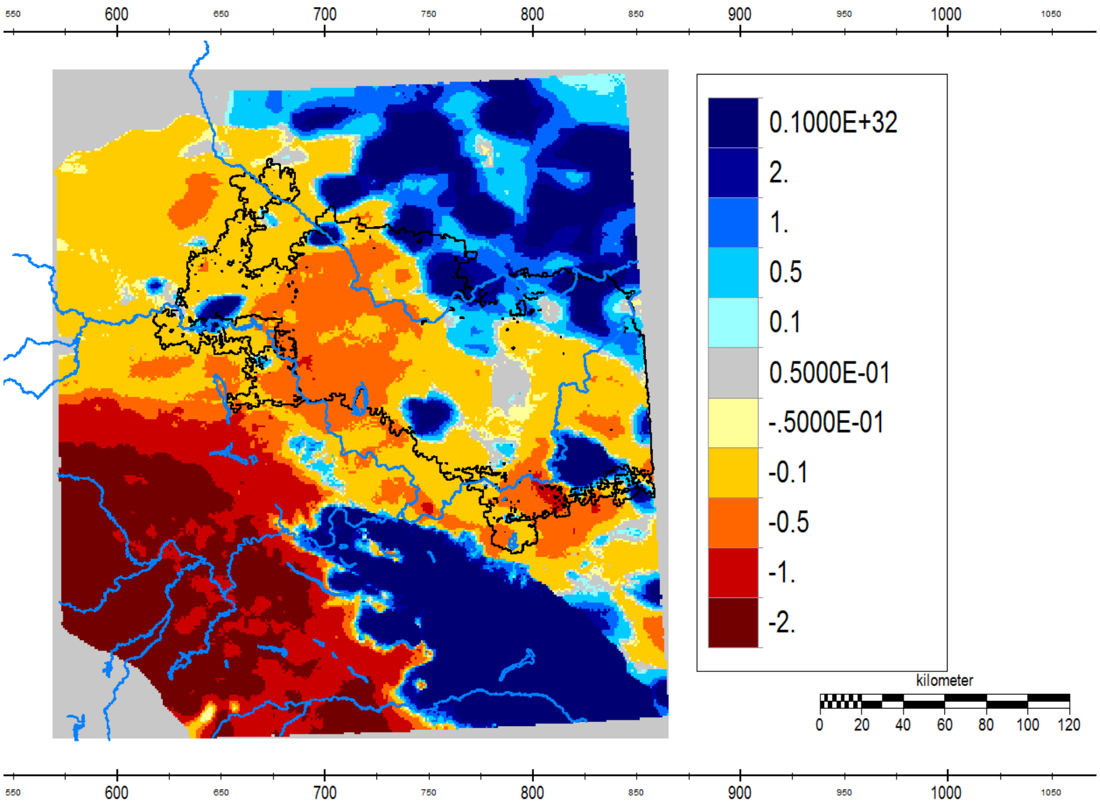

Figure 6.9 Difference in transmissivity values (in m^2/day) in Simulation 9 compared to Simulation 2. Black outline indicates the Alderson gas zone.

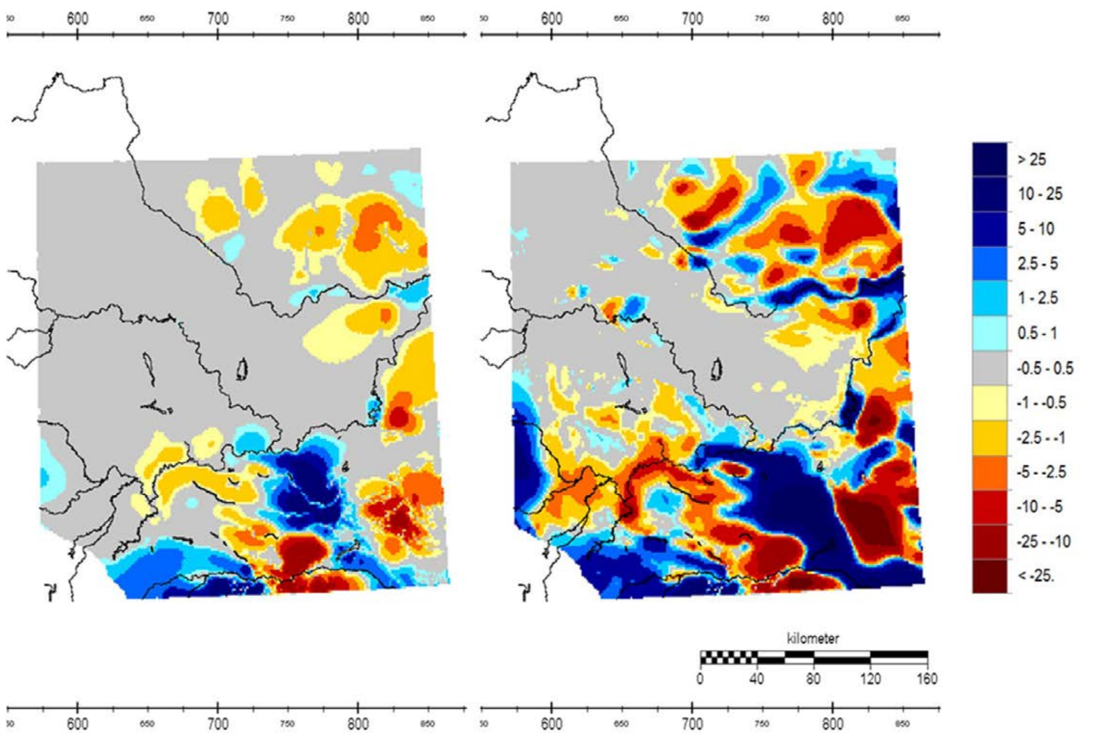

Figure 6.10 Computed difference between Simulation 9 and Simulation 2 for (left) the groundwater level and (right) the pressure head directly underneath the Pakowki Formation, all in meters of difference.

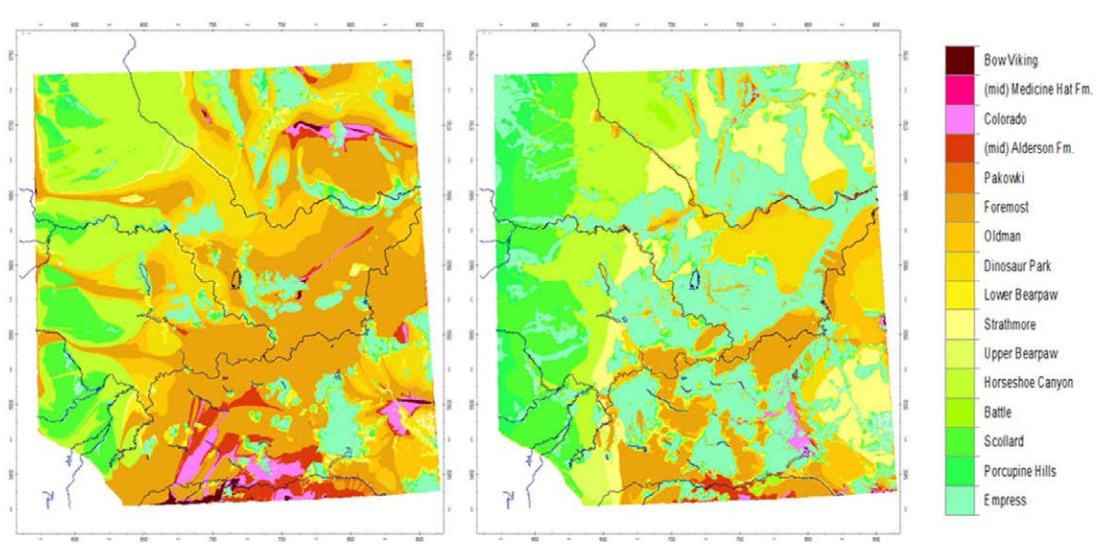

Figure 6.11 Maximal depth (expressed in Formation) for (left) particles that travel forwards to their outlet and (right) backwards to their origin for Simulation 9.

6.2.2 Simulation 4

6.2.2.1 Introduction and modeling adjustments

Simulation 4 aims to simulate the effect of a hydraulically connected Aquifer with an internally connected gas reservoir, and the influence of groundwater flow towards the gas reservoir on the seal strength. Within the gas reservoir, the seals are weak, which enables the simulation of the effect of a large gas column on a weak seal in the Alderson Formation. This simulation is performed solely to determine the effect on the groundwater flow. The capability of the seals to hold gas will be simulated in a later stage. Because this simulation is a modification of Simulation 9 in the boundary zone and the Alderson gas reservoir (Figure 2.7), the results are compared to Simulation 9.

Simulation 4 consists of the following elements introduced into Simulation 9:

Reservoir Building blocks:

A1: In the zone of the gas reservoir, there are two flavours of voxels: shale or sand. From the range of permeabilities in the property model in this zone, the highest 40% of K values ($k=1.13E^{-3}$ m/d) are sand ($k=4.32E^{-2}$ m/day), the lowest 60% permeabilities are shale.
C2: The k-value of the shale in the reservoir depends on the strength of the seals. The shale voxels in the reservoir have a k and n value that can hold 10 m of gas max. Therefore, $k = 3.41E^{-8}$ m/day.

Boundary zone Building Blocks:

B1: There is a gradual (log scale) change from sandy voxels in the south to shaly voxels in the north in layers:15 Alderson A, 17 Alderson B1 , 19 Alderson B2 and 21 Alderson C. The permeability of the sand is ($k=4.32E^{-2}$ m/day), the rest is shale ($k = 3.41E^{-8}$ m/day).
D1: The k-value of the shale in the boundary zone depends on the strength of the seals. The shale voxels in the reservoir have a k and n value that can hold 230 m of gas max. Therefore, $k=8.31E^{-10}$ m/day

6.2.2.2 Results

The adjustments in the boundary zone and in the gas zone do not lead to notable changes in the water balance (Table 6.5). The effect on transmissivities is in general a lower transmissivity in the boundary zone, and a higher transmissivity in a distinct area within the gas zone (Figure 6.12). In the gas zone, the higher transmissivities are the areas in which sandstone is schematised. These areas are concentrated towards the edges of the gas zone. In the centre and in the west, the transmissivity is hardly altered, since it is going from a very low permeability to an even lower permeability. The lower transmissivities in the boundary zone show that the property model has a relatively high permeability in the southeastern part in this zone. This could also be partly the result of the assignment of cells from the property model to the formations in the layer model. The zone with slightly higher transmissivities in the southern edge shows the effect of the gradual transition from shale to sand towards the south.

The effects on groundwater level and hydraulic head (Figure 6.13) show mainly differences in head over the gas zone (with higher heads with upward flow and lower heads with downward flow) and around the Cypress Hills in the area with reduced transmissivities, where the opposite effect is visible. The flow paths (Figure 6.14) do not show notable differences.

Table 6.5 Overview of the change in water balance components between scenario 4 and 9.

	Waterbalance	Simulation 4		Simulation 9		Difference	
		Inflow million m3/year	Outflow million m3/year	Inflow million m3/year	Outflow million m3/year	Inflow million m3/year	Outflow million m3/year
1	Flow Montana	1.566	-0.081	1.537	-0.080	-0.029	0.001
2	River flux	1.936	-99.969	1.936	-99.943	0.000	0.026
2a	Red Deer River	0.000	-12.191	0.000	-12.152	0.000	0.039
2b	Bow River	0.006	-7.126	0.006	-7.133	0.000	-0.007
2c	Belly River	0.966	-2.423	0.966	-2.423	0.000	0.000
2d	Old Man River	0.147	-15.313	0.147	-15.313	0.000	0.000
2e	Saskatchewan River	0.005	-9.782	0.005	-9.828	0.000	-0.047
2f	Milk River	0.813	-0.796	0.813	-0.799	0.000	-0.003
2g	Rest (minor streams)	0.000	-52.339	0.000	-52.295	0.000	0.044
3	Lakes	9.211	-6.665	9.215	-6.664	0.003	0.002
4	Wells	0.000	0.000	0.000	0.000	0.000	0.000
5	Recharge	94.290	0.000	94.290	0.000	0.000	0.000
							0.000
6	Flow from Pakowki	4.024	-4.719	4.093	-4.756	0.069	-0.037
7	Flow from Colorado	0.497	-0.496	0.533	-0.532	0.036	-0.036
	Total (1+2+3+4+5)	107.004	-106.715	106.978	-106.687	-0.025	0.028
	Error		0.289		0.291		0.003

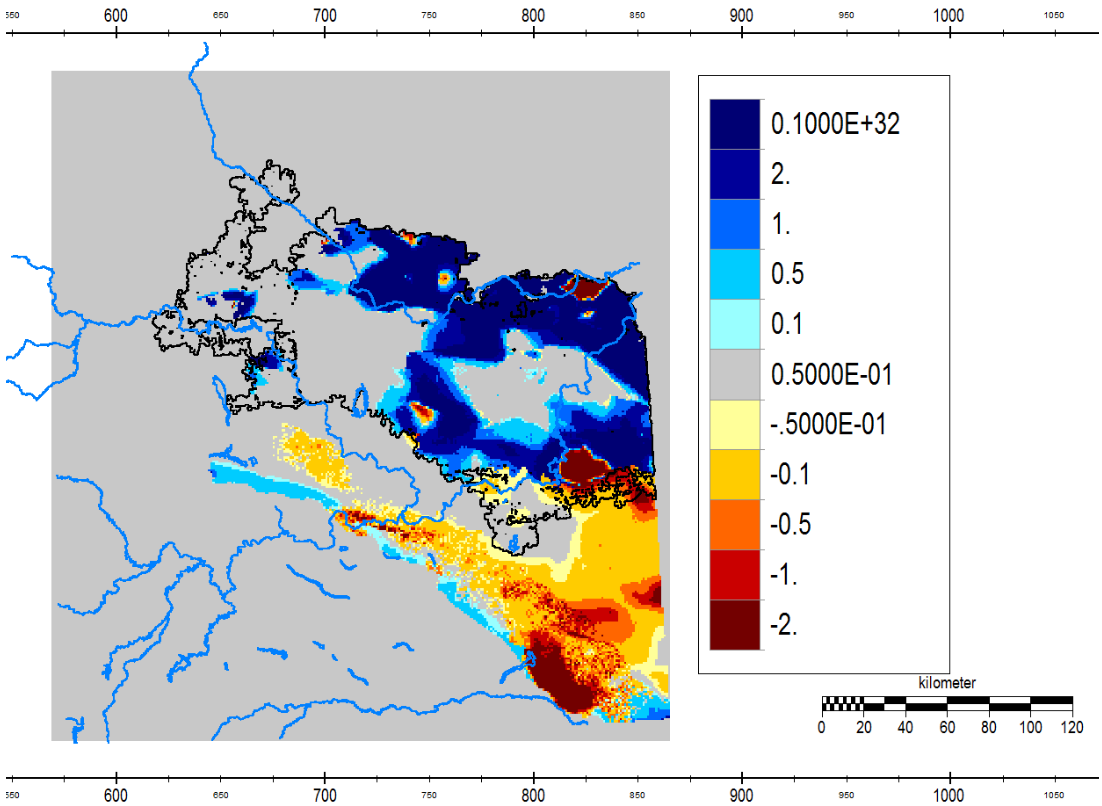

Figure 6.12 Difference in transmissivity values (in m^2/day) in Simulation 4 compared to Simulation 9. Black outline indicates the Alderson gas zone.

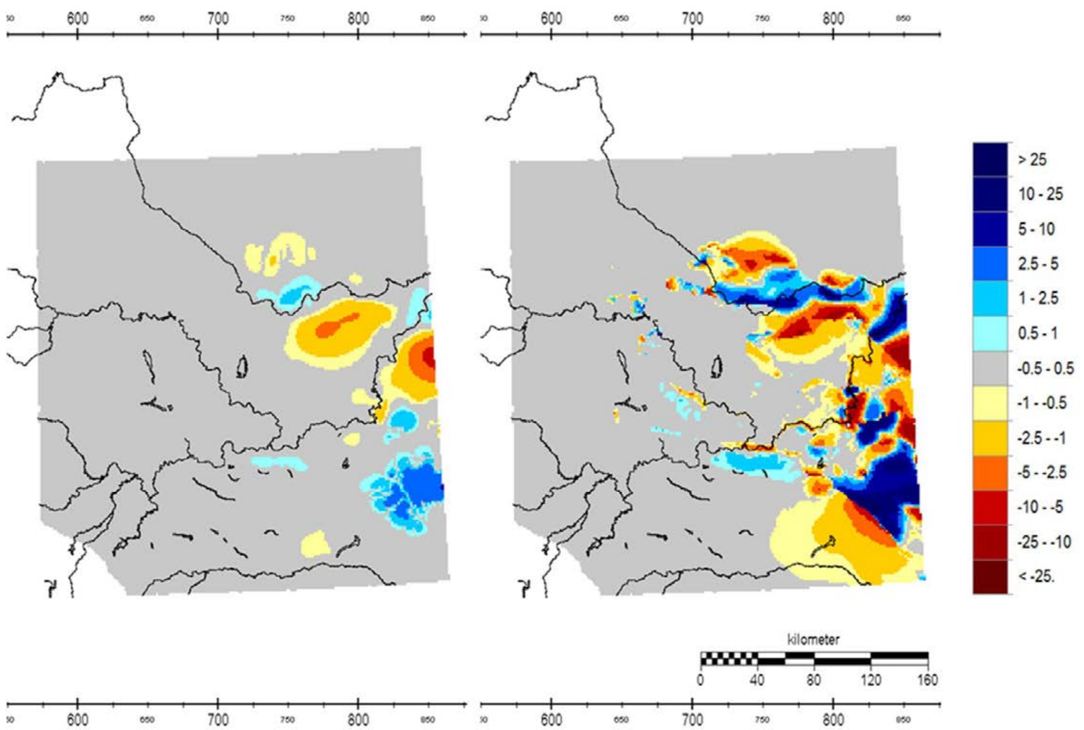

Figure 6.13 Computed difference between Simulation 4 and Simulation 9 for (left) the groundwater level and (right) the pressure head directly underneath the Pakowki Formation, all in meters of difference.

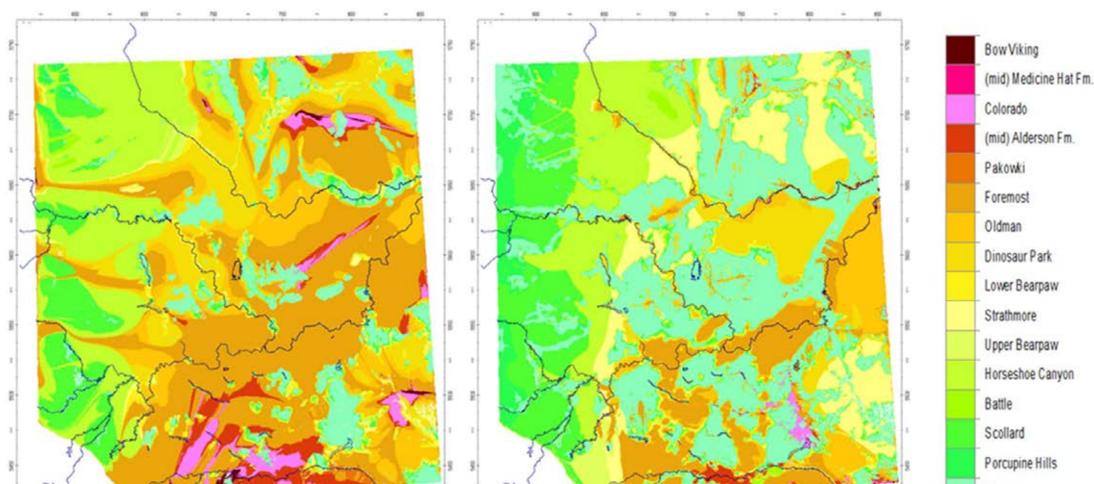

Figure 6.14 Maximal depth (expressed in Formation) for particles that travel forwards to their outlet and (right) backwards to their origin for Simulation 4.

6.2.3 Simulation 5

6.2.3.1 Introduction and modeling adjustments

Simulation 5 aims to simulate the effect of a hydraulically disconnected Aquifer and an internally connected gas reservoir. Within the gas reservoir, the seals are strong, which enables the simulation of the effect of a large gas column and a strong seal in the Alderson Formation. This simulation is performed solely to determine the effect on the groundwater flow. The capability of the seals to hold gas will be simulated in a later stage.
Because this simulation is a modification of Simulation 9 in the boundary zone and the Alderson gas reservoir (Figure 2.7), the results are compared to Simulation 9.

Simulation 5 consists of the following elements introduced into Simulation 9:

Reservoir Building blocks:

A1: In the zone of the gas reservoir, there are two flavours of voxels: shale or sand. From the range of permeabilities in the property model in this zone, the highest 40% of K values ($k=1.13E^{-3}$ m/d) are sand ($k=4.32E^{-2}$ m/day), the lowest 60% permeabilities are shale.
C1: The shale here should have such a k value (and effective porosity for later) to hold a gas column from the deepest base of the Alderson C Formation within the reservoir extent tot the highest top of the Alderson A (or base of the Pakowki Formation) within the reservoir extent. Therefore, $k = 8.31E^{-10}$ m/day (~230m).

Boundary zone Building Blocks:

B2: In the boundary zone, all voxels are shale. So all voxels in layers:15 Alderson A, 17 Alserson B1 , 19 Alderson B2 and 21 Alderson C are set to shale.
D1: The k-value of the shale in the boundary zone depends on the strength of the seals. The shale voxels in the reservoir have a k and n value that can hold 230 m of gas max. Therefore, $k=8.31E^{-10}$ m/day

6.2.3.2 Results

The water balance of Scenario 5 compared to Scenario 9 (Table 6.6) shows no notable differences, except for the in- and outflow from the Pakowki Formation. This is the result of the changed transmissivity values (Figure 6.15). Again, in the reservoir, the 40% sandstone shows up as a distinct area with higher transmissivities. The boundary zone is also similar to Simulation 4, except for the fact that the blue edge in the south is missing because the entire Alderson A, B and C members are low permeable shale in this Simulation. In the groundwater levels and hydraulic heads (Figure 6.16) this results into higher heads around the Cypress Hills, also compared to Simulation 4, and higher heads in zone bordering the boundary zone, caused by groundwater that is retained on its travel northward. These changes also have a notable effect on the groundwater levels.

In the flow paths (Figure 6.17), the effect of the low permeable Alderson boundary zone is visible in the Cypress Hills where the groundwater does not percolate as deep as in Simulation 4 and 9, and stops in the Pakowki Formation. This explains the differences in the water balance.

Table 6.6 Overview of the change in water balance components between scenario 5 and 9.

	Waterbalance	Simulation 5		Simulation 9		Difference	
		Inflow million m3/year	Outflow million m3/year	Inflow million m3/year	Outflow million m3/year	Inflow million m3/year	Outflow million m3/year
1	Flow Montana	1.436	-0.081	1.537	-0.080	0.101	0.001
2	River flux	1.936	-99.815	1.936	-99.943	0.000	-0.128
2a	Red Deer River	0.000	-12.188	0.000	-12.152	0.000	0.036
2b	Bow River	0.006	-7.108	0.006	-7.133	0.000	-0.026
2c	Belly River	0.966	-2.423	0.966	-2.423	0.000	0.000
2d	Old Man River	0.147	-15.314	0.147	-15.313	0.000	0.001
2e	Saskatchewan River	0.005	-9.573	0.005	-9.828	0.000	-0.256
2f	Milk River	0.813	-0.819	0.813	-0.799	0.000	0.020
2g	Rest (minor streams)	0.000	-52.390	0.000	-52.295	0.000	0.095
3	Lakes	9.181	-6.651	9.215	-6.664	0.033	-0.013
4	Wells	0.000	0.000	0.000	0.000	0.000	0.000
5	Recharge	94.290	0.000	94.290	0.000	0.000	0.000
							0.000
6	Flow from Pakowki	2.707	-3.243	4.093	-4.756	1.386	-1.512
7	Flow from Colorado	0.373	-0.376	0.533	-0.532	0.160	-0.156
	Total (1+2+3+4+5)	106.844	-106.547	106.978	-106.687	0.135	-0.140
	Error		0.297		0.291		-0.005

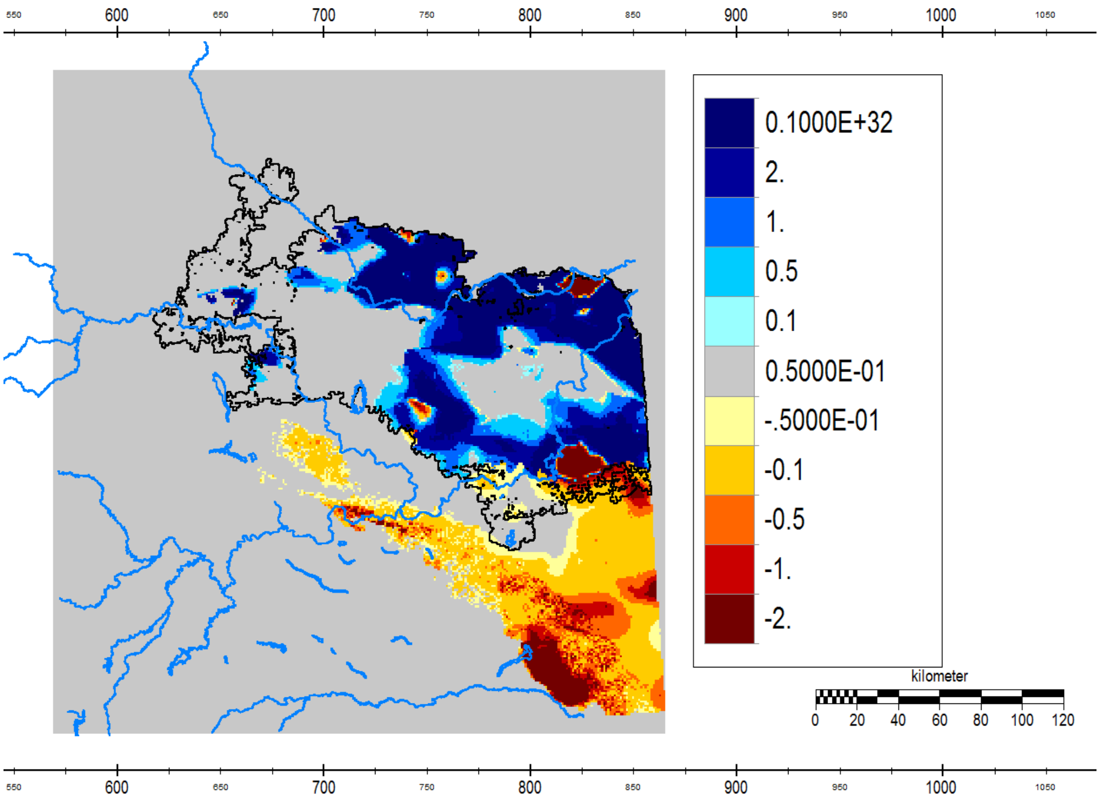

Figure 6.15 Difference in transmissivity values (in m^2/day) in Simulation 5 compared to Simulation 9. Black outline indicates the Alderson gas zone.

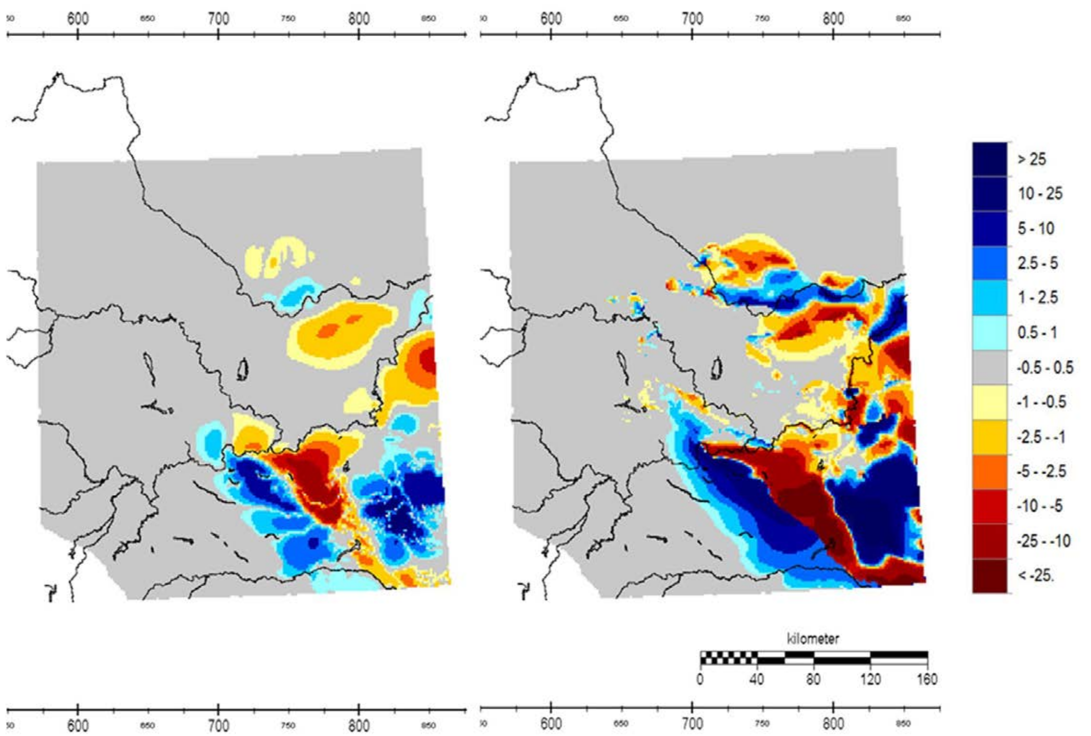

Figure 6.16 Computed difference between Simulation 5 and Simulation 9 for (left) the groundwater level and (right) the pressure head directly underneath the Pakowki Formation, all in meters of difference.

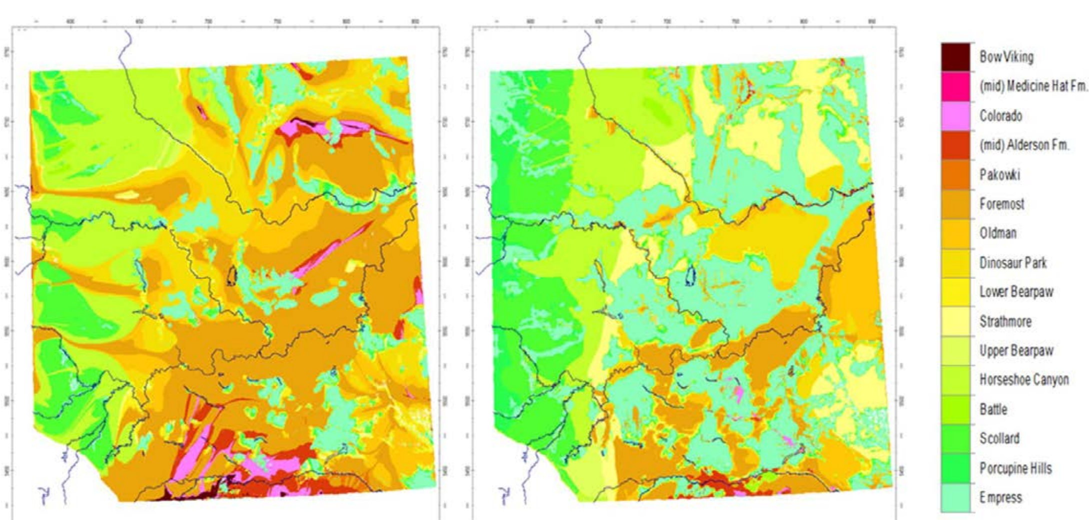

Figure 6.17 Maximal depth (expressed in Formation) for particles that travel forwards to their outlet and (right) backwards to their origin for Simulation 5.

6.2.4 Simulation 6

6.2.4.1 Introduction and modeling adjustments

Simulation 6 aims to simulate the effect of a hydraulically disconnected Aquifer and an internally disconnected gas reservoir. Within the gas reservoir and boundary zone, the seals are weak, which enables the simulation of the effect of a small gas column and weak seals in the Alderson Formation. This simulation is performed solely to determine the effect on the groundwater flow. The capability of the seals to hold gas will be simulated in a later stage.
Because this simulation is a modification of Simulation 9 in the boundary zone and the Alderson gas reservoir (Figure 2.7), the results are compared to Simulation 9.

Simulation 6 consists of the following elements introduced into Simulation 9:

Reservoir Building blocks:

A2: In the zone of the gas reservoir, there are two flavours of voxels: shale or sand. From the range of permeabilities in the property model in this zone, the highest 20% of K values (k=4.58E^{-3} m/d) are sand (k=4.32E^{-2} m/day), the lowest 80% permeabilities are shale.
C2: The k-value of the shale in the reservoir depends on the strength of the seals. The shale voxels in the reservoir have a k and n value that can hold 10 m of gas max. Therefore, k = 3.41E^{-8} m/day.

Boundary zone Building Blocks:

B1: There is a gradual (log scale) change from sandy voxels in the south to shaly voxels in the north in layers:15 Alderson A, 17 Alderson B1 , 19 Alderson B2 and 21 Alderson C. The permeability of the sand is (k=4.32E^{-2} m/day), the rest is shale (k = 3.41E^{-8} m/day).
D2: The shale voxels in the boundary zone have a k and n value that can hold a column of gas of 10m max. Therefore, k = 3.41E^{-8} m/day

6.2.4.2 Results

The water balance of Simulation 6 (Table 6.7) does not show notable changes compared to Simulaton 9, only a minor change in the flow from the Pakowki Formation. The differences in transmissivity (Figure 6.18) in the boundary zone are almost identical to Simulation 4. In the gas zone, the 20% sandy voxels concentrate mainly in the north, and to a lesser degree in the southeast along the edge of the reservoir. Areas with a reduced transmissivity result from voxels that were relatively permeable and are turned into shale in this simulation. The effects on the hydraulic head are similar to Simulation 1, and also in this simulation groundwater levels are hardly affected (Figure 6.19). The same goes up for the flow paths (Figure 6.20).

Table 6.7 Overview of the change in water balance components between scenario 6 and 9.

	Waterbalance	Simulation 6		Simulation 9		Difference	
		Inflow million m3/year	Outflow million m3/year	Inflow million m3/year	Outflow million m3/year	Inflow million m3/year	Outflow million m3/year
1	Flow Montana	1.563	-0.080	1.537	-0.080	-0.026	0.000
2	River flux	1.936	-99.968	1.936	-99.943	0.000	0.024
2a	Red Deer River	0.000	-12.156	0.000	-12.152	0.000	0.004
2b	Bow River	0.006	-7.132	0.006	-7.133	0.000	-0.001
2c	Belly River	0.966	-2.423	0.966	-2.423	0.000	0.000
2d	Old Man River	0.147	-15.313	0.147	-15.313	0.000	0.000
2e	Saskatchewan River	0.005	-9.741	0.005	-9.828	0.000	-0.088
2f	Milk River	0.813	-0.796	0.813	-0.799	0.000	-0.003
2g	Rest (minor streams)	0.000	-52.407	0.000	-52.295	0.000	0.112
3	Lakes	9.211	-6.665	9.215	-6.664	0.003	0.001
4	Wells	0.000	0.000	0.000	0.000	0.000	0.000
5	Recharge	94.290	0.000	94.290	0.000	0.000	0.000
							0.000
6	Flow from Pakowki	3.812	-4.505	4.093	-4.756	0.281	-0.251
7	Flow from Colorado	0.498	-0.497	0.533	-0.532	0.035	-0.036
	Total (1+2+3+4+5)	107.001	-106.713	106.978	-106.687	-0.023	0.026
	Error		0.288		0.291		0.003

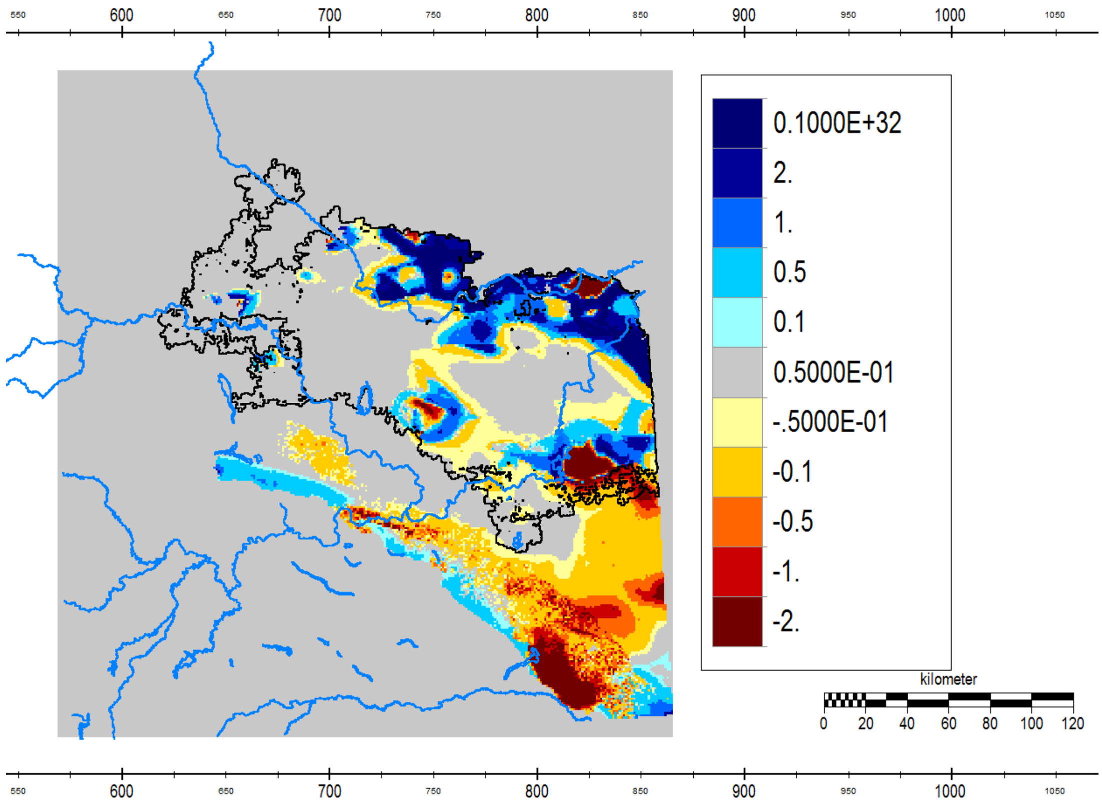

Figure 6.18 Difference in transmissivity values (in m^2/day) in Simulation 6 compared to Simulation 9. Black outline indicates the Alderson gas zone.

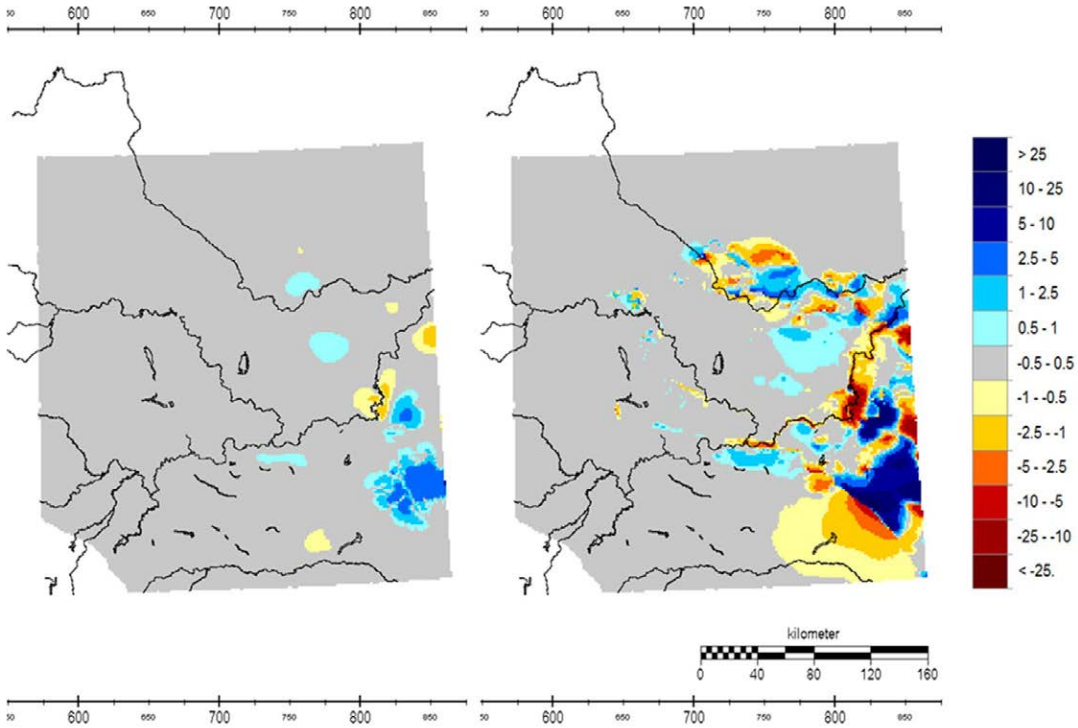

Figure 6.19 Computed difference between Simulation 6 and Simulation 9 for (left) the groundwater level and (right) the pressure head directly underneath the Pakowki Formation, all in meters of difference.

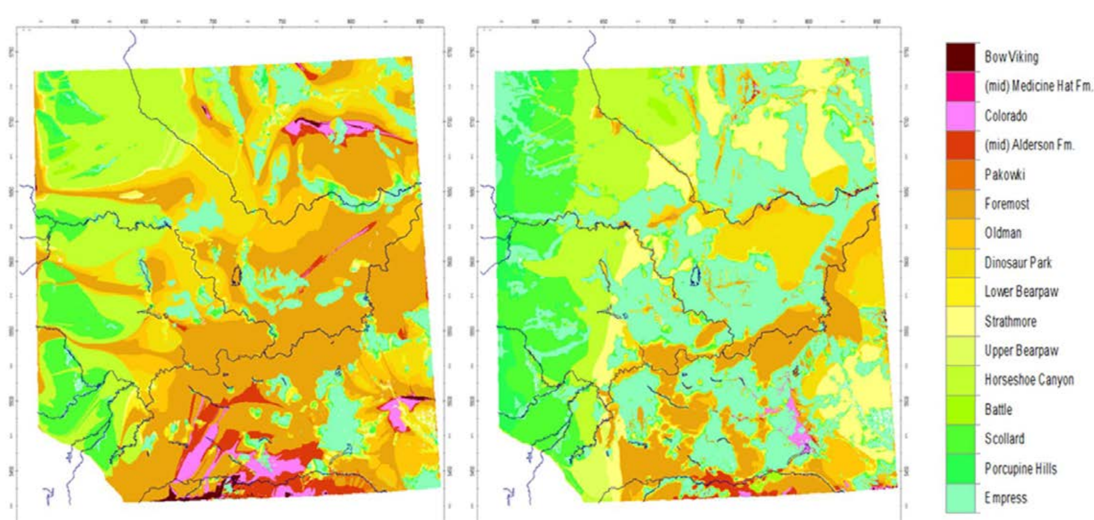

Figure 6.20 Maximal depth (expressed in Formation) for particles that (left) travel forwards to their outlet and (right) backwards to their origin for Simulation 6.

6.2.5 Simulation 7

6.2.5.1 Introduction and modeling adjustments

Simulation 7 aims to simulate the effect of a hydraulically connected Aquifer and an internally disconnected gas reservoir. Within the gas reservoir, the seals are strong, which enables the simulation of the effect of a short gas column and a strong seal in the Alderson Formation. This simulation is performed solely to determine the effect on the groundwater flow. The capability of the seals to hold gas will be simulated in a later stage.
Because this simulation is a modification of Simulation 9 in the boundary zone and the Alderson gas reservoir (Figure 2.7), the results are compared to Simulation 9.

Simulation 7 consists of the following elements introduced into Simulation 9:

Reservoir Building block:

A2: In the zone of the gas reservoir, there are two flavours of voxels: shale or sand. From the range of permeabilities in the property model in this zone, the highest 20% of K values (k=4.58E^{-3} m/d) are sand (k=4.32E^{-2} m/day), the lowest 80% permeabilities are shale.
C1: The shale here should have such a k value (and effective porosity for later) to hold a gas column from the deepest base of the Alderson C Formation within the reservoir extent tot the highest top of the Alderson A (or base of the Pakowki Formation) within the reservoir extent. Therefore, k = 8.31E^{-10} m/day (~230m).

Boundary zone Building Blocks:

B1: There is a gradual (log scale) change from sandy voxels in the south to shaly voxels in the north in layers:15 Alderson A, 17 Alderson B1 , 19 Alderson B2 and 21 Alderson C. The permeability of the sand is (k=4.32E^{-2} m/day), the rest is shale (k=8.31E^{-10} m/day).
D1: The k-value of the shale in the boundary zone depends on the strength of the seals. The shale voxels in the reservoir have a k and n value that can hold 230 m of gas max. Therefore, k=8.31E^{-10} m/day.

6.2.5.2 Results

In the water balances (Table 6.8), there is only a small effect visible in the Flow from the Pakowki Formation. The Transmissivity values (Figure 6.21) show a combination of the boundary zone of Simulation 4 and the gas zone of Simulation 6. Also the results for the hydraulic head and groundwater levels (Figure 6.22) are almost identical to the corresponding zones in those simulations, and so are the flow paths (Figure 6.23).

Table 6.8 Overview of the change in water balance components between scenario 6 and 9.

	Waterbalance	Simulation 7		Simulation 9		Difference	
		Inflow million m3/year	Outflow million m3/year	Inflow million m3/year	Outflow million m3/year	Inflow million m3/year	Outflow million m3/year
1	Flow Montana	1.567	-0.080	1.537	-0.080	-0.029	0.000
2	River flux	1.936	-99.961	1.936	-99.943	0.000	0.017
2a	Red Deer River	0.000	-12.156	0.000	-12.152	0.000	0.004
2b	Bow River	0.006	-7.131	0.006	-7.133	0.000	-0.002
2c	Belly River	0.966	-2.423	0.966	-2.423	0.000	0.000
2d	Old Man River	0.147	-15.313	0.147	-15.313	0.000	0.000
2e	Saskatchewan River	0.005	-9.711	0.005	-9.828	0.000	-0.117
2f	Milk River	0.813	-0.796	0.813	-0.799	0.000	-0.003
2g	Rest (minor streams)	0.000	-52.431	0.000	-52.295	0.000	0.136
3	Lakes	9.210	-6.666	9.215	-6.664	0.004	0.003
4	Wells	0.000	0.000	0.000	0.000	0.000	0.000
5	Recharge	94.290	0.000	94.290	0.000	0.000	0.000
							0.000
6	Flow from Pakowki	3.745	-4.433	4.093	-4.756	0.349	-0.323
7	Flow from Colorado	0.464	-0.463	0.533	-0.532	0.069	-0.069
	Total (1+2+3+4+5)	107.003	-106.707	106.978	-106.687	-0.025	0.020
	Error		0.296		0.291		-0.005

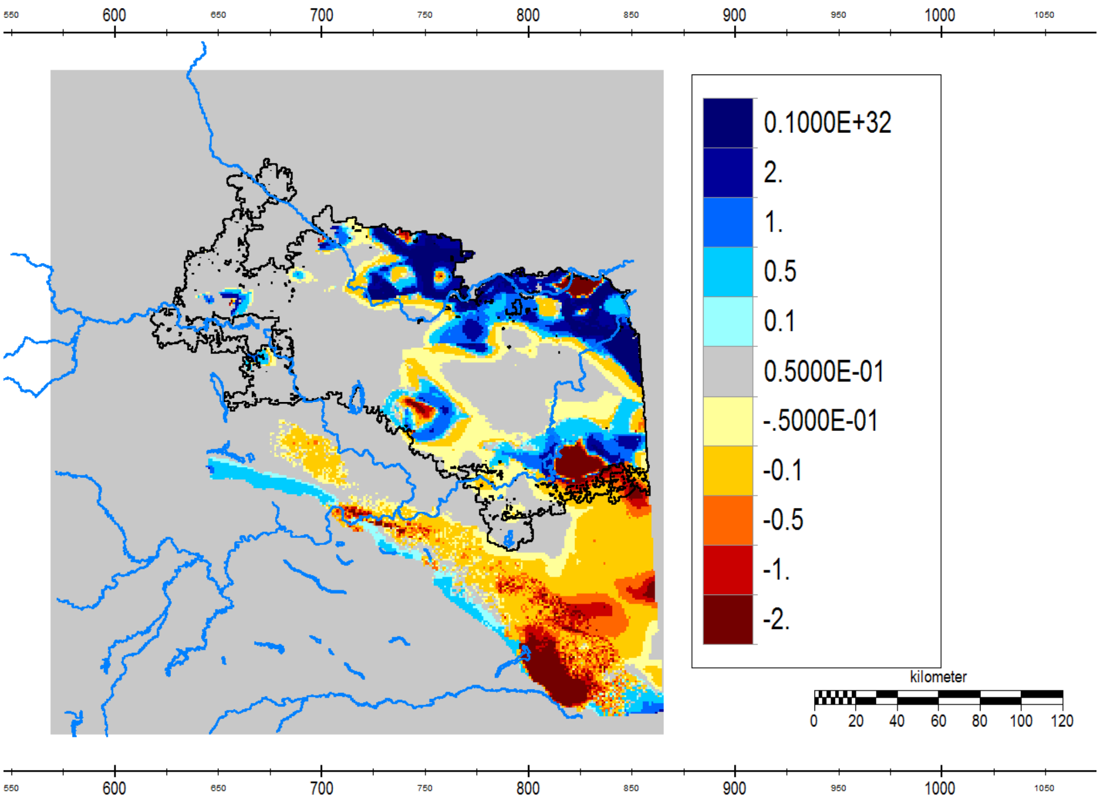

Figure 6.21 Difference in transmissivity values (in m^2/day) in Simulation 7 compared to Simulation 9. Black outline indicates the Alderson gas zone.

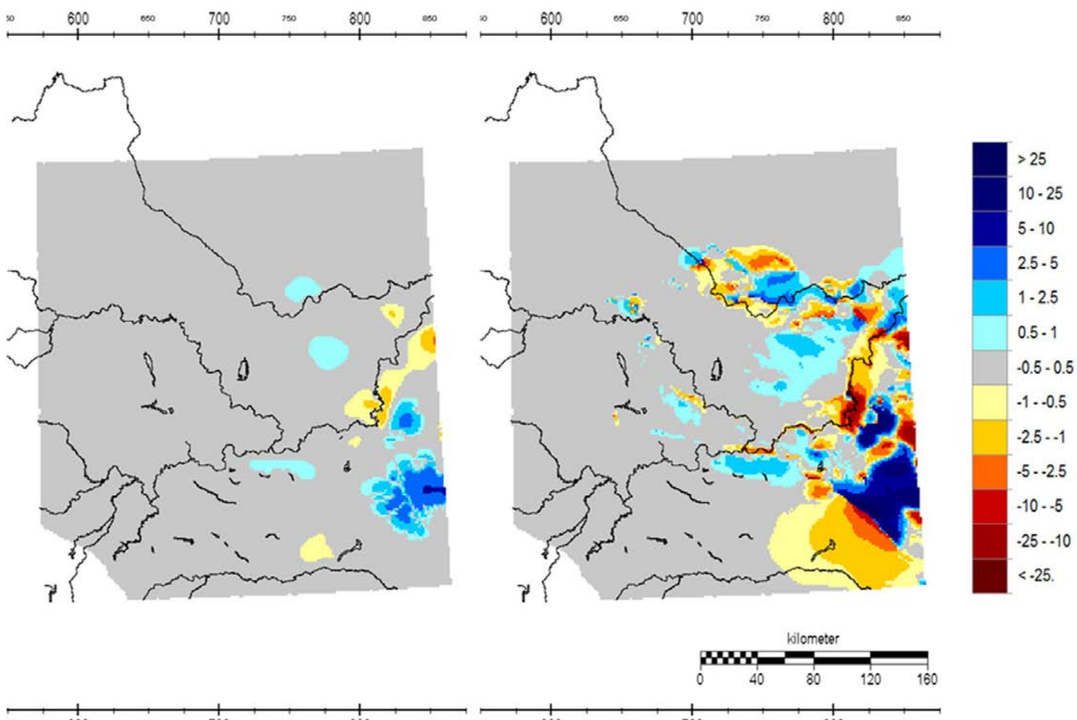

Figure 6.22 Computed difference between Simulation 7 and Simulation 9 for (left) the groundwater level and (right) the pressure head directly underneath the Pakowki Formation, all in meters of difference.

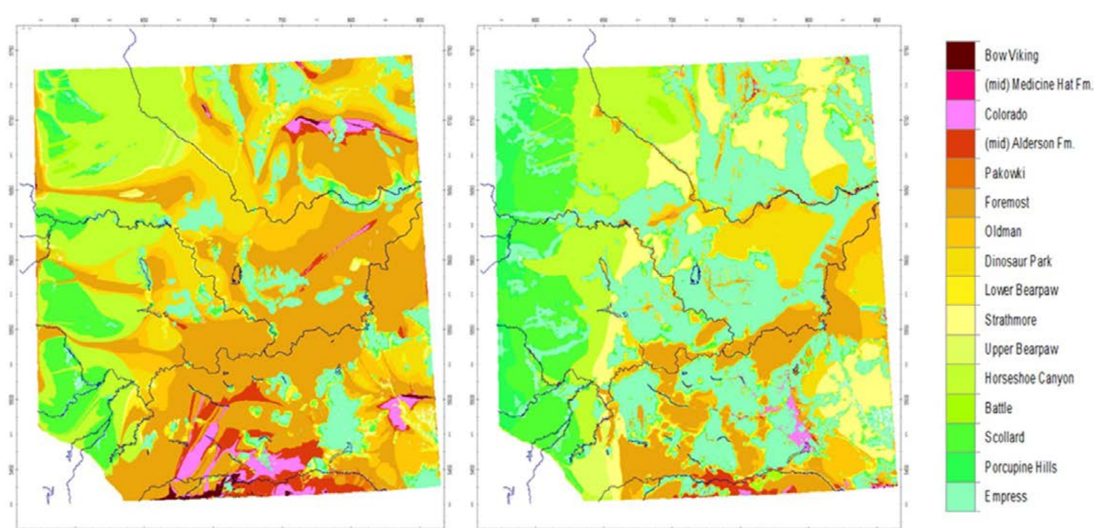

Figure 6.23 Maximal depth (expressed in Formation) for particles that travel forwards to their outlet and (right) backwards to their origin for Simulation 7.

6.2.6 Simulation 8

6.2.6.1 Introduction and modeling adjustments

Simulation 8 aims to simulate the effect of a hydraulically disconnected Aquifer and an internally disconnected gas reservoir. Within the gas reservoir, the seals are strong, which enables the simulation of the effect of a short gas column and a strong seal in the Alderson Formation. This simulation is performed solely to determine the effect on the groundwater flow. The capability of the seals to hold gas will be simulated in a later stage.
Because this simulation is a modification of Simulation 9 in the boundary zone and the Alderson gas reservoir (Figure 2.7), the results are compared to Simulation 9.

Simulation 8 consists of the following elements introduced into Simulation 9:

Reservoir Building blocks:

A2: In the zone of the gas reservoir, there are two flavours of voxels: shale or sand. From the range of permeabilities in the property model in this zone, the highest 20% of K values (k=4.58E^{-3} m/d) are sand (k=4.32E^{-2} m/day), the lowest 80% permeabilities are shale.
C1: The shale here should have such a k value (and effective porosity for later) to hold a gas column from the deepest base of the Alderson C Formation within the reservoir extent tot the highest top of the Alderson A (or base of the Pakowki Formation) within the reservoir extent. Therefore, k = 8.31E^{-10} m/day (~230m).

Boundary zone Building Blocks:

B2: In the boundary zone, all voxels are shale. So all voxels in layers:15 Alderson A, 17 Alderson B1 , 19 Alderson B2 and 21 Alderson C are set to shale.
D1: The k-value of the shale in the boundary zone depends on the strength of the seals. The shale voxels in the reservoir have a k and n value that can hold 230 m of gas max. Therefore, k=8.31E^{-10} m/day

6.2.6.2 Results

The water balance (Table 6.9) shows no notable differences with Simulation 9, except for the flow from the Pakowki Formation. This is similar to the effects of the disconnected reservoir in Simulation 5. Also the transmissivity values (Figure 6.24) for the boundary zone are identical to Simulation 5. The transmissivity values in the gas zone are identical to Simulation 7. Also the results for the hydraulic head and groundwater levels (Figure 6.25) are almost identical to the corresponding zones in those simulations, and so are the flow paths (Figure 6.26).

Table 6.9 Overview of the change in water balance components between scenario 6 and 9.

	Waterbalance	Simulation 8		Simulation 9		Difference	
		Inflow million m3/year	Outflow million m3/year	Inflow million m3/year	Outflow million m3/year	Inflow million m3/year	Outflow million m3/year
1	Flow Montana	1.433	-0.080	1.537	-0.080	0.104	0.000
2	River flux	1.936	-99.807	1.936	-99.943	0.000	-0.136
2a	Red Deer River	0.000	-12.157	0.000	-12.152	0.000	0.005
2b	Bow River	0.006	-7.109	0.006	-7.133	0.000	-0.024
2c	Belly River	0.966	-2.423	0.966	-2.423	0.000	0.000
2d	Old Man River	0.147	-15.314	0.147	-15.313	0.000	0.001
2e	Saskatchewan River	0.005	-9.513	0.005	-9.828	0.000	-0.315
2f	Milk River	0.812	-0.820	0.813	-0.799	0.000	0.020
2g	Rest (minor streams)	0.000	-52.472	0.000	-52.295	0.000	0.177
3	Lakes	9.180	-6.652	9.215	-6.664	0.034	-0.012
4	Wells	0.000	0.000	0.000	0.000	0.000	0.000
5	Recharge	94.290	0.000	94.290	0.000	0.000	0.000
							0.000
6	Flow from Pakowki	2.447	-2.981	4.093	-4.756	1.647	-1.775
7	Flow from Colorado	0.354	-0.355	0.533	-0.532	0.178	-0.178
	Total (1+2+3+4+5)	106.840	-106.540	106.978	-106.687	0.138	-0.147
	Error		0.300		0.291		-0.009

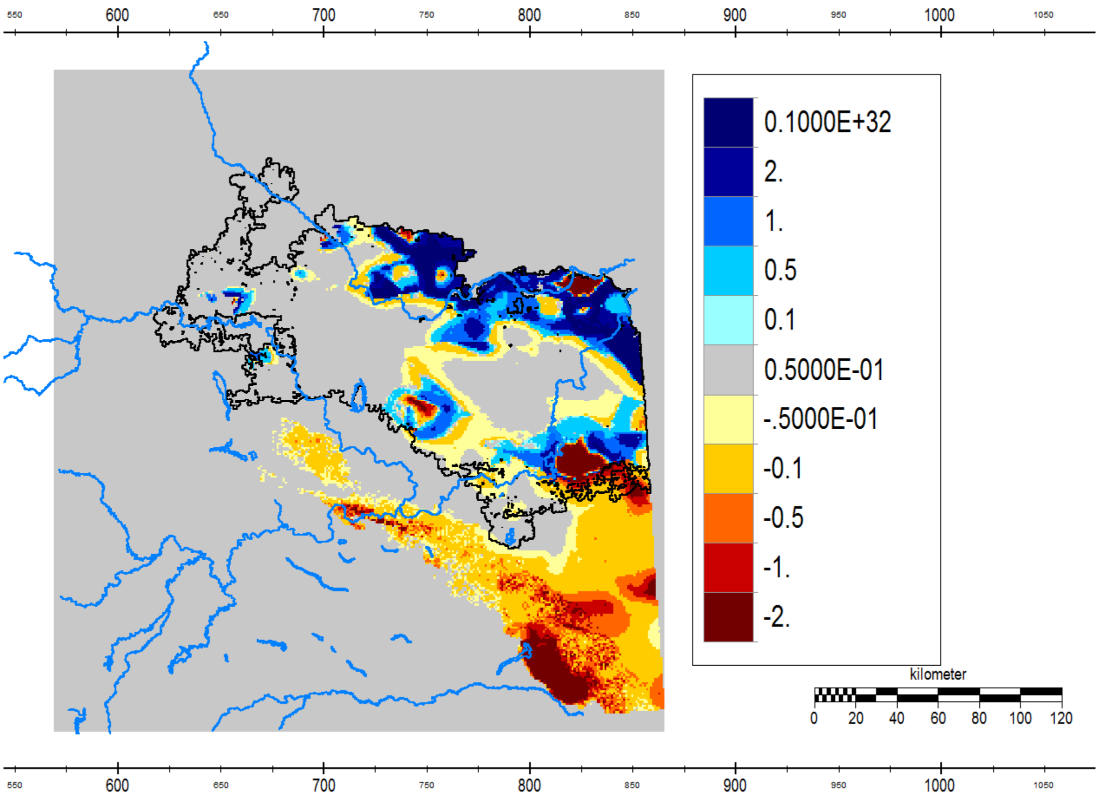

Figure 6.24 Difference in transmissivity values (in m^2/day) in Simulation 8 compared to Simulation 9. Black outline indicates the Alderson gas zone.

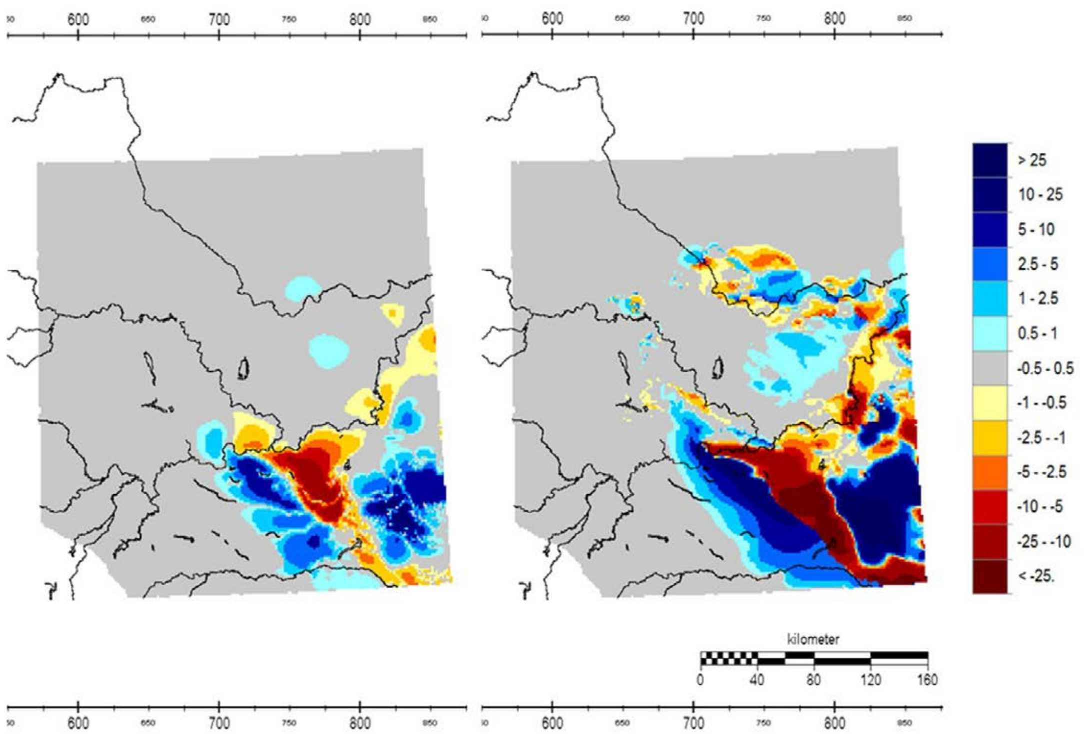

Figure 6.25 Computed difference between Simulation 8 and Simulation 9 for (left) the groundwater level and (right) the pressure head directly underneath the Pakowki Formation, all in meters of difference.

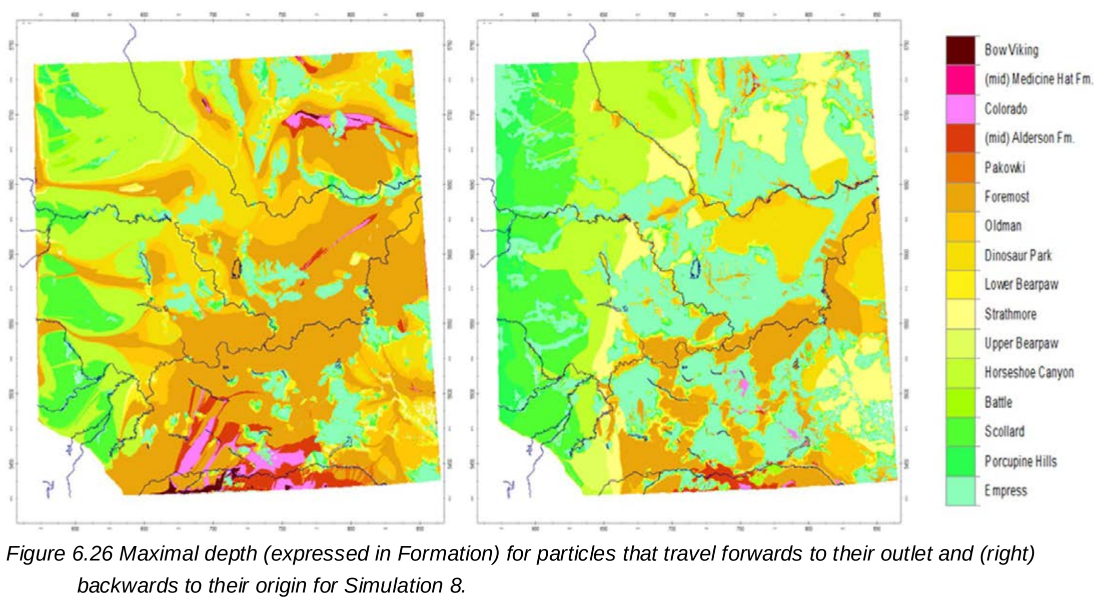

Figure 6.26 Maximal depth (expressed in Formation) for particles that travel forwards to their outlet and (right) backwards to their origin for Simulation 8.

6.3 Phase 4 Two phase modelling

6.3.1 Simulation 15

6.3.2 Simulation 15

Simulation 15 represents the 201 layer model with the well-log derived permeability values for the Milk River / Alderson Formations and for the Medicine Hat Formation. Since this model forms the basis for the scenario simulations 10-14, this scenario is discussed first. The subsequent scenario simulations will be compared to the results of this model.
In this simulation the property model as used in simulation 9 in iMOD is implemented in STOMP.

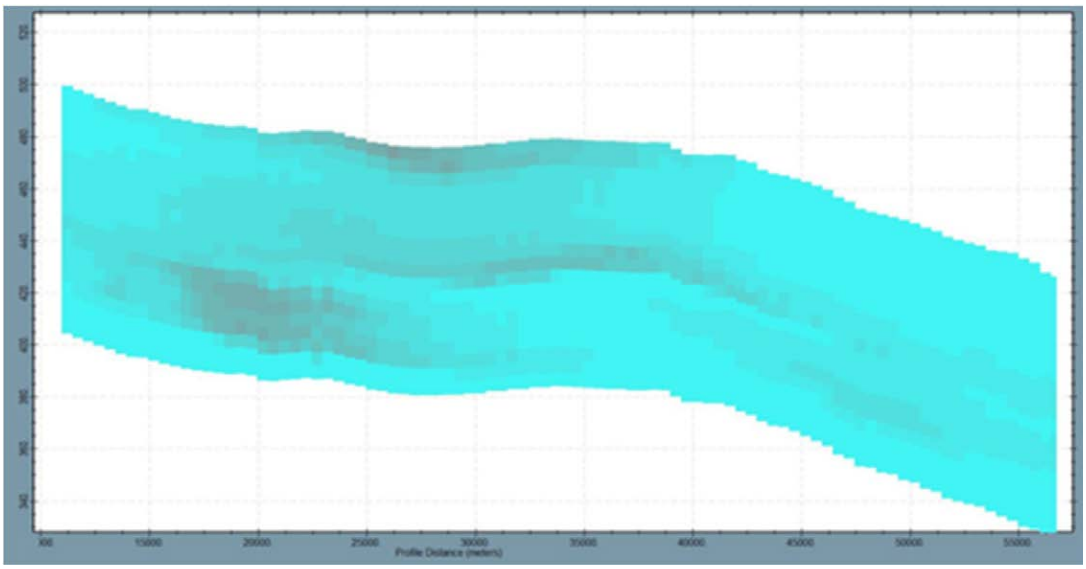

Figure 6.27 we see that the gas saturation is spread through the reservoir and are around 0.1. The highest saturations are in the zones with the highest permeabilities: the gas pressure spreads the gas according to the permeability. After 1 year

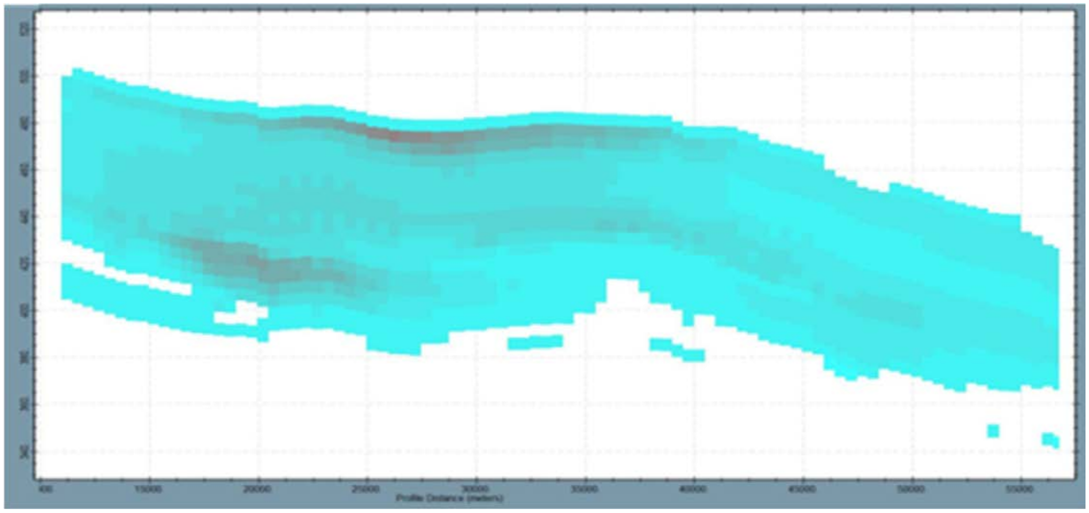

Figure 6.28 the gas moves vertically towards the Pakowki. The saturation in the upper sand layers increases until the saturation becomes 0.3125. After 50 years

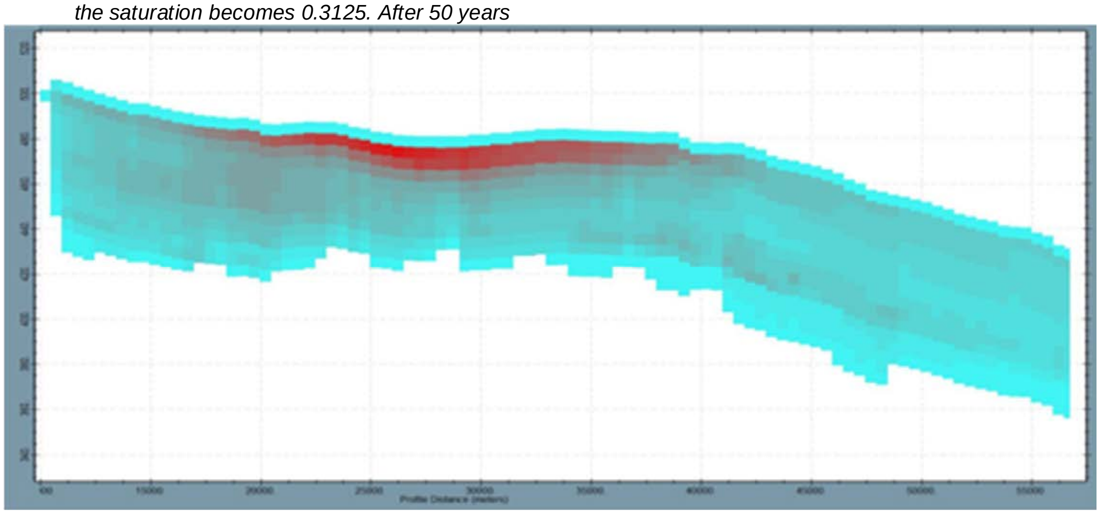

Figure 6.29 *the gas moves laterally to the south site outside the gas reservoir.*

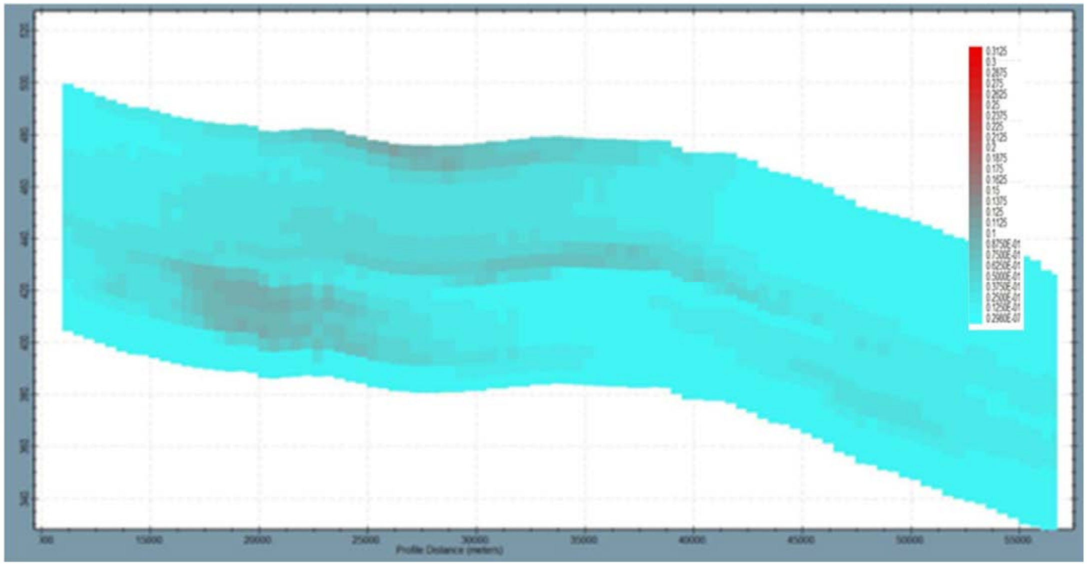

Figure 6.27 Simulation 15 at t=0.

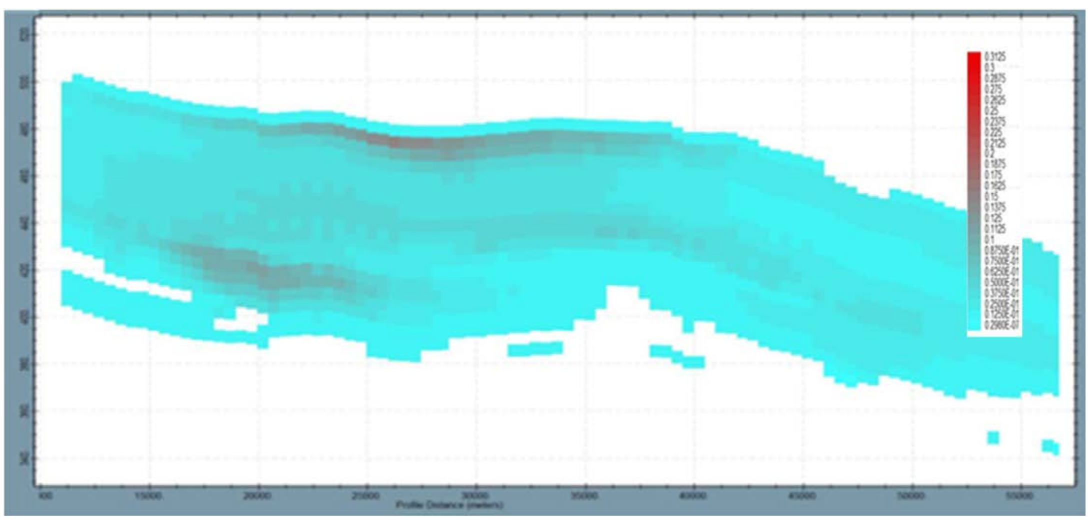

Figure 6.28 Simulation 15 at t=1 year.

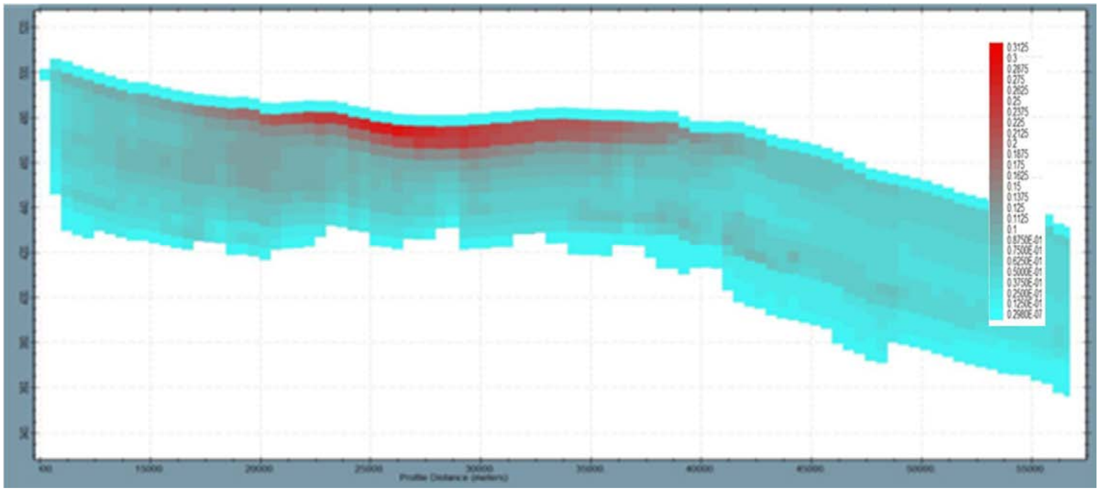

Figure 6.29 Simulation 15 at t=50 years.

6.3.3 Simulation 10

In this simulation we see at T=0 (Figure 6.30) a different distribution of the gas compared to simulation 15: the gas is mainly present in the cells with the sand permeabilities (40%) at a saturation of approximately 0.15. The part of the reservoir with shale permeability has gas saturation of nearly 0. At t=3 year (Figure 6.31), the gas has moved significantly in the vertical direction: the gas saturation in the top of the sand bodies has become 0.3125, while the bottom has become approximately 0.

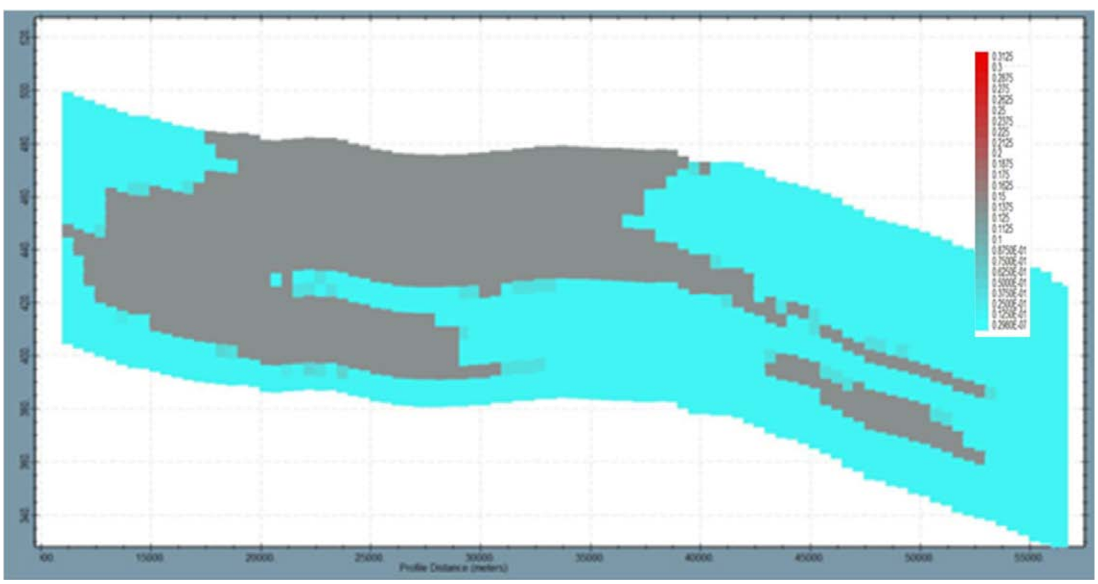

Figure 6.30 Simulation 10 at T=0

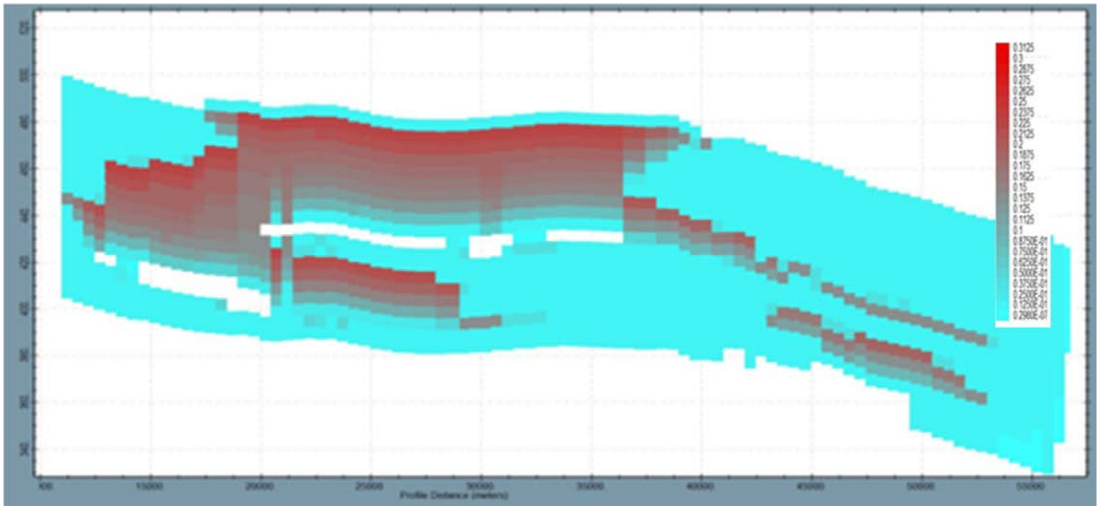

Figure 6.31 Simulation 10 at T=3 year.

6.3.4 Simulation 11

Simulation 11 shows at T=0 (Figure 6.32) the same distribution as simulation 10 since the division between sand and shale is the same. Before t=1 year (t=3 months, Figure 6.33), we see some vertical migration of the gas within the gas reservoir and at the south side of the model gas is moving towards the gas reservoir. The vertical migration is very small compared to simulation 10 because of the difference in the seal's strength.

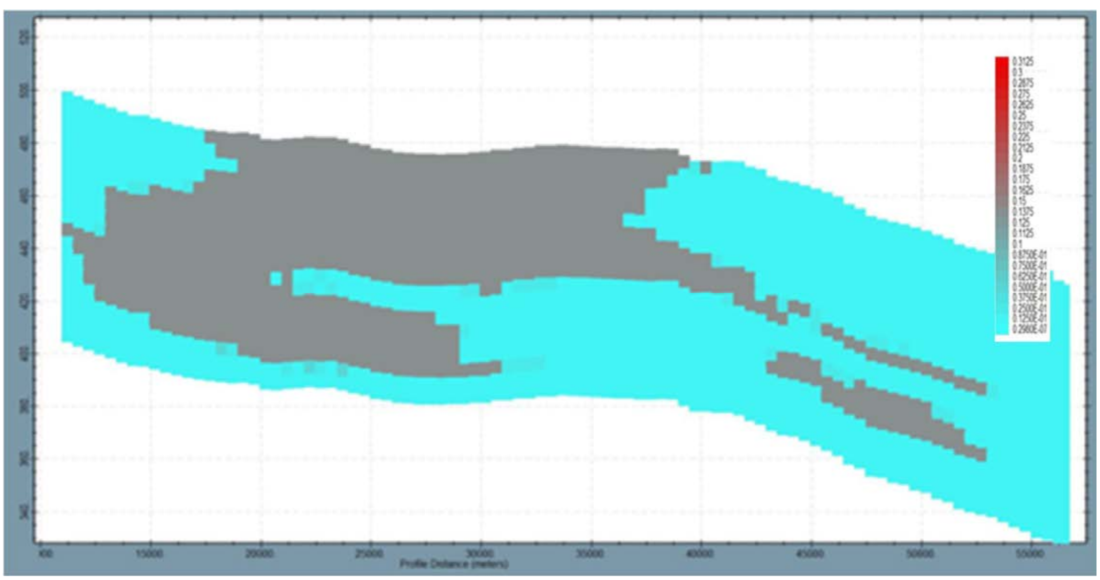

Figure 6.32 Simulation 11 at t=0.

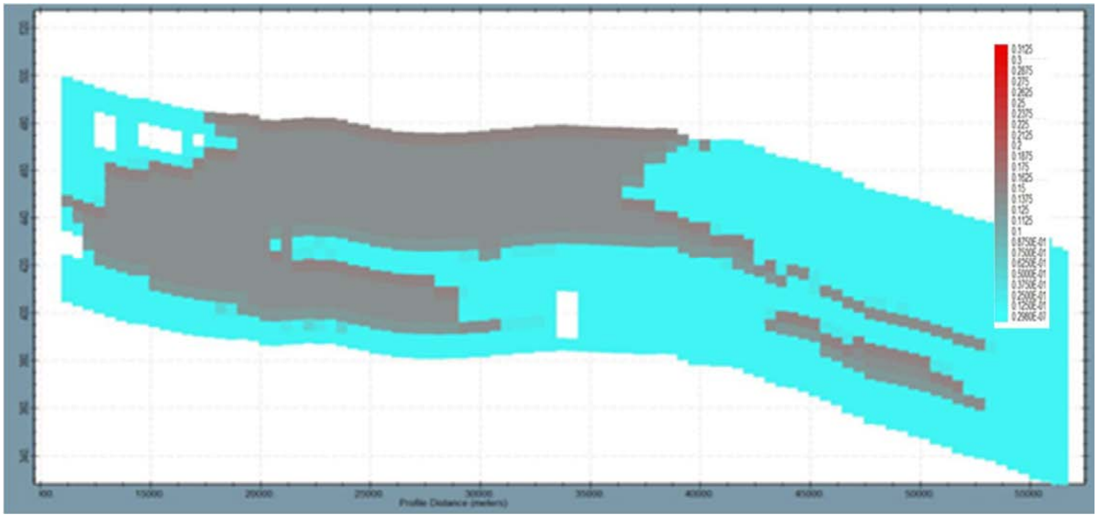

Figure 6.33 Simulation 11 at t=3 months

6.3.5 Simulation 12

Simulation 12 uses a permeability division of 20% sand and 80% shale. The gas saturation is mainly present in the cells with sand permeability at a saturation of approximately 0.15. Anywhere else the gas saturation is very low. There is some vertical migration within the sand formations. After 1 year (Figure 6.35), the saturation becomes approximately 0.2. At the north side the gas moves vertically and at the bottom of the reservoir, the saturation becomes 0. After 4 years there is no gas present at the north side. At t=500 years, the gas is mainly in the top layers of the sand formations (Figure 6.36).

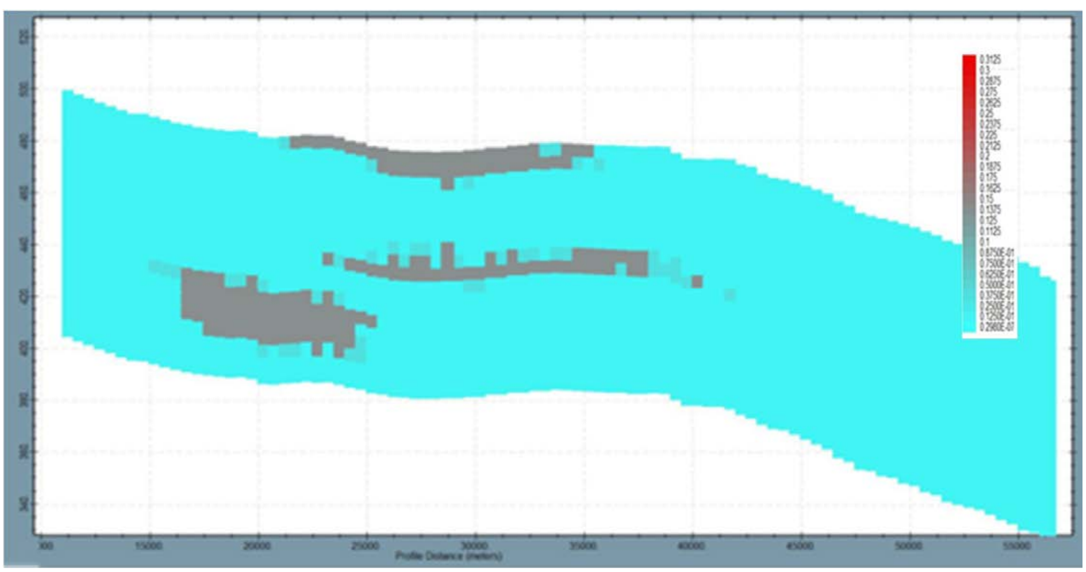

Figure 6.34 Simulation 12 at t=0.

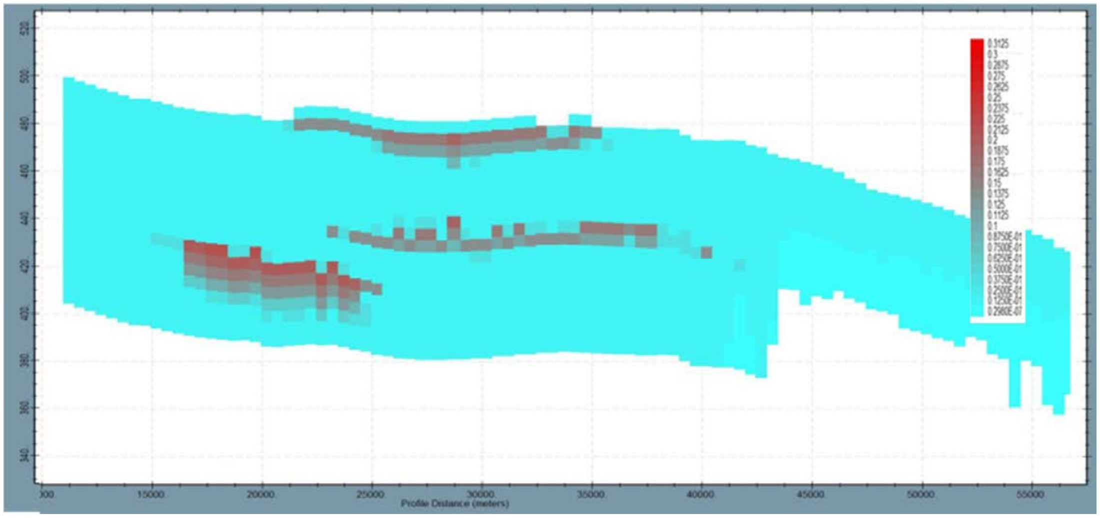

Figure 6.35 Simulation 12 at t=1 year

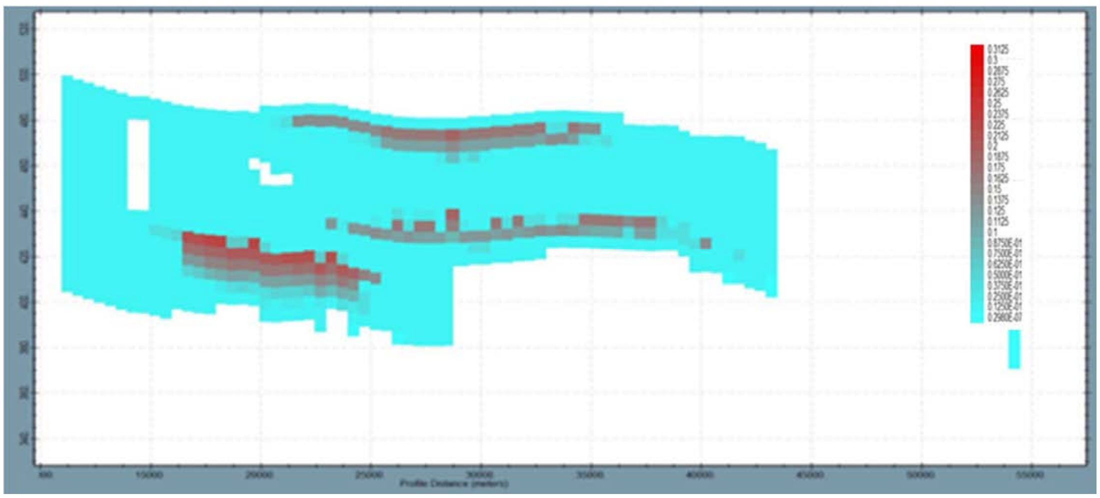

Figure 6.36 Simulation 12 at t=500 years.

6.3.6 Simulation 13

Simulation 13 has the same gas distribution as simulation 12 (20% sand and 80% shale) at t=0 (Figure 6.37). The gas moves vertically within the sand formations until a gas saturation of approximately 0.25 is reached after 28 years (Figure 6.38).

Just like simulation 12, the gas is mainly present in the 20% where sand formations are in this simulation.

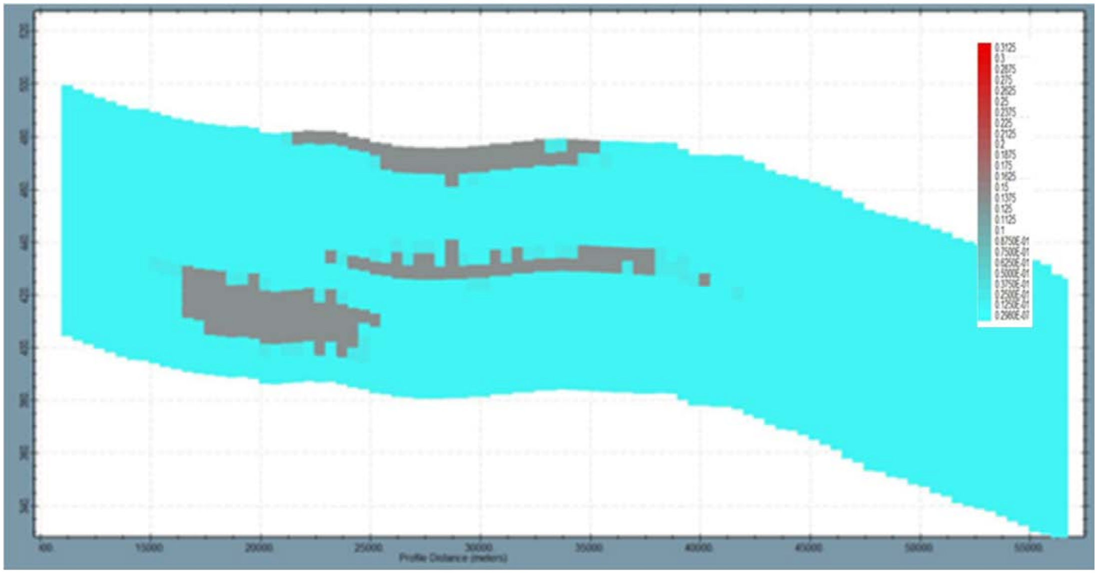

Figure 6.37 Simulation 13 at t=0.

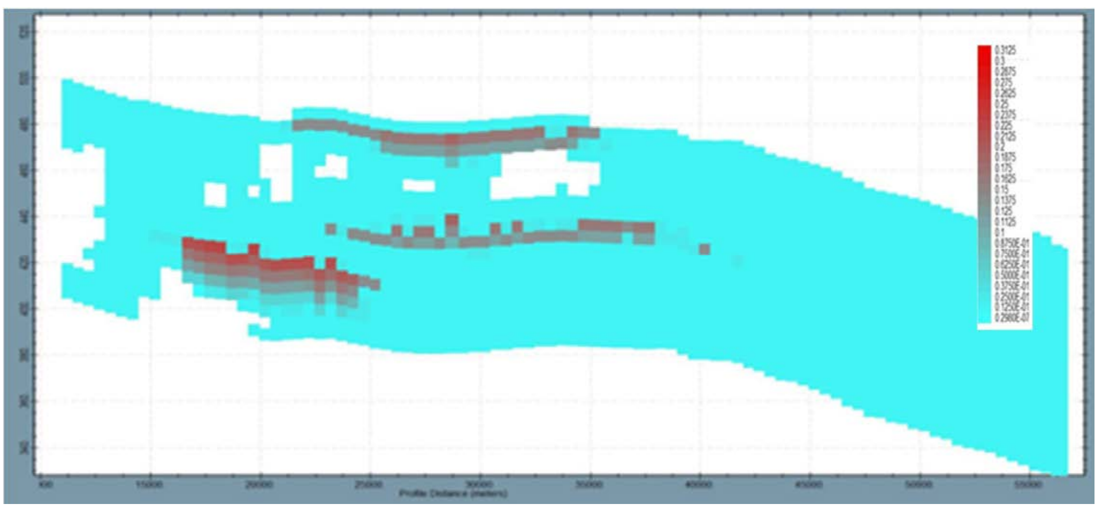

Figure 6.38 Simulation 13 at t=28 years.

6.3.7 Simulation 14

Just like simulation 12 and 13, simulation 14 has initially at t=0 (Figure *6.39*) gas in the sand formation (20% sand). After 18 years (Figure 6.40) the gas has moved vertically within the sand formations and the gas is mainly present at the top of the sand formations.

At the time frame for approximately 20 years, there is not much difference in gas distribution between simulation 12, 13 and 14.

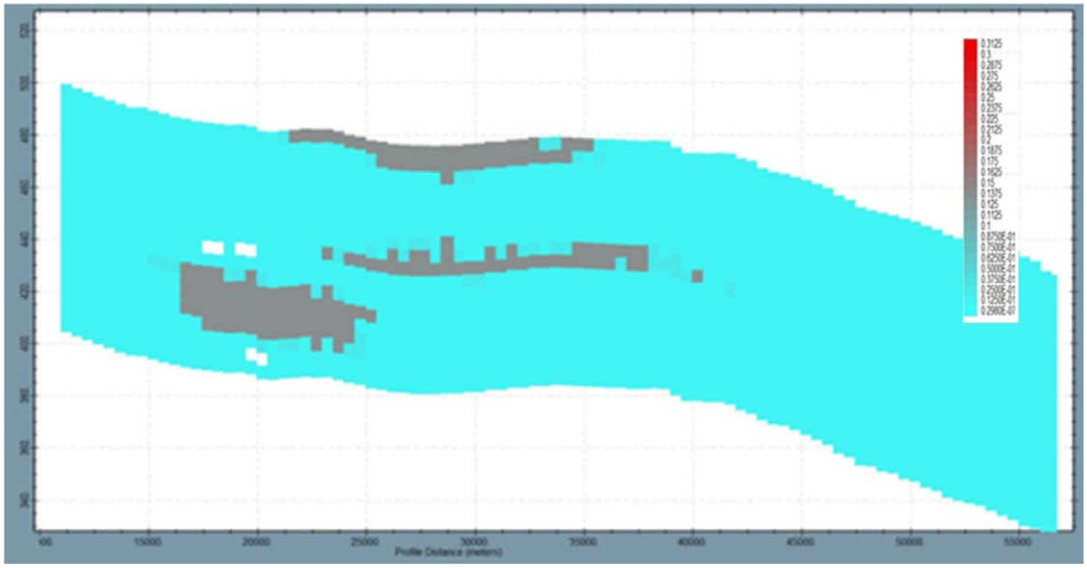

Figure 6.39 Simulation 14 at t=0

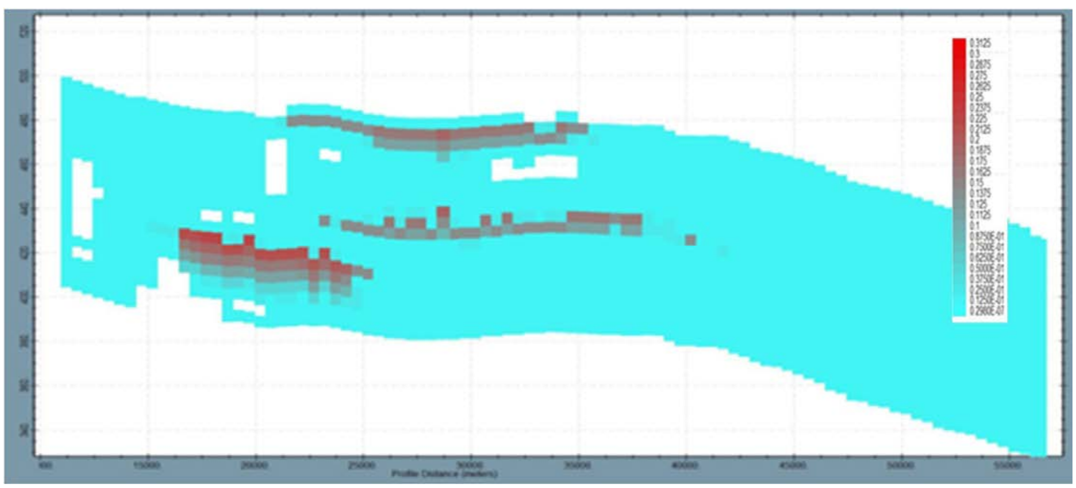

Figure 6.40 Simulation 14 at t=18 years.

7 Discussion

7.1 General

The simulations performed in Phase 1 show a large-scale gravity driven groundwater system. Recharge of the system is minimal and the total transmissivity is generally low. Inflow of 9 million m^3/year from Montana as estimated by Pétré (2016) is hard to realize with the schematized relatively low permeability in the Milk River Formation. The current model generates an inflow of 2 million m^3/year.

7.2 Phase I

A small general decrease in permeabilities in the subsoil in Simulation 2 compared to Simulation 1 and its large effect on hydraulic head and groundwater level (Figure 6.3) shows the extremely high sensitivity of the hydrogeological system to permeability. On the other hand, reducing permeabilities within the Alderson gas zone to zero (Simulation 3) only has a minor effect on groundwater levels and hydraulic heads. The is twofold, on the one hand the Pakowki Formation blocks almost any influence from underneath to the phreatic level, and secondly it suggests that this part of the Alderson system in the already low permeable gas zone is relatively insensitive to changes in permeability. Setting up the model also showed the high sensitivity to minor differences in recharge. The model runs performed show a realistic groundwater flow system in which the permeabilities and recharge are in relative balance, but the extreme sensitivity to these parameters should be kept in mind.

7.3 Phase II

The simulations performed in Phase 2 show that each Building Block has its typical signature to the hydrogeological system. These changes are mostly limited to the boundary zone and gas zone. The schematisation of the sand and shale voxels shows that there are distinct areas with higher permeabilities in the property model, and therefore in the conceptual model scenarios. These areas are concentrated along the edges of the gas zone in the eastern part of the Albertan gas zone. The more permeable northern edge and southern edge are almost disconnected by the low permeability centre. This configuration may have an effect on gas distribution and potential future gas migration.

The property model of Simulation 9 shows the highest transmissivity values in the Alderson Formation in the Northeast of the model domain. The largest part of this domain is not part of the commingled Alderson gas zone. Furthermore, the model shows relatively high transmissivities in the southeastern part of the boundary zone. By introducing an Alderson boundary zone consisting entirely of shale (e.g. Simulation 5 and 8), this part of the groundwater flow system is mostly affected. It causes less inflow into the Alderson Formation. In addition, the groundwater is retained on the southern border of the boundary zone. All other configurations of the boundary zone with a gradual decrease in permeability values towards the north appear to have a minor effect on the groundwater flow in the Alderson gas zone. This leads to the question if this schematisation really results in a hydraulically connected reservoir as initially planned.

7.4 Phase IV

The two phase flow simulations show that in simulation 10 to 14 the gas concentrates in the sand bodies, with an increasing gas saturation towards the top of these bodies. Hence, In these conceptual model scenarios, it is possible to simulate discovery conditions of the gas reservoir. In simulation 12, 13 and 14 with the disconnected sand bodies, the maximum gas saturation(0.18) is less relative to the maximum gas saturation in simulation 10 and 11 (0.22), because less gas pressure is build up towards the top.

No lateral southward migration of gas is simulated in simulation 10 to 14. This suggests that not enough gas pressures is built up to overcome the capillary forces in the boundary zone, also not in situations with a weak seal, at least not in the time range modelled.

In Simulation 15, most of the gas migrates towards the top and lateral migration into the boundary zone in the south is present. Hence, it is impossible to simulate the discovery conditions of the Alderson gas reservoir in the property model based on well-logs. A reason for this could be that the property model contains average permeability over 2m intervals derived from well logs. It could well be that thin layers of tight mudstone or diagenetic planes that could play a role in gas capture are not taken into account when using this method. Also, the derivation of permeabilities could have a systemetic error towards too high values.

The effect of groundwater flow on the gas migrationis not observed in the simulations so far. This could be the result of the schematisation of the hydraulically connected boundary zone. In the simulations, the different scenarios gave similar results for the groundwater flow. A boundary zone with higher permeabilities would probably enable the investigation of the effects of the possible hydraulic connectivity better.

The comparison between the simulations remains difficult in this stage, because not all scenarios have finished the preferred simulation time of 500 years. The results so far give confidence that the discovery conditions can be simulated well with the scenarios.

8 Conclusions

The specific questions are:

1. *Can a regional gravity-driven groundwater flow system as conceptualized be generated in the model domain, given our hydrostratigraphy and choices of boundaries when no natural gas deposits are included in the system? What is the effect of groundwater pumping?*

   Yes, such a gravity driven groundwater flow system can be generated. It has to be kept in mind that this system is highly sensitive to the balance between recharge and permeability. A small change in one of these variables leads to large changes in the groundwater flow system.
   The effect of groundwater pumping is not yet investigated in this stage. It will be investigated in Phase 3 which is skipped, as it forms the basis of Phase 6 and 8.

2. *If the Alderson Member gas-zone is replaced by a simple aquiclude in 1, does the gravity-flow system match observed patterns of regional gravity-driven groundwater flow in southern Alberta as conceptualized in the companion report?*

   The introduction of an impermeable gas zone (Simulation 3) does not lead to large differences in the regional hydrogeology. The modelled differences are too small to be used for comparison to observed patterns in the conceptual model. In Phase 2, the simulations do show notable differences when the permeability voxels in the property model are replaced by sand and shale. These differences are however mainly related to the replacement of voxels by sand, and not by the replacement by low permeability shale. This suggests a low dependency to of the groundwater flow to lowering the permeabilities in the Alderson as-zone.

3. *If the Alderson Member is parameterized as conceptualized under each alternative model described in the companion report, can it trap natural gas under pre-development conditions?*

   The parameterized sand bodies in the Alderson gas zone do appear to trap natural gas. The gas saturation at the top of these sand bodies is up to 31% when a buoyancy pressure of 96kPA (equivalent to a gas column of 10m) is introduced. If the higher buoyancy pressures are applied, the gas saturation may be higher.

4. *If the Alderson Member is parameterized as conceptualized under each alternative model, can it still trap natural gas under conditions where the underlying Medicine Hat Member gas zone is left permanently commingled with the Alderson Member after the two gas zones are commercially exhausted?*

   The effect of commingling will be investigated in a later stage. In this Phase 5, the results form Phase 4 containing equilibrium two-phase flow models with gas included, will be perturbed by higher pressures representing the commingled gas wells.

5. *If 4 is true, will gas leak out of the Alderson Member by diffusion?*

   Also this effect of diffusion will be investigated in a later stage (Phase 7 and 8).

6. *Will groundwater pumping in the Milk River Aquifer (Virgelle Member) cause natural gas to pass through capillary seals that could otherwise trap natural gas under 4?*

   The effect of groundwater pumping on the seal integrity will be investigated in a later stage, Phase 6.

7. *Will groundwater pumping in the Milk River Aquifer (Virgelle Member) affect trap leakage by diffusion?*

   The effect of groundwater pumping on the seal integrity in combination with diffusion will be investigated in a later stage, Phase 8.

8. *If natural gas leaked out through seals in a separate phase due to buoyant forces or pumping-related reduction in capillary forces, would it go into the Milk River Aquifer (Virgelle Member) or elsewhere? Does groundwater pumping affect this?*

   The effect of groundwater pumping on the seal integrity in combination with diffusion will be investigated in a later stage, Phase 8.

9. *If natural gas leaked through seals by diffusion instead would it go into the Milk River Aquifer (Virgelle Member) or elsewhere? Does groundwater pumping affect this?*

   The effect of groundwater pumping on the seal integrity in combination with diffusion will be investigated in a later stage, Phase 8.

9 References

Barnett et al, 2012, *Australian groundwater modelling guidelines*, Waterlines report, National Water Commission, Canberra.

McDonald, M. and A. Harbaugh, 1988. A modular three-dimensional finite-difference ground-water flow model: Techniques of Water-Resources Investigations of the United States Geological Survey. Tech. rep., USGS.

Dobson and Houseworth, 2014. Inventory of Shale Formations in the US, Including Geologic, Geochemical, Hydrological, Mechanical, and Thermal Characteristics. Fual cycle research and development. Lawrence Berkeley National Laboratory, September, 2014. FCRD-UFD-2014-000512

Kaluarachchi, J.J. and Parker, J.C. (1992) Multiphase flow with a simplified model for oilentrapment. Transport in Porous Media 7, 1-14.

Lenhard, R.J. and Parker, J.C. (1987) Measurement and prediction of saturation-pressure relationships in three-phase porous media. J. Contam. Hydrol. 1, 407-424.

Lenhard, R.J., Oostrom, M., White, M.D. (1995) Modeling fluid flow and transport in variably saturated porous media with the STOMP simulator. 2. Verification and validation exercises.Adv. Water Resources 18(6), 365-373.

Marsman, A. (2002) The influence of water pollution on the flow of light non aqueous phase liquids in soil. Phd Thesis Wageningen University, ISBN 90-5808-734-4.

Mualem, Y. (1976) A new model for predicting the hydraulic conductivity of unsaturated porous media. Water Resources Research 12: 513–522. doi:10.1029/WR012i003p00513.

Parker, J.C. and Lenhard, R.J. (1987) A model for hysteretic constitutive relations governing multiphase flow. 1. Saturation pressure relations. Water Resour. Res. 23, 2187-2196.

Pétré, M., A., 2016. Étude hydrogéologique de l'aquifère transfrontalier Milk River (Canada): modèles géologique, conceptuel et numérique pour la gestion raisonnée de la resource. Thèse. Quebec, Université du Quebec, Institut national de la recherche sicentifique, Doctorat en sciences de la terre.

Pétré, M., A. Rivera, and R. Lefèbvre, 2015. Three-dimensional unified geological model of the Milk River Transboundary Aquifer (Alberta, Canada – Montana, USA); Canadian Journal of Earth Sciences, v. 52, p. 96–111 dx.doi.org/10.1139/cjes-2014-0079

Van Genuchten, M.T. (1980) A closed form equation for predicting the hydraulic conductivity of unsaturated soils. Soil. Sci. Soc. Am. J. 44, 892-898.

Vermeulen, P.T.M, L.M.T. Burgering, F.J. Roelofsen and B. Minnema, J. Verkaik, 2017. *iMOD user manual*. version 4.0, July 2017. Deltares, The Netherlands. (http://oss.deltares.nl/web/iMOD).

White, M.D., Oostrom, M., Lenhard, R. J. (1995) Modeling fluid flow and transport in variably saturated porous media with the STOMP simulator. 1. Non-volatile three-phase model description. Adv. Water Resources 18, 53-77.

Appendix A: simulation overview

Phase	Simulation	Parameters	Recipe for Parameterization	Intention, Purpose or Test
	Basic	recharge (USA+direct)		water balance, flow directions, output at poc's
Single Phase, Steady State Modeling with Particles	Simulation 1	Simplest Layer Model:	Assign single values of K from literature reports to each layer.	Replicate gravity flow system, get reasonable water balances and flow directions at steady state without gas field.
	Simulation 2	Simplest Voxel Model	Assign single values of K from literature reports to each voxel.	Replace layers above with voxels and get a stable model running.
	Simulation 3	Simplest Voxel Model with Impermeable Gas Field	Turn all the Alderson voxels in the gas zone to no-flow cells (K=0).	Add the presence of gas field in Alderson. Do comparative analysis of location of recharge, discharge, head values, flow directions, travel times, water balance, from model to observations and literature. Calibrate layer K, boundary conditions+ accordingly. Validate that we can replace lowermost layers below the Medicine Hat with GHB or make inactive with. Compare this to the GSC results and explain any divergences.
	Simulation 4	Conceptual Model 010; Connected reservoir, strong seals, Alderson sst persists to north.	1. Parameterize voxels lying immediately above Telgraph Creek top as well as the Alderson A, B, and C tops as shale everywhere as shale. Parameterize the k and n of shale to be such that they can hold back very long columns as suggested by Corcoran and Dore (2002) Figure 3. 2. In the gas zone, parameterize Alderson voxels as a binary system of either "sandstone" or "shale". Assign the voxel class by Vsh value, tuning Vsh to be such that sandstone voxels represent at least 40% of the Alderson voxels in the gas zone. Parameterize the k and n of shale to be such that they can only hold back very short columns, less than 10 m as suggested by Chen et al.(2015). Parameterize sandstone voxels with values from Simulation 3. Verify that the assigned sandstone voxels line up with the short perforated intervals in the field.	Test if a 010 Parameterization can still replicate the observed flow patterns seen in 3. If so, retain for mutlimodel ensemble. If not, remove and document.
	Simulation 5	Conceptual Model 011: Connected reservoir, strong seals, Alderson sst localized to south.	1. In the boundary zone, parameterize Alderson voxels as a binary system of either "sandstone" or "shale". Using the voxel model, find the highest value of voxel Vsh (i.e., the least sandy) that creates a continuous and unbroken 3D boundary in the zone between the north edge of the Alderson sand and the south boundary of the gas field. Any voxel with this value of Vsh or higher will be a shale in this boundary zone. Set the values of k and n for shale to be strong seals. 2.In the gas zone, parameterize Alderson voxels as a binary system of either "sandstone" or "shale". Assign the voxel class by Vsh value, tuning Vsh to be such that sandstone voxels represent at least 40% of the Alderson voxels in the gas zone. Parameterize the k and n of shale to be such that they can only hold back very short columns, less than 10 m as suggested by Chen et al. (2015). Parameterize sandstone voxels with values from Simulation 3. Verify that the assigned sandstone voxels line up with the short perforated intervals in the field.	Test if a 011 Parameterization can still replicate the observed flow patterns. If so, retain for mutlimodel ensemble. If not, remove and document.
	Simulation 6	Conceptual Model 100: Disconnected reservoir, weak seals, Alderson sst persists north.	1. In the boundary zone, parameterize the Alderson voxels as a binary system of either "sandstone or shale". Assign the voxel class by Vsh value, tuning Vsh cutoff to be such that sandstone voxels represent at least 40% of the voxels in the boundary zone. Parameterize the k and n of the shale voxels to be weak seals and parameterize k of sandstone voxels as per Simulation 3. 2. In the gas zone, parameterize Alderson voxels as a binary system of either "sandstone" or "shale". Assign the voxel class by Vsh value, tuning Vsh to be such that shale voxels represent at least 70% of the Alderson voxels. Parameterize the k and n of shale to be such that they can only hold back very short columns, less than 10 m as suggested by Chen et al. (2015). Parameterize sandstone voxels with values from Simulation 3. Verify that the assigned sandstone voxels line up with the short perforated intervals in the field.	Test if a 100 Parameterization can still replicate the observed flow patterns seen in 3. If so, retain for mutlimodel ensemble. If not, remove and document.
	Simulation 7	Conceptual Model 110: Disconnected reservoir, strong seals , Alderson sst persists north.	1. In the boundary zone, parameterize the Alderson voxels as a binary system of either "sandstone or shale". Assign the voxel class by Vsh value, tuning Vsh cutoff to be such that sandstone voxels represent at least 40% of the voxels in the boundary zone. Parameterize the k and n of the shale voxels to be weak seals and parameterize k of sandstone voxels as per Simulation 3. 2. In the gas zone, parameterize Alderson voxels as a binary system of either "sandstone" or "shale". Assign the voxel class by Vsh value, tuning Vsh cutoff to be such that shale voxels represent at least 70% of the Alderson voxels. Parameterize the k and n of shale to be such that they can hold back very long columns as suggested by Corcoran and Dore (2002) Figure 3. Parameterize sandstone voxels with values from Simulation 3. Inspect that the sandstone voxels line up with the short perforated intervals in the field.	Test if a 110 Parameterization can still replicate the observed flow patterns seen in 3. If so, retain for mutlimodel ensemble. If not, remove and document.
	Simulation 8	Conceptual Model 111: Disconnected reservoir, strong seals, Alderson sst restricted to south.	Parameterize all Alderson voxels in the boundary zone and the gas zone as a binary system of either "sandstone" or "shale". Assign the voxel class by Vsh value, tuning Vsh cutoff to be such that shale voxels represent at least 70% of the Alderson voxels. Parameterize the k and n of shale to be such that they can hold back very long columns as suggested by Corcoran and Dore (2002) Figure 3. Parameterize sandstone voxels with values from Simulation 3. Inspect that the sandstone voxels line up with the short perforated intervals in the field.	Test if a 111 Parameterization can still replicate the observed flow patterns seen in 3. If so, retain for mutlimodel ensemble. If not, remove and document.
	Simulation 9	AGS Distributed Property Geomodel	Use log-derived voxel properties in the AGS geomodel directly.	Test if a data-driven model can still replicate the observed flow patterns seen in 3. If so, retain for mutlimodel ensemble. If not, remove and document.

Two Phase STOMP model: discovery conditions	Simulation 10	Conceptual Model 010; Connected reservoir, strong seals, Alderson sst persists to north.	Parameters for 2-phase flow appropriate to conceptual model as per voxels that are "sandstone" versus "shale".	Test if the modeled geosystem traps gas in the Alderson gas-field zone under natural hydrogeological conditions.
	Simulation 11	Conceptual Model 011: Connected reservoir, strong seals, Alderson sst localized to south.	Parameters for 2-phase flow appropriate to conceptual model as per voxels that are "sandstone" versus "shale".	Test if the modeled geosystem traps gas in the Alderson gas-field zone under natural hydrogeological conditions.
	Simulation 12	Conceptual Model 100: Disconnected reservoir, weak seals, Alderson sst persists north.	Parameters for 2-phase flow appropriate to conceptual model as per voxels that are "sandstone" versus "shale".	Test if the modeled geosystem traps gas in the Alderson gas-field zone under natural hydrogeological conditions.
	Simulation 13	Conceptual Model 110: Disconnected reservoir, strong seals , Alderson sst persists north.	Parameters for 2-phase flow appropriate to conceptual model as per voxels that are "sandstone" versus "shale".	Test if the modeled geosystem traps gas in the Alderson gas-field zone under natural hydrogeological conditions.
	Simulation 14	Conceptual Model 111: Disconnected reservoir, strong seals, Alderson sst restricted to south.	Parameters for 2-phase flow appropriate to conceptual model as per voxels that are "sandstone" versus "shale".	Test if the modeled geosystem traps gas in the Alderson gas-field zone under natural hydrogeological conditions.
	Simulation 15	AGS Distributed Property Geomodel	Parameters for 2-phase flow appropriate to conceptual model as per voxels that are "sandstone" versus "shale".	Test if the modeled geosystem traps gas in the Alderson gas-field zone under natural hydrogeological conditions.
Two Phase STOMP model: closure conditions, commingled abandonments	Simulation 16	Conceptual Model 010; Connected reservoir, strong seals, Alderson sst persists to north.	Add source term or fix Alderson pressures to replicate the expected equilibrium conditions with commingled abandonments linking Alderson gas zone with residual natural gas pressures in the Medicine Hat zone(s).	Test if the modeled geosystem traps gas in the Alderson+Medicine Hat residual gas under natural hydrogeological conditions.
	Simulation 17	Conceptual Model 011: Connected reservoir, strong seals, Alderson sst localized to south.	Add source term or fix Alderson pressures to replicate the expected equilibrium conditions with commingled abandonments linking Alderson gas zone with residual natural gas pressures in the Medicine Hat zone(s).	Test if the modeled geosystem traps gas in the Alderson+Medicine Hat residual gas under natural hydrogeological conditions.
	Simulation 18	Conceptual Model 100: Disconnected reservoir, weak seals, Alderson sst persists north.	Add source term or fix Alderson pressures to replicate the expected equilibrium conditions with commingled abandonments linking Alderson gas zone with residual natural gas pressures in the Medicine Hat zone(s).	Test if the modeled geosystem traps gas in the Alderson+Medicine Hat residual gas under natural hydrogeological conditions.
	Simulation 19	Conceptual Model 110: Disconnected reservoir, strong seals , Alderson sst persists north.	Add source term or fix Alderson pressures to replicate the expected equilibrium conditions with commingled abandonments linking Alderson gas zone with residual natural gas pressures in the Medicine Hat zone(s).	Test if the modeled geosystem traps gas in the Alderson+Medicine Hat residual gas under natural hydrogeological conditions.
	Simulation 20	Conceptual Model 111: Disconnected reservoir, strong seals, Alderson sst restricted to south.	Add source term or fix Alderson pressures to replicate the expected equilibrium conditions with commingled abandonments linking Alderson gas zone with residual natural gas pressures in the Medicine Hat zone(s).	Test if the modeled geosystem traps gas in the Alderson+Medicine Hat residual gas under natural hydrogeological conditions.
	Simulation 21	AGS Distributed Property Geomodel	Add source term or fix Alderson pressures to replicate the expected equilibrium conditions with commingled abandonments linking Alderson gas zone with residual natural gas pressures in the Medicine Hat zone(s).	Test if the modeled geosystem traps gas in the Alderson+Medicine Hat residual gas under natural hydrogeological conditions.
Two Phase STOMP model: closure conditions, commingled abandonments, diffusion	Simulation 22	Conceptual Model 010; Connected reservoir, strong seals, Alderson sst persists to north.	Add diffusion processes to see if diffusion causes release of methane mass in solution with or without capillary entrapment.	If the geosystem can trap gas under closure conditions, natural gradients, test if diffusion is an important mechanism of leakage.
	Simulation 23	Conceptual Model 011: Connected reservoir, strong seals, Alderson sst localized to south.	Add diffusion processes to see if diffusion causes release of methane mass in solution with or without capillary entrapment.	If the geosystem can trap gas under closure conditions, natural gradients, test if diffusion is an important mechanism of leakage.
	Simulation 24	Conceptual Model 100: Disconnected reservoir, weak seals, Alderson sst persists north.	Add diffusion processes to see if diffusion causes release of methane mass in solution with or without capillary entrapment.	If the geosystem can trap gas under closure conditions, natural gradients, test if diffusion is an important mechanism of leakage.
	Simulation 25	Conceptual Model 110: Disconnected reservoir, strong seals , Alderson sst persists north.	Add diffusion processes to see if diffusion causes release of methane mass in solution with or without capillary entrapment.	If the geosystem can trap gas under closure conditions, natural gradients, test if diffusion is an important mechanism of leakage.
	Simulation 26	Conceptual Model 111: Disconnected reservoir, strong seals, Alderson sst restricted to south.	Add diffusion processes to see if diffusion causes release of methane mass in solution with or without capillary entrapment.	If the geosystem can trap gas under closure conditions, natural gradients, test if diffusion is an important mechanism of leakage.
	Simulation 27	AGS Distributed Property Geomodel	Add diffusion processes to see if diffusion causes release of methane mass in solution with or without capillary entrapment.	If the geosystem can trap gas under closure conditions, natural gradients, test if diffusion is an important mechanism of leakage.
Two Phase STOMP model or IMOD model: closure conditions, commingled abandonments, diffusion, groundwater pumping	Simulation 28	Conceptual Model 010; Connected reservoir, strong seals, Alderson sst persists to north.	Add Milk River Aquifer pumping.	Test to see if pumping groundwater in the Milk River Aquifer under present day patterns and levels of development change the trap function or diffusive flux.
	Simulation 29	Conceptual Model 011: Connected reservoir, strong seals, Alderson sst localized to south.	Add Milk River Aquifer pumping.	Test to see if pumping groundwater in the Milk River Aquifer under present day patterns and levels of development change the trap function or diffusive flux.
	Simulation 30	Conceptual Model 100: Disconnected reservoir, weak seals, Alderson sst persists north.	Add Milk River Aquifer pumping.	Test to see if pumping groundwater in the Milk River Aquifer under present day patterns and levels of development change the trap function or diffusive flux.
	Simulation 31	Conceptual Model 110: Disconnected reservoir, strong seals , Alderson sst persists north.	Add Milk River Aquifer pumping.	Test to see if pumping groundwater in the Milk River Aquifer under present day patterns and levels of development change the trap function or diffusive flux.
	Simulation 32	Conceptual Model 111: Disconnected reservoir, strong seals, Alderson sst restricted to south.	Add Milk River Aquifer pumping.	Test to see if pumping groundwater in the Milk River Aquifer under present day patterns and levels of development change the trap function or diffusive flux.
	Simulation 33	AGS Distributed Property Geomodel	Add Milk River Aquifer pumping.	Test to see if pumping groundwater in the Milk River Aquifer under present day patterns and levels of development change the trap function or diffusive flux.

Two Phase STOMP model or IMOD model: closure conditions, commingled abandonments, diffusion, groundwater pumping	Simulation 34	Conceptual Model 010; Connected reservoir, strong seals, Alderson sst persists to north.	Add Milk River Aquifer pumping without diffusion.	Test to see if pumping groundwater in the Milk River Aquifer under present day patterns and levels of development change the trap function or diffusive flux.
	Simulation 35	Conceptual Model 011: Connected reservoir, strong seals, Alderson sst localized to south.	Add Milk River Aquifer pumping without diffusion.	Test to see if pumping groundwater in the Milk River Aquifer under present day patterns and levels of development change the trap function or diffusive flux.
	Simulation 36	Conceptual Model 100: Disconnected reservoir, weak seals, Alderson sst persists north.	Add Milk River Aquifer pumping without diffusion.	Test to see if pumping groundwater in the Milk River Aquifer under present day patterns and levels of development change the trap function or diffusive flux.
	Simulation 37	Conceptual Model 110: Disconnected reservoir, strong seals , Alderson sst persists north.	Add Milk River Aquifer pumping without diffusion.	Test to see if pumping groundwater in the Milk River Aquifer under present day patterns and levels of development change the trap function or diffusive flux.
	Simulation 38	Conceptual Model 111: Disconnected reservoir, strong seals, Alderson sst restricted to south.	Add Milk River Aquifer pumping without diffusion.	Test to see if pumping groundwater in the Milk River Aquifer under present day patterns and levels of development change the trap function or diffusive flux.
	Simulation 39	AGS Distributed Property Geomodel	Add Milk River Aquifer pumping without diffusion.	Test to see if pumping groundwater in the Milk River Aquifer under present day patterns and levels of development change the trap function or diffusive flux.

Appendix B: model design and construction

This report follows guidance of best modeling practice as documented in the Australian Groundwater Modeling Guidelines (Barnett et al., 2012). The choice to follow the Australian Modeling Guidelines (hereafter referred to as the Guidelines) is to ensure that this study will be viewed as competent and unbiased, containing credible and reliable information and advice for decision makers at the Alberta Energy Regulator (AER). The sections of the Guidelines most relevant to this simulation plan are sections 4 and 5. How this work addresses each of the guiding principles listed in the Guidelines can be found below.

Guiding Principle 4.1: The size, discretization and the dimensionality of the model domain should be chosen to reflect the modelling objectives, conceptual model and target confidence-level classification.

The extent of the model domain is consistent with the regulatory question being asked. The model covers the area of the AER's Southeast Alberta Management Unit, where questions about the risks to groundwater in the Milk River Formation from widespread abandonment of comingled wells in the Alderson/Medicine Hat gas field have prompted the project's work.
The discretization of the model is based on the data available. In one of the simulations, a simple layer model will be used and the results will be compared with the detailed model.

Guiding Principle 4.2: Spatial discretization of the model domain should be chosen so that it will not lead to excessive model run times that may prevent or hamper the successful development of the model within the available project time frame.

The MODFLOW model will use the smallest discretization possible since the run time of this model is not an obstacle considering the capabilities of iMOD. For the multiphase flow, cross sections (semi 3-D) models (STOMP) will be used to limit the calculation time.

Guiding Principle 4.3: The model grid should provide sufficient refinement to be able to adequately represent the problem geometry, including the layout of proposed developments and the processes of importance.

The refinement of the numerical model grid from the geologic model grid is expected to be minimal. In STOMP we will chose refinement where necessary if gas flow or gas entrapment is expected.

Guiding Principle 4.4: If temporal variation (including periodic fluctuations or long-term trends) is important in either the groundwater stresses to be modelled or the model results being sought, transient simulations are required. Otherwise steady state predictions should be considered.

In the designed conceptual models temporal variation is not an issue so steady state will be used.

Guiding Principle 4.5: Initial conditions in a transient simulation should be obtained, wherever possible, from a previous model run (e.g. a steady state solution) to avoid spurious results at early times in the transient model run.

Does not apply

Guiding Principle 4.6: A model should be constructed according to the design, and documented as built. It is reasonable and sometimes essential for the design and construction to change as more is learned about the system and the way it can be represented.

All the simulations (shown in the simulation overview in Appendix 1) will be documented.

Appendix C: guiding principles for calibration and sensitivity analysis

Guiding Principle 5.1: All available information should be used to guide the parameterisation and model calibration. All parameters should initially be considered to be uncertain.

Guiding Principle 5.2: The calibration process should be used to find model parameters that prepare a model for use during predictions of future behaviour, rather than finding model parameters that explain past behaviour.

Guiding Principle 5.3: The modeller should find a balance between simplicity (parsimony) and complexity (highly parameterised spatial distribution of some properties). Non-uniqueness should be managed by reducing the number of parameters or by regularisation, which is a way of ensuring that parameter estimates do not move far from initial estimates that are considered to be reasonable.

Guiding Principle 5.4: Performance measures should be agreed prior to calibration, and should include a combination of quantitative and non-quantitative measures. The scaled root mean squared error (SRMS) is a useful descriptor of goodness of fit when the only objective is to fit historical measurements of heads, but is less useful when automated calibration methods are used. A target SRMS of 5% or 10% is only meaningful when those setting the target know that it is achievable for a particular kind of problem and a particular environment with a known density of informative data.

Guiding Principle 5.5: Sensitivity analysis should be performed to compare model outputs with different sets of reasonable parameter estimates, both during the period of calibration (the past) and during predictions (in the future).

Guiding Principle 5.6: A formal verification process should only be attempted where a large quantity of calibration data is available and it is possible to set aside a number of key observations that could otherwise be used for calibration.

As discussed in the companion conceptual model report,

> "*The Guidelines affirm that consideration of alternative conceptual models is good modeling practice, as their use represents acknowledgement of our uncertainty in our description of the hydrogeological domain and the physical processes. The use of alternative models also allows for exploration of the space of uncertainty. … It is a good geological practice to have several working concepts in mind when interpreting scarce, incomplete, noisy, and sometimes contradictory field observations.*"

In keeping with these best practices, this modeling exercise will use the 6 conceptual models, describing the nature of groundwater flow and the gas accumulation in the Alderson Member to complete a series of 33 simulations . The interpretation of the results of these simulations will provide the opportunity to examine the nature of uncertainty in our models. These simulations will be validated as potentially representative of the natural system based on their ability to replicate the field data for flow directions and regional discharge. The simulations that fit with reality will all be used for risk analysis.